Platensimycin and Platencin Biosynthesis in *Streptomyces platensis*: Exploring Nature's Biological Machinery for the Discovery and Development of Useful Compounds

by

Ryan Matthew Peterson

A dissertation submitted in partial fulfillment of

the requirements for the degree of

Doctor of Philosophy

(Pharmaceutical Sciences)

at the

UNIVERSITY OF WISCONSIN-MADISON

2012

Date of final oral examination: 06/04/2012

The dissertation is approved by the following members of the Final Oral Committee:

Ben Shen, Professor, Pharmaceutical Sciences
Charles T. Lauhon, Associate Professor, Pharmaceutical Sciences
Weiping Tang, Assistant Professor, Pharmaceutical Sciences
Tim S. Bugni, Assistant Professor, Pharmaceutical Sciences
Michael G. Thomas, Associate Professor, Bacteriology

PLATENSIMYCIN AND PLATENCIN BIOSYNTHESIS IN *STREPTOMYCES PLATENSIS:* EXPLORING NATURE'S BIOLOGICAL MACHINERY FOR THE DISCOVERY AND DEVELOPMENT OF USEFUL COMPOUNDS

Ryan M. Peterson

Under the supervision of Professor Ben Shen

At The University of Wisconsin-Madison, Madison, WI and

At The Scripps Research Institute, Jupiter, FL

Platensimycin (PTM) and platencin (PTN) are recently discovered secondary metabolites produced by strains of *Streptomyces platensis.* They are potent, selective inhibitors of bacterial and mammalian fatty acid synthases and have emerged as promising drug leads for both antibacterial and antidiabetic therapies. In addition to traditional medicinal chemistry approaches to lead small molecule optimization for drug development, characterization of the organisms responsible for production of complex natural products complements synthetic efforts. Advantages of studying the biosynthetic pathways of antibiotic small molecules include (i) discovery of novel enzymes providing access to new chemistry, biochemistry and mechanisms of catalysis; (ii) discovery of regulatory elements providing methods for increasing titers of lead compounds; (iii) identification of self-resistance mechanisms providing insight for prediction and prevention of clinical resistance; and finally, (iv) identification of opportunities for combinatorial biosynthesis, pathway engineering, and improved methods of drug discovery and development. The genetic loci responsible for PTM/PTN production in *S. platensis* MA7327 and PTN production in *S. platensis* MA7339 were cloned and sequenced to reveal genes involved in

biosynthesis, regulation, and resistance. Ultimately, the structural differences between PTM and PTN lie in their unique diterpenoid moieties. Herein, the divergence in the PTM and PTN biosynthetic pathways dictated by novel diterpene synthases is explored as the producing strains of PTM and PTN present a unique opportunity for the comparative study of biosynthetic pathways producing related – but distinct – compounds. By studying the strategies Nature employs for increasing structural diversity in secondary metabolic pathways, we may gain insight into exploiting these strategies for developing methods for generating new and useful compounds. Additionally, the self-resistance mechanisms in the producing organisms of PTM and PTN are presented and serve as excellent models to understand and thereby predict future resistance mechanisms to new lead antibiotic compounds. The outcomes of these studies promise not only in-depth understanding of the unique biosynthetic reactions leading to PTM and PTN production but offer the potential for key advances in preparing PTM, PTN, and future analogs for the clinic.

Acknowledgements

I would like to first and foremost thank Professor Ben Shen for supporting my graduate research and providing an excellent environment to learn and grow as a scientist. His guidance has truly been invaluable. I would also like to extend my gratitude to all of the past and present members of the Shen group, who over the years have offered advice, insight, and most of all, a friendly work environment. In particular, I would like to thank Dr. Steven Van Lanen, for encouraging me to join the Shen lab during my first-year rotation; Dr. Yihua Chen for insightful discussions on science (and fishing); Dr. Geoff Horsman, for his kindness and technical expertise; Dr. Scott Rajski, for his support and contributions to the platensimycin project; Evelyn Wendt-Pienkowski, for the countless answers you had for my questions about cloning, *Streptomyces*, and why my experiments didn't work; Dr. Jeremy Lohman, for being a great colleague, friend, and roommate; and finally, Dr. Michael Smanski, who has been an excellent colleague, mentor, and friend over the years we had working on the platensimycin project together. I want to thank all the faculty, staff, and fellow graduate students in the Pharmaceutical Sciences Division and the School of Pharmacy – Chuck Lauhon, Ken Niemeyer, Joni Mitchell, Gary Girdaukas, and countless others who have made life a little bit easier. I would also like to thank our new friends and colleagues at The Scripps Research Institute who have welcomed the Shen group to a new home in Jupiter, FL. Finally, I would like to thank my friends and family for their unconditional love and support – and in particular, Emily, who has provided a source of strength and happiness.

Table of Contents

List of Figures

List of Tables

List of Abbreviations

A	alanine
AA	amino acid
ACP	acyl carrier protein
ADHBA	3-amino-2,4-dihydroxybenzoic acid
ADHOHP	2-amino-4,5-dihydroxy-6-one-heptanoic acid-7-phosphate
ADP/ATP	adenosine di/triphosphate
AHBA	aminohydroxybenzoic acid
$Apra^{R/S}$	apramycin resistant/sensitive
ASA	aspartate-4-semi-aldehyde
AT	acyl transferase
ATCC	American Type Culture Collection
AU	absorbance units
BLAST	basic local alignment search tool
ºC	degrees Celsius
CDC	Centers for Disease Control and Prevention
CDP-ME	4-(cytidine 5'-diphospho)-2-*C*-methyl-D-erythritol
CDP-ME2P	CDP-ME 2-phosphate
CDP-MEK	CDP-ME kinase
CIAP	calf-intestinal alkaline phosphatase
CoA	coenzyme-A
CPP	copalyl pyrophosphate (copalyl diphosphate)
CPT-1	carnitine palmitoyl transferase 1

CTP	cytidine triphosphate
D	aspartate
Da	dalton
DH	dehydratase
DHAP	dihyroxyacetone phosphate
DMAPP	dimethylallyl pyrophosphate
DMSO	dimethyl sulfoxide
DNA	deoxyribonucleic acid
DNase	deoxyribonuclease
dNTP	deoxyribonucleotide triphosphate
DTS	diterpene synthase
DXP	1-deoxy-D-xylulose 5-phosphate
DXPR	DXP reductase
DXPS	DXP synthase
E	glutamate
EDTA	ethylene diaminetetraacetic acid
ent-	prefix for an enantiomer of a natural product when the trivial name only refers to one enantiomer
ER	enoyl reductase
eV	electron volt
FAO	fatty acid oxidation
FASI	type I fatty acid synthase
FASII	type II fatty acid synthase

GAs	gibberellins
GA3P	glyceraldehyde-3-phosphate
GC-MS	gas chromatography-mass spectroscopy
GGDP	geranylgeranyl diphosphate **(**all trans-3,7,11,15-tetramethyl-2,6,10,14-hexadecatetraenyl pyrophosphate)
GGOH	geranylgeraniol (all trans-3,7,11-15-Tetramethyl-2,6,10,14-hexadecatetraen-1-ol)
His	histidine
HIV	human immunodeficiency virus
HMBPP	1-hydroxy-2-methyl-2-(*E*)-butenyl 4-pyrophosphate
HMBPPR	HMBPP reductase
HMBPPS	HMBPP synthase
HMG	3-hydroxy-3-methylglutarate
HMGR	HMG reductase
HMGS	HMG synthase
HPLC	high-performance liquid chromatography
hr	hours
HTS	high-throughput screening
IC_{50}	half maximal inhibitory concentration
IPP	isopentenyl pyrophosphate
IPTG	isopropyl β-D-1-thiogalactopyranoside
$Kan^{R/S}$	kanamycin resistant/sensitive
Kb	kilobase

kDa	kilodalton
KR	ketoreductase
LB	Luria-Bertani
LC-MS	liquid chromatography-mass spectroscopy
µg	microgram
µm	micrometer
µmol	micromoles
M	molar
M5P	mevalonate 5-phosphate
M5PP	mevalonate 5-pyrophosphate
MECPP	2-*C*-methyl-D-erythritol 2,4-dicyclopyrophosphate
MECPPS	MECPP synthase
MEP	2-*C*-methyl-D-erythritol 4-phosphate
mg	milligram
MHz	megahertz
MIC	minimal inhibitory concentration
min	minute
MK	mevalonate kinase
mL	milliliter
MLC	minimal lysis concentration
mm	millimeter
mM	millimolar
mmol	millimoles

MOPS	3-(N-morpholino)propanesulfonic acid
MPLC	medium pressure liquid chromatography
MRSA	methicillin-resistant *S. aureus*
MW	molecular weight
MSSA	methicillin-sensitive *S. aureus*
MWCO	molecular weight cut-off
m/z	mass/charge
N	asparagine
NADH	nicotinamide adenine dinucleotide, reduced
NCBI	National Center for Biotechnology Information
NCE	new chemical entity
nd	not determined
nm	nanometer
NMR	nuclear magnetic resonance
NP	natural product
NRPS	nonribosomal peptide synthetase
ORF	open reading frame
PCR	polymerase chain reaction
PKS	polyketide synthase
PP_i	inorganic pyrophosphate
ppm	parts per million
PTM	platensimycin
PTN	platencin

Q	glutamine
rDNA	ribosomal DNA
R_f	retardation factor (in TLC, the ratio of the distance traveled by the center of a spot to the distance traveled by the solvent front)
RNA	ribonucleic acid
RNase	ribronuclease
rpm	rotations per minute
R2YE	rich media for Streptomyces (see Appendix for media recipes)
S	serine
SAR	structure-activity-relationship
SNA	soft nutrient agar
sp.	species (undefined or unnamed)
spp.	species (plural)
syn-	prefix indicating a stereoisomer of a molecule
T	threonine
TCA	tricarboxylic acid cycle (citric acid cycle/Krebs cycle)
TF	trigger factor fusion tag
TE	thioesterase
TSB	tryptic soy broth (see Appendix for media recipes)
TLC	thin layer chromatography
UV-vis	ultraviolet-visible light
VISA	vancomycin intermediate *S. aureus*
VRE	vancomycin resistant enterococci

v/v	volume per volume
WT	wild-type
w/v	weight per volume
X	any amino acid
YME	yeast malt extract (see Appendix for media recipes)

Chapter 1: Nature as a source for drugs and therapeutics

1.1 A brief history of natural products and their sources

Nature has provided humans with the means for treatment of disease for thousands of years as societies have always sought remedies for common ailments, pain, and untimely death. Plants or their extracts have served as the basis for medicinal preparations for millennia and remain a major component of curative medicine in many cultures today, including in Ayurvedic Medicine and Traditional Chinese Medicine (1, 2). Traditional knowledge of medicinally beneficial flora, or pharmacognosy, was eventually combined with advancements in chemistry, and new methods of isolation, chemical characterization, and biological testing were developed in order to better understand the roles of the individual components – or "natural products" – within traditional preparations. The success of this approach is exemplified by the isolation of morphine from crude opium (extracted from the poppy, *Panus somniferum*) by Friedrich Sertürner in 1817, which represents the first pure, pharmacologically active natural product isolated for therapeutic use (3). Subsequent isolations of quinine from *Cinchona calisaya*, (an antimalarial, 1820), salicin and salicylic acid from *Salix alba* (precursors to aspirin, 1826-1838), and digitoxin from *Digitalis purpurea* (a cardiac glycoside, 1875) contributed to the rise of a so-called Western medicine approach (**Figure 1.1**) (4, 5). The ability to identify and purify active

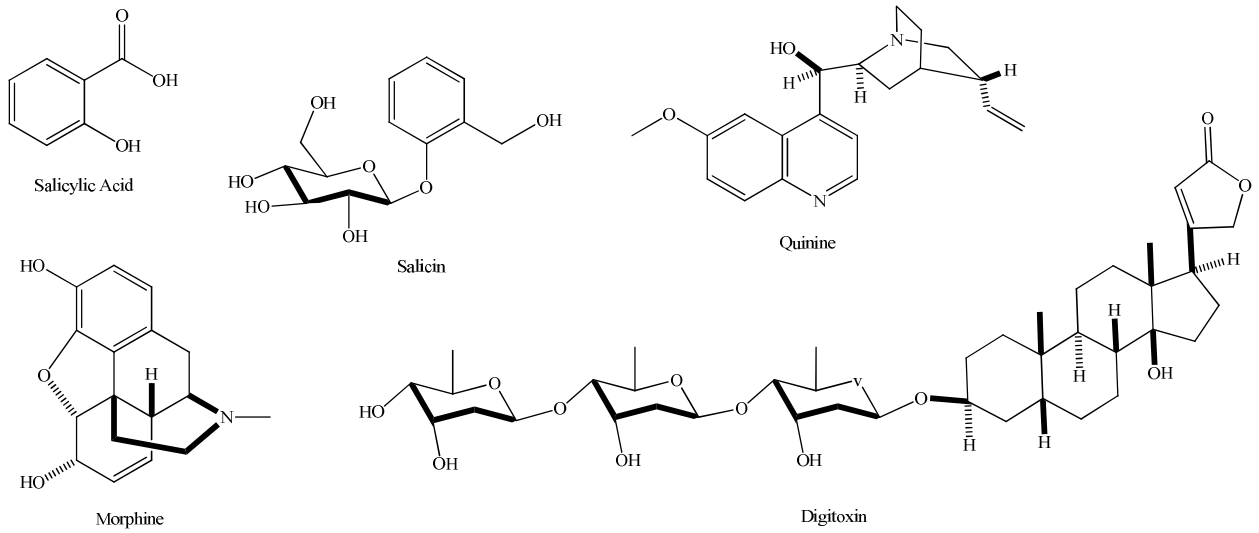

Figure 1.1 – Biologically active natural products isolated in the 19th century

compounds from natural sources, characterize their individual effects on the human body, and prescribe an accurate dosing of compounds to alleviate disease or its symptoms was a major advancement in modern medicine.

The twentieth century brought with it additional advancements and progress in science and medicine, but more importantly, a new source of medicinally useful natural products was unveiled: microorganisms. The infamous and fortuitous discovery of penicillin (produced by *Penicillium* mold) by Alexander Fleming in 1928 – and its successful industrial development and commercialization during World War II – provided a "miracle" cure to previously deadly and seemingly untreatable infections (6, 7). The unparalleled success of penicillin expanded the focus of pharmaceutical research and development to include microorganisms and their relatively unknown pharmaceutical potential. As a result of massive efforts to screen microorganisms for new antibiotics – combined with established programs to isolate biologically active compounds from plants – the twentieth century saw amazing developments in medicine and the treatment of disease. The discovery of new and effective antibiotics, antiparasitics,

antimalarials, lipid control agents, immunosuppressants, and anticancer agents likely contributed greatly to the average life expectancy nearly doubling throughout most of the world by the end of the century (8, 9). By 1990, nearly 80% of the pharmaceuticals on the world market were natural products, or synthetic analogs of naturally occurring compounds, further highlighting the contribution of natural products to modern medicine (2, 9).

Despite an obvious "golden age" of natural product-derived drug discovery in the middle to latter part of the twentieth century, the onset of the twenty-first century saw a major shift in drug discovery efforts by pharmaceutical companies. Many companies scaled back, if not completely abandoned, their natural product discovery programs (9, 10). High throughput screening (HTS) programs combined with new combinatorial chemistry methods for producing very large synthetic libraries of "drug-like" compounds better adapted to a new model of drug discovery: rapid synthesis of large, combinatorial libraries followed by HTS methods for identification of compounds that target known biological targets for treatment of disease (11). However, the success of these target-based screening approaches and their reliance on medicinal chemical engineering for lead compound synthesis has not been realized as the attrition rates for compound libraries are much higher than expected, drug approvals from the Food and Drug Administration (FDA) have fallen, the number of new chemical entities (NCEs) is steadily declining, and pharmaceutical industry growth is stagnant (8, 12, 13). The industry is again at a crossroads and its drug discovery approaches are in need of reevaluation. As programs shift back to phenotypic screening in complex biological systems in order to reevaluate the best possible targets (or combinations thereof) for drug leads, the advantages of natural products are clear: they provide "privileged" scaffolds that have evolved to interact with biological macromolecules, which can act as drug leads or as biochemical probes for investigation of

cellular function and disease (11, 13–16); they provide unmatched structural diversity and complement synthetic and combinatorial libraries, as well as guide synthetic efforts (17–22); and finally, although the number of known natural products from all living sources has now surpassed over one million compounds, the vast number of species of plants, fungi, and bacteria that have yet to be isolated, characterized, or screened for bioactivity – one source estimates more than 90% of the world's biodiversity remains unexplored – suggests that Nature remains a virtually untapped reservoir of novel compounds and structural diversity (2, 20, 23).

1.2 The metabolic pathways responsible for natural products

Natural products are products of both primary and secondary metabolic pathways. Primary metabolism is essential to an organism and provides the means for breakdown of food, generation of energy, as well as production of the building blocks necessary for biosynthesis of macromolecules – such as polysaccharides, peptides, DNA, RNA, and lipids – common and essential for life in all biological systems. Importantly, primary metabolism is a well-organized and highly efficient process. While primary metabolites such as amino acids, nucleotides, vitamins and organic acids can have important industrial value, secondary metabolites are the main source for unique, structurally-diverse, and pharmacologically-active natural products (6, 20). Secondary metabolites are typically low molecular weight molecules (MW <3000 Da) and while structurally complex, are ultimately derived from relatively few and simple precursors, which are shunted from primary metabolic pathways. In stark contrast to primary metabolites, secondary metabolites and their intermediates characteristically accumulate inside or outside the cell (5). Furthermore, production of individual secondary metabolites can be unique to a genus, a species, or even a single microbial strain (6, 20). Although the precise role(s) of secondary metabolites can be ambiguous, by definition they do not contribute to basic growth and

development; yet, while they are not essential to their producers, they must provide some survival advantage (6, 24).

1.3 Organization of secondary metabolites by common precursor(s)

Natural products produced by secondary metabolism are derived from the same simple building blocks generated and utilized by primary metabolism in biological systems. These precursors for secondary metabolism are generally shunted from energy-generating pathways such as glycolysis, photosynthesis, or the Krebs (TCA) cycle. Diverse natural products can therefore be arranged into several general classes according to the common precursor(s) utilized and the chemistry employed by enzymes involved in building their hydrocarbon- and nitrogen-containing skeletons. **Figure 1.2** illustrates the grouping of representative natural products derived from secondary metabolism into seven common classes: fatty acids, peptides, alkaloids, aminoglycosides, terpenoids, polyketides, and flavonoids (5). While a majority of natural products "fit" into these defined classes, the innate combinatorial nature observed in secondary metabolism leads to an expectation that shuffling of classical pathways should occur. Indeed, this prediction is exemplified by natural products that are "hybrid" molecules, including those of polyketide and peptide, or polyketide and terpene, origin (25–28). Furthermore, the multitude of possible downstream tailoring reactions, including rearrangement of carbon skeletons, oxidation reactions, and other modifications, can ultimately disguise each natural product's simple origins and contribute to the vast structural diversity inherent to secondary metabolism (5).

1.4 *Streptomyces* are major producers of microbial natural products

Among microorganisms, species within the genus *Streptomyces* (order *Actinomycetales*, or "actinomycetes") are some of the most prolific producers of natural products discovered so far. Beginning with the discovery and isolation of streptothricin in 1942, and the more clinically

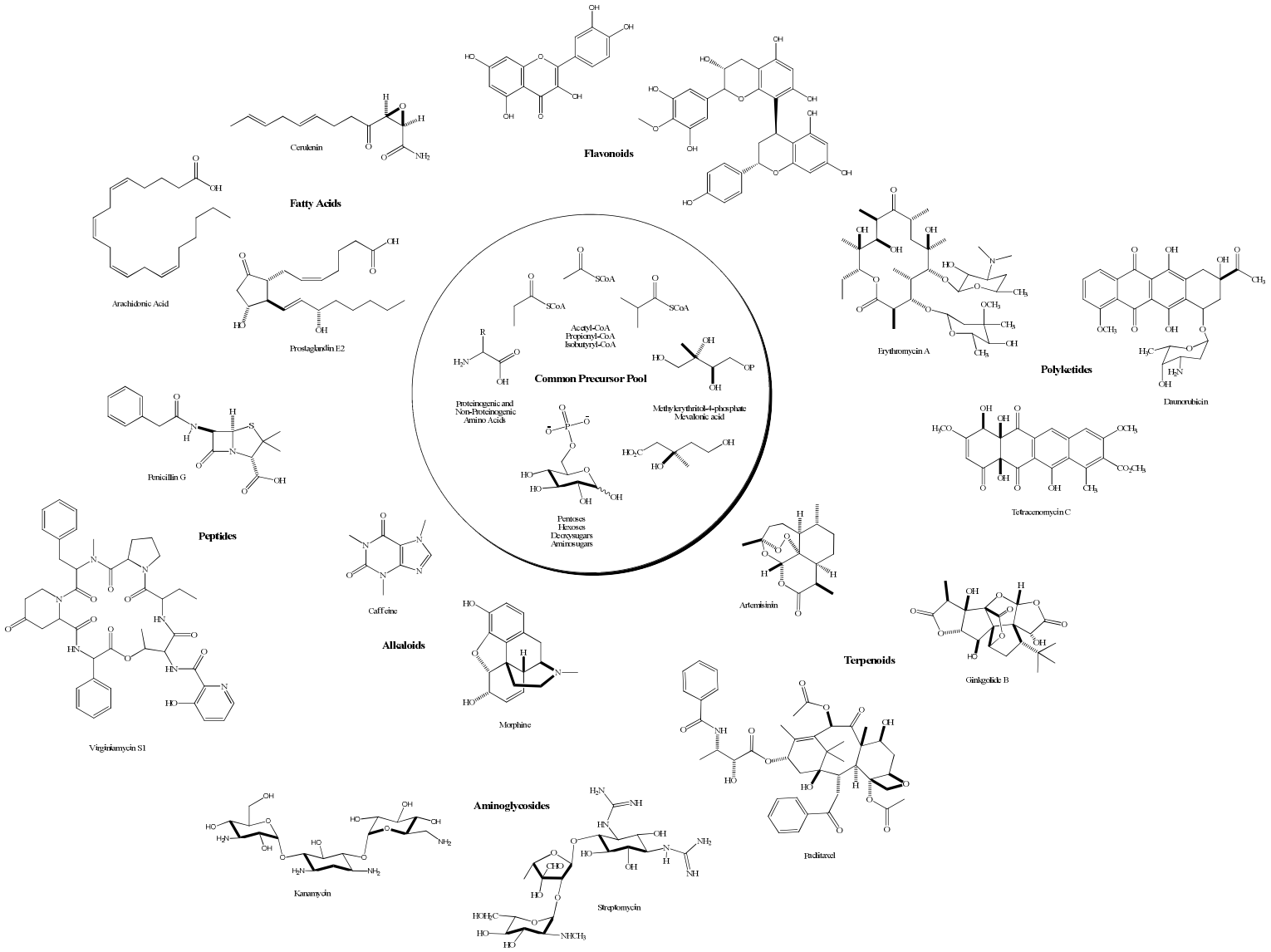

Figure 1.2 – General classes of natural products derived from secondary metabolism based on common precursor origin

relevant streptomycin in 1944, *Streptomyces* have become one of the largest contributors of clinical antimicrobial compounds and serve as a model for secondary metabolite production in bacteria (29). **Table 1.1** summarizes a recent estimation by Bérdy of the total number of known natural products (as of 2002) and the approximate number of natural products isolated from plants, animals, fungi, and various bacteria (20). *Streptomyces* species are responsible for approximately 34% of presently known bioactive microbial metabolites. A large percentage (~86%) of these metabolites have been identified as having "antibiotic" (i.e. antibacterial, antifungal, antiprotozoal, antitumor, or antiviral) bioactivities; yet, the distinctiveness (<1% overlap in similarity between structures produced by fungal and *Streptomyces* species) and complexity of metabolites isolated from *Streptomyces* species suggest these compounds are ideal candidates in new screens for additional pharmaceutically or agriculturally relevant bioactivities (20).

Table 1.1 – Approximate number of known natural products from various sources

Source	Antibiotics	Total bioactive metabolites	Total known compounds
All Natural Product Sources:	25,000-30,000	>250,000	>1,000,000
Animal Kingdom:	5,000	50,000-100,000	300,000-400,000
Higher Plants:	11,500	>100,000	>500,000
Microbes:	16,500	22,500	>50,000
Fungi:	4,900	8,600	-
Order *Actinomycetales:*	8,700	10,100	-
Genus *Streptomyces:*	6550	7630	-
Other bacteria:	2900	3800	-

Streptomyces belong to the phylum, *Actinobacteria*, which is one of the largest and earliest lineages within the prokaryotes (30). Although the morphology, physiology, and metabolism within this phylum varies considerably, its members are Gram-positive organisms

with characteristically high G+C content in their DNA (>70%) (31). *Actinobacteria* are prevalent in all types of environments and can interact with other organisms in both friendly and unfriendly ways. Remarkably, just as the genus, *Streptomyces*, is the largest producer of clinically useful antibiotics, another genus, *Mycobacterium*, includes pathogens responsible for the largest number of human deaths worldwide caused by bacterial infection (30, 32). The capacity of *Actinobacteria* to flourish as animal and plant pathogens, as well as thrive as prolific producers of novel secondary metabolites, has warranted continued discovery and characterization of unique species within this phylum (29, 33–36).

Members of the genus, *Streptomyces*, are also ubiquitous in Nature and typically colonize soil and vegetation (37). They display an unusually complex morphology and life cycle, compared with traditional unicellular bacteria, in that they form differentiated mycelial "tissues" and spores (31). The typical life cycle of *Streptomyces* begins with growth of substrate, or vegetative, mycelium from a resting spore. Germ tubes extend out of the spore by apical growth to form hyphae – long, thread-like filamentous structures – and as the cells divide, cross walls – or "septa" – are formed at regular intervals in each hypha (38). Lateral branching occurs from these subapical cells, forming newly extending hyphal tips, and creating a mat of vegetative mycelium. Chromosomal DNA replicates in dividing cells and moves toward the extending tips and into new branches in a process called nucleoid migration (39). When nutrients are limiting or other environmental stress occurs, a short period of growth arrest is followed by formation of aerial, or reproductive, hyphae through lateral branching from the substrate mycelium. As these aerial hyphae extend out of, or away from, the soil, their tips differentiate into chains of spores, with each spore compartment containing a single chromosome (31, 38, 39). The spores represent a semi-dormant stage in the life cycle, resist low nutrient and water availability in the soil, and

can survive for long periods of time (37). As antibiotic production is generally growth-phase dependent, detailed knowledge of the complex *Streptomyces* life cycle is important for understanding the physiology and regulation involved in production of useful secondary metabolites as well as for general growth, fermentation, preservation, and genetic manipulation of producing *Streptomyces* strains (37, 39).

1.5 A need for novel antibiotics

Microbial natural products-guided drug discovery yielded many robust and clinically useful antibacterial antibiotics in the approximately twenty years following the widespread success of penicillin (**Table 1.2**, **Figure 1.3)**. Despite a declared "victory against infectious disease" by the U.S. Surgeon General in December, 1967, a serious threat had already surfaced in laboratories and clinics: antibiotic resistance in pathogenic bacteria (40). Unfortunately, acquired resistance to antibiotics is now recognized as an inevitable consequence of antibiotic use, as observed clinical resistance emerges very soon after approved use in all major classes of antibiotics (**Table 1.3**).

Infection caused by multidrug resistant bacteria is a serious public health concern. A 2002 Centers for Disease Control (CDC) report estimates that at least two million people acquire bacterial infections in U.S. hospitals each year, with around 70% of these infections caused by strains resistant to at least one commonly used antibiotic. As a result, approximately 90,000 people die from these infections (41). With an undeniable rise in bacterial resistance to clinically used antibiotics, the potential severity of the problem is compounded by the fact that there are simply not enough new and effective drugs coming out of the pharmaceutical pipeline to combat newly emergent and resistant strains (41). This is evidenced by an approximately 32-year gap (1968-2000) without discovery or approval of a new class of antibiotic (**Table 1.2**), before the

Table 1.2 – Timeline of the discovery of the major classes of clinical antibiotics by year (42)

Year	Antibiotic	Class	NP	Synthetic
1932	Sulfapyridine	Sulfonamide		X
1940	Penicillin	beta-Lactam	X	
1944	Streptomycin	Aminoglycoside	X	
1945	Cephalosporin	beta-Lactam	X	
1947	Chloramphenicol	Phenypropanoid	X	
1948	Chlortetracycline	Tetracycline	X	
1950	Erythromycin	Macrolide	X	
1955	Vancomycin	Glycopeptide	X	
1955	Virginiamycin	Streptogramin	X	
1955	Amphotericin	Polyene (antifungal)	X	
1955	Lincomycin	Lincosamide	X	
1959	Rifamycin	Ansamycin	X	
1962	Nalidixic Acid	Quinolone		X
1969	Fosfomycin	Phosphonate	X	
2000	Linezolid	Oxazolidinone		X
2003	Daptomycin	Lipopeptide	X	

Table 1.3 –History of observed clinical resistance to major classes of antibiotics (41, 43, 44)

Year	Bacteria	Antibiotic
1947	*Staphylococcus aureus*	Penicillin
1967	*Streptococcus pneumoniae*	Penicillin
1967	*Neisseria gonorrhea*	Penicillin
1970	*Staphylococcus aureus*	Methicillin
1983	*Enterococcus faecium*	Penicillin
1983	*Shigella*	Multidrug resistance
1983	*Escherichia coli*	Fluroquinolones
1984	*Mycobacterium tuberculosis*	Multidrug resistance
1989	*Enterococcus*	Vancomycin
2001	*Campylobacter*	Fluroquinolones
2002	*Staphylococcus aureus*	Vancomycin

oxazolidinones and lipopeptides were approved for clinical use in 2000 and 2003, respectively (45). While functional modifications to existing classes of antibiotics have yielded new "generations" of antibiotics effective in treating resistant pathogens, this practice is not a

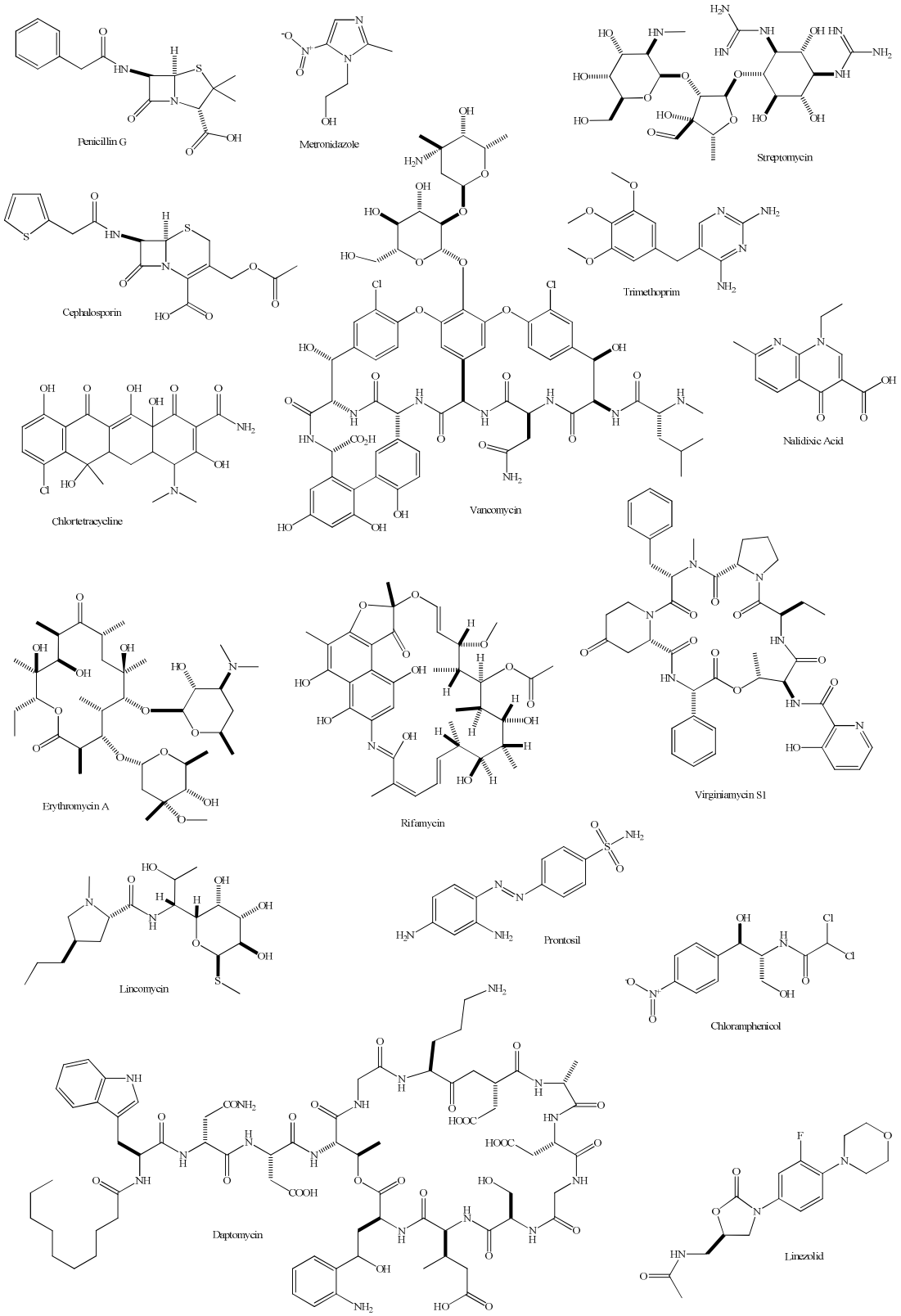

Figure 1.3 – Chemical structures of clinically relevant classes of antibiotics

sustainable approach for future antibiotic development. Consequently, new approaches to the treatment and prevention of infectious disease are desperately needed, and discovery of new classes of compounds targeting novel bacterial targets may provide a critical first step (46).

1.6 Validated targets for antibiotic development

Despite remarkable efforts to identify new therapeutic targets in pathogenic bacteria, relatively few essential targets have been validated by clinical use (45). **Figure 1.4** illustrates these five cellular processes/targets and the classes of antibiotics inhibiting these processes are noted below. The chemical structures of clinically used antibiotics targeting these processes are highlighted in **Figure 1.3**.

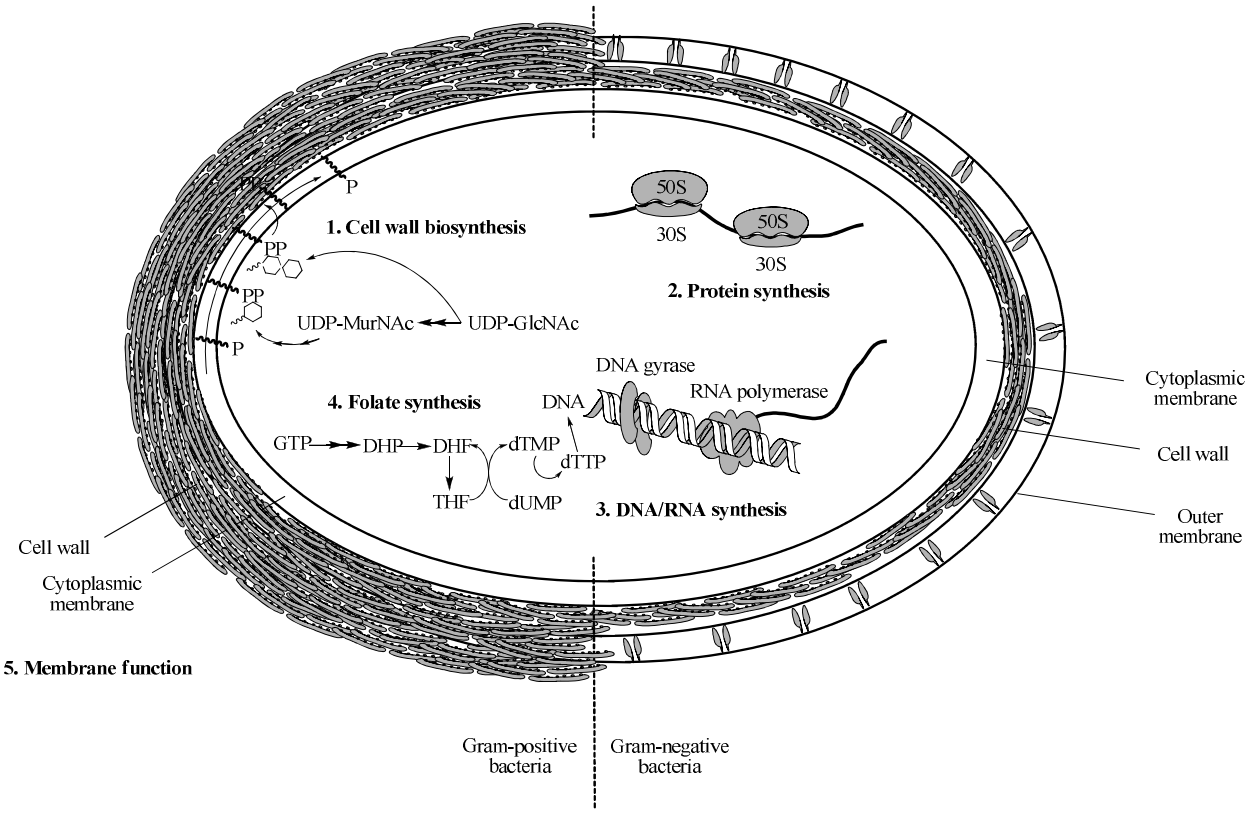

Figure 1.4 – Validated cellular targets in typical Gram-positive and Gram-negative bacteria for currently used antibacterial antibiotics

1. **Inhibition of bacterial cell wall synthesis**: β-lactams (e.g., penicillin G/cephalosporin) inhibit formation of peptidoglycan cross-linking; and glycopeptides (e.g., vancomycin) inhibit peptidoglycan synthesis
2. **Inhibition of bacterial protein synthesis**: aminoglycosides (e.g., streptomycin); tetracyclines (e.g., chlortetracycline); macrolides (e.g., erythromycin A); lincosamides (e.g., lincomycin); streptogramins (e.g., virginiamycin); phenylpropanoids (e.g., chloramphenicol); and oxazolidinones (e.g., linezolid); each of these classes specifically inhibit bacterial protein synthesis through binding of either the 30S ribosomal unit (aminoglycosides and tetracyclines) or the 50S ribosomal subunit (macrolides, lincosamides, streptogramins, phenylpropanoids, and oxazolidinones)
3. **Inhibition of nucleic acid synthesis or replication inhibitors**: quinolones (e.g., nalidixic acid) bind to DNA gyrase and prevent DNA supercoiling; and ansamycins (e.g., rifamycin) bind DNA-dependent RNA polymerase inhibiting initiation
4. **Inhibition of folic acid synthesis**: sulfonamides (e.g., prontosil) act as competitive inhibitors of dihydropteroate synthetase; and trimethoprim interferes with dihydrofolate reductase
5. **Disruption of membrane function:** lipopeptides (e.g., daptomycin) bind the cell membrane and cause rapid depolarization leading to cell death

1.7 Type II fatty acid synthesis (FASII) in bacteria as a target for novel antibiotics

Fatty acids are cellular building blocks and are, among other things, the major constituents of biological membranes. Hence, *de novo* synthesis of fatty acids is essential in all kingdoms of life, and a conserved set of biochemical reactions are responsible for fatty acid

synthesis in most organisms (47, 48). Yet, distinct variations of this conserved pathway for fatty acid synthesis (FAS) exist in Nature. In mammals, a single homodimer of a 270 kD polypeptide containing seven functional domains, is responsible for the entire catalytic cycle of FAS. Similarly, fungal FAS utilizes a heterodimer of two distinct, multidomain polypeptide chains. Each of these type I fatty acid synthesis (FASI) systems are characterized by multifunctional enzyme complexes, or "megasynthases", containing multiple domains and reaction centers, and catalyzing all of the reaction steps involved in the fatty acid biosynthetic pathway (49–51). In contrast, a type II fatty acid synthesis (FASII) system is found in bacteria (as well as in plants and some protozoan parasites), which utilizes discrete proteins, with each catalytic step in the fatty acid biosynthetic pathway carried out by a single, monofunctional protein (52). The essentiality of fatty acids combined with clear differences among FASII dissociated enzymes and the megasynthases of FASI in mammals (including humans) suggest that FASII should be an attractive target for broad-spectrum antibacterial antibiotics. Indeed, numerous natural and synthetic compounds inhibiting bacterial growth have now been identified as specific inhibitors of bacterial FASII enzymes (47, 49, 52–58). Specifically, the continued clinical use of the antituberculosis drug, isoniazid, as well as the commercial use of the antiseptic, triclosan, both inhibitors of the enoyl-ACP reductase, FabI, further validate FASII pathway enzymes as effective antibacterial targets (52). Although lipid metabolism has been extensively studied in *E. coli* and its pathway has become a paradigm for bacterial fatty acid biosynthesis (**Figure 1.5, Table 1.4**), significant diversity in FASII enzymology and essentiality among various genera of bacteria is becoming more evident (59–62). Although this may hinder development of broad spectrum antibiotics targeting diverse strains, it nonetheless provides opportunities to develop highly specific inhibitors against major pathogens, including multi-drug-resistant strains

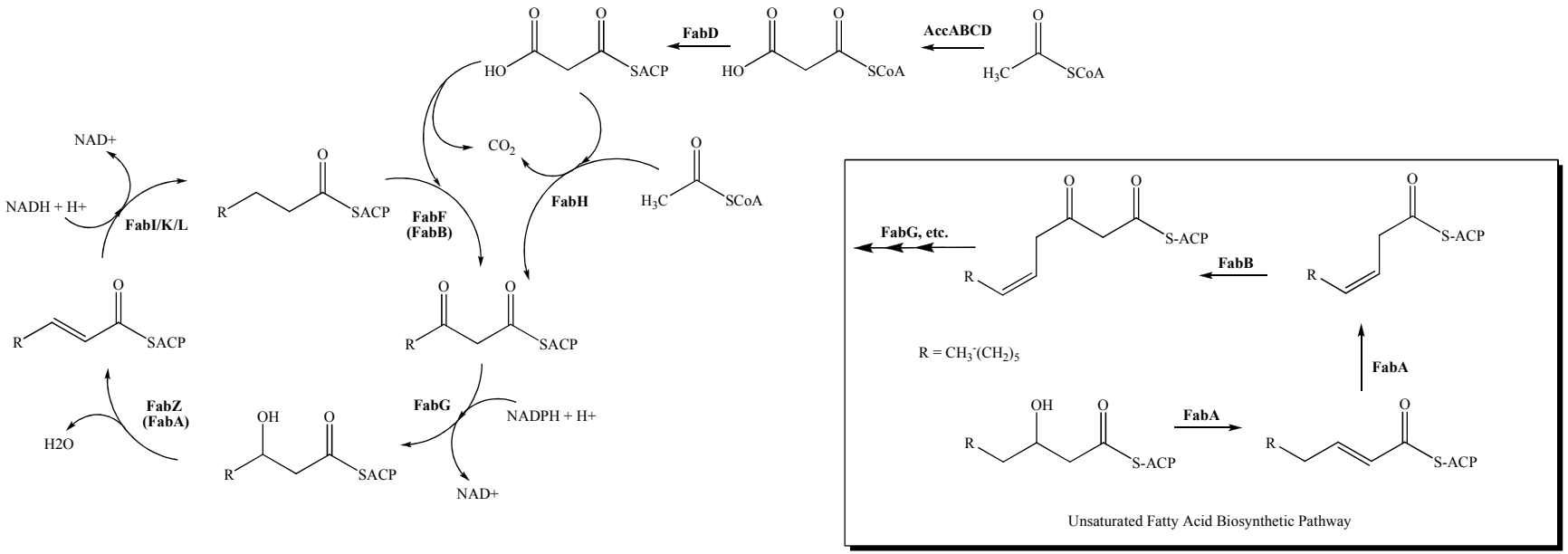

Figure 1.5 – Schematic of type II fatty acid synthesis in bacteria

Table 1.4 – Enzymes of type II fatty acid synthesis in bacteria

Pathway/Enzyme:	Function:	Protein size (#AA):	Source:	Accession number:
Acetyl-CoA Carboxylase:				
AccA	Carboxyl-transferase subunit	319	*E. coli*	BAA08425
AccB	Biotin carboyxl carrier protein (BCCP)	156	*E. coli*	BAE77296
AccC	Biotin carboxylase	449	*E. coli*	BAE77297
AccD	Carboxyl-transferase subunit	304	*E. coli*	BAA16173
Saturated Fatty Acid Synthesis:				
AcpP	apo-ACP	78	*E. coli*	BAA35902
FabD	Malonyl-CoA:ACP transacylase	309	*E. coli*	BAA35900
FabF	3-Ketoacyl-ACP synthase II	413	*E. coli*	BAA35903
FabG	3-Ketoacyl-ACP reductase	244	*E. coli*	BAA35901
FabH	3-Ketoacyl-ACP synthase III	317	*E. coli*	BAA35899
FabI	Enoyl-ACP reductase I (NADH)	262	*E. coli*	BAA14841
FabK	Enoyl-ACP reductase II (FAD, NADH)	324	*S. pneumoniae*	AAF98273
FabL	Enoyl-ACP reductase III (NADPH)	250	*B. subtilis*	ADM36925
FabZ	3-hydroxyacyl-ACP dehydrase	151	*E. coli*	BAA77855
Unsaturated Fatty Acid Synthesis:				
FabA	3-Hydroxydecanoyl- ACP dehydrase/ isomerase	172	*E. coli*	BAA35712
FabB	3-Ketoacyl-ACP synthase I	406	*E. coli*	BAA16180
Additional Enzymes:				
AcpS	ACP synthase	126	*E. coli*	BAE76739
BirA	Biotin protein ligase	321	*E. coli*	BAE77342
FabR	Transcriptional activator/repressor	234	*E. coli*	BAE77348
FadR	Transcriptional activator/repressor	239	*E. coli*	BAA36042

for which FASII provides an entirely new set of cellular targets that are not currently exploited in the clinic (62).

1.8 Discovery of platensimycin and platencin as potent inhibitors of FASII

The renewed interest in the targeting enzymes of bacterial fatty acid synthesis has culminated in the recent discovery of platensimycin (PTM) and platencin (PTN) (**Figure 1.6**), isolated from two distinct strains of *Streptomyces platensis* (63, 64). Both molecules were discovered through a systematic screening of 250,000 natural product extracts (83,000 strains in three growth conditions) using a clever high-throughput, whole cell-based antisense strategy, designed to detect selective inhibitors of FabF (57). Further investigation revealed PTM as a selective and potent FabF inhibitor (IC_{50} = 48nM, *Staphylococcus aureus* FabF), and PTN as a dual inhibitor of both FabF (IC_{50}=4.6μM, *S. aureus* FabF) and FabH (IC_{50}=9.2μM, *S. aureus* FabH) (**Table 1.5**). Importantly, both molecules display broad spectrum, Gram-positive, antibacterial activity, do not exhibit cross-resistance to clinically relevant pathogens (i.e. MRSA, MSSA, and VRE), and have shown *in vivo* efficacy without toxicity through clearance of a *S. aureus* infection in a mouse model (63–66). Unfortunately, the pharmacokinetic profiles of both PTM and PTN have proven suboptimal stalling further advancement of PTM and PTN toward becoming effective, clinically-relevant antibiotics (62-67).

Remarkably, PTM has recently emerged as a new lead for the treatment of diabetes and related disorders (67). Further pharmacokinetic evaluation of PTM in mice revealed that orally administered PTM concentrates in the liver where it subsequently inhibits *de novo* lipogenesis (through apparent inhibition of mammalian fatty acid synthesis, FASI), reduces fatty acid oxidation, and increases glucose oxidation. These immediate effects ultimately result in chronically lower liver triglyceride levels and improved insulin sensitivity, both therapeutically

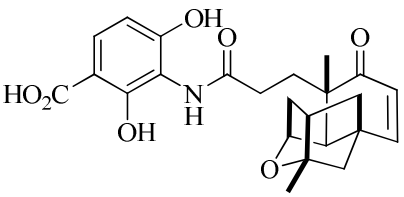

Platensimycin
$C_{24}H_{27}NO_7$, MW: 441.47

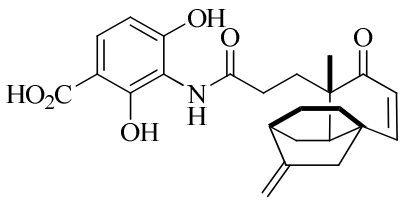

Platencin
$C_{24}H_{27}NO_6$, MW: 425.47

Figure 1.6 – Chemical structures of platensimycin (PTM) and platencin (PTN)

beneficial effects in a diabetes disease model (67). The mechanism by which inhibition of FASI also results in reduced levels of fatty acid oxidation, but increased levels of glucose oxidation is thought to be mediated through the accumulation of hepatic malonyl-CoA, a substrate for FASI. Increased levels of malonyl-CoA negatively regulate carnitine palmitoyltransferase 1 (CPT-1), which participates in a rate-limiting step in fatty acid oxidation. Inhibition of CPT-1 reduces fatty acid oxidation requiring an alternative catabolic (energy-generating) pathway – such as glucose oxidation – to compensate (67, 68). An *in vitro* assay for FASI activity confirmed that PTM inhibits purified rat and human FASI (IC_{50} values of 0.18 µM and 0.30 µM, respectively). The revelation that PTM accumulates in the liver where it can specifically inhibit hepatic FASI, has provided new insight into the biological activities of PTM. More importantly, it has validated specific inhibition of hepatic fatty acid synthase (FASI) as a target for treatment for diabetes and related metabolic disorders (67).

Yet, PTM and PTN remain remarkably potent inhibitors of bacterial FASII. The mechanism by which PTM inhibits bacterial FabF has been investigated (64). Briefly, FabF, or β-ketoacyl-ACP synthase II (KASII), catalyzes the condensation of malonyl-ACP with an acyl-ACP intermediate, elongating the acyl chain by two carbons in the first of four stages in the

Table 1.4 –Antimicrobial and toxicity profiles of PTM, PTN, and linezolid

	MIC (μg/mL)		
Organism	**PTM**	**PTN**	**linezolid**
S. aureus (MSSA)	0.5	0.5	4
S. aureus (+serum)	2	8	4
S. aureus (MRSA)	0.5	1	2
S. aureus (MRSA, macrolide^R)	0.5	1	2
S. aureus (MRSA, linezolid^R)	1	1	32
S. aureus (VISA, vancomycin^R)	0.5	0.5	2
E. faecalis (macrolide^R)	1	2	1
E. faecium (VRE)	0.1	<0.06	2
S. pneumoniae	1	4	1
E. coli (WT)	>64	>64	>64
E. coli (tolC)	16	2	32
	Toxicity (μg/mL)		
Organism	**PTM**	**PTN**	**linezolid**
C. albicans (MIC)	>64	>64	>64
HeLa MTT (IC_{50})	>1000	>100	>100
RBC lysis (MLC)	>67	>67	>67

* 1μg/mL concentration equals 2.27 μM for platensimycin, 2.35 μM for platencin, and 2.96 μM for linezolid

Abbreviations: MIC, minimal inhibitory concentration; IC_{50}, half maximal inhibitory concentration; MRSA, methicillin-resistant S. aureus; MSSA, methicillin-susceptible S. aureus; MTT, 3-(4,5-dimethylthiazol-2-yl)-2,5-diphenyl-2H-tetrazolium bromide; VISA, vancomycin-intermediate S. aureus; VRE, vancomycin-resistant Enterococcus; RBC, red blood cell; MLC, minimum lysis concentration; WT, wild-type; tolC, *E.coli* multidrug efflux pump

elongation cycle of fatty acid synthesis (49). The reaction mechanism by which this Claisen condensation proceeds is a three step, ping-pong reaction: (i) acyl-ACP is covalently transferred to the active site cysteine and reduced ACP is released; (ii) malonyl-ACP binds and is decarboxylated, releasing CO_2; and (iii) the condensation reaction occurs and the final product is released (69). Crystallographic studies have revealed that PTM preferentially interacts with the FabF active site only after an acyl-enzyme intermediate has been formed. Interestingly, a "gatekeeping" phenylalanine (Phe-400) residue appears to prevent PTM binding prior to acyl-

enzyme intermediate formation (**Figure 1.7**). A conformational change after intermediate formation allows binding of PTM in the active site where PTM apparently outcompetes malonyl-ACP and inhibits the condensation reaction (64). Although similar studies of PTN-bound FabF or FabH have not been reported, PTN is expected to interact with these enzymes in a manner similar to PTM. Slight differences in structure between the two molecules likely determine the basis for PTN – but not PTM – inhibition of FabH, as well as the higher affinity of FabF for PTM (65). The biological activities of PTM and PTN as antibacterial antibiotics, with a mode of

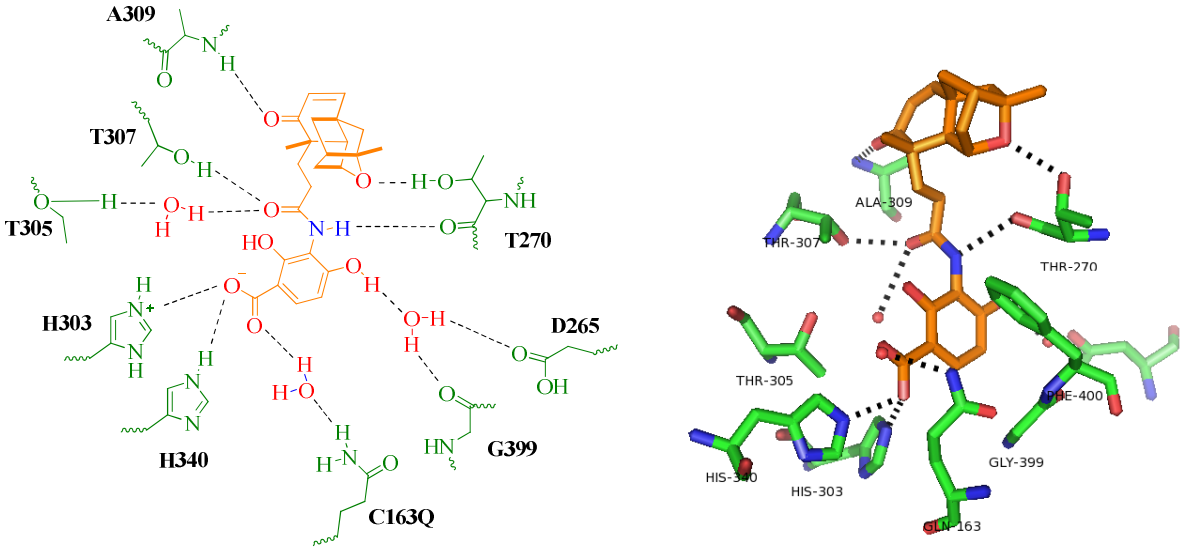

Figure 1.7 – Models of the *E. coli* FabF (C163Q) active site with bound platensimycin and predicted hydrogen bonding with active site residues. (PDB: 2GFX)

action not currently exploited by clinically used antibiotics, has generated significant excitement in this new class of compounds (70–74). Furthermore, the discovery of PTM and PTN highlights the value of maintaining programs for natural products drug discovery and incorporating new and innovative screening methods to ensure successful outcomes.

In addition to traditional medicinal chemistry approaches to lead small molecule optimization for drug development, characterization of the organisms responsible for production of complex lead natural products complements total synthetic efforts. Advantages of studying biosynthetic pathways of lead small molecules include: (i) discovery of novel enzymes providing access to new chemistry, biochemistry and mechanisms of catalysis; (ii) discovery of regulatory elements providing methods for increasing titers of lead compounds; (iii) identification of self-resistance mechanisms providing insight for prediction and prevention of clinical resistance; and finally, (iv) identification of opportunities for combinatorial biosynthesis, pathway engineering, and improving methods of drug discovery and development. In the proceeding chapters, each of these advantages will be highlighted through identification and characterization of the biosynthetic machinery responsible for production of platensimycin (PTM) and platencin (PTN) in strains of *Streptomyces platensis*.

1.9 References

1. Ji H-F, Li X-J, Zhang H-Y (2009) Natural products and drug discovery. *EMBO Reports* 10:194-200.

2. Harvey A (2000) Strategies for discovering drugs from previously unexplored natural products. *Drug Discovery Today* 5:294-300.

3. Huxtable RJ, Schwarz SK (2001) The isolation of morphine - first principles in science and ethics. *Molecular Interventions* 1:189-91.

4. Singh SB (2012) in *Antibiotic Discovery and Development*, eds Dougherty TJ, Pucci MJ (Springer US, Boston, MA), pp 821-847.

5. Dewick PM (2009) in *Medicinal Natural Products: A Biosynthetic Approach* (John Wiley & Sons Inc). 3rd Ed.

6. Demain AL, Fang A (2000) The natural functions of secondary metabolites. *Advances in Biochemical Engineering/Biotechnology* 69:1-39.

7. Elander RP (2002) University of Wisconsin contributions to the early development of penicillin and cephalosporin antibiotics. *SIM News* 52:270-278.

8. Kola I, Landis J (2004) Can the pharmaceutical industry reduce attrition rates? *Nature Reviews Drug Discovery* 3:711-715.

9. Li JW-H, Vederas JC (2009) Drug discovery and natural products: end of an era or an endless frontier? *Science* 325:161-165.

10. Baker DD, Chu M, Oza U, Rajgarhia V (2007) The value of natural products to future pharmaceutical discovery. *Natural Product Reports* 24:1225-1244.

11. Wagenaar MM (2008) Pre-fractionated microbial samples – the second generation natural products library at Wyeth. *Molecules* 13:1406-1426.

12. Newman DJ, Cragg GM (2007) Natural products as sources of new drugs over the last 25 years. *Journal of Natural Products* 70:461-477.

13. Carter GT (2011) Natural products and pharma 2011: strategic changes spur new opportunities. *Natural Product Reports* 28:1783-1789.

14. Hong J (2011) Role of natural product diversity in chemical biology. *Current Opinion in Chemical Biology* 15:350-354.

15. Verdine G (1996) The combinatorial chemistry of nature. *Nature* 384:S11-S13.

16. Nisbet LJ, Moore M (1997) Will natural products remain an important source of drug research for the future? *Current Opinion in Biotechnology* 8:708-12.

17. Ward DM, Weller R, Bateson MM (1990) 16S rRNA sequences reveal numerous uncultured microorganisms in a natural community. *Nature* 345:63-65.

18. Davies J (1999) Millennium bugs. *Trends in Cell Biology* 9:M2-M5.

19. Henkel T, Brunne RM, Müller H, Reichel F (1999) Statistical investigation into the structural complementarity of natural products and synthetic compounds. *Angewandte Chemie* 38:643-647.

20. Bérdy J (2005) Bioactive microbial metabolites. *The Journal of Antibiotics* 58:1-26.

21. Feher M, Schmidt JM (2003) Property distributions: differences between drugs, natural products, and molecules from combinatorial chemistry. *Journal of Chemical Information and Computer Sciences* 43:218-227.

22. Breinbauer R, Vetter IR, Waldmann H (2002) From protein domains to drug candidates - natural products as guiding principles in the design and synthesis of compound libraries. *Angewandte Chemie* 41:2879-2890.

23. Cragg GM, Newman DJ, Snader KM (1997) Natural products in drug discovery and development. *Journal of Natural Products* 60:52-60.

24. Davies J, Ryan KS (2012) Introducing the parvome: bioactive compounds in the microbial world. *ACS Chemical Biology* 7:252-259.

25. Iida M et al. (2008) Three new polyketide−terpenoid hybrids from Penicillium sp. *Organic Letters* 10:845-848.

26. Kawasaki T et al. (2006) Biosynthesis of a natural polyketide-isoprenoid hybrid compound , furaquinocin A□: identification and heterologous expression of the gene cluster. *Journal of Bacteriology* 188:1236-1244.

27. Shen B et al. (2001) The biosynthetic gene cluster for the anticancer drug bleomycin from Streptomyces verticillus ATCC15003 as a model for hybrid peptide-polyketide natural product biosynthesis. *Journal of Industrial Microbiology and Biotechnology* 27:378-385.

28. Bandow JE, Metzler-Nolte N (2009) New ways of killing the beast: prospects for inorganic-organic hybrid nanomaterials as antibacterial agents. *ChemBioChem* 10:2847-2850.

29. Watve MG, Tickoo R, Jog MM, Bhole BD (2001) How many antibiotics are produced by the genus Streptomyces? *Archives of Microbiology* 176:386-390.

30. Gao B, Gupta RS (2012) Phylogenetic framework and molecular signatures for the main clades of the phylum Actinobacteria. *Microbiology and Molecular Biology Reviews* 76:66-112.

31. Hopwood DA (2006) Soil to genomics: the Streptomyces chromosome. *Annual Review of Genetics* 40:1-23.

32. Cole S et al. (1998) Deciphering the biology of Mycobacterium tuberculosis from the complete genome sequence. *Nature* 393:537–544.

33. Baltz RH (2008) Renaissance in antibacterial discovery from actinomycetes. *Current Opinion in Pharmacology* 8:557-63.

34. Kurtböke I (2010) Biodiscovery from microbial resources□: Actinomycetes leading the way. *Microbiology Australia* 31:53-57.

35. Goodfellow M, Fiedler H-P (2010) A guide to successful bioprospecting: informed by actinobacterial systematics. *Antonie van Leeuwenhoek* 98:119-142.

36. Nett M, Ikeda H, Moore BS (2009) Genomic basis for natural product biosynthetic diversity in the actinomycetes. *Natural Product Reports* 26:1362-1384.

37. Kieser T, Bibb MJ, Buttner M, Chater KF, Hopwood DA E(2000) *Practical streptomyces genetics* (The John Innes Foundation Norwich, UK).

38. Manteca A, Alvarez R, Salazar N, Yagüe P, Sanchez J (2008) Mycelium differentiation and antibiotic production in submerged cultures of Streptomyces coelicolor. *Applied and Environmental Microbiology* 74:3877-3886.

39. Flärdh K (2003) Growth polarity and cell division in Streptomyces. *Current Opinion in Microbiology* 6:564-571.

40. Fauci AS (2001) Infectious diseases: considerations for the 21st century. *Clinical Infectious Diseases* 32:675-685.

41. Taubes G (2008) The bacteria fight back. *Science* 321:356-361.

42. IDSA (2004) *Bad Bugs, No Drugs: As Antibiotic R&D Stagnates, a Public Health Crisis Brews* (Oxford University Press).

43. Palanichamy K, Kaliappan KP (2010) Discovery and syntheses of “superbug challengers”-platensimycin and platencin. *Chemistry - An Asian Journal* 5:668-703.

44. Mayers DL (2009) *Antimicrobial Drug Resistance* (Humana Press, Totowa, NJ).

45. Walsh C, Wright G (2005) Introduction: antibiotic resistance. *Chemical Reviews* 105:391-394.

46. Overbye K, Barrett J (2005) Antibiotics: Where did we go wrong? *Drug Discovery Today* 10:45–52.

47. Campbell J, Cronan JE (2001) Bacterial fatty acid biosynthesis: targets for antibacterial drug discovery. *Annual Review of Microbiology* 55:305-332.

48. Gago G, Diacovich L, Arabolaza A, Tsai S-C, Gramajo H (2011) Fatty acid biosynthesis in actinomycetes. *FEMS Microbiology Reviews* 35:475-497.

49. White SWS, Zheng J, Zhang YY-M, Rock C, Rock (2005) The structural biology of type II fatty acid biosynthesis. *Annual Review of Biochemistry* 74:791-831.

50. Jenni S, Leibundgut M, Maier T, Ban N (2006) Architecture of a fungal fatty acid synthase at 5Å resolution. *Science* 311:1263-1267.

51. Maier T, Jenni S, Ban N (2006) Architecture of mammalian fatty acid synthase at 4.5Å resolution. *Science* 311:1258-1262.

52. Wright HT, Reynolds KA (2007) Antibacterial targets in fatty acid biosynthesis. *Current Opinion in Microbiology* 10:447-53.

53. Heath R, White S, Rock C (2001) Lipid biosynthesis as a target for antibacterial agents. *Progress in Lipid Research* 40:467-497.

54. Payne DJ, Warren PV, Holmes DJ, Ji Y, Lonsdale JT (2001) Bacterial fatty-acid biosynthesis: a genomics-driven target for antibacterial drug discovery. *Drug Discovery Today* 6:537-544.

55. Heath R (2004) Fatty acid biosynthesis as a target for novel antibacterials. *Current Opinion in Investigational Drugs* 5:146-153.

56. Ondeyka JG et al. (2006) Discovery of bacterial fatty acid synthase inhibitors from a Phoma species as antimicrobial agents using a new antisense-based strategy. *Journal of Natural Products* 69:377-380.

57. Young K et al. (2006) Discovery of FabH/FabF inhibitors from natural products. *Antimicrobial Agents and Chemotherapy* 50:519-526.

58. Zhang Y-M, White SW, Rock CO (2006) Inhibiting bacterial fatty acid synthesis. *Journal of Biological Chemistry* 281:17541-17544.

59. Brinster S, Lamberet G, Staels B, Trieu-Cuot P, Gruss A (2009) Type II fatty acid synthesis is not a suitable antibiotic target for Gram-positive pathogens. *Nature* 457:83-86.

60. Heath RJ, Su N, Murphy CK, Rock CO (2000) The enoyl-[acyl-carrier-protein] reductases FabI and FabL from Bacillus subtilis. *Journal of Biological Chemistry* 275:40128-40133.

61. Heath RJ, Rock CO (2000) A triclosan-resistant bacterial enzyme. *Nature* 406:145-146.

62. Parsons JB, Rock CO (2011) Is bacterial fatty acid synthesis a valid target for antibacterial drug discovery? *Current Opinion in Microbiology* 14:1-6.

63. Wang J et al. (2007) Discovery of platencin, a dual FabF and FabH inhibitor with in vivo antibiotic properties. *Proceedings of the National Academy of Sciences of the United States of America* 104:7612-7616.

64. Wang J et al. (2006) Platensimycin is a selective FabF inhibitor with potent antibiotic properties. *Nature* 441:358-361.

65. Jayasuriya H et al. (2007) Isolation and structure of platencin: a FabH and FabF dual inhibitor with potent broad-spectrum antibiotic activity. *Angewandte Chemie* 46:4684-4688.

66. Singh SB et al. (2006) Isolation, structure, and absolute stereochemistry of platensimycin, a broad spectrum antibiotic discovered using an antisense differential sensitivity strategy. *Journal of the American Chemical Society* 128:11916-11920.

67. Wu M et al. (2011) Antidiabetic and antisteatotic effects of the selective fatty acid synthase (FAS) inhibitor platensimycin in mouse models of diabetes. *Proceedings of the National Academy of Sciences of the United States of America* 108:5378-5383.

68. Foster DW (2004) The role of the carnitine system in human metabolism. *Annals of the New York Academy of Sciences* 1033:1-16.

69. Rock CO, Jackowski S (2002) Forty years of bacterial fatty acid synthesis. *Biochemical and Biophysical Research Communications* 292:1155-1166.

70. Palanichamy K, Kaliappan KP (2010) Discovery and syntheses of “superbug challengers”-platensimycin and platencin. *Chemistry - An Asian Journal* 5:668-703.

71. Manallack DT, Crosby IT, Khakham Y, Capuano, B (2008) Platensimycin: a promising antimicrobial targeting fatty acid synthesis. *Current Medicinal Chemistry* 15:705-710.

72. Häbich D, von Nussbaum F (2006) Platensimycin, a new antibiotic and “superbug challenger” from nature. *ChemMedChem* 1:951-954.

73. Lu X, You Q (2010) Recent advances on platensimycin: a potential antimicrobial agent. Current Medicinal Chemistry 17:1139-1155.

74. Martens E, Demain AL (2011) Platensimycin and platencin: promising antibiotics for future application in human medicine. The Journal of Antibiotics 64:705-710.

Chapter 2: Bacterial diterpenoid biosynthesis as a source for new natural product diversity

*Content from this chapter has been published previously:

> Smanski MJ, Peterson RM, Huang S-X, Shen B (2012) Bacterial diterpene synthases: new opportunities for mechanistic enzymology and engineered biosynthesis. *Current Opinion in Chemical Biology* 16:132-141.

2.1 Introduction

The discovery of PTM and PTN as first-in-class antibacterial antibiotics, with a mode of action not currently exploited by clinically used antibiotics was a great achievement in natural product drug discovery and an encouraging first step towards addressing a desperate need for novel antibiotic therapies. The characterization of their biosynthetic pathways will provide key advancements in optimizing these lead compounds for therapeutic use. Furthermore, the unique structures of these compounds, products of secondary metabolism in *Streptomyces,* provide opportunities for discovery of novel enzymes and their mechanisms of catalysis, which can ultimately be exploited for engineered biosynthesis, generating further structural diversity. As the following chapters will highlight, PTM and PTN are diterpenoid natural products. This chapter provides a brief overview on the biosynthesis of terpenoid natural products, surveys currently know diterpenoid natural products of bacterial origin, and identifies unique advantages in studying novel bacterial diterpenoid natural products and their biosynthetic machinery.

2.2 Terpenoids and their building blocks

Terpenoids are present in all organisms and often have key metabolic roles. Steroid hormones in mammals, carotenoid pigments in plants, and the electron carrying species, menaquinone, of bacterial anaerobic respiration, are all examples of essential terpenoids (*1*). Terpenoids are also products of secondary metabolism and, ultimately, represent the largest and

most structurally diverse family of natural products with now over 60,000 known terpenoid compounds (*2*). All terpenoids are derived from five-carbon isoprene units, isopentenyl diphosphate (IPP) and dimethylallyl diphosphate (DMAPP), which are condensed consecutively to form linear intermediates with the general formula, $(C_5H_8)_n$ – where n is the number of isoprene units utilized (*3*). Condensation reactions occur in a "head-to-tail" manner: DMAPP aligns its pyrophosphate group (the "head") with the terminal double bond of isopentenyl pyrophosphate (the "tail") where elimination of the pyrophosphate forms a carbocation, which reacts with the isopentenyl double bond. The initial condensation reaction forms a linear, ten-carbon polyprenyl diphosphate intermediate. Additional head-to-tail condensations with IPP, or alternatively, "head-to-head" condensations among advanced intermediates, further elongate these linear chains (*4*). The polyprenyl diphosphate intermediates can then undergo intramolecular cyclization and rearrangement, facilitated by terpene synthases (also referred to as "terpene cyclases"), leading to a multitude of possible scaffolds. These parent terpene scaffolds are categorized into classes according to the number of isoprene units incorporated: monoterpenes (C_{10}), sesquiterpenes (C_{15}), diterpenes (C_{20}), sesterterpenes (C_{25}), and triterpenes (C_{30}). The opportunity for further enzymatic derivatization of these parent scaffolds allows for the enormous, natural diversity of isoprene-derived compounds (*5*).

IPP and DMAPP can be formed by either of two known pathways: the mevalonate pathway and a non-mevalonate pathway. The mevalonate pathway is characterized by formation of mevalonate from three molecules of acetyl-CoA. Mevalonate proceeds through two phosphorylation reactions and decarboxylation to yield IPP, which is isomerized into DMAPP (*6*). The more recently discovered non-mevalonate pathway is characterized by formation of 1-deoxy-D-xylulose 5-phosphate (DXP) from a condensation reaction between pyruvate and

glyceraldehyde 3-phosphate (GA3P), followed by a reduction and isomerization to 2-C-methyl-erythritol 4-phosphate (MEP). MEP can be converted – via five additional enzymatic steps – into IPP and DMAPP (*7*, *8*). Although the mevalonate pathway is considered a major pathway in higher eukaryotes, the non-mevalonate pathway has been found to be essential in plants and some bacteria. Notably, *Streptomyces* contain complete sets of non-mevalonate pathway genes, but components of the mevalonate pathway have been found to contribute to non-essential terpenoid production in some species as well (*1*, *7*). Unfortunately, there is no clear relationship between terpenoid natural product structure and precursor origin (*1*).

2.3 Terpene synthases: mechanisms of intramolecular cyclization and rearrangement

Terpene synthases catalyze the multi-step cyclization cascades responsible for transforming linear, achiral polyprenyl intermediates into unique scaffolds with multiple chiral centers (*5*). The active sites within these enzymes are able to initiate and propagate highly reactive carbocation intermediates required for carbon-carbon bond formation and rearrangements. Furthermore, these enzymes can proceed with high structural and stereochemical precision forming a single product, or they can be naturally promiscuous, producing as many as fifty products from a common substrate (*2*, *9*). Terpene synthases are divided into two classes based on the mechanism they use for initial carbocation formation: type I, or ionization-dependent, and type II, or protonation-dependent. Type I terpene synthases generate reactive carbocation intermediates through a metal-triggered ionization of the substrate diphosphate group, whereas type II terpene synthases utilize protonation of an epoxide ring or carbon-carbon double bond to form a reactive intermediate (**Figure 2.1**). Type I terpene synthases contain two functional sequence motifs, located on separate helices within the protein, which cooperatively bind a trinuclear magnesium cluster responsible for coordinating and

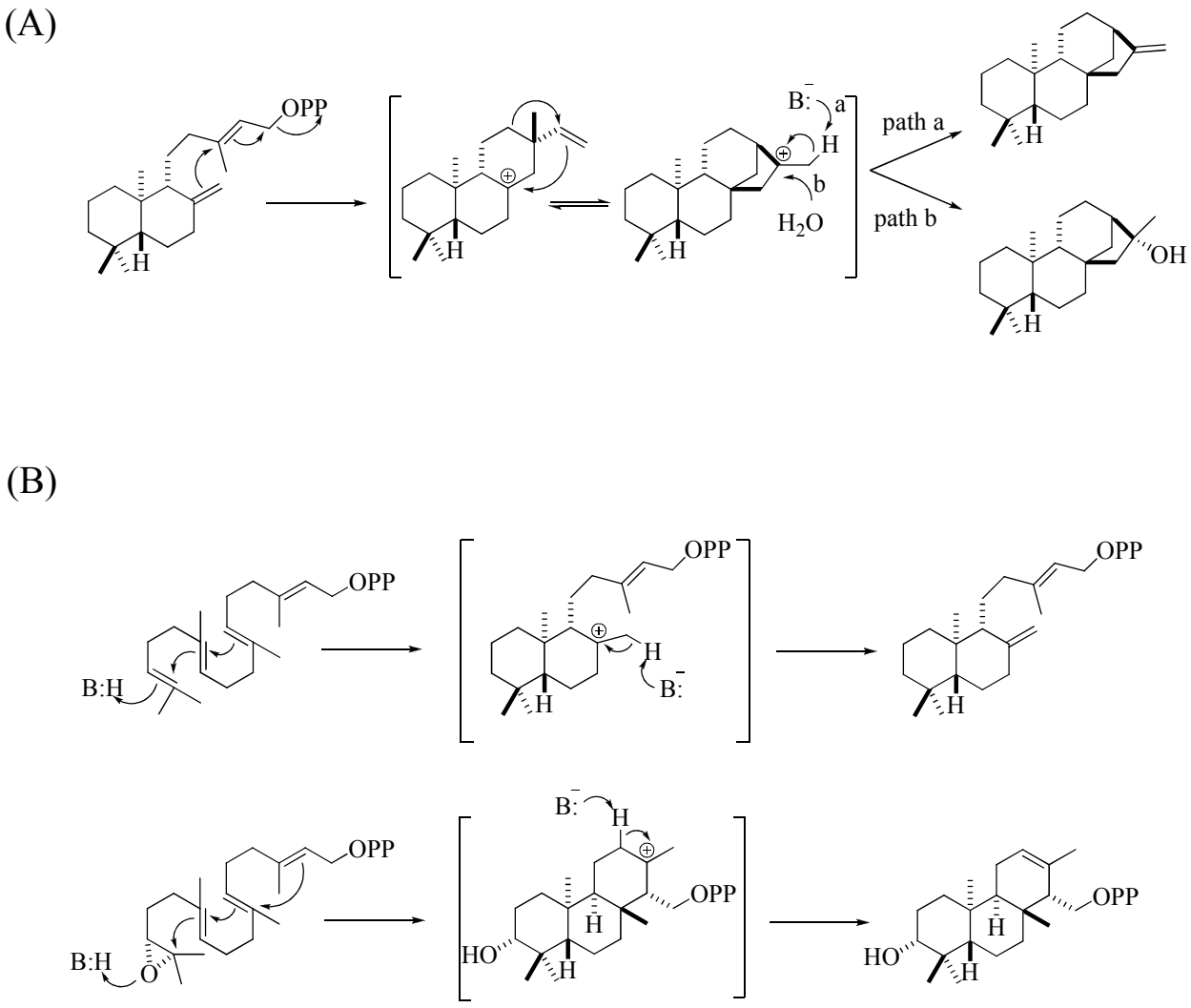

Figure 2.1 – Mechanisms of type I and type II terpene synthases. (A) Ionization of diphosphate-containing substrate leading to carbocation formation, intramolecular cyclization and rearrangements, and quenching of the reactive carbocation by proton abstraction (path a) or electrophilic attack by a water molecule (path b) catalyzed by type I terpene synthases; and (B) protonation of a double bond- (top) or epoxide- (bottom) containing substrate leading to carbocation formation, intramolecular cyclization and rearrangements, and quenching of the reactive carbocation by proton abstraction catalyzed by type II terpene synthases.

triggering ionization of the substrate diphosphate leaving group. The consensus sequences for these two motifs are DDXXD/E, an "aspartate-rich" motif, and (L,V)(V,L,A)(N,D)D(L,I,V)-X(S,T)XXXE, or the "NSE/DTE" motif. Type II terpene synthases contain a single functional motif, with the consensus sequence, DXDD. The central aspartate residue within this motif acts

as a proton donor to an double bond or epoxide ring, triggering carbocation formation (*5*, *10*). The hydrophobic active sites within both type I and type II terpene synthases serve as inert reaction cavities capable of stabilizing transiently formed carbocation intermediates via interactions with the π-systems of amino acid side chains such as phenylalanine, tyrosine, or tryptophan within the active site (*11*). The active site cavity participates both as a template, guiding folding and stabilization of the flexible polyisoprene substrate prior to carbocation formation, and as a chaperone, guiding reactive intermediates through an intricate reaction cascade toward a final product (*5*, *11–14*). Quenching of the carbocation through proton abstraction, or in some cases electrophilic attack by a water molecule, ultimately ends the cyclization cascade (**Figure 2.1**) (*5*, *15*, *16*).

2.4 Diterpenoids and bacteria

Diterpenoid natural products all derive from the same twenty-carbon linear intermediate, (*E*,*E*,*E*)-geranylgeranyl diphosphate (GGDP), which is transformed by diterpene synthases (DTSs) into one of many diverse scaffolds. Diterpenoids have primarily been isolated from plants and fungi and include many medicinally and agriculturally relevant compounds (*17–22*). In particular, an emphasis has been placed on a group of agriculturally relevant compounds called gibberellins (*5*, *23*). Gibberellins (GAs) are tetracyclic diterpenoid acids and have key roles in plant development and physiology: seed germination and emergence, stem and leaf growth, flowering, fruit growth, etc. (*23*, *24*). Over 136 different GAs have been identified from plants and fungi, and their complex roles as phytohormones have encouraged their continued isolation and examination over the past fifty years (*24*). Production of GAs was eventually discovered in the nitrogen-fixing, Gram-negative soil bacteria, *Rhizobium phaesoli*, in 1988, and these compound represent some of the first reported bacterial diterpenoids (*25*). While bacteria

are traditionally excellent sources of diverse natural products, the number of terpenoids – and in particular, diterpenoids – isolated from bacterial sources has been surprisingly limited, and they have not been extensively identified through classical structure-guided or activity-guided screening of bacterial culture extracts (*6*, *26*, *27*). In addition to the discovery of GA production in various bacterial genera (*24*, *25*, *28*), relatively few reports of bacterial diterpenoid natural products have followed in the past twenty-five years (**Figure 2.2**): terpentecin (*Kitasatosporia griseola*, now referred to as *Streptomyces griseolosporeus*, 1985) (*29–31*); UCT4B (*Streptomyces* sp. S-464, 1992) (*32*); verrucosan-2β-ol from (*Chloroflexus aurantiacus*, 1993) (*33*); isoagathenediol (*Rhodospirillum rubrum*, 1995) (*34*); brasilicardins (*Nocardia brasiliensis*, 1999) (*35*); neoverrucosanes (*Saprospira grandis*, 2003) (*36*); phenalinolactones (*Streptomyces sp*. Tu6071, 2006) (*37*); PTM (*Streptomyces platensis*, 2006) (*38*); PTN (*Streptomyces platensis, 2007*) (*39*); viguiepinol and oxaloterpins (*Streptomyces sp*. KO-3988, 2007) (*40*, *41*); cyslabdan (*Streptomyces sp*. K04-0144, 2008) (*42*); cyclooctatin (*Streptomyces melanosporofaciens*, 2009) (*43*); tuberculosinol and isotuberculosinols (*Mycobacterium tuberculosis*, 2009) (*44–47*); the gifhornenolones (*Verrucosispora gifhornesis* YM28-088, 2010) (*48*); and JBIR-65 (*Actinomadura sp.*, 2010) (*49*). Not surprisingly, *Streptomyces* and other actinomycetes are major contributors of bacterial diterpenoid natural products (*1*, *6*, *50*). Rapid advances in technology throughout the past decade have contributed to an increased understanding of the biosynthetic pathways leading to terpenoid production and have provided new access to previously unknown bacterial terpenoid compounds. Furthermore, the rapid development of sequencing technologies, and their application for whole genome sequencing efforts of numerous bacterial genera and species, has revealed the genetic potential for terpenoid production by

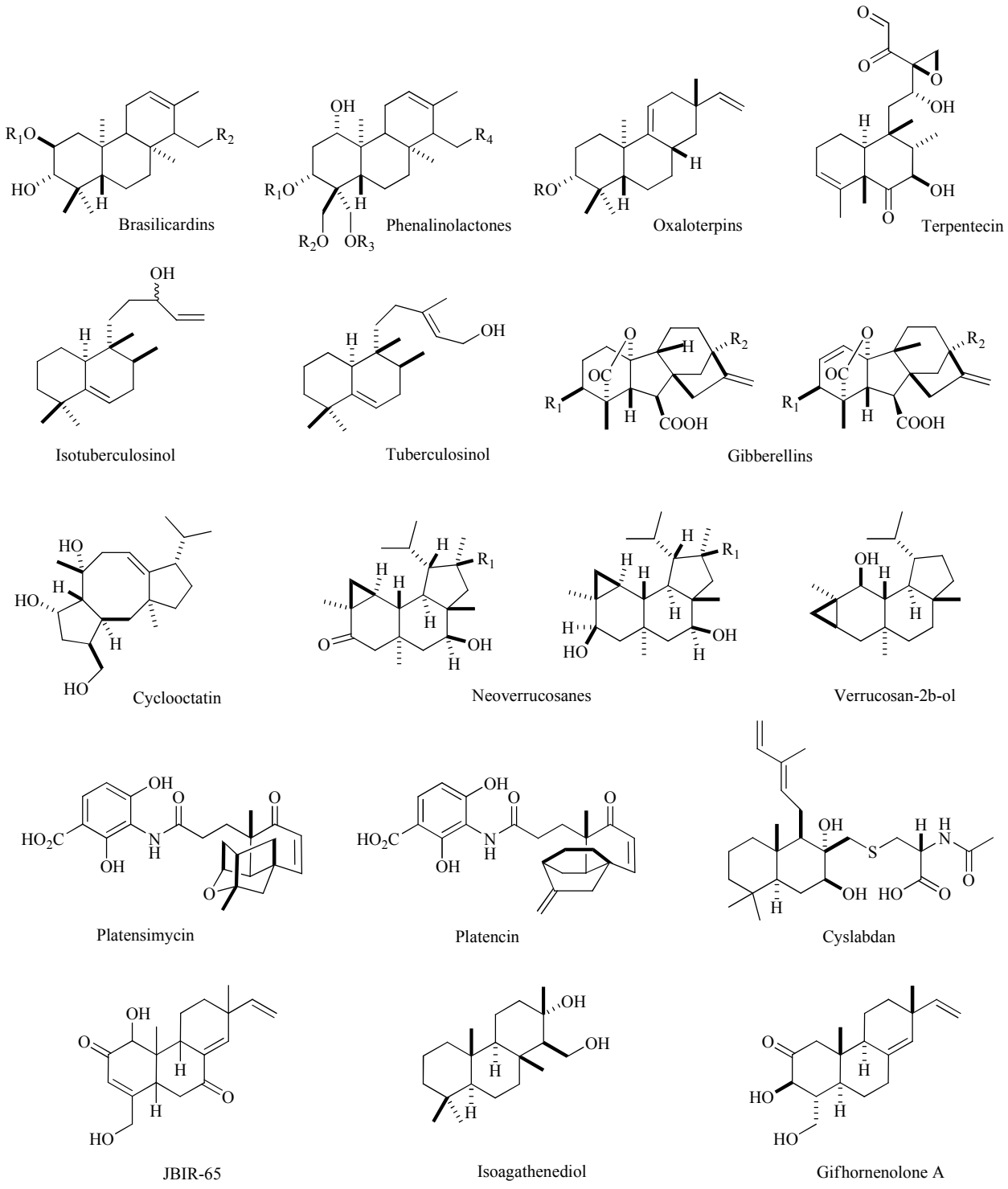

Figure 2.2 – Chemical structures of diterpenoid natural products isolated from bacteria

bacteria (and in particular, actinomycetes) is widespread and likely represents an unexploited source of natural product diversity (*27*, *51*, *52*).

2.5 Bacterial diterpene synthases

The biosynthetic pathways of terpenoid natural products and the catalytic mechanisms of terpene synthases have been mainly described from higher plants and fungi; yet, characterization and manipulation of these pathways and their enzymes remains challenging (*53*, *54*). For example, despite the large number of known diterpenoid compounds (~12,000), relatively few diterpenoid biosynthetic genes have been cloned from plants and fungi (**Table 2.2**). The technical feasibility of isolating typically membrane-bound enzymes from limited natural resources (plant or fungal specimen), or attempting to successfully identify, clone, and recombinantly express genes that are scattered throughout an entire chromosome, has made reconstituting terpenoid biosynthetic pathways from these organisms difficult (*50*). In contrast, the unique phenomenon of genes encoding secondary metabolism in bacteria nearly always being arranged on the chromosome as a "cluster" of biosynthetic genes exemplifies an immediate advantage for studying terpenoid pathways from bacteria (*52*, *55*). The recent characterization of several DTSs and their pathways from actinomycetes and other bacterial genera (**Table 2.1, Figure 2.3**) has demonstrated the utility of studying bacterial diterpenoid biosynthesis. These studies suggest that bacteria offer new opportunities for discovery of novel compounds, characterization of unique enzymes, and ultimately, straightforward platforms for combinatorial engineering efforts to further increase terpenoid structural diversity (*52*).

The first bacterial DTSs to be reported were a terpentedienyl diphosphate synthase (a type II DTS) and a terpentetriene synthase (a type I DTS), two essential enzymes for

Table 2.1 – Summary of reported bacterial diterpene synthases

Organism	Enzyme(s)	Protein Accession Number	Substrate	Product	Final Natural Product
Mycobacterium tuberculosis	Rv3377c	NP_217894	GGDP	halimadienyl diphosphate	(13R,13S)-Isotuberculosinol, Tuberculosinol
Bradyrhizobium japonicum, *Streptomyces sp.* KO-3988	Blr2149 (BjCPS), ORF2	BAC47414, BAD86797	GGDP	*ent*-copalyl diphosphate	Gibberellins, Oxaloterpins
Streptomyces melanosporofaciens MI614-43F2	CotB2	BAI44338	GGDP diphosphate	cyclooctat-9-en-7-ol	Cyclooctatin
Streptomyces griseolosporeus	Cyc1 (ORF11)	BAB39206	GGDP	terpentedienyl diphosphate	Terpentecin
Nocardia brasiliensis IFM 0406	Bra4	BAG16278	(epoxy-GGDP)	(unknown)	Brasilicardin A
Streptomyces sp. Tu6071	PlaT2	ABB69743	(epoxy-GGDP)	(unknown)	Phenalinolactone A
Bradyrhizobium japonicum	Blr2150 (BjKS)	BAC47415	ent-CPP	*ent*-kaurene	Gibberellins
Streptomyces sp. KO-3988	ORF3	BAD86798	ent-CPP	pimara-9(11),15-diene	Oxaloterpins
Mycobacterium tuberculosis	Rv3378c	NP_217895	halimadienyl diphosphate	(13R,13S)-isotuberculosinol, tuberculosinol	(13R,13S)-Isotuberculosinol, Tuberculosinol
Streptomyces griseolosporeus	Cyc2 (ORF12)	BAB39207	terpentedienyl diphosphate	terpentetriene	Terpentecin

terpentecin production in *S. griseolosporeus* (**Figure 2.3**) (*30*, *31*). Bioinformatics analysis of the putative terpentedienyl diphosphate synthase (Cyc1/ORF11) in *S. griseolosporeus* revealed low sequence similarity with N-terminal regions of characterized eukaryotic DTSs responsible for type II DTS activity: *Phaeosphaeria sp*. FCPS/KS, 29% identity over 494 amino acids; and *Gibberella fujikuroi* GfCPS/KS, 27% identity over 444 amino acids. However, the presence of the conserved type II, aspartate-rich DXDD motif corroborated its initial functional assignment as a type II DTS, which was ultimately confirmed *in vitro* (*30*, *56*). Similarly, the terpentetriene synthase (Cyc2/ORF12) was predicted to be a type I DTS prior to *in vitro* characterization, based not only on modest sequence similarity to a previously characterized bacterial type I sesquiterpene synthase (*Streptomyces sp*. UC5319 pentalenene synthase, 25% sequence identity over 331 amino acids), but by the presence of the characteristic type I metal-binding "DDXXD" and "NSE/DTE" motifs (*30*, *31*, *57*).

Five type II bacterial DTSs, contributing to unique bacterial diterpenoid biosynthetic pathways, have been reported since the DTSs responsible for terpentecin production were reported in 2001 (**Table 2.1, Figure 2.3**). Three of these type II bacterial DTSs (halimadienyl diphosphate synthase, Rv3377c, from *Mycobacterium tuberculosis*; and ent-copalyl diphosphate synthases, ORF2 and BjCPS, from *Streptomyces. sp*. KO-3988 and *Bradyrhizobium japonicum*, respectively) contain characteristic DXDD motifs and convert GGDP into bicyclic, diphosphate-containing scaffolds, which serve as substrates for further cyclization by type I DTSs (*40*, *41*, *44–47*, *58*). Interestingly, two type II DTSs (Bra4, from *Nocardia brasilensis*; and PlaT2, from *Streptomyces sp.* Tu6071), responsible for brasilicardin and phenalinolactone production, respectively, contain atypical catalytic motifs: (E/D)SA(E/N) replaces the canonical type II DXDD motif. Furthermore, an additional gene, adjacent to Bra4 or PlaT2 in each of their

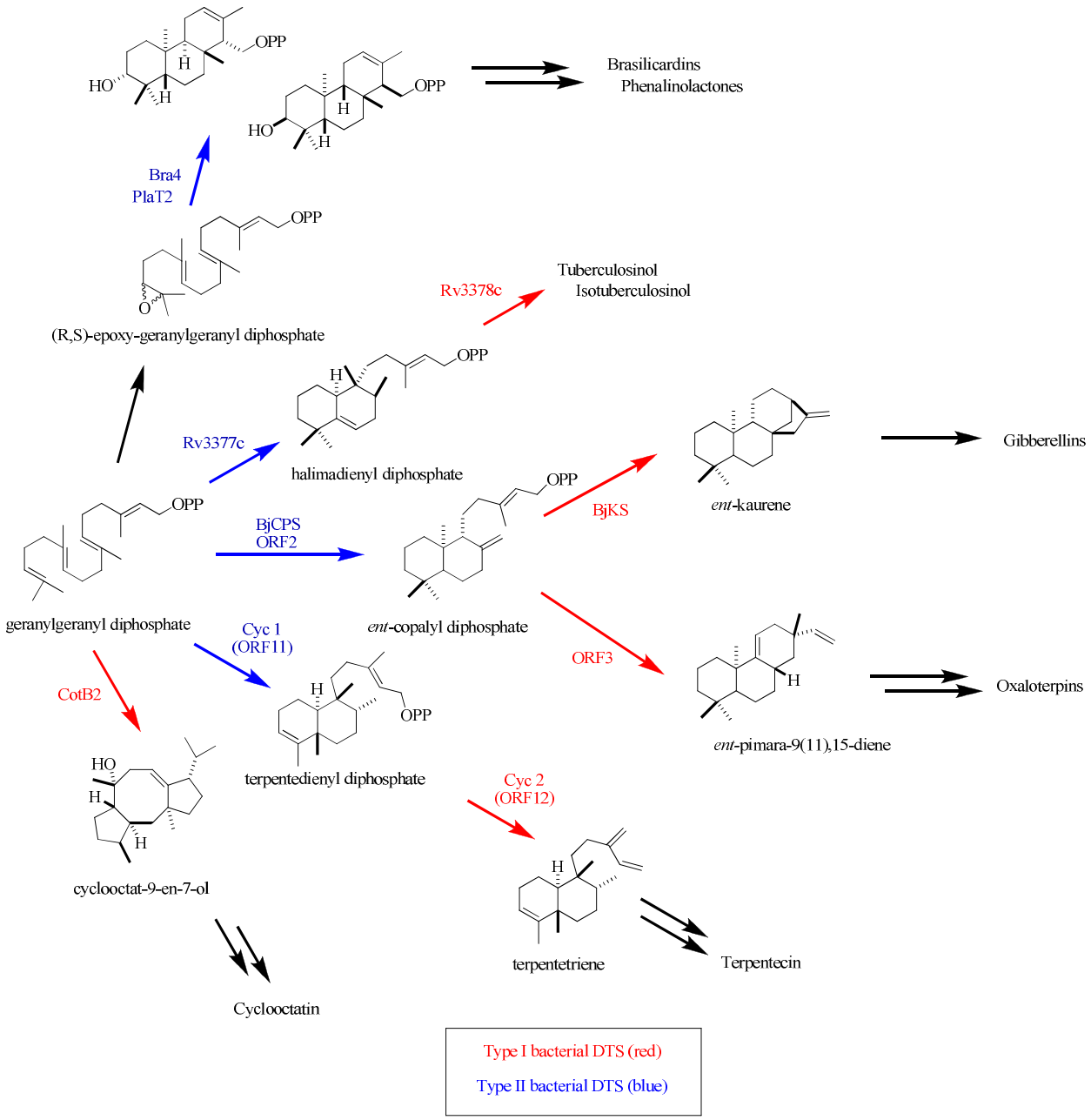

Figure 2.3 – Biosynthetic pathways of known bacterial diterpenoid natural products. Each diterpenoid is derived from a common twenty-carbon linear diterpene intermediate, geranylgeranyl diphosphate (GGDP), and cyclized by the action of type II (blue) and/or type I (red) diterpene synthases. See **Figure 2.2** for chemical structures of final diterpenoid products.

respective clusters, is homologous to eukaryotic squalene epoxidase and is predicted to convert GGDP to epoxy-GGDP. Although complete *in vitro* characterizations have not yet been reported, Bra4 and PlaT2 are expected to be non-canonical type II DTSs, acting on an epoxy-GGDP substrate and initiating carbocation formation through protonation of an epoxide rather than a double bond, a type II mechanism more commonly seen in plant triterpenoid biosynthesis from squalene (**Figure 2.1**) (*59–61*). A minimum evolution phylogentic tree highlights the sequence diversity displayed among each of these bacterial type II DTSs and in comparison to their homologs in plants and fungal species (**Figure 2.5**).

Additionally, four type I bacterial DTSs have been reported: ent-kaurene synthase, BjKS, from *Bradyrhizobium japonicum;* pimaradiene synthase, ORF3, from *Streptomyces. sp*. KO-3988; tuberculosinol/isotuberculosinol synthase, Rv3378c, from *Mycobacterium tuberculosis*; and cyclooctatenol synthase, CotB2, from *S. melanosporofaciens* (**Table 2.1**) (*43*, *46*, *58*, *62*). Primary sequence comparison among these first five type I bacterial DTSs reveals a surprising level of sequence diversity: pairwise alignment averages just 12.5% sequence identity. The diversity among type I bacterial DTSs compared with that among plant and fungal type DTSs is apparent on a minimum evolution phylogentic tree (**Figure 2.4**) by the profound branching of individual bacterial type I DTSs. Sequence similarity among DTSs, even those acting on identical substrates, is characteristically low compared with that seen among homologs in other classes of biosynthetic enzymes: average pairwise identity among plant and fungal type I DTSs is just 28% and 25%, respectively. Yet, continued discovery and characterization of novel DTS enzymes and the scaffolds they produce, will increase our understanding of how primary sequence and structural variation contribute to diterpenoid product diversity.

2.6 Evolutionary relationship between bacterial and eukaryotic DTSs

A number of structures for type I and type II terpene synthases of bacterial, fungal, or plant origin have now been reported; however, no structure of a bacterial DTS has been solved (*2*, *5*, *63*, *64*). Yet, these studies coupled with detailed bioinformatic analyses of bacterial DTSs now provide insight into DTS evolution. Bacterial type II DTSs are homologous to bacterial triterpene synthases, such as squalene-hopene synthase, and primary sequence alignments suggest a conservation of overall topology and active site location (*65*, *66*). Furthermore, bacterial type II DTSs are hypothesized to contain the same βγ-didomain structure deriving from an ancient duplication of two $(\alpha/\alpha)_6$ barrels (*66*). Bacterial type I DTSs are predicted to have a single α-domain "isoprenoid fold" based on primary sequence alignments to the bacterial type I sesquiterpene synthases, pentalenene synthase and epi-isozizaene synthase – both from *Streptomyces* species. (*67–69*). Ancestral bifunctional plant DTSs, containing a αβγ-tridomain and catalyzing both types of TS mechanisms but in separate active sites, likely evolved from an early fusion of bacterial type I (α) and II (βγ) enzymes. These tridomain DTSs are still observed: in the bifunctional ent-kaurene synthase from the moss, *Physcomitrella patens,* or the bifunctional abietadiene synthase from *Abies grandis* (*70, 71*). Furthermore, monofunctional type I or type II DTSs found in plants often retain vestigial domains from apparent ancestral enzymes, and while lacking functional active site motifs, these domains likely remain for structural support (*63*, *64*, *72*). The ancient roots of bacterial DTSs might explain the greater sequence diversity observed in these enzymes (**Figures 2.4 and 2.5**), but more importantly, these predictions reveal key insights into studying the structural and mechanistic features of unique bacterial DTS enzymes.

2.7 Discovery of novel bacterial diterpenoid natural products and DTSs responsible for their unique scaffolds

Low sequence similarity among bacterial DTSs presents difficulties for attempting conventional sequence-based strategies for identifying new DTS enzymes. Yet, identification of bacterial DTSs can be facilitated if they are adjacent to more recognizable/conserved terpene biosynthetic genes, such as those involved in the mevalonate pathway (*30*, *73*). The biosynthetic gene clusters responsible for bacterial diterpenoid natural products have also been identified by screening for predicted genes contributing to biosynthesis of other structural moieties in the final structure or tailoring modifications (*37*, *58*, *74*, *75*). Finally, the utilization of the common substrate GGDP and the synthases responsible for its production can be exploited as a probe for discovering novel diterpenoid biosynthetic clusters (*76*). Each of these methods has provided novel bacterial DTS enzymes for study and characterization. By optimizing methods for recognizing new members of bacterial DTSs, we can further expand the structural and catalytic landscape of terpenoid natural products. The efforts described in the following chapters to characterize platensimycin (PTM) and platencin (PTN) biosynthesis serve as a model for discovery and characterization new bacterial DTSs and not only expand the sequence diversity associated with DTSs, but contribute towards efforts for identification of novel DTSs and their associated natural products.

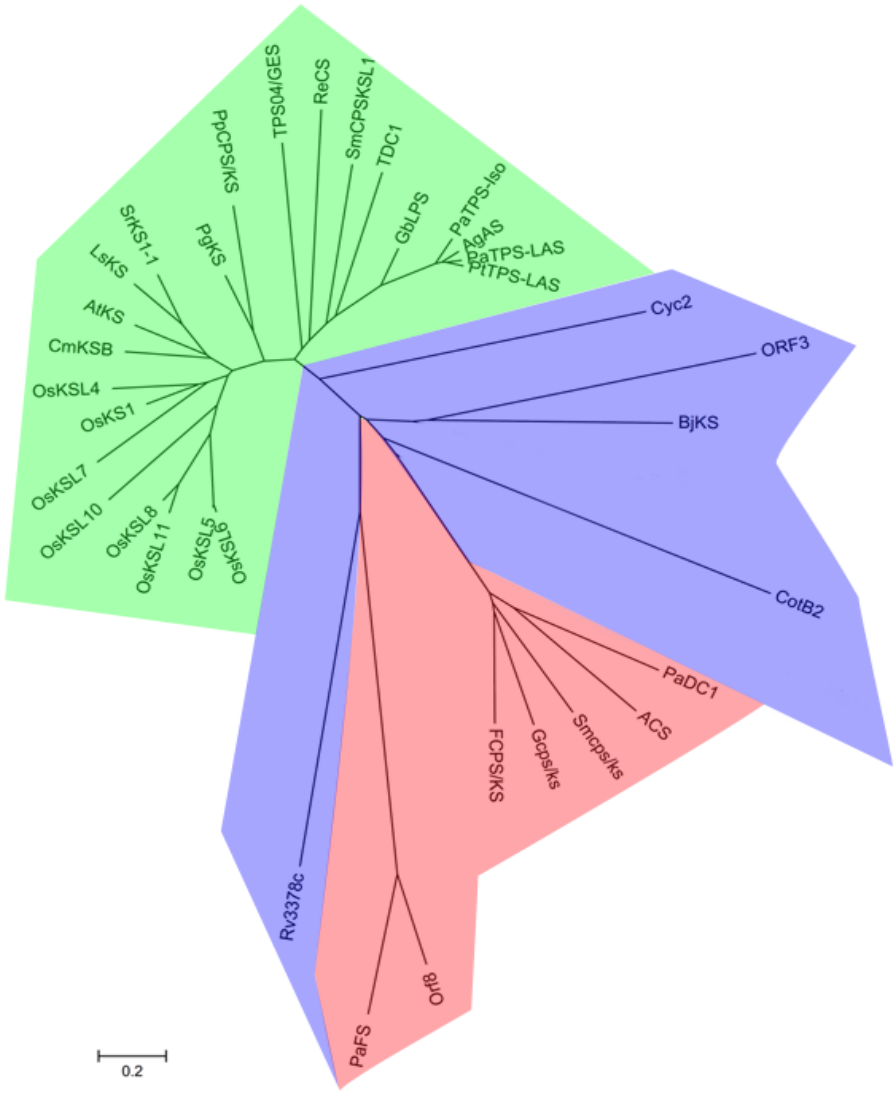

Figure 2.4 – Minimum evolution tree of primary amino acid sequences of type I DTSs from plants (green), fungi (red), and bacteria (blue). Trees were generated using CLUSTALW alignments (*77*). The branch lengths represent the extent of sequence diversity found in bacterial DTSs compared with enzymes in plants and fungi. Names and accession numbers of the DTS enzymes compared are listed below: Bacterial type I DTSs: Cyc2 (BAB39207), ORF3 (BAD86798), BjKS (BAC47415), PtmT3 (ACO31279), CotB2 (BAI44338), and Rv3378 (P_217895); Fungal type I DTSs: PaDC1 (BAG30961), ACS (BAB62102), Smcps/ks (CAP07655), Gfcps/ks (Q9UVY5), FCPS/KS (BAA22426), Orf8 (bsc8) (BAI44849), and PaFS (BAF45925); Plant type I DTSs: OsKSL6 (ABH10733), OsKSL5 (ABH10732), OsKSL11 (AAZ76733), OsKSL8 (BAD34478), OsKSL10 (ABH10735), OsKSL7 (ABH10734), OsKS1 (AAQ72559), OsKSL4 (AAU05906), CmKSB (AAB39482), AtKS (AAC39443), LsKS (BAB12441), SrKS1-1 (AF097310_1), PgKS (ADB55708), PpCPS/KS (BAF61135), TPS04/GES (NP_564772), RcCS (XP_002513340), SmCPSKSL1 (AEK75338), TDC1 (AAC49310), GbLPS (AAL09965), PaTPS-Iso (AAS47690), AgAS (Q38710), PaTPS-LAS (AAS47691), and PtTPS (AAX07435).

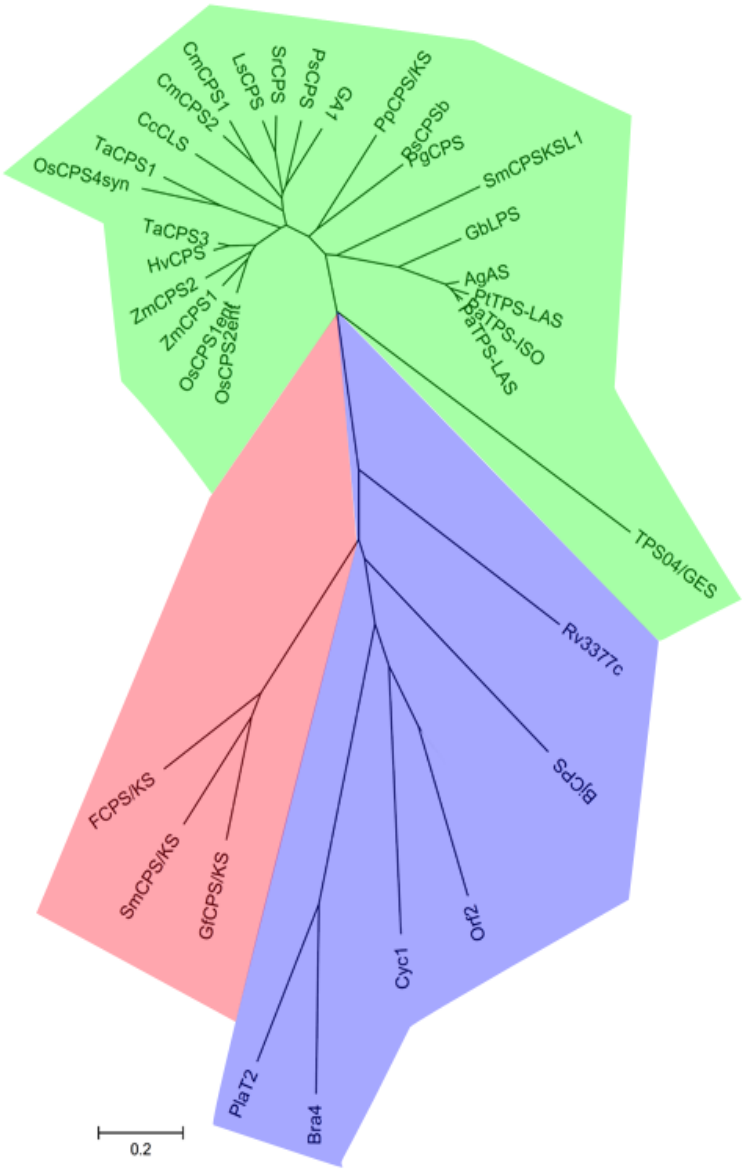

Figure 2.5 – Minimum evolution tree of primary amino acid sequences of type II DTSs from plants (green), fungi (red), and bacteria (blue). Trees were generated using CLUSTALW alignments (*77*). The branch lengths represent the extent of sequence diversity found in bacterial DTSs compared with enzymes in plants and fungi. Names and accession numbers of the DTS enzymes compared are listed below: Bacterial type II DTSs: Rv3377c (NP_217894), BjCPS (BAC47414), Orf2 (BAD86797), Cyc1 (BAB39206), Bra4 (BAG16278), and PlaT2 (ABB69743); Fungal type II DTSs: FCPS/KS (BAA22426), SmCPS/KS (CAP07655), and GfCPS/KS (Q9UVY5); Plant type II DTSs: OsCPS1ent (BAD42449), OsCPS2ent (Q6ET36), ZmCPS1 (AAT49065), ZmCPS2 (ADB55709), HvCPS (BAH56560), TaCPS3 (AAT70083), OsCPS4syn (NP_0010521), TaCPS1 (BAH56558), CcCLS (ADJ93862), CmCPS1 (AAD04292), CmCPS2 (AAD04923), LsCPS (BAB12440), SrCPS (AAB87091), PsCPS (AAB58822), GA1 (AAA53632), PpCPS/KS (BAF61135), PsCPSb (ADB55709), PgCPS (ADB55707), GbLPS (AAL09965), AgAS (Q38710), PtTPS-LAS (AAX07435), PaTPS-ISO (AAS47690), PaTPS- LAS (AAS47691), SmCPSKSL1 (AEK75338), and TPS04/GES (NP_564772).

Table 2.2 – Summary of characterized plant and fungal DTSs (*16*, *70*, *76*, *78–102*)

Organism(s)	Enzyme(s)	Accession Number	Substrate(s)	Product	Final NP
Phoma betae	ACS	BAB62102	*syn*-CPP	aphidicolan-16-ol	Aphidicolin
P. betae	ACS	BAB62102	*syn*-CPP	aphidicol-16-ene	Aphidicolin
Oryza sativa	OsKSL4	AAU05906	*syn*-CPP	*syn*-pimara-7,15-diene	Momilactones
O. sativa	OsKSL8	BAD34478	*syn*-CPP	*syn*-stemar-13-ene	Oryzalexins
O. sativa	OsKSL11	AAZ76733	*syn*-CPP	*syn*-stemod-13(17)-ene	-
Phomopsis amygdali	PaDC1	BAG30961	(+)-CPP	(+)-kaurene	-
P. amygdali	PaDC1	BAG30961	(+)-CPP	(+)-phyllocladene	-
P. amygdali	PaDC1	BAG30961	(+)-CPP	pimara-8,15-diene	-
P. amygdali	PaDC1	BAG30961	(+)-CPP	(+)-isopimar-8,15-diene	-
P. amygdali	PaDC1	BAG30961	(+)-CPP	phyllocaldan-16-ol	-
P. amygdali	PaDC1	BAG30961	(+)-CPP	(+)-pimara-8(14),15-diene	-
P. amygdali, Abies grandis	PaDC1, AgAS	BAG30961, Q38710	(+)-CPP, GGDP/(+)-CPP	sandaracopimar-8(14),15-diene	-
A. grandis, Picea abies, Pinus taeda	AgAS, PaTPS-LAS, PtTPS-LAS	Q38710, AAS47691, AAX07435	GGDP/(+)-CPP	abieta-8(14),13(15)-diene (neoabietadiene)	-
A. grandis, P.abies, P. taeda	AgAS, PaTPS-LAS, PtTPS-LAS	Q38710, AAS47691, AAX07435	GGDP/(+)-CPP	abieta-7,13-diene (abietadiene)	-
P. abies, P. taeda	PaTPS-LAS, PtTPS-LAS	AAS47691, AAX07435	GGDP/(+)-CPP	abieta-8-13-diene (palustradiene)	-
A.grandis, Ginkgo biloba, P. abies, P. taeda	AgAS, GbLPS, PaTPS-LAS, PtTPS-LAS	Q38710, AAL09965, AAS47691, AAX07435	GGDP/(+)-CPP	abieta-8(14),12-diene (levopimaradiene)	Ginkgolides
A. grandis, P. abies	AgAS, PaTPS-Iso	Q38710, AAS47690	GGDP/(+)-CPP	isopimar-7,15-diene	-
Physcomitrella patens	PpCPS/KS	BAF61135	GGDP/ent-CPP	*ent*-16-hydroxy-kaurene	-

Table 2.2 – (continued)

O. sativa	OsKSL5	ABH10732	*ent*-CPP	*ent*-pimara-8(14),15-diene	-
O. sativa	OsKSL6	ABH10733	*ent*-CPP	*ent*-(iso)kaur-15-ene	-
O. sativa	OsKSL7	ABH10734	*ent*-CPP	*ent*-cassa-12,15-diene	Phytocassanes
O. sativa	OsKSL10	ABH10735	*ent*-CPP	*ent*-sandaracopimara-8(14),15-diene	Oryzalexins
O. sativa, P. patens, Phaeosphaeria sp. L487, Gibberella fujikuroi, Stevia rebaudiana, Cucurbita maxima, Arabidopsis thaliana, Lactuca sativa, Sphaceloma manihoticola, Picea glauca, Picea sitchensis	OsKS1, PpCPS/KS, FCPS/KS, Gfcps/ks, SrKS1-1, SrKS22-1, CmKSB, AtKS, LsKS, Smcps/ks, PgKS, PsKS	AAQ72559, BAF61135, BAA22426, Q9UVY5, AF097310_1, AAB39482, AAC39443, BAB12441, CAP07655, ADB55708, ADB55710	*ent*-CPP, GGDP/*ent*-CPP	*ent*-kaur-16-ene	Gibberellins
Pseudopterogorgia elisabethae	ELS	-	GGDP	elisabethatriene	Pseudopterosins
O. sativa, S. rebaudiana, C. maxima, A. thaliana, L. sativa, Triticum aestivum, Hordeum vulgare, Pisum sativum, Zea mays, P. glauca, P. sitchensis	OSCPS1/2ent, SrCPS, CmCPS1/2, GA1, LsCPS, TaCPS1-3, HvCPS, PsCPS, ZmCPS1/ZmCPS2, PgCPS, PsCPS	AK10033/AY602991, AF034545, AAD04292/AAD04293, U11034, AB031204, AB439588-AB439590, AAT49065, AAB58822, AAA73960/AAT70083, ADB55707, ADB55709	GGDP	*ent*-copalyl diphosphate	-
O. sativa	OsCPS4syn	AY530101	GGDP	*syn*-copalyl diphosphate	-

Table 2.2 – (continued)

P. amygdali, A. grandis, G. biloba, P. abies, P. taeda	PaDC2, AgAS, GbLPS, PaTPS-LAS, PtTPS-LAS	AB252835, Q38710, AF331704, AY473621, AY779541	GGDP	(+)-copalyl diphosphate/labdadienyl diphosphate	-
Taxus brevifolia	TDC1	AAC49310	GGDP	taxa-4(20),11(12)-diene	-
T. brevifolia	TDC1	AAC49310	GGDP	taxa-4(5),11(12)-diene	Paclitaxel
T. brevifolia	TDC1	AAC49310	GGDP	taxa-3(4),11(12)-diene	-
A. thaliana	TPS04/GES	NP_564772	GGDP	geranyllinalool	(E,E)-4,8,12-trimethyltrideca-1,3,7,11-tetraene (TMTT)
Selaginella moellendorffii	SmCPSKSL1	AEK75338	GGDP	labda-7,13E-dien-15-ol	-
Cistus creticus	CcCLS	ADJ93862	GGDP	labd-13-ene-8a,15-diol (copal-8-ol)	-
Ricinus communis	RcCS	XP_002513340	GGDP	casbene	-
P. amygdali, Alternaria brassicicola	PaFS, Orf8	BAF45925, BAI44849	GGDP, IPP+DMAPP/GGDP	fusicocca-2,10(14)-diene	Brassicicene, Fusicoccin, Cotylenin

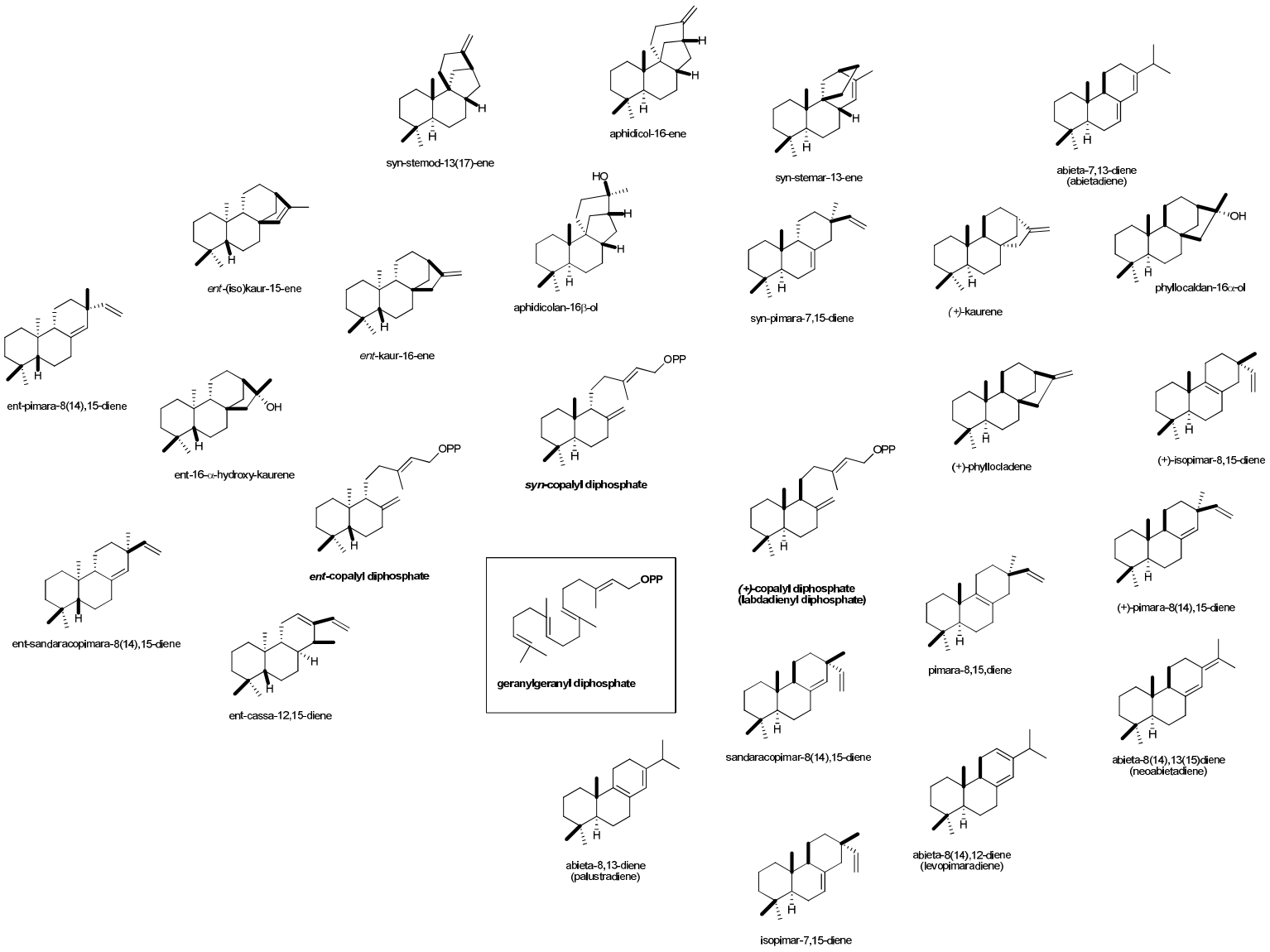

Figure 2.6 – Diterpene scaffolds isolated from plant and fungal organisms – Part I (see Table 2.2)

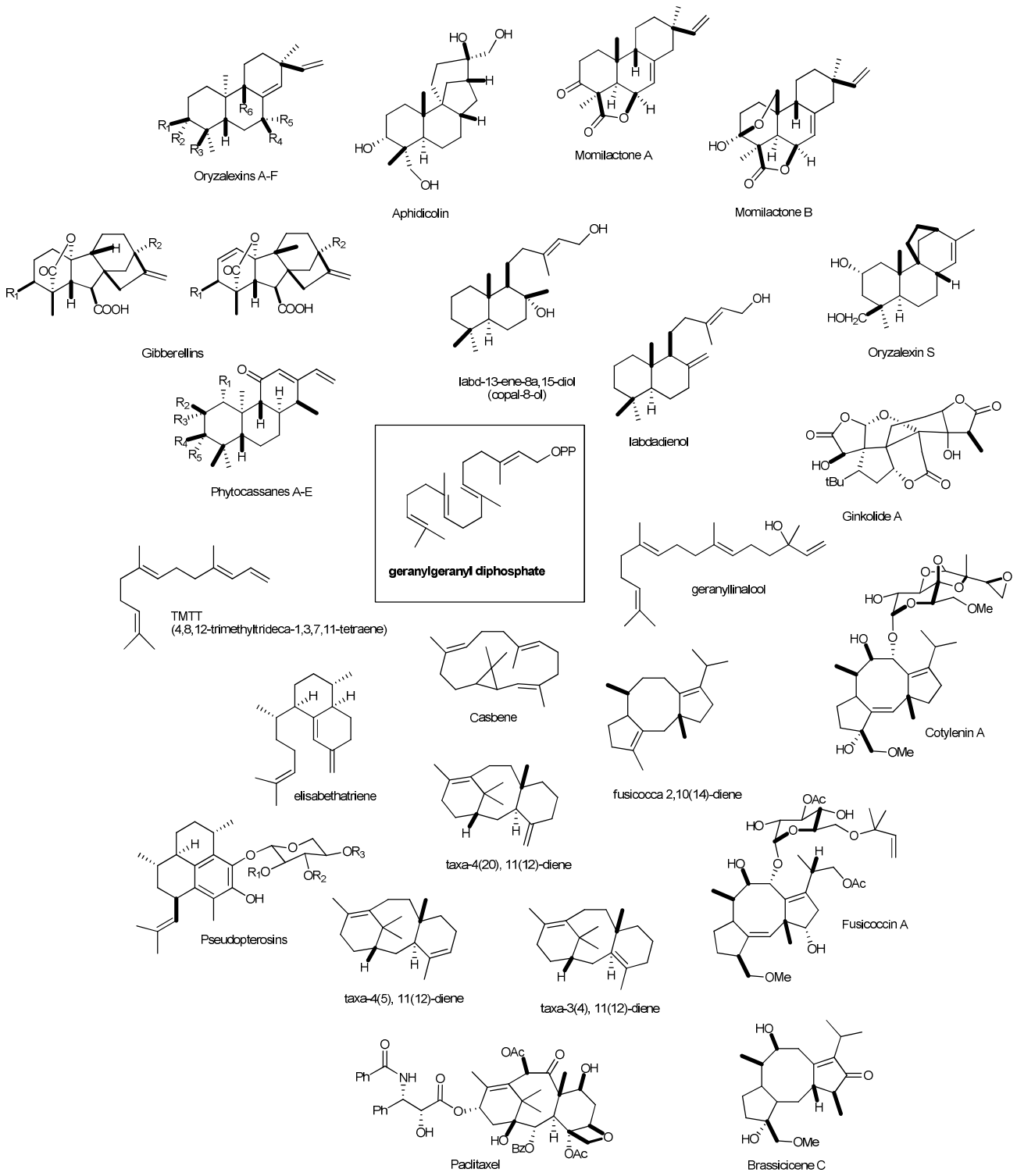

Figure 2.7 – Diterpenoid scaffolds isolated from plant and fungal organisms – Part II (see Table 2.2)

2.8 References

1. Kuzuyama T, Seto H (2003) Diversity of the biosynthesis of the isoprene units. *Natural Product Reports* 20:171-183.

2. Christianson DW (2008) Unearthing the roots of the terpenome. *Current Opinion in Chemical Biology* 12:141-150.

3. Ruzicka L (1953) The isoprene rule and the biogenesis of terpenic compounds. *Cellular and Molecular Life Sciences* 9:357-367.

4. Oldfield E, Lin F-Y (2012) Terpene biosynthesis: modularity rules. *Angewandte Chemie* 51:1124-37.

5. Christianson DW (2006) Structural biology and chemistry of the terpenoid cyclases. *Chemical Reviews* 106:3412-3442.

6. Daum M, Herrmann S, Wilkinson B, Bechthold A (2009) Genes and enzymes involved in bacterial isoprenoid biosynthesis. *Current Opinion in Chemical Biology* 13:180-188.

7. Eisenreich W, Bacher A, Arigoni D, Rohdich F (2004) Biosynthesis of isoprenoids via the non-mevalonate pathway. *Cellular and Molecular Life Sciences* 61:1401-1426.

8. Rohmer M (1999) The discovery of a mevalonate-independent pathway for isoprenoid biosynthesis in bacteria, algae and higher plants. *Natural Product Reports* 16:565-574.

9. Steele CL, Crock J, Bohlmann J, Croteau R (1998) Sesquiterpene synthases from grand fir (Abies grandis). *Journal of Biological Chemistry* 273:2078-2089.

10. MacMillan J, Beale M (1999) in *Comprehensive Natural Products Chemistry: Isoprenoids including carotenoids and steroids*, ed Nakanishi K (Elsevier), pp 217-241.

11. Lesburg C, Caruthers J, Paschall C, Christianson DW (1998) Managing and manipulating carbocations in biology: terpenoid cyclase structure and mechanism. *Current Opinion in Structural Biology* 8:695–703.

12. Jenson C, Jorgensen WL (1997) Computational investigations of carbenium ion reactions relevant to sterol biosynthesis. *Journal of the American Chemical Society* 119:10846-10854.

13. Tantillo D (2011) Biosynthesis via carbocations: theoretical studies on terpene formation. *Natural Product Reports* 28:1035-1053.

14. Tantillo DJ (2010) The carbocation continuum in terpene biosynthesis--where are the secondary cations? *Chemical Society Reviews* 39:2847-2854.

15. Kawaide H et al. (2011) Identification of the single amino acid involved in quenching the ent-kauranyl cation by a water molecule in ent-kaurene synthase of Physcomitrella patens. *FEBS Journal* 278:123-133.

16. Mafu S, Hillwig ML, Peters RJ (2011) A novel labda-7,13-dien-15-ol-producing bifunctional diterpene synthase from Selaginella moellendorffii. *ChemBioChem* 12:1984-7.

17. Kingston D, Newman D (2007) Taxoids: cancer-fighting compounds from nature. *Current Opinion in Drug Discovery & Development* 10:130-144.

18. Greay SJ, Hammer K a. (2011) Recent developments in the bioactivity of mono- and diterpenes: anticancer and antimicrobial activity. *Phytochemistry Reviews* in press (available online).

19. Brahmachari G, Mandal LC, Roy R, Mondal S, Brahmachari AK (2011) Stevioside and related compounds - molecules of pharmaceutical promise: a critical overview. *Archiv der Pharmazie* 344:5-19.

20. Klayman D (1985) Qinghaosu (artemisinin): an antimalarial drug from China. *Science* 228:1049-1055.

21. Klayman DL et al. (1984) Isolation of artemisinin (qinghaosu) from Artemisia annua growing in the United States. *Journal of Natural Products* 47:715-717.

22. Puri M, Sharma D, Tiwari AK (2011) Downstream processing of stevioside and its potential applications. *Biotechnology Advances* 29:781-791.

23. Hedden P, Kamiya Y (1997) Gibberellin biosynthesis: enzymes, genes and their regulation. *Annual Review of Plant Physiology and Plant Molecular Biology* 48:431-460.

24. Bottini R, Cassán F, Piccoli P (2004) Gibberellin production by bacteria and its involvement in plant growth promotion and yield increase. *Applied Microbiology and Biotechnology* 65:497-503.

25. Atzorn R, Crozier A, Wheeler C, Sandberg G (1988) Production of gibberellins and indole-3-acetic acid by Rhizobium phaseoli in relation to nodulation of Phaseolus vulgaris roots. *Planta* 175:532–538.

26. Kuzuyama T, Seto H (2003) Diversity of the biosynthesis of the isoprene units. *Natural Product Reports* 20:171-183.

27. Cane DE, Ikeda H (2012) Exploration and mining of the bacterial terpenome. *Accounts of Chemical Research* 45:463-472.

28. Gutierrez-Manero FJ et al. (2001) The plant-growth-promoting rhizobacteria Bacillus pumilus and Bacillus licheniformis produce high amounts of physiologically active gibberellins. *Physiologia Plantarum* 111:206-211.

29. Tamamura T et al. (1985) Isolation and characterization of terpentecin, a new antitumor antibiotic. *The Journal of Antibiotics* 38:1664-1669.

30. Dairi T et al. (2001) Eubacterial diterpene cyclase genes essential for production of the isoprenoid antibiotic terpentecin. *Journal of Bacteriology* 183:6085-6094.

31. Hamano Y et al. (2002) Functional analysis of eubacterial diterpene cyclases responsible for biosynthesis of a diterpene antibiotic, terpentecin. *The Journal of Biological Chemistry* 277:37098-37104.

32. Kawada S et al. (1995) Terpentecin and ECT4B, new family of topoisomerase II targeting antitumor antibiotics produced by Streptomyces: producing organism, fermentation and large scale purification. *The Journal of Antibiotics* 48:211-216.

33. Hefter J, Richnow H, Fischer U (1993) (-)-Verrucosan-2beta-ol from the phototrophic bacterium Chloroflexus aurantiacus: first report of a verrucosane-type diterpenoid from a prokaryote. *Journal of General Microbiology* 139:2757-2761.

34. Chuck J-A, Barrow KD (1995) The isolation of isoagathenediol: a new tricyclic diterpene from the lipids of Rhodospirillum rubrum. *Microbiology* 141:2659-2663.

35. Shigemori H et al. (1999) Biosynthesis of diterpenoid moiety of brasilicardin A via non-mevalonate pathway in Nocardia brasiliensis. *Tetrahedron Letters* 40:4353-4354.

36. Spyere A, Rowley DC, Jensen PR, Fenical W (2003) New neoverrucosane diterpenoids produced by the marine gliding bacterium Saprospira grandis. *Journal of Natural Products* 66:818-822.

37. Dürr C et al. (2006) Biosynthesis of the terpene phenalinolactone in Streptomyces sp. Tü6071: analysis of the gene cluster and generation of derivatives. *Chemistry & Biology* 13:365-377.

38. Wang J et al. (2006) Platensimycin is a selective FabF inhibitor with potent antibiotic properties. *Nature* 441:358-361.

39. Wang J et al. (2007) Discovery of platencin, a dual FabF and FabH inhibitor with in vivo antibiotic properties. *Proceedings of the National Academy of Sciences of the United States of America* 104:7612-7616.

40. Ikeda C, Hayashi Y, Itoh N, Seto H, Dairi T (2007) Functional analysis of eubacterial ent-copalyl diphosphate synthase and pimara-9(11),15-diene synthase with unique primary sequences. *Journal of Biochemistry* 141:37-45.

41. Motohashi K et al. (2007) Studies on terpenoids produced by actinomycetes: oxaloterpins A, B, C, D, and E, diterpenes from Streptomyces sp. KO-3988. *Journal of Natural Products* 70:1712-1717.

42. Fukumoto A et al. (2008) Cyslabdan, a new potentiator of imipenem activity against Methicillin-resistant Staphylococcus aureus, produced by Streptomyces sp. K04-0144. *The Journal of Antibiotics* 61:7–10.

43. Kim S-Y et al. (2009) Cloning and heterologous expression of the cyclooctatin biosynthetic gene cluster afford a diterpene cyclase and two P450 hydroxylases. *Chemistry & Biology* 16:736-743.

44. Nakano C, Hoshino T (2009) Characterization of the Rv3377c gene product, a type-B diterpene cyclase, from the Mycobacterium tuberculosis H37 genome. *ChemBioChem* 10:2060-2071.

45. Mann FM et al. (2009) Edaxadiene: a new bioactive diterpene from Mycobacterium tuberculosis. *Journal of the American Chemical Society* 131:17526-17527.

46. Nakano C et al. (2011) Characterization of the Rv3378c gene product, a new diterpene synthase for producing tuberculosinol and (13R,S)-isotuberculosinol (nosyberkol), from the Mycobacterium tuberculosis H37Rv genome. *Bioscience, Biotechnology, and Biochemistry* 75:75-81.

47. Maugel N, Mann FM, Hillwig ML, Peters RJ, Snider BB (2010) Synthesis of (±)-Nosyberkol (Isotuberculosinol, Revised Structure of Edaxadiene) and (±)-Tuberculosinol. *Organic Letters* 12:2626-2629.

48. Shirai M et al. (2010) Terpenoids produced by actinomycetes: isolation, structural elucidation and biosynthesis of new diterpenes, gifhornenolones A and B from Verrucosispora gifhornensis YM28-088. *The Journal of Antibiotics* 63:245-250.

49. Takagi M, Motohashi K, Khan ST, Hashimoto J, Shin-ya K (2010) JBIR-65, a new diterpene, isolated from a sponge-derived Actinomadura sp. SpB081030SC-15. *The Journal of Antibiotics* 63:401-403.

50. Dairi T (2005) Studies on biosynthetic genes and enzymes of isoprenoids produced by actinomycetes. *The Journal of Antibiotics* 58:227-243.

51. Citron CA, Gleitzmann J, Laurenzano G, Pukall R, Dickschat JS (2011) Terpenoids are widespread in Actinomycetes: a correlation of secondary metabolism and genome data. *ChemBioChem* 13:202-214.

52. Smanski MJ, Peterson RM, Huang S-X, Shen B (2012) Bacterial diterpene synthases: new opportunities for mechanistic enzymology and engineered biosynthesis. *Current Opinion in Chemical Biology* 16:132-141.

53. Ajikumar PK et al. (2008) Terpenoids: opportunities for biosynthesis of natural product drugs using engineered microorganisms. *Molecular Pharmaceutics* 5:167-190.

54. Kirby J, Keasling JD (2008) Metabolic engineering of microorganisms for isoprenoid production. *Natural Product Reports* 25:656-661.

55. Fischbach M, Walsh C, Clardy J (2008) The evolution of gene collectives: how natural selection drives chemical innovation. *Proceedings of the National Academy of Sciences of the United States of America* 105:4601-4608.

56. Hamano Y et al. (2001) Cloning of a Gene Cluster Encoding Enzymes Responsible for the Mevalonate Pathway from a Terpenoid-antibiotic-producing Streptomyces Strain. *Bioscience, Biotechnology, and Biochemistry* 65:1627-1635.

57. Cane DE et al. (1994) Pentalenene synthase. Purification, molecular cloning, sequencing, and high-level expression in Escherichia coli of a terpenoid cyclase from Streptomyces UC5319. *Biochemistry* 33:5846-5857.

58. Morrone D et al. (2009) Gibberellin biosynthesis in bacteria: separate ent-copalyl diphosphate and ent-kaurene synthases in Bradyrhizobium japonicum. *FEBS Letters* 583:475-480.

59. Hayashi Y et al. (2008) Cloning of the gene cluster responsible for the biosynthesis of brasilicardin A, a unique diterpenoid. *The Journal of Antibiotics* 61:164-174.

60. Daum M et al. (2010) Functions of genes and enzymes involved in phenalinolactone biosynthesis. *ChemBioChem* 11:1383-1391.

61. Phillips DR, Rasbery JM, Bartel B, Matsuda SP (2006) Biosynthetic diversity in plant triterpene cyclization. *Current Opinion in Plant Biology* 9:305-314.

62. Ikeda C, Hayashi Y, Itoh N, Seto H, Dairi T (2007) Functional analysis of eubacterial ent-copalyl diphosphate synthase and pimara-9(11),15-diene synthase with unique primary sequences. *Journal of Biochemistry* 141:37-45.

63. Köksal M, Jin Y, Coates RM, Croteau RB, Christianson DW (2011) Taxadiene synthase structure and evolution of modular architecture in terpene biosynthesis. *Nature* 469:116-120.

64. Köksal M, Hu H, Coates RM, Peters RJRJ, Christianson DW (2011) Structure and mechanism of the diterpene cyclase ent-copalyl diphosphate synthase. *Nature Chemical Biology* 7:431-433.

65. Wendt KU, Poralla K, Schulz GE (1997) Structure and function of a squalene cyclase. *Science* 277:1811-1815.

66. Cao R et al. (2010) Diterpene cyclases and the nature of the isoprene fold. *Proteins* 78:2417-2432.

67. Lesburg CA, Zhai G, Cane DE, Christianson DW (1997) Crystal structure of pentalenene synthase: mechanistic insights on terpenoid cyclization reactions in biology. *Science* 277:1820-1824.

68. Aaron JA, Lin X, Cane DE, Christianson DW (2010) Structure of epi-isozizaene synthase from Streptomyces coelicolor A3(2), a platform for new terpenoid cyclization templates. *Biochemistry* 49:1787-1797.

69. Seemann M et al. (2002) Pentalenene synthase. Analysis of active site residues by site-directed mutagenesis. *Journal of the American Chemical Society* 124:7681-7689.

70. Hayashi K-I et al. (2006) Identification and functional analysis of bifunctional ent-kaurene synthase from the moss Physcomitrella patens. *FEBS Letters* 580:6175-6181.

71. Peters RJ et al. (2000) Abietadiene synthase from grand fir (Abies grandis): characterization and mechanism of action of the “pseudomature” recombinant enzyme. *Biochemistry* 39:15592-15602.

72. Peters RJ, Carter OA, Zhang Y, Matthews BW, Croteau RB (2003) Bifunctional abietadiene synthase: mutual structural dependence of the active sites for protonation-initiated and ionization-initiated cyclizations. *Biochemistry* 42:2700-2707.

73. Kawasaki T et al. (2006) Biosynthesis of a natural polyketide-isoprenoid hybrid compound, furaquinocin A□: identification and heterologous expression of the gene cluster. *Journal of Bacteriology* 188:1236-1244.

74. Tully RE, Berkum PV, Lovins KW, Eister DL (1998) Identification and sequencing of a cytochrome P450 gene cluster from Bradyrhizobium japonicum. *Biochimica et Biophysica Acta* 1398:243-255.

75. Smanski MJ et al. (2011) Dedicated ent-kaurene and ent-atiserene synthases for platensimycin and platencin biosynthesis. *Proceedings of the National Academy of Sciences of the United States of America* 108:13498-13503.

76. Toyomasu T et al. (2008) Identification of diterpene biosynthetic gene clusters and functional analysis of labdane-related diterpene cyclases in Phomopsis amygdali. *Bioscience, Biotechnology, and Biochemistry* 72:1038-1047.

77. Tamura K et al. (2011) MEGA5: Molecular evolutionary genetics analysis using maximum likelihood, evolutionary distance, and maximum parsimony methods. *Molecular Biology and Evolution* 28:2731-2739.

78. Oikawa H et al. (2001) Cloning and functional expression of cDNA encoding aphidicolan-16 beta-ol synthase: a key enzyme responsible for formation of an unusual diterpene skeleton in biosynthesis of aphidicolin. *Journal of the American Chemical Society* 123:5154-5155.

79. Otomo K et al. (2004) Diterpene cyclases responsible for the biosynthesis of phytoalexins, momilactones A, B, and oryzalexins A-F in rice. *Bioscience, Biotechnology, and Biochemistry* 68:2001-2006.

80. Morrone D et al. (2006) An unexpected diterpene cyclase from rice: functional identification of a stemodene synthase. *Archives of Biochemistry and Biophysics* 448:133-140.

81. Nemoto T et al. (2004) Stemar-13-ene synthase, a diterpene cyclase involved in the biosynthesis of the phytoalexin oryzalexin S in rice. *FEBS Letters* 571:182-186.

82. Vogel BS, Wildung MR, Vogel G, Croteau RB (1996) Abietadiene synthase from grand fir (Abies grandis). cDNA isolation, characterization, and bacterial expression of a bifunctional diterpene cyclase involved in resin acid biosynthesis. *The Journal of Biological Chemistry* 271:23262-23268.

83. Schepmann HG, Pang J, Matsuda SP (2001) Cloning and characterization of Ginkgo biloba levopimaradiene synthase which catalyzes the first committed step in ginkgolide biosynthesis. *Archives of Biochemistry and Biophysics* 392:263-269.

84. Ro D-K, Bohlmann J (2006) Diterpene resin acid biosynthesis in loblolly pine (Pinus taeda): functional characterization of abietadiene/levopimaradiene synthase (PtTPS-LAS) cDNA and subcellular targeting of PtTPS-LAS and abietadienol/abietadienal oxidase (PtAO, CYP720B1). *Phytochemistry* 67:1572-1578.

85. Wilderman PR, Peters RJ (2007) A single residue switch converts abietadiene synthase into a pimaradiene specific cyclase. *Journal of the American Chemical Society* 129:15736-15737.

86. Martin DM, Fäldt J, Bohlmann J (2004) Functional characterization of nine Norway spruce TPS genes and evolution of gymnosperm terpene synthases of the TPS-d subfamily. *Plant Physiology* 135:1908-1927.

87. Yamaguchi S et al. (1996) Molecular cloning and characterization of a cDNA encoding the gibberellin biosynthetic enzyme ent-kaurene synthase B from pumpkin (Cucurbita maxima L.). *The Plant Journal* 10:203-212.

88. Ait-Ali T, Swain SM, Reid JB, Sun T, Kamiya Y (1997) The LS locus of pea encodes the gibberellin biosynthesis enzyme ent-kaurene synthase A. *The Plant Journal* 11:443-454.

89. Xu M et al. (2007) Functional characterization of the rice kaurene synthase-like gene family. *Phytochemistry* 68:312-326.

90. Kawaide H, Imai R, Sassa T, Kamiya Y (1997) Ent-kaurene synthase from the fungus Phaeosphaeria sp. L487. cDNA isolation, characterization, and bacterial expression of a bifunctional diterpene cyclase in fungal gibberellin biosynthesis. *The Journal of Biological Chemistry* 272:21706-21712.

91. Yamaguchi S, Sun TP, Kawaide H, Kamiya Y (1998) The GA2 locus of Arabidopsis thaliana encodes ent-kaurene synthase of gibberellin biosynthesis. *Plant Physiology* 116:1271-1278.

92. Toyomasu T et al. (2000) Cloning of a full-length cDNA encoding ent-kaurene synthase from Gibberella fujikuroi: functional analysis of a bifunctional diterpene cyclase. *Bioscience, Biotechnology, and Biochemistry* 64:660-664.

93. Keeling CI et al. (2010) Identification and functional characterization of monofunctional ent-copalyl diphosphate and ent-kaurene synthases in white spruce reveal different patterns for diterpene synthase evolution for primary and secondary metabolism in gymnosperms. *Plant Physiology* 152:1197-1208.

94. Kohl AC, Kerr RG (2004) Identification and characterization of the pseudopterosin diterpene cyclase, elisabethatriene synthase, from the marine gorgonian, Pseudopterogorgia elisabethae. *Archives of Biochemistry and Biophysics* 424:97-104.

95. Lin X, Hezari M, Koepp a E, Floss HG, Croteau RB (1996) Mechanism of taxadiene synthase, a diterpene cyclase that catalyzes the first step of taxol biosynthesis in Pacific yew. *Biochemistry* 35:2968-2977.

96. Hezari M, Lewis NG, Croteau RB (1995) Purification and characterization of taxa-4(5),11(12)-diene synthase from Pacific yew (Taxus brevifolia) that catalyzes the first committed step of taxol biosynthesis. *Archives of Biochemistry and Biophysics* 322:437-444.

97. Herde M et al. (2008) Identification and regulation of TPS04/GES, an Arabidopsis geranyllinalool synthase catalyzing the first step in the formation of the insect-induced volatile C16-homoterpene TMTT. *The Plant Cell* 20:1152-1168.

98. Minami A et al. (2009) Identification and functional analysis of brassicicene C biosynthetic gene cluster in Alternaria brassicicola. *Bioorganic & Medicinal Chemistry Letters* 19:870-4.

99. Falara V, Pichersky E, Kanellis AK (2010) A copal-8-ol diphosphate synthase from the angiosperm Cistus creticus subsp. creticus is a putative key enzyme for the formation of pharmacologically active, oxygen-containing labdane-type diterpenes. *Plant Physiology* 154:301-310.

100. Hill AM, Cane DE, Mau CJ, West CA (1996) High level expression of Ricinus communis casbene synthase in Escherichia coli and characterization of the recombinant enzyme. *Archives of Biochemistry and Biophysics* 336:283-289.

101. Bömke C, Rojas MC, Gong F, Hedden P, Tudzynski B (2008) Isolation and characterization of the gibberellin biosynthetic gene cluster in Sphaceloma manihoticola. *Applied and Environmental Microbiology* 74:5325-39.

102. Hillwig ML et al. (2011) Domain loss has independently occurred multiple times in plant terpene synthase evolution. *The Plant Journal* 68:1051-1060.

Chapter 3: Cloning, sequencing, annotation, and manipulation of the gene clusters responsible for platensimycin and platencin production in strains of *Streptomyces platensis*

*Content from this chapter has been published previously:

Smanski MJ, Yu Z, Casper J, Lin S, Peterson RM, Chen Y, Wendt-Pienkowski E, Rajski SR, Shen B (2011) Dedicated ent-kaurene and ent-atiserene synthases for platensimycin and platencin biosynthesis. *Proceedings of the National Academy of Sciences of the United States of America* 108:13498-13503.

Yu Z, Smanski MJ, Peterson RM, Marchillo K, Andes D, Rajski SR, Shen B (2010) Engineering of Streptomyces platensis MA7339 for overproduction of platencin and congeners. *Organic Letters* 12:1744-1747.

Smanski MJ, Peterson RM, Rajski SR, Shen B (2009) Engineered Streptomyces platensis strains that overproduce antibiotics platensimycin and platencin. *Antimicrobial Agents and Chemotherapy* 53:1299-1304.

3.1 Introduction

PTM and PTM are composed of two structurally distinct moieties: a 3-amino-2,4-dihydroxybenzoic acid (ADHBA) polar "head" group linked by a propionamide chain to a 17-carbon tetracyclic or tricyclic "cage" moiety in PTM and PTN, respectively. Stable isotope feeding studies have suggested biosynthetic origins for these compounds (*1*, *2*). The ADHBA moiety is derived from three-carbon and four-carbon primary metabolites from glycolysis and the TCA cycle, respectively. It is predicted to follow a pathway similar to the recently reported grixazone biosynthetic pathway: a non-shikimate-type route utilizing primary metabolites, aspartate 4-semialdehyde (ASA) and dihydroxyacetone phosphate (DHAP), to form 3,4-aminohydroxybenzoic acid (AHBA) (**Figure 3.1**) (*3–6*). The unique cage moieties differentiating PTM from PTN have each been shown to originate from the MEP (non-mevalonate) pathway for terpene biosynthesis, utilizing the primary metabolites, pyruvate and

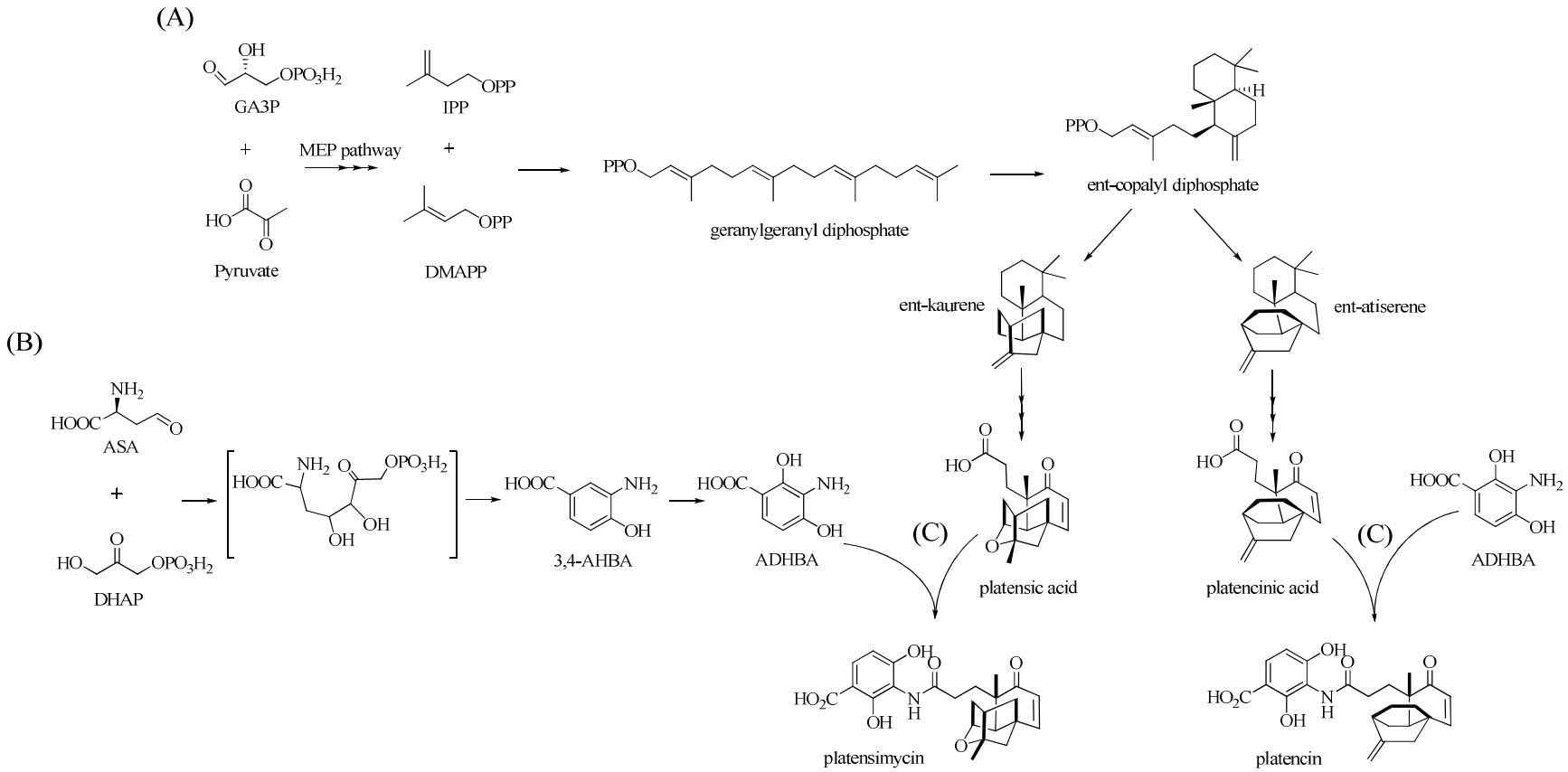

Figure 3.1 – Proposed pathway for the biosynthesis of platensimycin and platencin. (A) Diterpene biosynthesis utilizing the MEP pathway for isoprene precursors, IPP and DMAPP; the common diterpene intermediate GGDP is converted to *ent*-CPP, which can be converted to either *ent*-kaurene or *ent*-atiserene; (B) biosynthesis of the common ADHBA moiety from ASA and DHAP; and (C) coupling between the modified diterpenoid moieties, platensic acid (a modified *ent*-kaurene scaffold) and platencinic acid (a modified *ent*-atiserene scaffold), and the ADHBA moiety as the final step in biosynthesis of PTM and PTN.

GA3P (*7*). Biosynthesis is predicted to proceed through the twenty-carbon diterpene intermediate, GGDP, which can be cyclized by DTSs into each of the unique aliphatic cage moieties. The carbon scaffold of the PTM cage moiety resembles that of *ent*-kaurene, while the distinct cage moiety of PTN resembles an *ent*-atiserene skeleton, and natural products derived from these related skeletons are known (*1*, *2*, *8–14*). These preliminary biosynthetic studies of PTM and PTN, by assessment of stable-isotope precursor incorporation, provide a first look at a potential pathway leading to production of these novel compounds (**Figure 3.1**).

This chapter highlights the efforts to (i) confirm production and validate the chemical profiles of the producing organisms, *S. platensis* MA7327 and *S. platensis* MA7339; (ii) clone, sequence, and annotate the genetic loci responsible for PTM and PTN production; and (iii) establish a set of protocols for genetic manipulation and engineering of the producing organisms. Ultimately, these methods have provided the foundation for detailed investigation of all aspects of PTM and PTN biosynthesis.

3.2 Production profiles of *S. platensis* MA7327 and *S. platensis* MA339

We obtained the reported PTM- and PTN-producing strains, *Streptomyces platensis* MA7327 and *Streptomyces platensis* MA7339 (Merck Research Laboratories, Rahway, NJ) and verified the ability of these strains to produce PTM or PTN. Each strain was fermented under previously reported conditions, or slightly modified versions, for PTM or PTN production (*1*, *15*, *16*). Importantly, *S. platensis* MA7327, a previously reported PTM producer, was revealed to be a "dual producer" of both PTM and PTN compounds (**Table 3.1, Figure 3.2**) (*17*). The S. platensis MA7339 strain was confirmed to be a "PTN-only producer" (**Table 3.1, Figure 3.2**) (*18*). These two strains presented a unique opportunity for the comparative study of

Figure 3.1 – Summary of platensimycin and platencin production by *Streptomyces platensis*

Compound	Titer (mg/L)	
	***S. platensis* MA7327**	***S. platensis* MA7339**
Platensimycin:		
in PTM medium:	10.1 ± 3.6	not detected
in PTN medium:	1.7 ± 1.0	not detected
Platencin:		
in PTM medium:	0.2 ± 0.1	0.26 ± 0.10
in PTN medium:	1.2 ± 0.5	0.05 ± 0.04

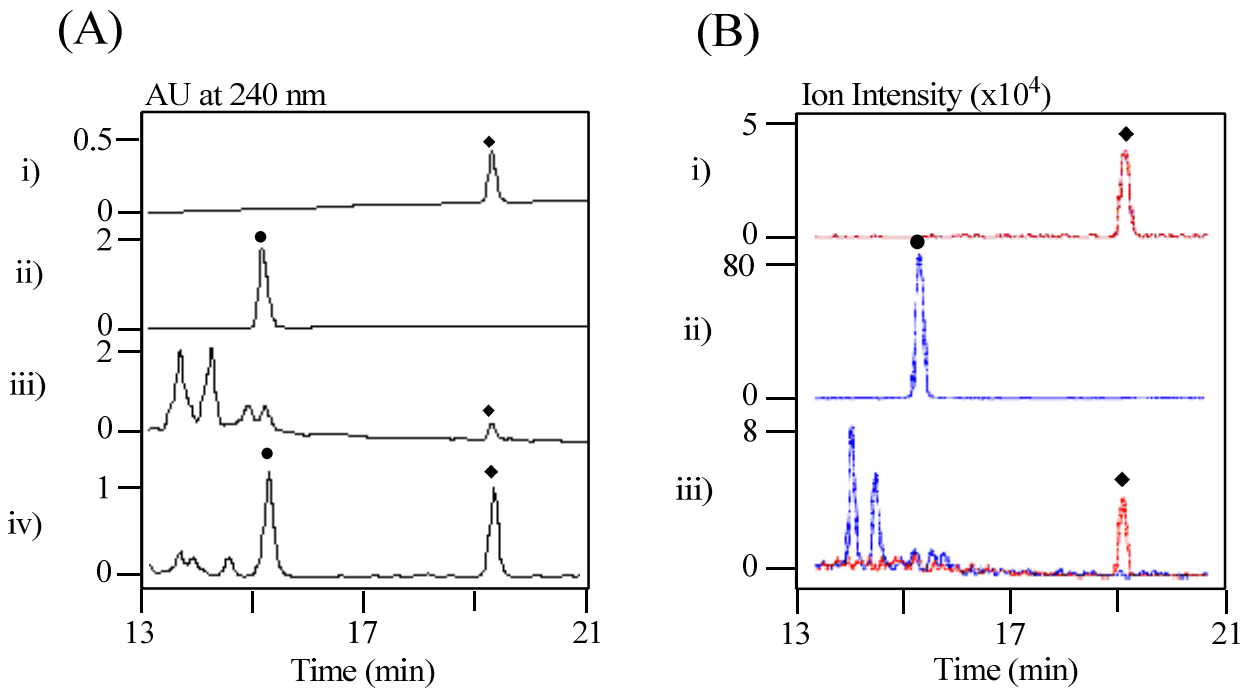

Figure 3.2 - Production of platensimycin and platencin by *S. platensis*. (A) HPLC chromatogram of (i) platencin and (ii) platensimycin standards and crude extracts from the fermentations of (iii) *S. platensis* MA7339 and (iv) *S. platensis* MA7327 in PTM production medium. (B) LC-MS chromatogram of (i) platencin standard, (ii) platensimycin standard and (iii) crude extracts from *S. platensis* MA7339 fermentation showing extracted ion chromatograms, m/z = 426 (red trace, PTN ♦) and m/z = 442 (blue trace, PTM ●)

two biosynthetic pathways producing related – but distinct – compounds. By exploring the strategies Nature employs for increasing structural diversity in secondary metabolic pathways, we may gain insight into exploiting these strategies for developing methods for generating new and useful compounds.

3.3 Methods for identifying the genetic loci responsible for PTM and PTN biosynthesis

3.3.1 PCR amplification of a single AHBA synthase gene contributing to both PTM and PTN biosynthesis

A PCR-based method was used to establish the genetic loci responsible for PTM and PTN production in the *S. platensis* producing organisms. The predicted involvement of the recently described non-shikamate pathway leading to 3,4-AHBA biosynthesis (**Figure 3.1**) provided a suitable target gene for attempted amplification and probe design: the putative AHBA synthase. Primers were designed from conserved regions identified from an alignment of GriH (GenBank: BAF36650), the AHBA synthase gene from the grixazone biosynthetic pathway, and two highly similar, putative AHBA synthases, Francci3_2069 and Francci3_4206 (GenBank: YP_481771 and YP-483283). A single fragment was amplified from *S. platensis* MA7327 genomic DNA and was confirmed to consist of a single sequence. Importantly, this revealed that a single AHBA synthase gene resides in the genome of *S. platensis* MA7327 and supported a shared pathway for PTM and PTN production.

3.3.2 Cloning, sequencing, and annotation of the *ptm* and *ptn* gene clusters

In order to identify genes surrounding the AHBA synthase, a genomic library from *S. platensis* MA7327 was constructed and screened by colony hybridization using the labeled AHBA synthase fragment (see above section) as a probe. Cosmids with genomic DNA inserts (~30–42 kb) containing the AHBA synthase gene were identified and used for sequencing

upstream and downstream of the AHBA synthase gene. Shotgun sequencing was performed by subcloning *Bam*HI or *Eco*RI digested fragments into the cloning vector, pGEM-3zf (Promega, Madison, WI) and sequencing with M13 forward and reverse primers. Ultimately, a 47-kb contiguous DNA sequence was assembled and open reading frames (ORFs) were identified. Putative ORFs were annotated using BLAST analyses to identify homologous sequences deposited in sequence databases. A similar approach was used to assemble and annotate a 41-kb contiguous DNA sequence from cosmids, containing the AHBA synthase gene, isolated from a *S. platensis* MA7339 genomic library. Annotated DNA sequences are available using the GenBank accession numbers, FJ655920 and CG398492. A combination of bioinformatics analysis and i*n vivo* gene inactivation methods was ultimately used to define the boundaries of a single biosynthetic gene cluster, the "*ptm* cluster", from *S. platensis* MA7327, responsible for production of both PTM and PTN (*19*). A highly similar gene cluster, the "*ptn* cluster", was also identified from *S. platensis* MA7339, responsible for PTN production (*19*). Comparison of the overall genetic organization between the two clusters as well as a summary of predicted functions for the putative genes encoding PTM and PTN production is presented in **Figure 3.3**. A complete list of annotated genes, identified database homologs, and proposed gene product functions are summarized in **Table 3.2**.

3.4 Inactivation of *ptmR1* and characterization of strains overproducing PTM and PTN

Both producing strains of *S. platensis* were confirmed to be amenable to established methods of genetic manipulation in *Streptomyces* (*20*). Importantly, they are capable of intergenic conjugation with an *E. coli* donor strain for delivery of DNA into the *Streptomyces* strain. Moreover, the producing strains are sensitive to antibiotics apramycin, kanamycin, and thiostrepton commonly used as selection markers for genetic manipulation. Targeted gene

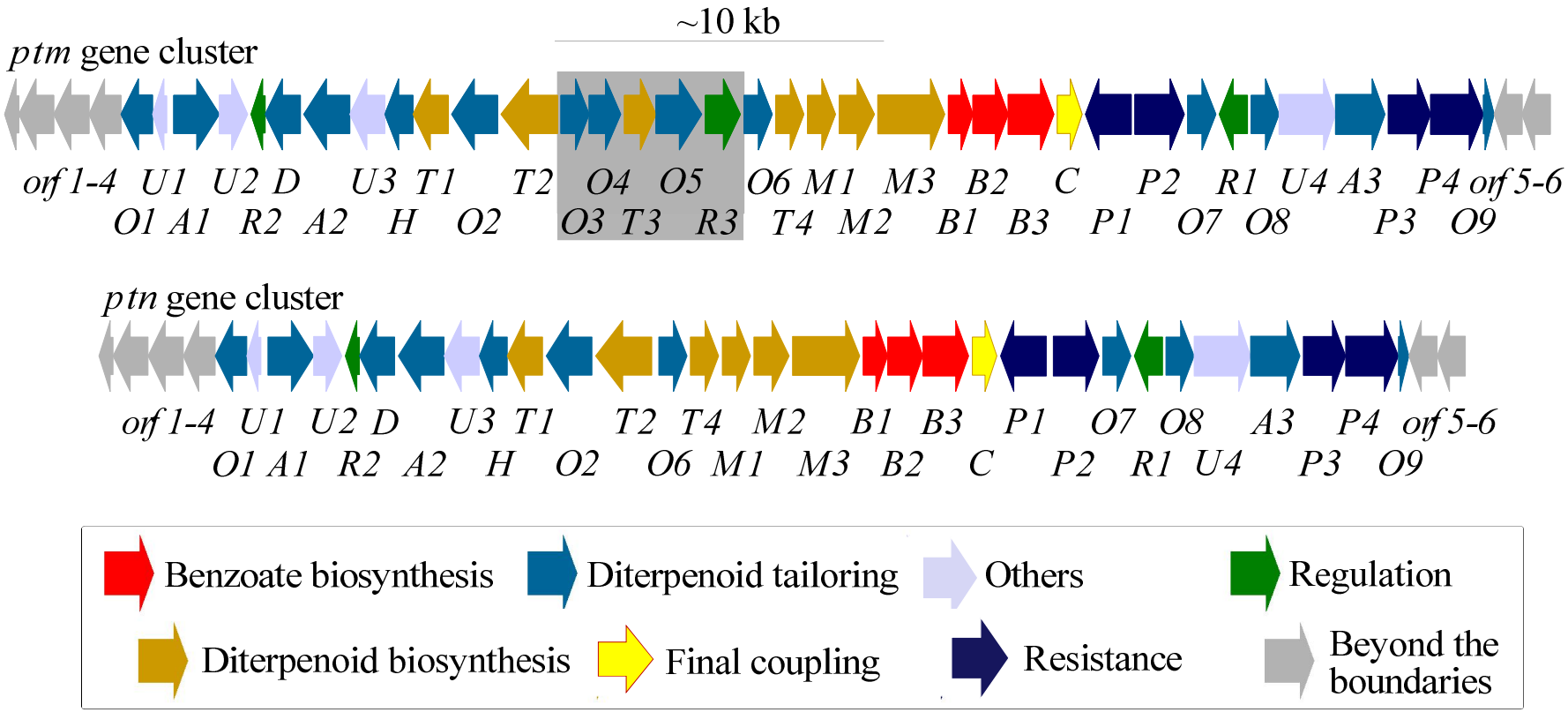

Figure 3.3 - Genetic organization of the ptm and ptn biosynthetic gene clusters. The *ptm* cluster from *S. platensis* MA7327 (top) encodes for both platensimycin and platencin production, while the *ptn* cluster from *S. platensis* MA7339 (bottom) encodes only platencin production. Each arrow represents a putative gene and the direction indicates direction of transcription. Unique colors indicate predicted functions in biosynthesis, resistance, and regulation (see legend). The shaded box encompassing genes *ptmO3-ptmR3* designates the "PTM cassette", containing genes that are only found in the ptm cluster and are essential for PTM production, but not PTN production.

Table 3.2 – Summary and deduced functions of ORFs from the *ptm* and *ptn* gene clusters

Gene (*ptn* cluster)	# AA	Identity	Gene (*ptm* cluster)	# AA	Protein Homolog (Accession #)	Homology (% ID / % Similarity)	Proposed Function
orf1-4			*orf 1-4*				(ORFs beyond the upstream boundary)
ptnO1	254	97%	*ptmO1*	254	DitI (AAD21071)	35/48	Dehydrogenase
ptnU1	184	96%	*ptmU1*	184	SSEG-08609(YP-02208525)	68/73	Unknown
ptnA1	434	96%	*ptmA1*	434	PaaK (CAD76926)	24/40	Acyl-CoA Synthetase
ptnU2	236	96%	*ptmU2*	236	SSEG-08597(YP-02208498)	47/64	Unknown
ptnR2	133	96%	*ptmR2*	133	SSEG-08605(YP-02208515)	65/76	Regulatory (DNA Binding Protein)
ptnD	385	97%	*ptmD*	385	DitF (AAD21068)	27/40	Thiolase
ptnA2	522	98%	*ptmA2*	522	Fcs (CAC18323)	30/42	Acyl-CoA Synthetase
ptnU3	360	99%	*ptmU3*	360	BarH (AAN32982)	28/44	Hydrolase
ptnH	284	94%	*ptmH*	284	Hsd4B (ABW74860)	46/61	2-Enoyl Acyl-CoA Hydratase
ptnT1	308	96%	*ptmT1*	308	Neut-1128 (YP-747348)	26/42	Type I DTS (ent-Atiserene synthase)
ptnO2	441	98%	*ptmO2*	440	HctG (AAY42399)	27/46	P-450 Monooxygenase
ptnT2	533	98%	*ptmT2*	533	*ent*-Cdps (BAD86797)	44/57	Type II DTS (*ent*-CDP Synthase)
			ptmO3	285	TfdA (ACF35485)	27/38	Fe(II)/α-KG-Dependent Dioxygenase
			ptmO4	388	CaiA (CAA5211)	26/43	Long-Chain Acyl CoA Dehydrogenase
			ptmT3	309	KSB (Q39548)	19/36[1]	Type I DTS (*ent*-Kaurene Synthase)
			ptmO5	430	CphP (BAG16627)	46/57	P-450 Monooxygenase
			ptmR3	355	MAV-2666 (YP-881857)	30/42	Regulatory (Hypothetical Kinase)
pnO6	280	96%	*ptmO6*	280	TfdA (ACF35485)	26/37	Fe(II)/α-KG Dependent Dioxygenase
ptnT4	348	99%	*ptmT4*	348	Ggdps (BAB07816)	66/77	GGDP Synthase
ptnM1	448	94%	*ptmM1*	448	IspH (AAL38655)	51/69[2]	HMBDP Reductase (MEP Pathway)
ptnM2	366	99%	*ptmM2*	366	PlaT5 (ABB69755)	77/84	HMBDP Synthase (MEP Pathway)
ptnM3	587	97%	*ptmM3*	587	PlaT6 (ABB69756)	62/71	DXP Synthase (MEP Pathway)
ptnB1	277	98%	*ptmB1*	277	GriI (BAF36651)	63/76	ADHOHP Synthase (AHBA)
ptnB2	368	98%	*ptmB2*	368	GriH (BAF36650)	71/81	3,4-AHBA Synthase (AHBA)
ptnB3	396	95%	*ptmB3*	396	MhbM (AAW63416)	29/45	Flavin-Dependent Hydroxylase (ADHBA)
ptnC	291	96%	*ptmC*	291	NfNAT (3D9W-A)	27/37	Amide Synthase (N-Acetyl Transferase)
ptnP1	474	96%	*ptmP1*	474	PhlA (AAB48109)	23/34[3]	Putative Resistance (KASIII)
					PhlB (AAB48107)	21/36[4]	
ptnP2	414	99%	*ptmP2*	414	PhlC (AAB48108)	22/35	Putative Resistance (Thiolase)
ptnO7	301	95%	*ptmO7*	301	ORF27 (BAD66689)	43/57	Oxidoreductase
ptnR1	238	99%	*ptmR1*	238	KorSA (CAA79637)	16/32	Regulatory (GntR family)
ptnO8	278	99%	*ptmO8*	278	PsfG (ACA09736)	37/55	Dehydrogenase
ptnU4	596	95%	*ptmU4*	596	QbsK (AAL65280)	31/42	Acyl-CoA Transferase
ptnA3	536	95%	*ptmA3*	537	Fcs (CAC18323)	28/40	Acyl-CoA Synthetase
ptnP3	405	96%	*ptmP3*	405	*Ti*KAS II (1J3N-A)	46/63	Putative Resistance (KASII)
ptnP4	520	97%	*ptmP4*	520	Pep (AAG31689)	30/48	Putative Resistance (Efflux Pump)
ptnO9	111	99%	*ptmO9*	111	FdxA (P24496)	74/83	(ORFs beyond downstream boundary)
orf5-7			*orf5-7*				

[1]values from alignment of full length PtmT3 with residues 393-773 of KSB; [2]values from alignment of full length IspH with residues 124-448 of PtmM1; [3]values from alignment of full length PhlA with residues 1-334 of PtmP1; [4]values from alignment of full length PhlB with residues 335-474 of PtmP1; AA, amino acids.

inactivation in *S. platensis* was facilitated by using λ-RED-mediated PCR-targeting methods for modifying cosmids containing the *ptm* and *ptn* gene clusters (*21*). The modified cosmid DNA – in which a target sequence/gene has been replaced with a "disruption cassette", containing a selectable resistance marker and an origin of transfer (*oriT*) – is introduced into *S. platensis* by conjugation, and replacement of the chromosomal target gene with the disruption cassette occurs via homologous recombination (**Figure 3.4**).

One gene target that was identified as a candidate for *in vivo* inactivation based on its deduced function, was *ptmR1*. Its gene product (PtmR1) shows sequence similarity to the GntR family of transcriptional repressors suggesting it may be involved in the regulation of PTM and PTN production (*22, 23*). We hypothesized that inactivation of *ptmR1* could lead to altered

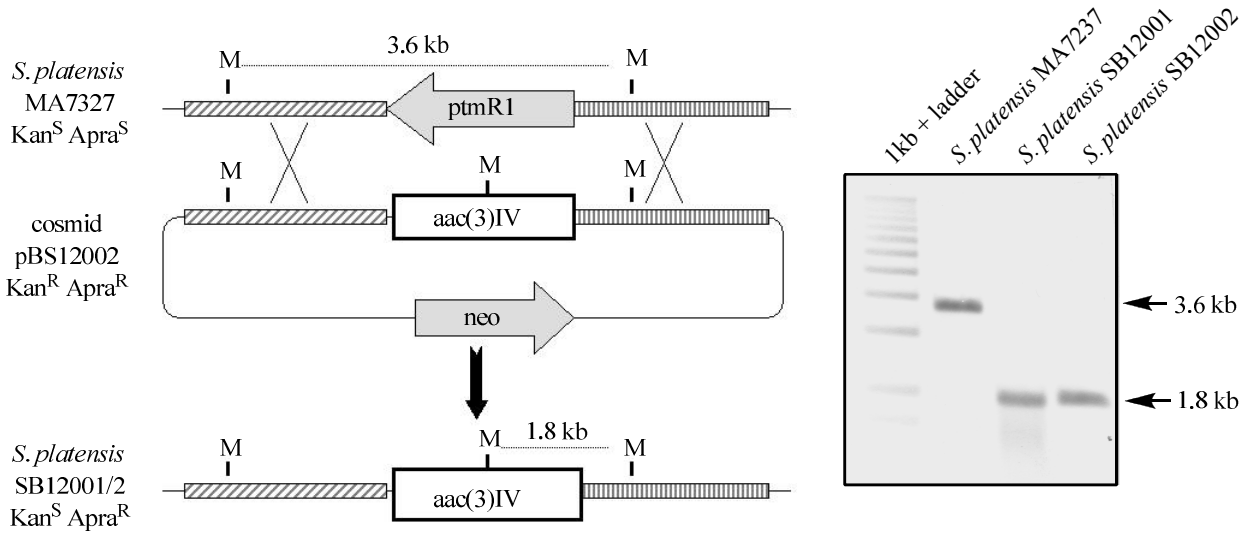

Figure 3.4 – Inactivation of *ptmR1* in *S. platensis* MA7327. Homologous recombination with modified cosmid, pBS12002, and southern analysis verifying genotypes of S. platensis MA7327 and mutant strains, SB12001 and SB12002. (M , MluI restriction site used for southern analysis, neo, kanamycin resistance cassette; aac(3)IV, apramycin resistance cassette; Apra^S, apramycin sensitive; Apra^R, apramycin resistant; Kan^S, kanamycin sensitive; Kan^R, kanamycin resistant)

production of these compounds. Replacement of *ptmR1* in *S. platensis* MA7327, with an apramycin resistance cassette (aac(3)IV), using the aforementioned PCR-targeting methods (*21*), yielded two strains, *S. platensis* SB12001 and SB12002, whose genotypes were confirmed by Southern analysis (**Figure 3.4**). HPLC analysis of the crude extracts from the fermentation of these Δ*ptmR1* strains under PTM or PTN production conditions showed considerable improvements in the titers of each compound (**Figure 3.5, Table 3.3**) (*17*). These overproducing strains produce PTM and PTN with yields of ~323 mg/L and ~255 mg/L, respectively, and ensure the availability of large amounts of PTM and PTN for the development and characterization of these compounds. Additionally, these overproducing strains provided a platform for isolating numerous pathway intermediates in sufficient quantity for structure elucidation (*18*).

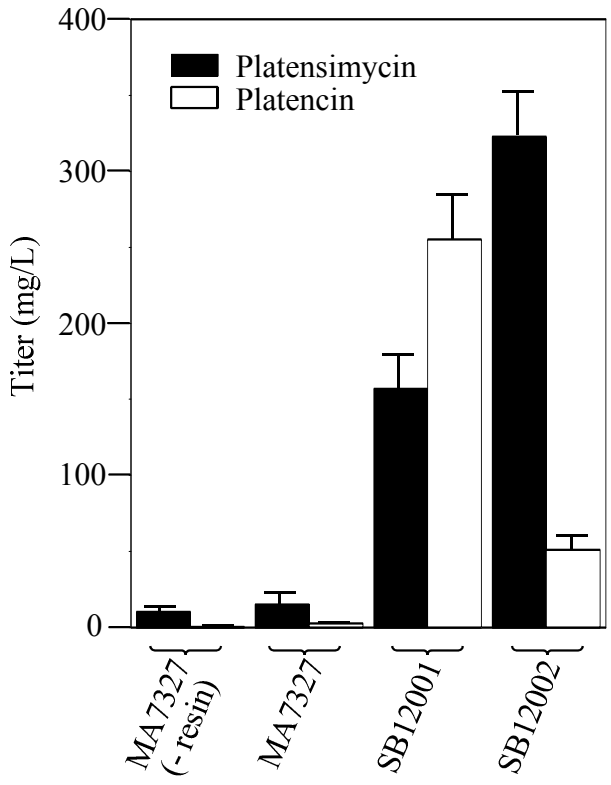

Figure 3.5 – Platensimycin and platencin production by S. platensis MA7327 WT and Δptmr1 mutant strains (17)

Compound	Titer (mg/L)		
	***S. platensis* MA7327**	**S. platensis SB12001**	**S. platensis SB12002**
Platensimycin:			
in PTM medium[a]:	15.1 ± 3.6	157 ± 22	323 ± 29
in PTN medium[a,b]:	2.1	43	122
Platencin:			
in PTM medium[a]:	2.5 ± 0.7	255 ± 30	51 ± 9.2
in PTN medium[a,b]:	0.8	122	29

[a] Media contained 3% w/v XAD-16 resin, [b] Values are the average of two independent trials

3.5 References

1. Herath K, Attygalle AB, Singh SB (2008) Biosynthetic studies of platencin. *Tetrahedron Letters* 49:5755-5758.

2. Herath KB, Attygalle AB, Singh SB (2007) Biosynthetic studies of platensimycin. *Journal of the American Chemical Society* 129:15422-15423.

3. Gould SJ, Melville CR, Cone MC (1996) 3-amino-4-hydroxybenzoic acid is derived from the tricarboxylic acid cycle rather than the shikimic acid pathway. *Journal of the American Chemical Society* 118:9228-9232.

4. Li Y, Gould SJ, Proteau PJ (2000) Biosynthesis of 3-amino-4-hydroxybenzoic acid in Streptomyces murayamaensis: incorporation of [4-13C]oxalacetate. *Tetrahedron Letters* 41:5181-5185.

5. Suzuki H, Ohnishi Y, Furusho Y, Sakuda S, Horinouchi S (2006) Novel benzene ring biosynthesis from C3 and C4 primary metabolites by two enzymes. *Journal of Biological Chemistry* 281:36944–36951.

6. Walsh CT, Haynes SW, Ames BD (2012) Aminobenzoates as building blocks for natural product assembly lines. Natural Product Reports 29:37-59.

7. Rohmer M (1999) The discovery of a mevalonate-independent pathway for isoprenoid biosynthesis in bacteria, algae and higher plants. *Natural Product Reports* 16:565-574.

8. Wang LQ, Qin GW, Chen SN, Li CJ (2001) Three diterpene glucosides and a diphenylamine derivative from Pieris formosa. *Fitoterapia* 72:779-787.

9. Kume T et al. (2002) Isolation of a diterpenoid substance with potent neuroprotective activity from fetal calf serum. *Proceedings of the National Academy of Sciences of the United States of America* 99:3288-3293.

10. Hanson J (2009) Diterpenoids. *Natural Product Reports* 26:1156-1171.

11. Dev S (1986) in *CRC Handbook of Terpenoids* (CRC Press), pp 7-57.

12. Hao X, Nie J (1998) Diterpenes from Spiraea japonica. *Phytochemistry* 48:1213-1215.

13. Hanson JR (1992) The microbiological transformation of diterpenoids. *Natural Product Reports* 9:139-151.

14. García PA, de Oliveira AB, Batista R (2007) Occurrence, biological activities and synthesis of kaurane diterpenes and their glycosides. *Molecules* 12:455-483.

15. Jayasuriya H et al. (2007) Isolation and structure of platencin: a FabH and FabF dual inhibitor with potent broad-spectrum antibiotic activity. *Angewandte Chemie* 46:4684-4688.

16. Singh SB et al. (2006) Isolation, structure, and absolute stereochemistry of platensimycin, a broad spectrum antibiotic discovered using an antisense differential sensitivity strategy. *Journal of the American Chemical Society* 128:11916-11920.

17. Smanski MJ, Peterson RM, Rajski SR, Shen B (2009) Engineered Streptomyces platensis strains that overproduce antibiotics platensimycin and platencin. *Antimicrobial Agents and Chemotherapy* 53:1299-1304.

18. Yu Z, Smanski MJ, Peterson RM, Marchillo K, Andes D, Rajski SR, Shen B (2010) Engineering of Streptomyces platensis MA7339 for overproduction of platencin and congeners. *Organic Letters* 12:1744-1747.

19. Smanski MJ, Yu Z, Casper J, Lin S, Peterson RM, Chen Y, Wendt-Pienkowski E, Rajski SR, Shen B (2011) Dedicated ent-kaurene and ent-atiserene synthases for platensimycin and platencin biosynthesis. *Proceedings of the National Academy of Sciences of the United States of America* 108:13498-13503.

20. Kieser T, Bibb MJ, Buttner M, Chater KF, Hopwood DA (2000*) Practical streptomyces genetics* (The John Innes Foundation Norwich, UK).

21. Gust B, Kieser T, Chater K (2002) *REDIRECT technology: PCR-targeting system in Streptomyces coelicolor.* (The John Innes Foundation Norwich, UK).

22. Rigali S, Derouaux A, Giannotta F, Dusart J (2002) Subdivision of the helix-turn-helix GntR family of bacterial regulators in the FadR, HutC, MocR, and YtrA subfamilies. *Journal of Biological Chemistry* 277:12507-12515.

23. Hillerich B, Westpheling J (2006) A new GntR family transcriptional regulator in streptomyces coelicolor is required for morphogenesis and antibiotic production and controls transcription of an ABC transporter in response to carbon source. *Journal of Bacteriology* 188:7477-7487.

Chapter 4: Bacterial diterpene synthases contributing to platensimycin and platencin biosynthesis

*Content from this chapter has been published previously or has been submitted for publication:

> Smanski MJ, Peterson RM, Shen B (2012) Platensimycin and platencin biosynthesis in Streptomyces platensis showcasing discovery and characterization of novel bacterial diterpene synthases. *Methods in Enzymology,* in press.
>
> Smanski MJ, Yu Z, Casper J, Lin S, Peterson RM, Chen Y, Wendt-Pienkowski E, Rajski SR, Shen B (2011) Dedicated ent-kaurene and ent-atiserene synthases for platensimycin and platencin biosynthesis. *Proceedings of the National Academy of Sciences of the United States of America* 108:13498-13503.

4.1 Introduction

The cloning, sequencing, and annotation of the *ptm* and *ptn* gene clusters from S. *platensis* MA7327 and *S. platensis* MA7339, respectively, now provide the genetic information necessary to characterize the biosynthetic machinery contributing to PTM and PTN production (*1*, *2*). Ultimately, the structural differences between PTM and PTN lie in their unique diterpenoid moieties. One or more DTSs are predicted to be responsible for this structural diversity. This chapter describes identification and functional characterization of the DTSs responsible for the distinctive diterpenoid scaffolds in PTM and PTN.

4.1.1 Identification of genes predicted to contribute to diterpene biosynthesis

Three genes within each cluster (*ptmM1*/*ptnM1*, *ptmM2*/*ptnM2*, and *ptmM3*/*ptnM3*) are predicted to encode essential genes contributing to the MEP pathway for biosynthesis of the isoprene precursors, IPP and DMAPP. Notably, these genes are located in a putative operon with another gene, *ptmT4*/*ptnT4*, which is homologous to geranylgeranyl diphosphate synthases (**Figure 3.3, Table 3.2**). These observations are consistent with previous labeling studies, indicating that the PTM and PTN diterpene moieties originate from pyruvate and glyceraldehyde

3-phosphate via the MEP pathway, and verify a source of GGDP for cyclization by DTSs into the aliphatic cage moieties of PTM and PTN (*3*, *4*).

Two candidate DTSs in the *ptm* cluster were identified based on sequence homology to proteins of known function: PtmT2 and PtmT3. PtmT2 shows high sequence similarity (45% identity / 58% similarity over 518 amino acids) to a bacterial *ent*-CPP synthase from *Streptomyces sp*. KO-3988 (**Table 2.1**) (*5*). Furthermore, an aspartate-rich motif (DXDD) was present in the primary amino acid sequence of PtmT2, characteristic of type II, protonation-dependent DTSs (*6*). Preliminary analysis of the primary amino acid sequence of PtmT3 revealed no characterized prokaryotic homologs in the NCBI database; yet, it is homologous (19% identity / 36% similarity over 380 amino acids) to a characterized *ent*-kaurene synthase from the chloroplasts of the plant species, *Cucurbita maxima* L. (*7*). As with PtmT2, PtmT3 also revealed two aspartate-rich sequence motifs, characteristic of type I ionization-dependent DTSs, further confirming functional assignment: magnesium-binding DDXXE and NDLXTXXXD motifs (*6*). These observations confirm the presence of both a type II DTS and a type I DTS in the *ptm* cluster, consistent with a two-enzyme pathway from GGDP leading to multiple cyclic diterpene scaffolds, which has been demonstrated in other organisms (*8*, *9*): (i) GGDP is converted to *ent*-CPP through the action of a type II DTS; and, (ii) *ent*-CPP is converted, through the action of a promiscuous type I DTS, into two or more diterpene scaffolds, including both the predicted *ent*-kaurene and *ent*-atiserene type intermediates, and leading to PTM and PTN diterpenoid scaffolds, respectively (see **Chapter 3, Figure 3.1**).

Yet, comparison between the *ptm* cluster and the *ptn* cluster reveals a surprising disparity: the *ptn* cluster does not contain a PtmT3 homolog. Although the *ptm* and *ptn* gene clusters share >97% sequence identity at the DNA level, and share the same overall genetic organization, the

ptn cluster entirely lacks a 5.4 kB DNA fragment and homologs to the annotated genes, *ptmO3*, *ptmO4*, *ptmT3*, *ptmO5*, and *ptmR3* from the ptm cluster (see **Chapter 3, Figure 3.3**). Intriguingly, this apparently leaves the *ptn* cluster without an obvious type I DTS, responsible for cyclization of *ent*-CPP into a predicted *ent*-atiserene type scaffold, and challenges the aforementioned prediction that promiscuity of PtmT3 could be responsible for both *ent*-kaurene and *ent*-atiserene type intermediates in the *ptm* cluster. A second inspection of the genes within the boundaries of the each cluster ultimately resulted in assignment of PtmT1/PtnT1 as putative candidates for a second type I DTS contributing to production of an *ent*-atiserene type intermediate for PTN biosynthesis. Notably, the functional assignment of PtmT1/PtnT1 was based on sequence homology to the UbiA family of aromatic prenyltransferases, distant structural and functional relatives of terpene synthases; however, PtmT1/PtnT1 contain no characteristic DTS or prenyltransferase sequence motifs (*6*, *10*).

4.2 Methods

4.2.1 Bacterial strains, plasmids, culture conditions, and chemicals

Escherichia coli DH5α was used for routine cloning and *Escherichia coli* BL21(DE3), BL21(DE3)pLysS, and BL21(DE3)Rosetta (New England Biolabs, Ipswich, MA) were used for recombinant protein expression (*11*). Vectors pGEM-T Easy (Promega Corporation, Madison, WI), pCDF-2 Ek/LIC Vector Kit (EMD Millipore, Billerica, MA), and pCold-TF (Clontech Laboratories, Inc., Mountain View, CA) were obtained from commercial sources. Platensimycin and platencin producers, *Streptomyces platensis* MA7327 and *Streptomyces platensis* MA7339, were kindly provided by Merck Research Laboratories (Rahway, NJ). *Streptosporangium roseum* DSM43021 was obtained from the American Type Culture Center (ATCC Number 12428). *E. coli* carrying plasmids were grown in Luria-Bertani (LB) medium and were selected

for with appropriate antibiotics (*11*). Standard media and protocols were used for *Streptomyces* growth and sporulation (*12*). Geranylgeranyl diphosphate (GGDP) and geranylgeraniol (GGOH) were obtained from Sigma-Aldrich (St. Louis, MO). All other media components and chemicals were from standard commercial sources. See **Appendix**, **section A1.2** for media recipes.

4.2.2 DNA manipulation and isolation

Plasmid preparation and gel extraction from *E. coli* was carried out with commercial kits (Qiagen, Valencia, CA) or according to standard protocols (*11*). Total *Streptomyces* DNA was isolated according to standard procedures (*12*), as were all restriction endonuclease digestions and ligations (*11*). Automated DNA sequencing and oligonucleotide primer synthesis were performed by the University of Wisconsin Biotechnology Center (Madison, WI), GENEWIZ (South Plainfield, NJ) or Integrated DNA Technologies (Coralville, IA).

4.2.3 Plasmids, primers, and strains

See **Appendix**, **Tables A1.1, A1.2, and A1.3**.

4.2.4 Inactivation of *ptmT1* and *ptmT3* in *S. platensis* MA7327

Following λRED-mediated PCR targeted gene replacement protocols (*13*), the modified cosmids, pBS12011 and pBS12012, were constructed by PCR-targeting pBS12003 to replace *ptmT1* and *ptmT3*, respectively, with the apramycin resistance cassette (**Table A1.1**). These cosmids were introduced into *S. platensis* MA7327 by intergenic conjugation to afford the Δ*ptmT1* and Δ*ptmT3* mutant strains, *S. platensis* SB12007 and *S. platensis* SB12008, respectively. Their genotypes were confirmed by Southern analysis.

4.2.5 Cloning of the "PTM cassette" for expression in *S. platensis* MA7339

A PCR approach was used to introduce convenient restriction sites flanking the PTM cassette. Because the entire cassette was not effectively amplified as a single product, smaller

fragments were amplified and cloned together to eventually yield the pSET152ermE* derivative, pBS12603, containing *ptmO3-ptmR3* under the expression of the *ermE** promoter. The construct was introduced into *S. platensis* MA7339 by intergenic conjugation yielding the strain, *S. platensis* SB12604.

4.2.6 Cloning *sros_3708* from *S. roseum* DSM43021 for expression in *S. platensis* SB12007

Streptosporangium roseum DSM43021 (ATCC Number 12428) was cultured on yeast malt extract (YME) agar at 28°C. Genomic DNA was isolated according to standard protocols from a YME liquid culture of *S. roseum* cells. Primers for amplification of *sros_3708* (NCBI Gene ID: 86669966) were designed using the database whole genome sequence for *S. roseum* (NCBI Reference Sequence: NC_013595.1). A DNA fragment containing *sros_3708* was amplified using primers, Sros_3708For and Sros_3708Rev (**Table A1.1**), and cloned into pGEM T-Easy vector using TA cloning methods (Promega, Madison, WI). The insert was subcloned into pANT841 via *SpeI* and *NcoI* restriction sites and then into pSET152ermE* via *SpeI* and *BamHI* sites. Finally, a fragment containing *sros_3708* and the upstream *ermE** promoter was cloned into pSET152AT via *EcoRI* and *BamHI* sites, creating the plasmid, pBS12017. The final construct was confirmed by sequencing.

4.2.7 Introduction of the *sros_3708* into S. *platensis* SB12007

Plasmid pBS12017 was introduced to SB12007 by a procedure similar to that previously described (*12*). In place of spores, SB12007 mycelial fragments were used during intergenic conjugation with donor strain *E. coli* ET12567/pUZ8002 harboring pBS12017. To obtain mycelial fragments, SB12007 was grown in 50 mL of R2YE liquid medium supplemented with apramycin (50 µg/mL) in a 250-mL baffled flask for 4 days at 30 °C in an incubated shaker. The resulting dense culture was pelleted by centrifugation at 4150rpm for 10 min and washed twice

with antibiotic-free medium. Finally, the pellet was resuspended in TSB medium, supplemented with 10% sucrose and 0.4% glycine prior to heat shock at 50 °C for 10 min, as in the previously described procedure (*12*). *E. coli* ET12567/pUZ8002 cells harboring pBS12017 were grown in 10mL LB + 100 μg/mL ampicillin to an OD_{600} of ~0.6, harvested, washed twice with antibiotic-free medium and resuspended in 1 mL of LB. A 0.5 mL aliquot of E. coli cells were added to 0.5 mL heat shocked mycelial fragments and plated. Recombinant strains were selected by overlaying conjugation plates with 2 mL soft nutrient agar (SNA) supplemented with thiostrepton and nalidixic acid (30 μg/mL and 25 μg/mL, respectively).

4.2.8 Fermentation of *S. platensis* strains and preparation of crude extract

Dense cultures were grown in R2YE (~3-5 days) and a 0.5 mL aliquot was used to inoculate 50 mL of ISM-3 seed medium. Seed cultures were grown at 28°C and 250 rpm in incubation shakers for ~48 hours. Flasks containing production media (generally, "PTM media" - see **Appendix, section A1.2**) were supplemented with 3% w/v of Amberlite XAD-16 resin before autoclaving. Production media was inoculated with a 1:100 dilution of seed culture and incubated for 6-10 days at 28°C and 250 rpm before the cells and resin were harvested, separated from the broth by centrifugation, and subsequently washed three times with equal volumes of H_2O. The resin/mycelial fragments were extracted with acetone (generally 4 x 6 mL acetone for cells from a 50 mL fermentation) to recover PTM and PTN. The acetone was removed under reduced pressure, and the crude extract was resuspended in methanol prior to analysis.

4.2.9 HPLC analysis of PTM and PTN

Analysis by HPLC using a Waters 510 system with a photodiode array detector (Waters, Milford, MA) and an Apollo C_{18} column (particle size, 5 μm; 4.6 mm x 250 mm; Grace Davison Discovery Sciences, Deerfield, IL) was performed using a 1 mL/min flow rate and a 20 min

gradient from 15% acetonitrile in H_2O with 0.1% formic acid to 90% acetonitrile in H_2O with 0.1% formic acid.

4.2.10 Construction of expression vectors containing *ptmT2* and *ptmT3*

The pCDF-2 Ek/LIC vector system was used to create expression vectors for overproducing PtmT2 and PtmT3 as N-terminally His_6-tagged fusion proteins. The gene encoding PtmT2 was amplified using the primers, PtmT2pCDF2For and PtmT2pCDF2Rev (**Table A1.1**). PCR was performed with the Expand High Fidelity PCR system as described by the manufacturer (Roche Applied Science). The amplified gene was treated with T4 DNA polymerase to generate single-stranded overhangs and annealed into the pCDF-2 Ek/LIC vector. The annealed vector/insert mixture was transformed directly into *E. coli* DH5α chemically competent cells according to standard protocols (*11*). The recombinant plasmid, pBS12250, containing *ptmT2*, was purified from E. coli DH5α cells and transformed into E. coli BL21(DE3) chemically competent cells. A similar procedure was used to amplify the gene encoding PtmT3, using the primers, PtmT3pCDF2For and PtmT3pCDF2Rev (**Table A1.1**), and yielded the recombinant plasmid, pBS12251.

4.2.11 Construction of expression vectors containing *ptmT1*

The gene encoding PtmT1 was amplified using the primers, PtmT1pCOLDFor and PtmT1pCOLDRev (**Table A1.1**). PCR was performed with the Expand High Fidelity PCR system as described by the manufacturer (Roche Applied Science). The resulting PCR product was digested and ligated into pCOLD-Tf via *NdeI* and *EcoRI* restriction sites, yielding pBS12252.

4.2.12 Overproduction and purification of recombinant enzymes in *E. coli*

Expression constructs were introduced into chemically competent *E. coli* BL21(DE3) cells by transformation and plated on LB containing 50 µg/mL streptomycin. A single colony was used to inoculate 50 mL of LB containing 50 µg/mL streptomycin and cultured overnight at 37°C. A 5 mL aliquot from the overnight culture was used to inoculate 500 mL of LB containing 50 µg/mL streptomycin, and the culture was incubated at 37°C and 250 rpm until it reached an OD_{600} of ~0.5. The culture was cooled to 18°C, and recombinant protein expression was induced by adding IPTG to a final concentration of 0.1 mM. Incubation was continued at 18°C with 250 rpm shaking for ~16-24 hrs before the cells were harvested by centrifugation at 4°C and 4150 rpm for 30 min. The cells were resuspended in 3-fold (w/v) lysis buffer (100 mM Tris, pH 8.0, 300 mM NaCl, 10% glycerol, 15 mM imidazole with ~1 mg/mL lysozyme and protease inhibitor cocktail (Roche)) and incubated with gentle mixing at room temperature for 30 min. The cells were cooled in an ice bath for 5 min prior to sonication on ice (medium power level output for 4 x 30 second cycles with one second pulses). The lysate was centrifuged at 15,000 rpm for 30 min, and the resulting supernatant was filtered through in-line 0.8 µm and 0.45 µm HPF Millex-HV 25 mm syringe driven filters prior to Ni-NTA mediated purification of His_6-tagged proteins.

4.2.13 FPLC methods for protein purification

An ÄKTA FPLC system (Amersham Pharmacia Biotech) with a HisTrap FF 5 mL column (GE Healthcare Life Sciences) was used to facilitate protein purification. Filtered supernatant was loaded onto the HisTrap FF column, washed with 10 column volumes Buffer A (50 mM Tris, pH 8.0, 15 0 mM NaCl, and 20 mM imidazole) and eluted with 50% Buffer B (50 mM Tris, pH 8.0, 100 mM NaCl, and 500 mM imidazole) at a flow rate of 2 mL/min. Fractions

(1.5 mL) were collected and analyzed using SDS-PAGE. Desired fractions were pooled and desalted using a HiPrep Desalting 26/10 column according to recommended protocols (Amersham Pharmacia Biotech). The desalted sample was concentrated using a Vivaspin 20 (30,000 MWCO, Sartorius-Stedim) and flash frozen in liquid nitrogen before storage at -80°C.

4.2.14 Synthesis and purification of GGDP from geranylgeraniol

Methods of synthesis and purification were modified from previously described reports (*14*, *15*). Geranylgeraniol (464 mg, 1600 µmol neat alcohol) was combined with trichloroacetonitrile (2 mL, ~20 mmol). A "TEAP" solution was prepared by slowly adding 3.64 mL of solution A (dilute 2 mL of concentrated phosphoric acid into 6.5 mL acetonitrile) to 6 mL solution B (5.5 mL triethylamine into 5 mL acetonitrile) with constant stirring. After mixing, 2 mL of the TEAP solution was added to the reaction mixture containing geranylgeraniol. The reaction mixture was incubated at 37°C for 5 min. This incubation was followed by 2 x 2 mL additions of TEAP solution with 5 min incubations at 37°C after each addition. A Buchi MPLC system (C-605/C-615) with a column (230 mm x 26 mm) packed with silica gel (230-400 mesh) was used for separation of the reaction mixture and purification of the desired GGDP product. The column was equilibrated at 10 mL/min using the following mobile phase: i-PrOH:NH_4OH:H_2O (6:2.5:0.5, v/v) before the reaction mixture (~8 mL, deep yellow in color) was applied to the column. The flow rate of mobile phase was resumed at 10 mL/min and the reaction mixture was subsequently eluted isocratically. Fractions (~8 mL/fraction) were collected just after a visible yellow band began to elute off the column (Note: a visible yellow band was observed previously on prep-TLC purification of smaller scale reaction mixture, with an R_f value of ~0.85-0.9). A total of 94 fractions were collected and analyzed by TLC for GGDP-containing fractions (see **Appendix, section A1.4.4)**. Pooled fractions were filtered,

concentrated with a rotary evaporator, diluted with equal volumes MeOH and 10 mM NH_3HCO_3, and stored at -20°C.

4.2.15 Enzyme assays

Enzyme reactions (500 µL) contained 50 mM Tris, pH 7, 1 mM $MgCl_2$, 5 mM 2-mercaptoethanol, 10% glycerol, and 100 µM GGDP substrate. The reactions were initiated by adding recombinant enzyme and incubated at 30°C for 1 hr. The reactions were terminated by extracting the assay mixtures with 3 x 0.5 mL of hexanes. The hexane extracts were pooled, concentrated by vacuum, and stored at -20°C prior to GC-MS analysis. A 10 U aliquot of calf-intestinal alkaline phosphatase (CIAP, 10,000 U/mL, New England Biolabs, Ipswich, MA) was then added to the previously extracted aqueous layer and allowed to incubate at 37°C for 4 hrs. This step enzymatically cleaves off the diphosphate moieties from GGDP substrate or diphosphate-containing products that remain in the aqueous layer. The dephosphorylated diterpene alcohols can then be extracted into an organic layer. The CIAP-treated aqueous layer was subsequently extracted three times with 3 x 0.5 mL of hexanes. This second pool of "CIAP-treated" hexane extracts was concentrated in vacuum and stored at -20°C prior to GC-MS analysis.

4.2.16 GC-MS analysis of products

Samples were resuspended in 100 µL hexanes before analysis. GC-MS analysis was performed on an Agilent Technologies 5973N MSD (electron-ionization mode, 70 eV) with a 6890 Series Gas Chromatograph containing an HP-5ms column [(5%-Phenyl)-methylpolysiloxane, 30 m x 0.25 mm ID x 25 µm film). The sample (0.5-1 µL) was injected at 275°C in splitless mode with the following program for the column oven temperature: (i) isothermal hold at 40°C for 3 min, (ii) a temperature gradient at 20°C/min to 300°C, and (iii)

isothermal hold at 300°C for an additional 4 min. The mass spectral data (50-500 *m/z*) were collected during the temperature ramp and final hold.

4.3 Results

4.3.1 Gene inactivation of *ptmT3* in *S. platensis* MA7327 abolishes PTM production

In order to confirm the functional assignment of PtmT3 as a type I DTS contributing to PTM biosynthesis, gene inactivation of *ptmT3* was carried out in *S. platensis* MA7327 to yield the Δ*ptmT3* mutant strain, *S. platensis* SB12008. This strain produced PTN exclusively under fermentation conditions for PTM and PTN production in wild-type *S. platensis* MA7327 (**Figure 4.1**). Furthermore, PTN was produced by SB12008 in approximately 9-fold greater titer than that observed in the wild type producing strain.

4.3.2 Gene inactivation of *ptmT1* in *S. platensis* MA7327 abolishes PTN production

Similarly, to investigate the role of PtmT1 as an apparent non-canonical DTS contributing to PTN biosynthesis, gene inactivation of *ptmT1* was carried out in *S. platensis* MA7327 to yield the Δ*ptmT1* mutant strain, *S. platensis* SB12007. Under the conditions for PTM and PTN production in wild-type *S. platensis* MA7327, the *S. platensis* SB12007 Δ*ptmT1* mutant strain did not produce PTN, but PTM production was unaffected (**Figure 4.1**).

4.3.3 Functional characterization of PtmT2 as a putative type II DTS

Recombinant overexpression of *ptmT2* in *E. coli* BL21(DE3) resulted in soluble N-terminally His_6-tagged fusion protein in high yield. Purification by FPLC, yielded ~22 mg of pure protein as determined by SDS-PAGE and Bradford assay (**Figure 4.2**). The enzymatic

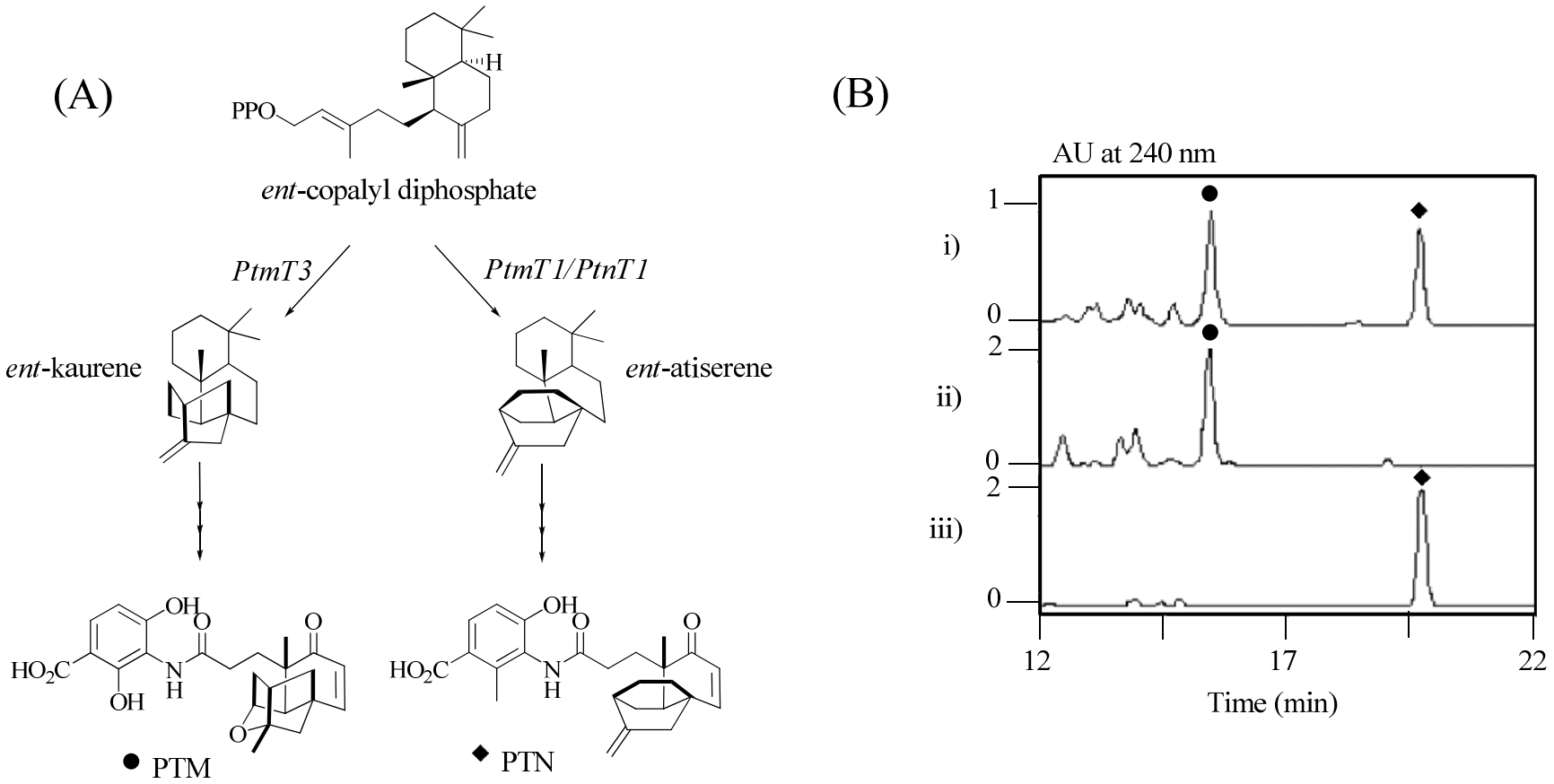

Figure 4.1 – Analysis of PTM and PTN production in wild-type and mutant strains of *S. platensis* MA7327. (A) Predicted pathway from *ent*-CPP to *ent*-kaurene (via PtmT3) or *ent*-atiserene (via PtmT1/PtnT1) and leading to PTM (●) or PTN (♦). (B) HPLC chromatograms of crude extracts produced by (i) wild-type *S. platensis* MA7327, (ii) Δ*ptmT1* mutant, *S. platensis* SB12007, and (iii) Δ*ptmT3* mutant, *S. platensis* SB12008.

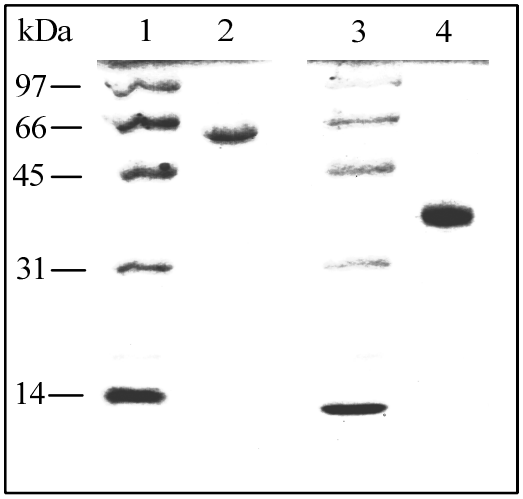

Figure 4.2 – SDS-PAGE of purified PtmT2 and PtmT3 proteins: lanes 1 and 3, low-range protein MW standards; lane 2, PtmT2 (57kDa); lane 4, PtmT3 (36kDa)

activity of purified PtmT2 was assayed using GGDP as a substrate and its product profile was analyzed by full-scan GC-MS analysis. After incubation of GGDP with the enzyme, the reaction was terminated by extraction with hexanes, yielding "extract A". The subsequent aqueous layer was treated with alkaline phosphatase and nonpolar compounds were again extracted with hexanes, yielding "extract B". Selected ion chromatograms monitoring m/z 257, m/z 272, or m/z 290 (fragment and molecular ion peaks of substrate and possible products) revealed no peaks in extract A, but two peaks in extract B corresponding to diterpene alcohols (**Figure 4.3**). Comparison of the mass spectra for each of these peaks to reference spectra confirmed their identity as geranylgeraniol, the diterpene alcohol of dephosphorylated GGDP substrate, and *ent*-copalol, the diterpene alcohol of dephosphorylated *ent*-CPP product (**Figure 4.3, Table 4.1**).

4.3.4 Functional characterization of PtmT3 as a putative type I DTS

Soluble, N-terminally His_6-tagged PtmT3 protein was obtained in similar high yields as PtmT2 from expression in *E. coli* BL21(DE3). After purification by FPLC, ~16 mg of pure protein was obtained as determined by SDS-PAGE and Bradford assay (**Figure 4.2**). Purified

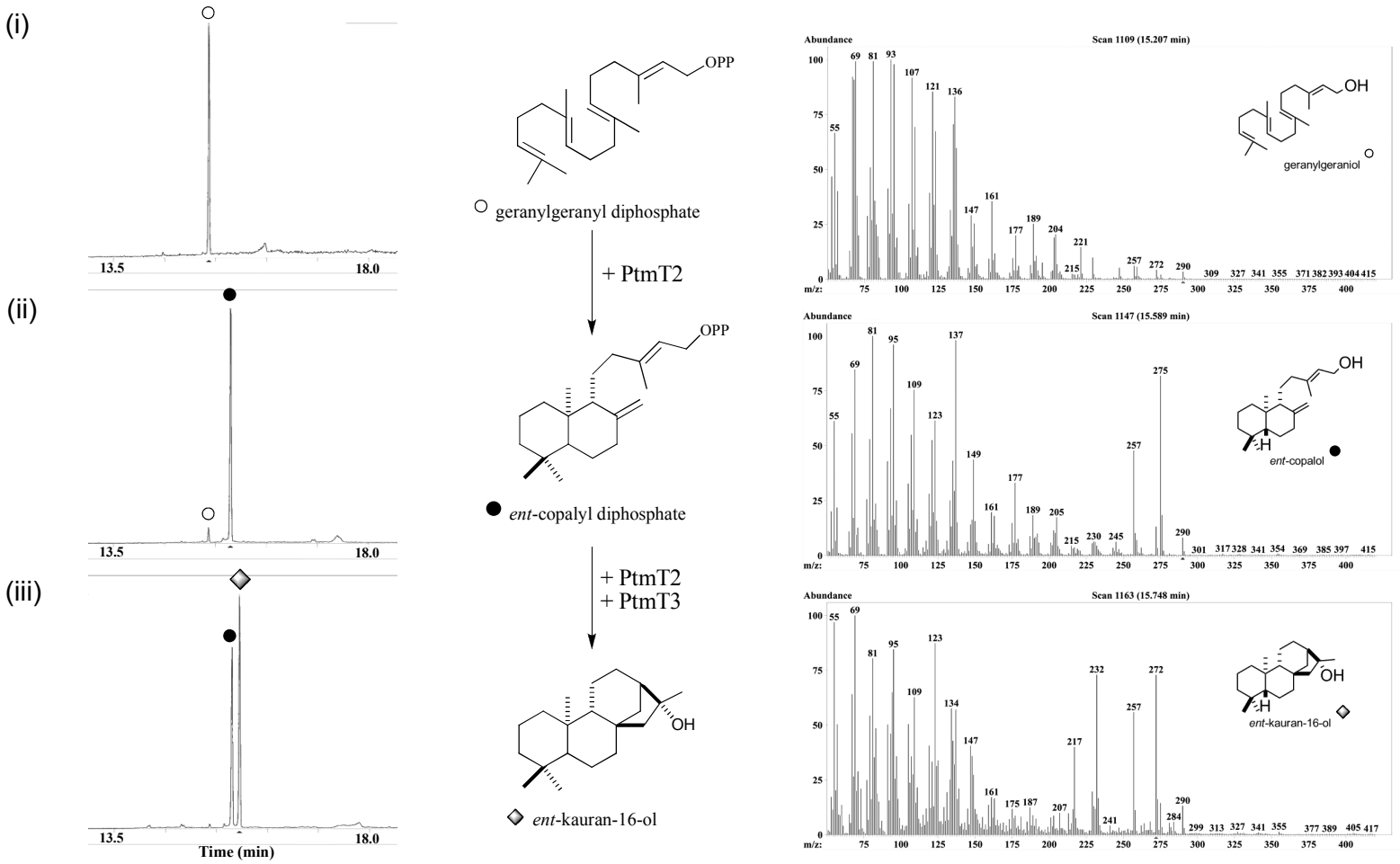

Figure 4.3 – Functional characterization of recombinant PtmT2 and PtmT3. GC-MS chromatogram (left) monitored ions at m/z 290 or m/z 272. GGDP substrate was incubated with PtmT2 alone, or PtmT2 and PtmT3. Mass spectra (right) of (i) geranylgeraniol (R_t = 15.207 min), open circle; (ii) *ent*-copalol (R_t = 15.589 min), closed circle; or (iii) *ent*-kauran-16-ol (R_t = 15.748 min), shaded diamond are shown. See **Appendix**, **section A1.5** for reference spectra.

Table 4.1 – Mass spectral data of the enzymatic products of PtmT2 and PtmT3

Recombinant Enzyme	Substrate	Product(s)	Retention time (min)	Parental and characteristic ions, m/z
PtmT2	GGDP	copalol[a]	15.589	290(M+), 275, 257, 177, 137, 109, 95, 81, 69
PtmT2 + PtmT3	GGDP	copalol[a]	15.589	290(M+), 275, 257, 177, 137, 109, 95, 81, 69
		kauran-16-ol	15.748	290(M+), 272, 257, 232, 123, 106, 94, 81, 69
Reference Standards:		geranylgeraniol[a]	15.207	290(M+), 275, 272, 257, 203, 93, 81, 69
		copalol[a]	nd[b]	290(M+), 275, 257, 177, 137, 109, 95, 81
		kaur-16-ene	nd[b]	272(M+), 257, 229, 213, 175, 147, 123
		kauran-16-ol	nd[b]	290(M+), 272, 257, 232, 134, 123, 94

[a]CDP/GGDP were treated with excess CIAP to detect as copalol or geranylgeraniol, respectively; [b]Compared with mass spectral data from literature and chemical databases

PtmT3 was assayed alone with GGDP, as well as in a coupled assay format with PtmT2, and the product profiles of these assays were analyzed by GC-MS analysis. The enzyme reaction mixtures were terminated by extraction with hexanes ("extract A") and the aqueous layer subjected to CIAP enzymatic dephosphorylation before a second extraction with hexanes ("extract B"). The reaction mixture containing PtmT3 and GGDP did not yield an enzymatic product – only the diterpene alcohol of GGDP, geranylgeraniol, was detected in selected ion chromatograms monitoring m/z 257, m/z 272, or m/z 290 in extract B. The coupled assay, containing GGDP substrate, PtmT2, and PtmT3 yielded two enzymatic products. Dephosphorylated diterpene alcohols of the GGDP substrate and PtmT2 product, *ent*-CPP, were detected in extract B, while a single, nonpolar product was detected in extract A. The nonpolar product was identified by comparison to reference spectra, and characteristic mass spectral fragmentation, as *ent*-kauran-16-ol (**Figure 4.3 and Table 4.1**) (*16*).

4.3.5 Expression, overproduction, and purification of PtmT1

In contrast to *ptmT2* and *ptmT3*, attempts for recombinant expression of *ptmT1* in E. coli were initially unsuccessful using a variety of expression vector systems. The *ptmT1* gene has now been cloned into the pCOLD-TF vector and expressed as a soluble form in *E. coli* BL21-CodonPlus cells. Although the enzyme can be purified by Ni-NTA chromatography and FPLC methods, it is still obtained in very low yield (**Figure 4.4**).

4.3.6 Expression of the "PTM cassette" (from *S. platensis* MA7327) in *S. platensis* MA7339 converts strain into a PTM/PTN dual producer

A 5.4 kB DNA fragment containing the annotated genes, *ptmO3*, *ptmO4*, *ptmT3*, *ptmO5*, and *ptmR3* in the *ptm* cluster was designated the "PTM cassette", as the complete absence of a homologous region in the *ptn* cluster suggested this locus contributes solely to PTM production.

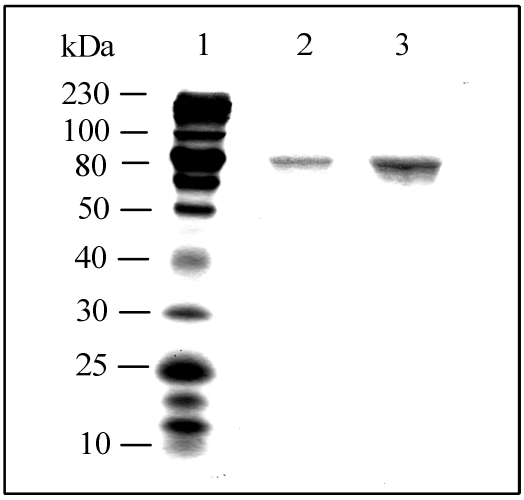

Figure 4.4 – SDS-PAGE of purified PtmT1 protein. Lane 1, broad-range protein MW standards; lanes 2 and 3, PtmT1 (33 kDa + 52 kDa TF fusion tag)

Fermentation and HPLC analysis of a recombinant *S. platensis* MA7339 strain containing a heterologous PTM cassette (*S. platensis* SB12604) revealed conferred PTM production at approximately 25 mg/L. PTN was still produced in trace amounts and was readily identified by LC-MS (**Figure 4.6**). The high level of PTM production compared with native PTN production is likely attributed to the high level expression of the PTM cassette by the *ErmE** promoter.

4.3.7 Identification of Sros_3708 from *Streptosporangium roseum* DSM43021 as a PtmT1/PtnT1 homolog

The primary amino acid sequence of PtmT1 shows no significant sequence similarity to known type I DTSs, nor does it contain any signature DTS sequence motifs. However, it is homologous to the UbiA family of aromatic prenyltransferases, which are distant structural and functional relatives of terpene synthases. Sequence alignments of PtmT1 with prototypical prenyltransferases revealed PtmT1 does not contain two canonical prenyltransferase DDxxD motifs, but does contain two putative atypical DxxxD motifs that align with the prenyltransferase active site regions (**Figure 4.5)** (*17*). Most of the PtmT1 homologs revealed in sequence

(A)

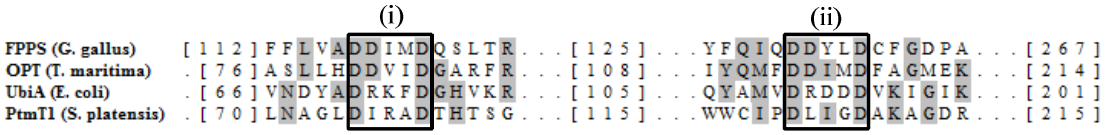

(B)

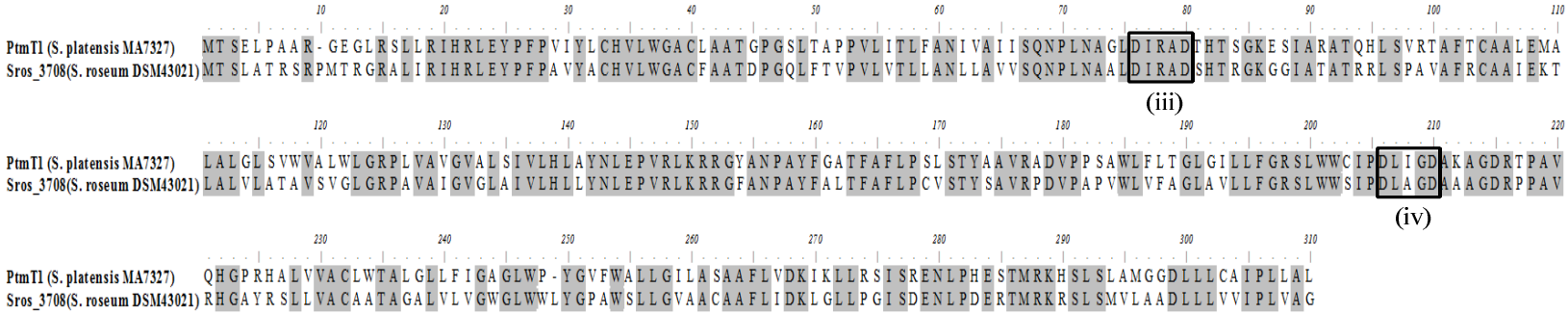

Figure 4.5 – Primary sequence alignments of PtmT1 and database homologs. (A) PtmT1 contains two atypical putative active site motifs, diverged from two canonical DDxxD motifs, (i) and (ii), present in characterized prenyltransferases: FPPS, farnesyl pyrophosphate synthase (P08836); OPT, octaprenyl pyrophosphate synthase (1V4E_B); UbiA, 4-HBA polyprenyltransferase (AEE59373); and PtmT1, ent-atiserene synthase (ACO31274). (B) PtmT1 shows high sequence similarity (63.5% identity over 309 aa), including two putative active site motifs DxxxD, (iii) and (iv), to a protein of unknown function from a whole genome sequence: Sros_3708 (ACZ86631), annotated as a hypothetical protein in *Streptosporangium roseum* DSM43021.

database searches are uncharacterized, putative proteins that have been identified through whole genome sequencing projects. None of these homologs are annotated as putative terpene synthases and many have not been assigned a predicted function based on sequence homology to proteins of known function. One such PtmT1 homolog, Sros_3708 (GenBank: ACZ86631), is annotated as a "protein of unknown function" and was identified from the complete genome sequence of *Streptosporangium roseum* DSM43021 (GenBank: CP001814). PtmT1 and Sros_3708 share 63.5% sequence identity including the two putative DxxxD motifs (**Figure 4.5**).

4.3.8 Expression of *sros_3708* in *S. platensis* SB12007 restores PTN production

The high sequence similarity between PtmT1 and Sros_3708 suggested these two proteins could share functional activity – as type I DTSs with non-canonical active site motifs. The *Streptosporangium roseum* DSM43021 strain was obtained and *sros_3708* was cloned from extracted genomic DNA for heterologous expression in *S. platensis*. The *S. platensis* MA7327 Δ*ptmT1* mutant strain, *S. platensis* SB12007, produces PTM, but has lost the ability to produce PTN (**Figure 4.6**). Complementation of the *ptmT1* mutant strain by overexpression of recombinant *sros_3708* was attempted. Notably, PTN production was restored in the *S. platensis* SB12007 strain harboring pBS12017 (a pSET152 derivative containing *sros_3708* and an upstream *ErmE** promoter) (**Figure 4.6**).

4.4 Discussion

4.4.1 PTM and PTN are "labdane-related" diterpenoids proceeding through a common *ent*-CPP intermediate

More than 12,000 diterpenoid natural products are known to date and all derive from the common linear precursor, (E,E,E)-geranylgeranyl diphosphate. A majority of diterpenoids contain polycyclic scaffolds, which can originate from either a single cyclization

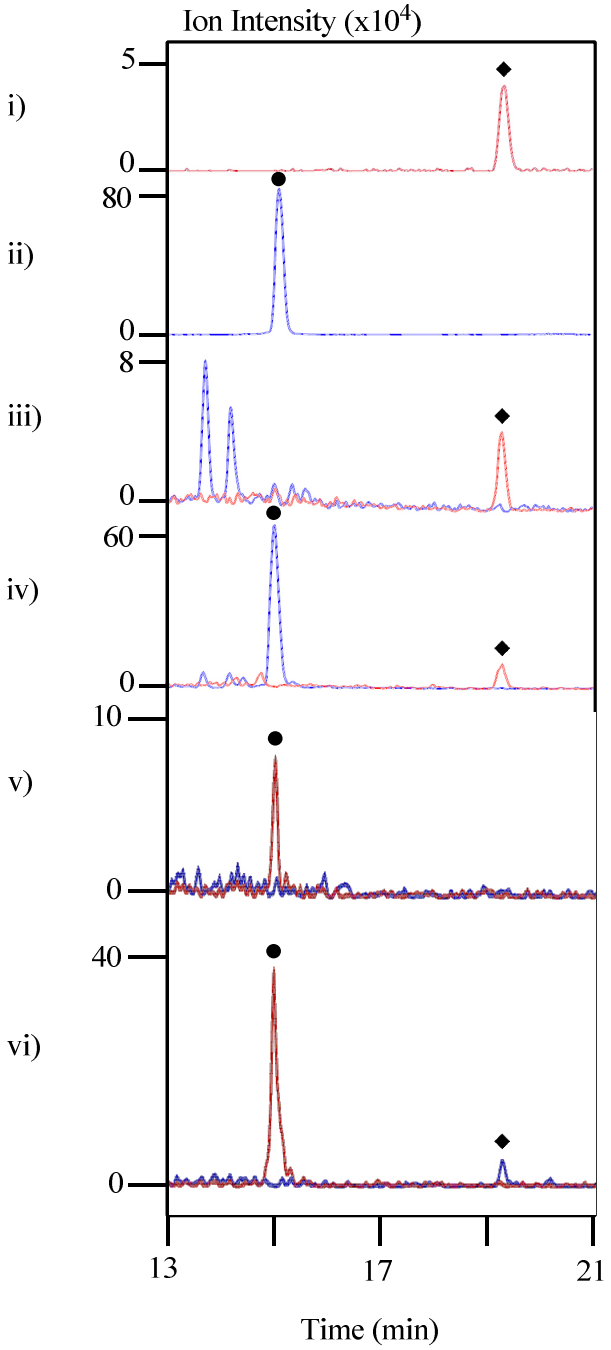

Figure 4.6 – Analysis of WT and modified strains of *S. platensis* containing recombinant DTS genes. LC-MS extracted ion chromatograms showing (i) authentic PTN, (ii) authentic PTM, (iii) crude extract produced by wild-type *S. platensis* MA7339, (iv) crude extract produced by the PTM cassette-containing mutant, *S. platensis* SB12604, (v) crude extract produced by the Δ*ptmT1* mutant, *S. platensis* SB12007, and (vi) crude extract produced by *S. platensis* SB12007 harboring the *sros_3708* over-expression construct, pBS12017. Traces show extracted m/z=426 for PTN (♦) or m/z=442 for PTM (●).

step, or as a result of two discrete cyclization/rearrangement reactions catalyzed by distinct enzymatic mechanisms. Notably, the two-step cyclization/rearrangement cascade is common among diterpenoid biosynthetic pathways, but is rarely seen in the biogenesis of other terpenoid natural product classes (e.g., mono-, sesqui-, or tri- terpenoids). The first step of the dual cyclization pathway for polycyclic diterpenoids involves a protonation-initiated cyclization (type II DTS mechanism) of GGDP. Interestingly, although mono- or tri-cyclization is theoretically possible, only bicyclization of GGDP to a labda-13-en-8-yl diphosphate intermediate has been observed. Stereochemical and skeletal diversity can be generated from this initial labda-13-en-8-yl diphosphate carbocation intermediate during the type II cyclization reaction step resulting in a number a possible bicyclic isoprenyl diphosphate scaffolds – designated "labdane-related" diterpenoid precursors (*18*). The most common of these bicyclic diphosphate intermediates are simply stereoisomers of copalyl/labdienyl diphosphate (CPP) – the stereochemistry depends on the prochiral conformation of the GGDP precursor prior to catalysis (**Figure 4.7**). However, other unique bicyclic scaffolds can be generated from rearrangements (e.g., hydride or methyl shifts) prior to the quenching of the reactive carbocation (**Figure 4.8**). Finally, since these bicyclic scaffolds retain the allylic diphosphate ester linkage from GGDP, they are substrates for ionization-dependent cationic cyclization (type I DTS mechanism), a cyclization mechanism more common among all terpene synthases. This second distinct cyclization reaction specifically converts the diphosphate-containing bicyclic precursors into unique tricyclic, tetracyclic, or even pentacyclic scaffolds, which are ultimately transformed via downstream tailoring steps into the myriad of diterpenoid natural products.

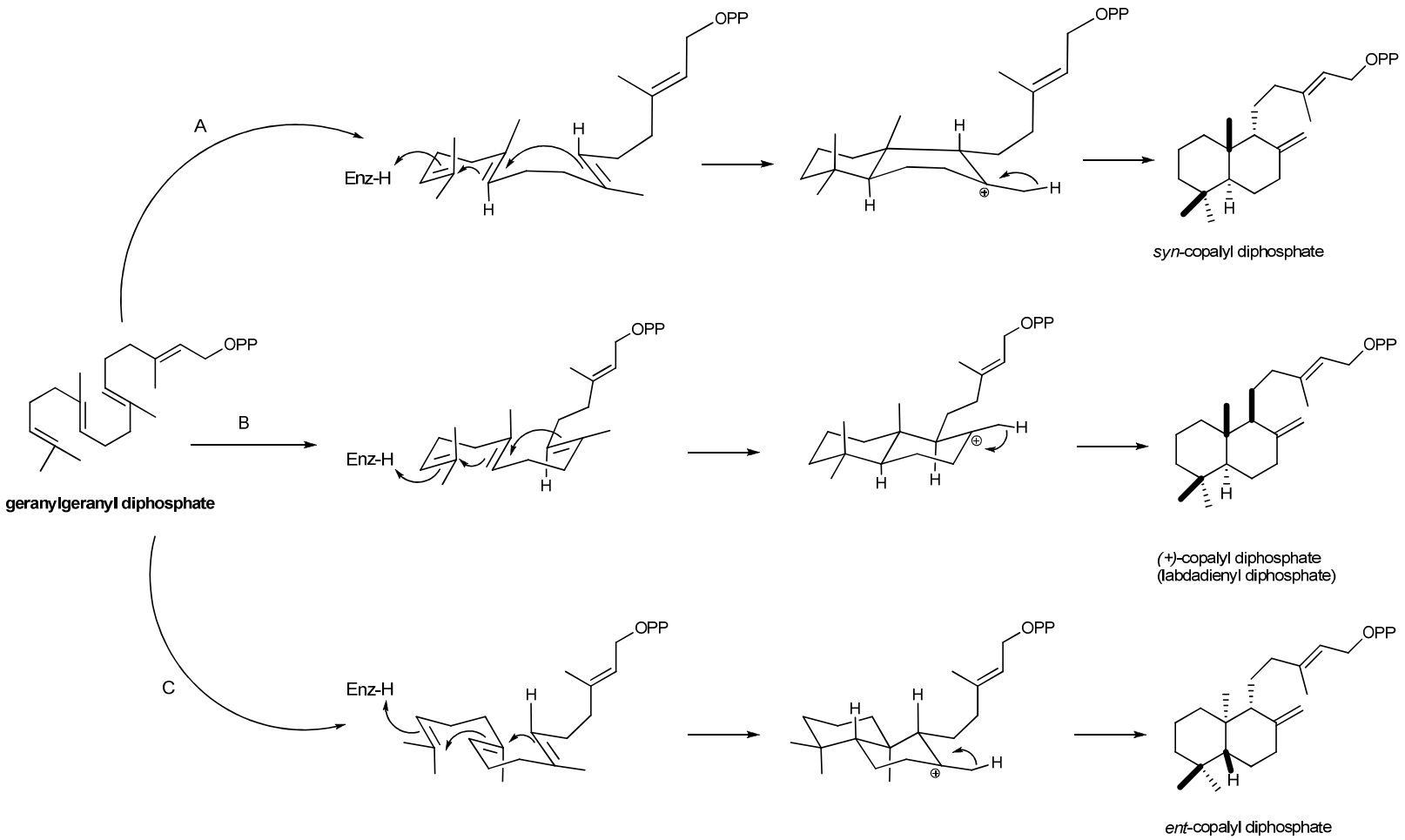

Figure 4.7 – Mechanisms of cyclization for stereoisomers of copalyl diphosphate. The stereochemistry depends on the prochiral conformation of the GGDP precursor in the active site prior to catalysis by a type II DTS. A pro-chair-boat conformation leads to "*syn*" orientation, (path A), while a pro-chair-chair conformation leads to either of two isomers, normal (+) or enatiomeric ("*ent*") orientation (path B and path C, respectively). (Normal orientation is defined as compared to the stereochemistry of the analogous A/B rings in cholesterol) (18).

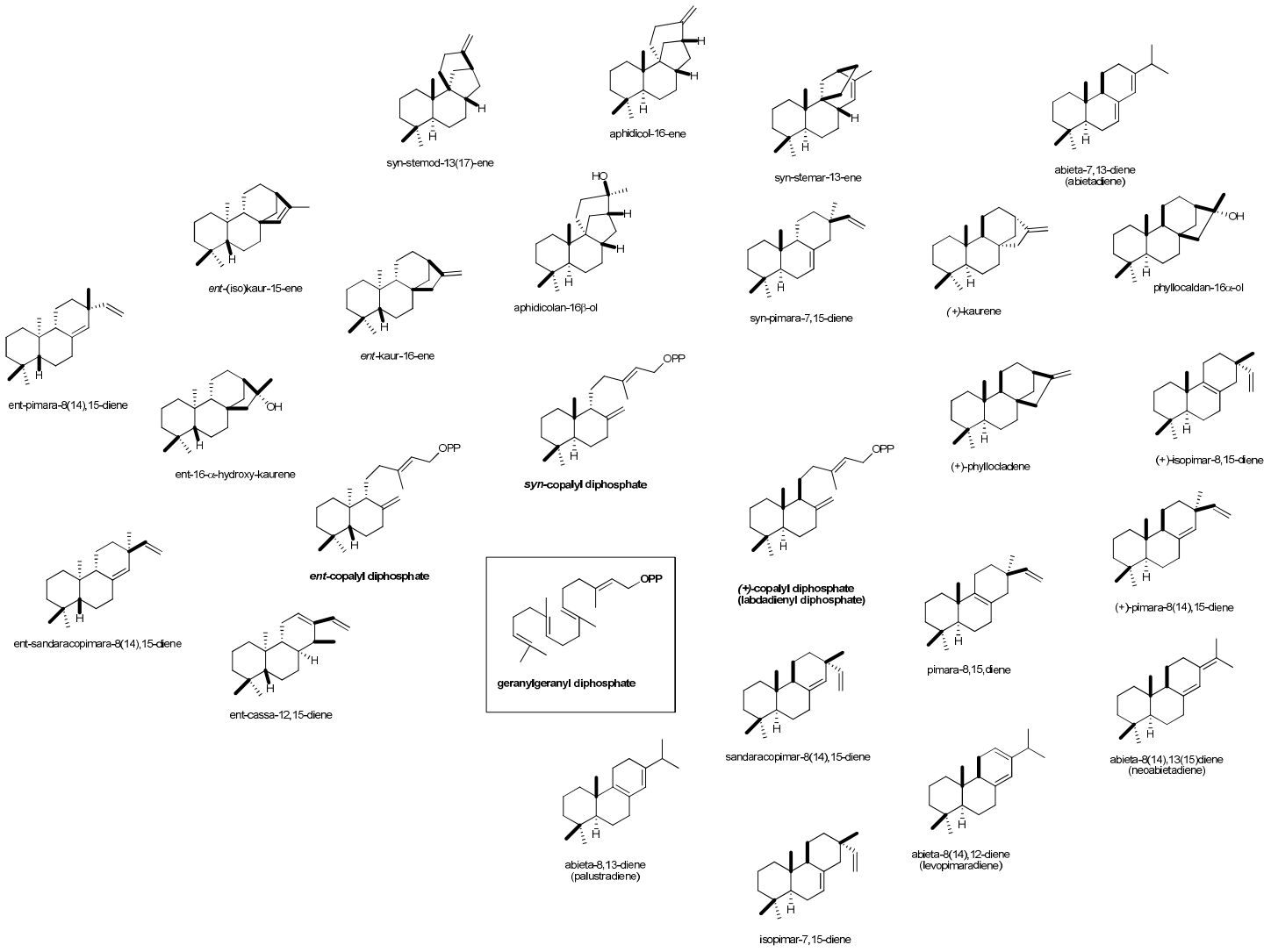

Figure 4.8 – Chemical structures of labdane-related diterpene scaffolds isolated from plant and fungal organisms. The structures shown each originate from GGDP and proceed through a bicyclic, labda-13-en-8-yl diphosphate intermediate.

The unique hydrocarbon scaffolds of PTM and PTN are structurally and stereochemically similar to *ent*-kaurene and *ent*-atiserene, diterpenes that are known intermediates in the biosynthetic pathways of many diterpenoid natural products. Furthermore, *ent*-kaurene and ent-atiserene are tetracyclic compounds that are produced via a type I DTS cyclization of the bicyclic diphosphate intermediate, *ent*-CPP. Characterization of the *ptm* and *ptn* clusters confirmed that PTM and PTN diterpenoid biosynthesis follows a typical two-step cyclization cascade for labdane-related diterpenoids. These studies have revealed that the initial cyclization step in each cluster, producing *ent*-CPP from the universal diterpenoid precursor, GGDP, is catalyzed by PtmT2 and PtnT2, type II DTS homologs that contain the canonical type II DTS active site motif. *In vitro* functional analysis confirmed PtmT2 is an *ent*-CPP synthase as it converts a GGDP substrate into a single *ent*-copalyl diphosphate product (**Figure 4.3**). PtmT2/PtnT2 provide the most advanced common diterpene intermediate in PTM and PTN biosynthesis and the substrate for type I DTSs responsible for catalyzing the second cyclization step into the predicted *ent*-kaurene and *ent*-atiserene type scaffolds.

4.4.2 PtmT3 and PtmT1/PtnT1 are discrete type I DTSs that channel *ent*-CPP into the PTM and PTN scaffolds, respectively

In order to clarify its role in either PTM or PTN biosynthesis, *ptmT3* was inactivated in *S. platensis* MA7327, a dual producer of PTM and PTN. Inactivation of *ptmT3* abolished PTM production, but increased PTN titer approximately nine-fold compared with the wild-type strain (**Figure 4.1**). These results now exclude PtmT3 from participating in PTN biosynthesis and support the functional assignment of PtmT3 as type I DTS dedicated to PTM biosynthesis. Furthermore, the increase in PTN titer in the Δ*ptmT3* mutant strain demonstrates that a discrete type I DTS is responsible for the PTN diterpenoid scaffold and channels excess *ent*-CPP

precursor toward PTN biosynthesis in the absence of PtmT3, which typically competes for this common substrate.

As described previously, in the absence of an obvious candidate type I DTS in the *ptn* cluster, PtnT1 was annotated as a putative atypical DTS contributing to an *ent*-atiserene type scaffold for PTN biosynthesis based on limited sequence similarity to the UbiA family of aromatic prenyltransferases. The *ptm* cluster homolog, PtmT1, was similarly annotated. In order to confirm any possible contribution PtmT1/PtnT1 may have in PTM or PTN biosynthesis, *ptmT1* was inactivated in *S. platensis* MA7327. Production of PTN was completely abolished in the subsequent Δ*ptmT1* mutant strain, while PTM production was unaffected (**Figure 4.1**). This result clearly established the role of PtmT1/PtnT1 in PTN biosynthesis. The exclusive production of an *ent*-atiserene intermediate by a DTS represents an as yet undescribed pathway for diterpenoid biosynthesis since no *ent*-atiserene synthase has been reported – notably, *ent*-atiserene production has only been observed *in vitro* as a minor product from an *ent*-pimaradiene synthase with a mutated active site (*9*). Furthermore, the lack of signature type I DTS metal-binding motifs and no significant sequence similarity to other DTSs may suggest that PtmT1/PtnT1 represent a new family of DTSs.

4.4.3 PtmT3 is a type I DTS producing *ent*-kauran-16-ol from *ent*-CPP

A mechanistic scheme for a cyclization/rearrangement pathway from *ent*-CPP leading to the tetracyclic diterpene, *ent*-kaur-16-ene, is illustrated in **Figure 4.9**. The pathway begins with formation of an *ent*-pimara-15-en-8-yl+ carbocation intermediate from diphosphate ionization-initiated tricyclization of *ent*-CPP. Tetracyclization then occurs, connecting C-16 to C-8 to form an *ent*-beyer-15-yl+ intermediate. This intermediate can undergo further ring rearrangement, including an alkyl shift where the C-12 to C-13 bond is broken and a new bond between C-12

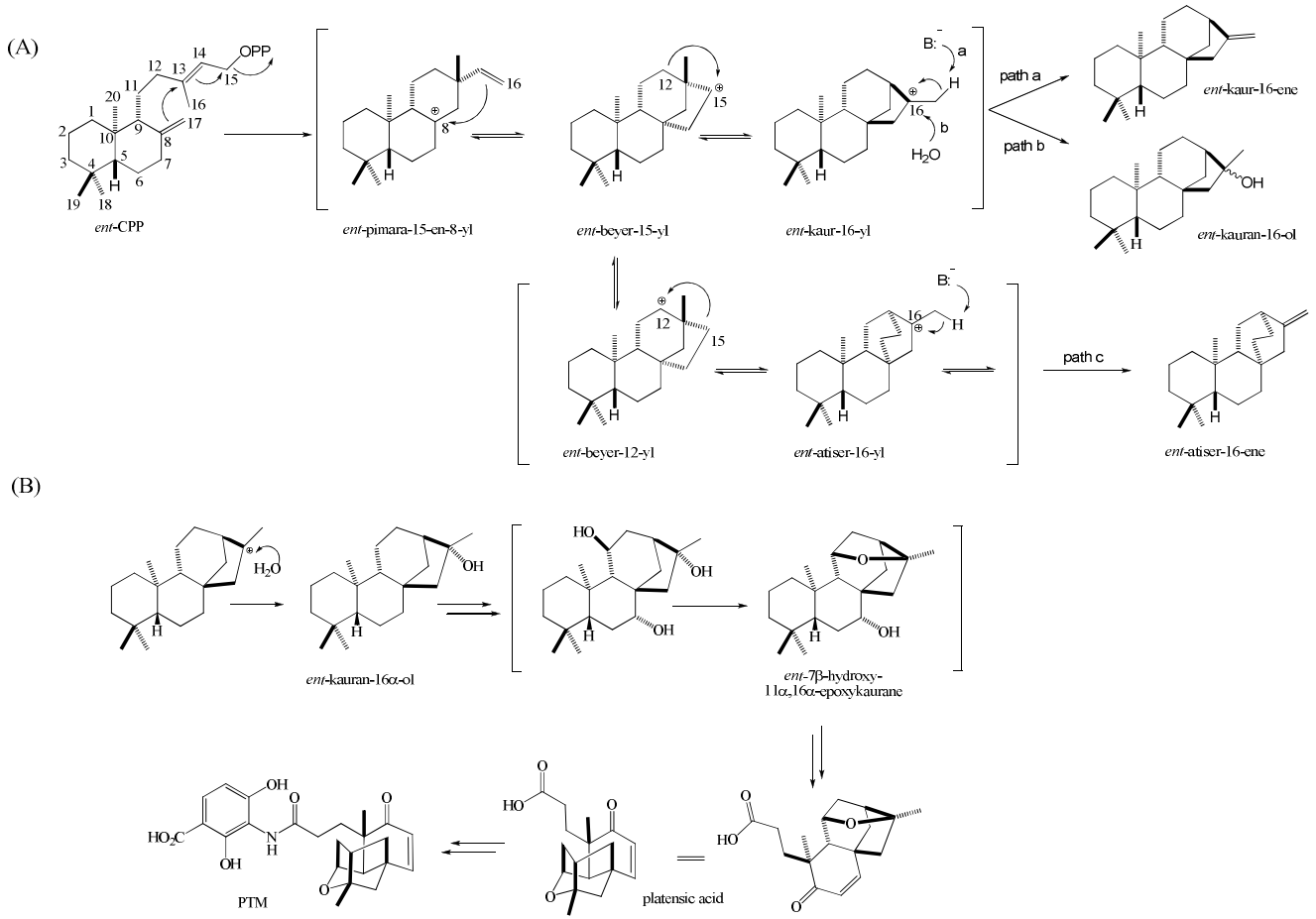

Figure 4.9 – Pathways for biosynthesis of tetracyclic diterpene scaffolds contributing to PTM and PTN production. (A) Proposed pathway from *ent*-CPP through various tricyclic and tetracyclic intermediates to *ent*-kaurene, *ent*-kauran-16-ol, and *ent*-atiser-16-ene products; quenching of an ent-kaur-16-yl+ carbocation occurs through deprotonation (path a) or addition of water prior to deprotonation (path b). (B) Proposed formation of the PTM ether bridge based on a similar pathway for formation of *ent*-7β-hydroxy-11α,16α-epoxykaurane from *ent*-kauran-16α-ol in *Gibberella fujikuroi* (*19*).

and C-15 is formed, followed by quenching of the carbocation by deprotonation of a neighboring methyl group to produce the *ent*-kaurene product (*9, 18*). Biosynthesis of PTM is predicted to proceed through an *ent*-kaurene intermediate and PtmT3 is likely responsible for its formation. Interestingly, functional analysis of recombinant PtmT3 enzyme *in vitro* revealed that PtmT3 selectively produces a hydroxylated, *ent*-kauran-16-ol product (**Figure 4.3, Table 4.1**). Biosynthesis of *ent*-kauran-16-ol is predicted to follow the same mechanistic steps involved in conversion of *ent*-CPP to *ent*-kaurene, with the exception that the ent-kaur-16-yl+ carbocation is captured by water prior to deprotonation, leading to the hydroxylated variant. Although the absolute stereochemistry of the hydroxyl has not yet been determined, there is precedence for the α-configuration: *ent*-kauran-16α-ol (also referred to as ent-16α-hydroxy- kaurene) has been isolated as a minor product from *Giberella fujikuroi* and also from a functionally characterized DTS in *Physcomitrella patens;* in addition, a related tetracyclic diterpene scaffold, phyllocladan-16α-ol (**Figure 4.8**), is a product of DTS from *Phomopsis amygdali* (*19–21*). The mechanisms underlying this unique variation of carbocation quenching have been explored in plant DTSs (*Physcomitrella patens*) and future comparative analyses among bacterial DTSs yielding kaurene and other tetracyclic products may also reveal insights into how DTS active site variation affects product profile (*20, 22*). Finally, the identification of *ent*-kauran-16-ol, rather than *ent*-kaure-16-ene, as the diterpene intermediate in the PTM biosynthetic pathway has implications in the downstream steps leading to the unique ether-containing PTM moiety. Specifically, formation of *ent*-7β-hydroxy-11α,16α-epoxykaurane from *ent*-kauran-16α–ol (**Figure 4.9**) has been observed in *Giberella fujikuroi*, although the biosynthetic machinery responsible for this transformation have not been characterized (*19*). The *ent*-7β-hydroxy-11α,16α-epoxykaurane structure is a feasible intermediate in a predicted pathway for modification of the ent-kauran-16-ol diterpene

moiety into platensic acid (**Figure 4.9**) and this insight may guide future studies on the oxidative tailoring steps involved in PTM biosynthesis.

4.4.4 Modularity in the PTM and PTN biosynthetic pathways

As all diterpenoids derive from a common origin, GGDP, a degree of modularity should exist among diterpenoid biosynthetic pathways. The utility of this inherent modularity has been demonstrated previously through recombinant "mixing and matching" of various (plant) type I and type II DTSs in an *E. coli* strain engineered to produce GGDP. These methods successfully yielded the desired diterpene scaffolds (*23*, *24*). Modularity in the PTM/PTN-producing strains was demonstrated by successfully converting the PTN-producing strain, *S. platensis* MA7339, into a PTM/PTN dual producer by heterologously expressing PtmT3, and other predicted PTM-specific tailoring genes located on the aforementioned "PTM cassette", in the MA7339 strain (**Figure 4.6**). The capacity of terpene pathways to swap in and out individual machinery, without an apparent need for protein-protein recognition or interaction among discrete enzymes, highlights the innate combinatorial nature of terpene biosynthesis and the source for the extraordinary structural diversity belonging to terpenoid natural products. Although the extent to which unique diterpene scaffolds can replace native scaffolds and proceed through existing biosynthetic pathways depends on the ability of the downstream tailoring enzymes to accept a new scaffold, the modular nature of these pathways can nonetheless be exploited for rational engineering of desired and novel diterpenoid compounds. In order for these methods to be successful, the full potential of diterpenoid biosynthetic pathways must be explored, including increasing the number of characterized DTSs, so as to begin to approximate the number of diterpenoid scaffolds available in Nature.

4.4.5 Discovery of new bacterial DTSs will expand the current catalytic landscape of DTS activity

Each new DTS characterized adds to a growing "biosynthetic toolbox" and further expands our understanding of the catalytic landscape contributing to DTS activity. Bacteria have emerged as significant producers of terpenoid – and now diterpenoid – natural products. As the evolutionary predecessors of eukaryotic DTSs, bacterial DTSs promise to extend our understanding of the minimal catalytic requirements of the core motifs and active site architecture. The number of characterized bacterial DTSs responsible for bacterial diterpenoid natural products has increased over the past decade, and these enzymes (and the biosynthetic pathways to which they belong) likely represent an underexplored source for chemical and catalytic diversity.

The characterization of the biosynthetic machinery responsible for PTM and PTN biosynthesis in *S. platensis* uncovered three new bacterial DTSs – PtmT1/PtnT2, PtnT2/PtnT2, and PtmT3 – increasing the number of sequences for comparison among the limited set of DTSs from bacterial origin. These enzymes have revealed conserved structural and mechanistic features: PtmT2 and PtmT3 are homologous to type II and type I DTSs, respectively, and have conserved signature asparatate motifs, and generate intermediates that are well-known among plant diterpenoid pathways. At the same time, both PtmT1 and PtmT3 now provide unique opportunities to expand the current understanding of the structural elements required for catalysis: PtmT3, although homologous to *ent*-kaurene synthases, displays a relatively unusual method for carbocation quenching through stereospecific addition of a water molecule to produce a hydroxylated version of a traditional *ent*-kaurene product; and, PtmT1, although lacking both the DDXXD and NSE/DTE motifs of typical type I DTS enzymes, is an apparent

atypical DTS converting an *ent*-CPP to an *ent*-atiserene type scaffold for PTN biosynthesis. Notably, PtmT1/PtnT1 represent a new family of DTSs responsible for a previously undescribed pathway for biosynthesis of diterpenoid natural products containing an atiserene type scaffold.

Although bioinformatics analysis provided little assistance in initial identification and annotation of PtmT1/PtnT1, the functional assignment of these enzymes as atypical DTSs now provides the means for discovery of previously unrecognized or misannotated homologs. The identification of Sros_3708 from *Streptosporangium roseum* DSM43021 as a homolog with high sequence similarity to PtmT1 provided a unique opportunity to test our hypothesis that uncharacterized and misannotated PtmT1 homologs deposited in sequence databases could also be atypical DTSs, with identical or similar catalytic activity and diterpene product profiles as PtmT1/PtnT1 (**Figure 4.5**). Significantly, Sros_3708 restored PTN production in a Δ*ptmT1* knockout mutant strain of *S. platensis* MA7327, confirming that Sros_3708 complements the loss of DTS activity provided by PtmT1 (**Figure 4.6**). Interestingly, the top four PtmT1 homologs identified in the NCBI database, including Sros_3708, are putative proteins that have been identified by whole genome sequencing methods. This allowed analysis of genetic organization on their respective chromosomes and insight into neighboring genes or clusters of genes. Remarkably, each of the four PtmT1 homologs are clustered in a three gene "set" that is homologous – both in sequence similarity and genetic organization – to PtmT2 (the ent-CPP synthase), PtmO2 (uncharacterized P450 monooxygenase), and PtmT1 in the *ptm* cluster and suggesting these clusters may represent previously unknown genetic loci for labdane-related diterpenoid natural products (**Figure 4.10**). These insights highlight the contributions that rapidly advancing technology now provide to traditional natural products discovery – in this case, the ever-growing number of sequenced bacterial genomes added to public databases allow

sequence gazing for novel enzymes (and entire biosynthetic pathways) with unique chemistries, which can then be cloned and characterized with incredible efficiency. Just as microorganisms have proven to be a rich source for other novel chemistry, they stand to provide significant contributions toward gaining access to the vast chemical space occupied by terpenoid natural products and will provide unique opportunities for engineered biosynthesis for drug discovery and industrial applications.

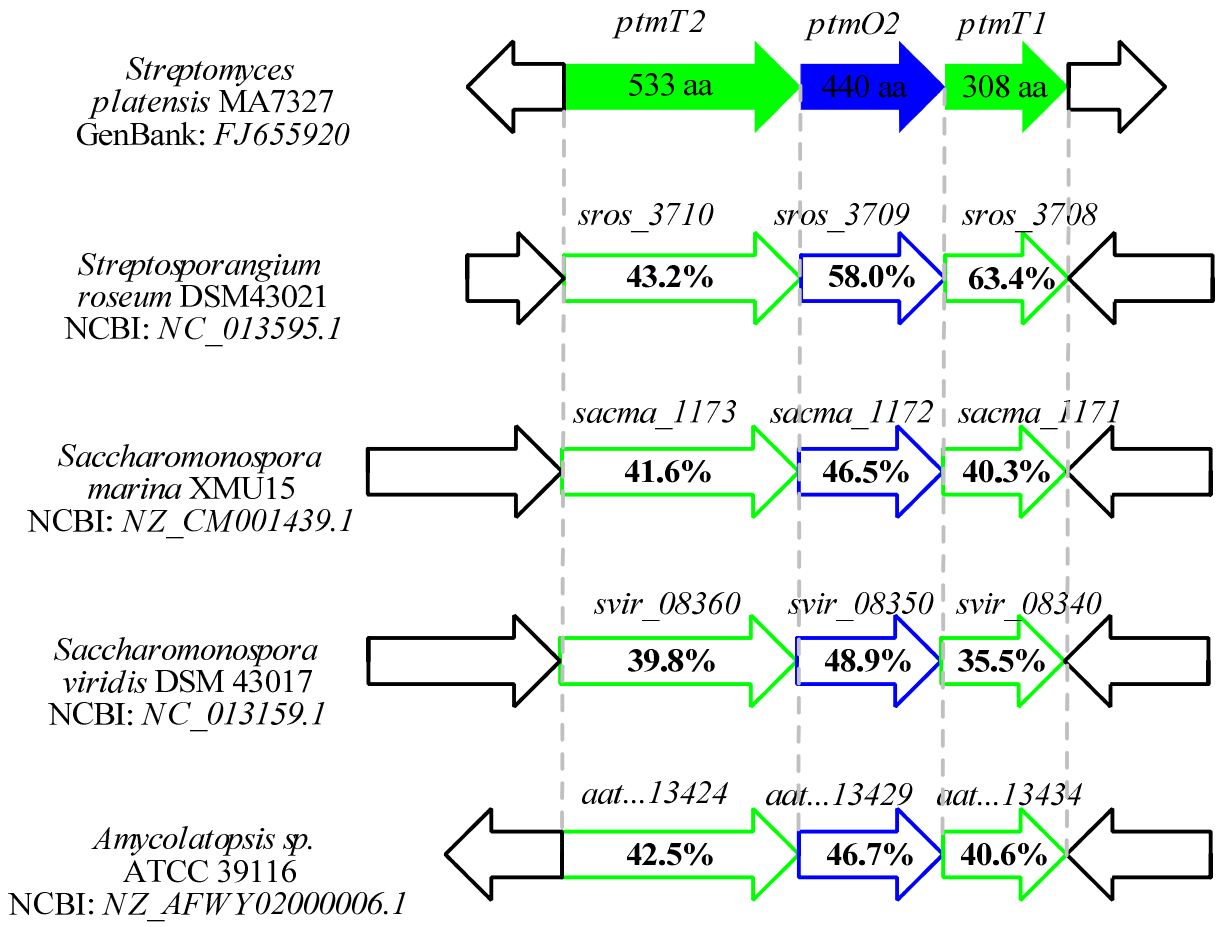

Figure 4.10 – Alignment of ORFs encoding homologs of PtmT1 and neighboring ORFs. Sequences obtained from NCBI whole genome sequences identified to contain PtmT1 homologs. Sequence identity (%) relative to homolog in *ptm* cluster (ptmT2, ptmO2, or ptmT1) is noted inside arrows indicating transcriptional direction of ORFs.

4.5 References

1. Smanski MJ, Yu Z, Casper J, Lin S, Peterson RM, Chen Y, Wendt-Pienkowski E, Rajski SR, Shen B (2011) Dedicated ent-kaurene and ent-atiserene synthases for platensimycin and platencin biosynthesis. *Proceedings of the National Academy of Sciences of the United States of America* 108:13498-13503.

2. Smanski MJ, Peterson RM, Shen B (2012) Platensimycin and platencin biosynthesis in Streptomyces platensis showcasing discovery and characterization of novel bacterial diterpene synthases. *Methods in Enzymology,* in press.

3. Herath KB, Attygalle AB, Singh SB (2007) Biosynthetic studies of platensimycin. *Journal of the American Chemical Society* 129:15422-15423.

4. Herath K, Attygalle AB, Singh SB (2008) Biosynthetic studies of platencin. *Tetrahedron Letters* 49:5755-5758.

5. Ikeda C, Hayashi Y, Itoh N, Seto H, Dairi T (2007) Functional analysis of eubacterial ent-copalyl diphosphate synthase and pimara-9(11),15-diene synthase with unique primary sequences. *Journal of Biochemistry* 141:37-45.

6. Christianson DW (2006) Structural biology and chemistry of the terpenoid cyclases. *Chemical Reviews* 106:3412-3442.

7. Yamaguchi S et al. (1996) Molecular cloning and characterization of a cDNA encoding the gibberellin biosynthetic enzyme ent-kaurene synthase B from pumpkin (Cucurbita maxima L.). *The Plant Journal* 10:203-212.

8. Christianson DW (2008) Unearthing the roots of the terpenome. *Current Opinion in Chemical Biology* 12:141-150.

9. Xu M, Wilderman P, Peters R (2007) Following evolution's lead to a single residue switch for diterpene synthase product outcome. *Proceedings of the National Academy of Sciences of the United States of America* 104:7397-7401.

10. Bräuer L, Brandt W, Schulze D, Zakharova S, Wessjohann L (2008) A structural model of the membrane-bound aromatic prenyltransferase UbiA from E. coli. *ChemBioChem* 9:982-992.

11. Sambrook J, Russel D (2001) *Molecular cloning: a laboratory guide* (Cold Spring Harbor Laboratory Press, Cold Spring Harbor).

12. Kieser T, Bibb MJ, Buttner M, Chater KF, Hopwood DA (2000) *Practical streptomyces genetics* (The John Innes Foundation Norwich, UK).

13. Gust B, Kieser T, Chater K (2002) *REDIRECT technology: PCR-targeting system in Streptomyces coelicolor* (The John Innes Foundation Norwich, UK).

14. Keller RK, Thompson R (1993) Rapid synthesis of isoprenoid diphosphates and their isolation in one step using either thin layer or flash chromatography. *Journal of Chromatography A* 645:161-167.

15. Cornforth R, Popjak G (1969) Chemical syntheses of substrates of sterol biosynthesis. *Methods in Enzymology* 81:359-390.

16. Kalinovsky AI et al. (1970) Mass spectrometry of kaurene derivatives I. The mass spectra of some (−)-kauran-16-ols. *Organic Mass Spectrometry* 3:1393-1400.

17. Bräuer L, Brandt W, Schulze D, Zakharova S, Wessjohann L (2008) A structural model of the membrane-bound aromatic prenyltransferase UbiA from E. coli. *ChemBioChem* 9:982-992.

18. Peters RJ (2010) Two rings in them all: the labdane-related diterpenoids. *Natural Product Reports* 27:1521-1530.

19. Fraga BM, Gonzalez P, Guillermo R, Hernandez MG (1996) The formation of an ent -11α,16α-epoxykaurane of biosynthetic significance by Gibberella fujikuroi. *Natural Product Letters* 8:257-262.

20. Hayashi K-I et al. (2006) Identification and functional analysis of bifunctional ent-kaurene synthase from the moss Physcomitrella patens. *FEBS Letters* 580:6175-6181.

21. Toyomasu T et al. (2008) Identification of diterpene biosynthetic gene clusters and functional analysis of labdane-related diterpene cyclases in Phomopsis amygdali. *Bioscience, Biotechnology, and Biochemistry* 72:1038-1047.

22. Kawaide H et al. (2011) Identification of the single amino acid involved in quenching the ent-kauranyl cation by a water molecule in ent-kaurene synthase of Physcomitrella patens. *FEBS Journal* 278:123-133.

23. Cyr A, Wilderman PR, Determan MK, Peters RJ (2007) A modular approach for facile biosynthesis of labdane-related diterpenes. *Journal of the American Chemical Society* 129:6684-6685.

24. Morrone D et al. (2010) Increasing diterpene yield with a modular metabolic engineering system in E. coli: comparison of MEV and MEP isoprenoid precursor pathway engineering. *Applied Microbiology and Biotechnology* 85:1893-1906.

Chapter 5: Mechanisms of self-resistance in the platensimycin and platencin producing strains, *Streptomyces platensis* MA7327 and *Streptomyces platensis* MA7339

5.1 Introduction

The rapid development of antibiotics beginning a little over sixty years ago was one of the most important advancements in the history of treating human disease (*1*). Unfortunately, pathogenic bacteria remain a threat to human health, and the inevitable tendency of microorganisms to become resistant to present therapeutics is a well recognized cause for concern (*2–4*). In addition to addressing a pharmaceutical pipeline that is simply not producing a sufficient number of drugs to treat newly emergent and resistant pathogens, studying the mechanisms of resistance to antibiotics will provide insight into preventing bacteria from disarming present and future therapies (*5*, *6*). Anticipating and counteracting resistance to novel antibiotics entering the clinical setting will be of the utmost importance to drug development efforts in the future.

5.1.1 Mechanisms of antibiotic resistance

Acquired resistance to antibiotics by bacteria generally resembles at least one of three major mechanisms: antibiotic destruction or modification, target modification, or alteration of the uptake and/or efflux of the antibiotic. Detoxification of antibiotics through enzyme-catalyzed destruction or modification of the drug has a broad impact on antimicrobial therapy. These resistance mechanisms not only protect the organisms deploying them, but effectively lower the concentration of the biologically active form of the antibiotic in the host/environment

and can promote growth of neighboring organisms. Antibiotic destruction was one of the earliest observed resistance mechanisms, with penicillin-inactivating strains of bacteria reported shortly after introduction of the drug in the 1940s (*7*). It is also one of the more common forms of resistance, with essentially all antibiotics susceptible to some sort of enzymatic modification rendering them less effective in binding their target, or more frequently, completely neutralized. **Table 5.1** summarizes the common enzymatic mechanisms responsible for conferring resistance to clinically relevant classes of antibiotics.

Antibiotic resistance due to reduced uptake or increased efflux of a drug highlights the fact that minor alterations to even secondary targets can have significant effects on the efficacy of antibiotics (*8*). The cytoplasmic membrane, the periplasm/peptidoglycan, and the outer membrane (in Gram-negative bacteria) represent the innate barriers for entry into bacterial cells and mediate concentration of molecules within the cell. Antibiotics exploit a variety of mechanisms to cross these barriers and enter the cell. These include diffusion, porins, and membrane transporters, and the mode of uptake varies with the charge, size and hydrophobicity of the molecule. Similarly, antibiotic compounds encounter natural efflux systems for shuttling surplus metabolites or other toxic substances out of the cell, although these systems are often tightly regulated. These cellular components may not represent primary targets of antibiotics, but they directly affect antibiotic concentration in the cell and their ability to reach their therapeutic target. A number of mutational events in these systems can lead to suboptimal concentrations of an antibiotic inside the cell and ultimately, survival of the organism. Moreover, the lowered exposure of the cell's interior to the antibiotic provided by reduced permeability or increased efflux can further enhance the effects of, or promote selection of, additional resistance mechanisms (*6*).

Target modification is another method for microbes to reduce the effectiveness of antimicrobial agents. Point mutations can be introduced into target genes and those that provide a selective advantage (i.e. reducing antibiotic binding with minimal loss in efficiency of primary function) can lead to resistance, with examples of even single point mutations providing clinically relevant resistance (*9*). Typically, more advanced modification, involving several advantageous point mutations or variation through homologous recombination with foreign DNA, is required to alter the antibiotic-target interaction enough to provide high-level resistance. Other target-mediated mechanisms of resistance include overexpression of the target gene, enzymatic modification of the target to affect antibiotic binding, or acquisition of an entirely separate gene that encodes the same biological function of the inhibited target, but does not bind the antibiotic (*6*).

5.1.2 Origins of antibiotic resistance elements

Evolution is the result of two accepted phenomena: genetic variability and selection by environmental pressure. The evolution of antibiotic resistance can be similarly simplified: random mutation creates genetic variability and some of these mutations confer a resistance phenotype; additionally, the use or presence of antibiotic molecules in the environment selects for the resistant variants, which increases the frequency of the resistance phenotype. Yet, most clinical resistance mechanisms in pathogens are not the result of simple mutations to their pre-existing cellular machinery in response to acute exposure to antibiotics, but are often distinct, highly sophisticated elements. It is therefore likely that genes currently identified as antibiotic-resistance determinants may have evolved, at least in part, for functionally separate purposes and in a variety of environments. Whether defined as “pre-adaptation” (assumption of a new, potentially unrelated function (i.e. resistance) through minimal mutation of an existing gene) or

as “exaptation” (a genetic element serving one function being equally capable of performing a new function, such as resistance), this hypothesis is evident in many observed clinical resistance mechanisms (**Table 5.2**) (*6*, *10*). As with any complex, inheritable trait, Nature often uses a “shotgun” approach in the evolutionary refinement of these traits from a common ancestral origin. Indeed, it is now evident through studying the recently coined “antibiotic resistome” – the collection of all antibiotic resistance genes and their precursors in pathogenic and non-pathogenic bacteria – that many antibiotic resistance determinants have been redundantly and independently evolved and are common among environmental bacteria (*11*). Furthermore, for several classes of antibiotics the major routes to resistance in clinical pathogens mirror those used by the original producing organisms, another major contributor to the resistome (**Table 5.2**) (*6*, *11–15*). In these organisms, it is has been proposed that resistance should serve as a pre-condition for the production of antibiotics and thus, has co-evolved with increasing titer or diversity of the compounds produced (*6*, *11*, *16*, *17*). Although this hypothesis has not been proven, the antibiotic resistance elements found in antibiotic-producing strains are generally correlated with the antibiotic’s observed modes of action (*18*). Surveying the incredible diversity of antibiotic resistance mechanisms available in Nature will ultimately advance new antibiotic development efforts to ensure the success of new therapies and repurpose those that may have become obsolete due to overwhelming clinical resistance.

5.1.3 Putative resistance elements in the *ptm* and *ptn* biosynthetic gene clusters

Among our studies on the biosynthetic gene clusters responsible for PTM and PTN production in *S. platensis* strains, we have sought to identify the self-resistance mechanism(s) in

Table 5.1 – Summary of enzymatic mechanisms contributing to antibiotic resistance

Mechanisms	Enzyme(s)	Antibiotics affected
Acylation	Acetyltransferase	Aminoglycosides, chloramphenicol, type A streptogramins
Adenylation	AMP-transferase	Aminoglycosides, lincosamides
C-O bond cleavage	Lyase	Type B streptogramins
Glycosylation	UDP-, TDP- glucosyl transferases	Macrolides, rifamycin
Hydrolysis	β-Lactamase, esterase, epoxidase	β-Lactams, macrolides, fosfomycin
Monooxidation	Monooxygenase	Tetracyclines
Phosphorylation	Kinase	Aminoglycosides, macrolides, rifamycin
Thiol transfer	Thiol-transferase	Fosfomycin

Table 5.2 – Summary of clinical resistance mechanisms with an evolutionary link to natural proteins in environmental organisms

Class of antibiotic	Observed clinical resistance	Related natural protein	Natural reservoirs
Aminoglycosides	Acetylation	Histone-acetylases	*Streptomyces*
	Phosphorylation	Protein kinases	*Streptomyces*
Chloramphenicol	Acetylation	Acetylases	*Streptomyces*
	Efflux	Major faciliator superfamily	*Streptomyces*
Fluoroquinolones	Topoisomerase protection	Qnr-like protein	*Shewanella algae*
Glycopeptides (e.g. vancomycin)	Target site modification (Van operon, D-ala-D-ala replacement)	Van operon homologous genes	*Streptomyces*, *Amycolatopsis, and Paenibacillus*
β-lactams (e.g. methicillin)	PBP2a	Homologous PBP2a	*Staphyloccus sciuri*
β-lactams (e.g. cefotaxime)	CTX-M-3 β-lactamase	Homologous β-lactamases	*Kluyvera ascorbata*
Macrolides	Target site modification	rRNA methylases	*Streptomyces*
Tetracyclines	Efflux	Major faciliator superfamily	*Streptomyces*

these producing organisms, for which very little is known (*19*). Characterization of the PTM and PTN biosynthetic machineries has revealed that *S. platensis* MA7327 is a PTM and PTN dual-producer and must maintain resistance to both PTM and PTN. While *S. platensis* MA7339 is an exclusive PTN producer and must minimally maintain resistance to PTN, we have previously succeeded in converting this strain into a dual PTM and PTN producer by adding a 5.4 kb "PTM cassette" (**see Chapter 4**), suggesting that *S. platensis* MA7339 is naturally resistant to both antibiotics as well. Bioinformatics analysis of the open reading frames (ORFs) within both the *ptm* dual-producing cluster and the *ptn* cluster revealed the same set of four putative genes – *ptmP1/ptmP2/ptmP3/ptmP4* or *ptnP1/ptnP2/ptnP3/ptnP4* – without apparent roles in biosynthesis or regulation that might encode elements conferring resistance to PTM, PTN, or both (*19*).

Despite the wealth of research into PTM and PTN as possible clinical therapeutics, the mechanisms of resistance to these antibiotics have thus far remained elusive. This chapter describes identification of PtmP3 (and its *ptn* cluster homolog PtnP3) as the major self-resistance conferring elements in native producers of PTM and PTN, capable of providing naïve *Streptomyces* hosts with high-level resistance to both PTM and PTN. We hypothesized that PtmP3 confers resistance by acting as a functional replacement for the FASII condensing enzymes targeted by PTM and PTN. Site-directed mutagenesis of a putative conserved active site residue in PtmP3 resulted in a loss of its ability to confer resistance. Furthermore, we have created Δ*fabF* and Δ*fabH* knockout mutants in the *S. platensis* MA7327 background, demonstrating an apparent ability of this strain to fully complement a loss of either one of these essential enzymes. Finally, investigation of the housekeeping FabF and FabH enzymes within the conserved fatty acid biosynthesis (*fab)* cluster from the *S. platensis* producing strains

revealed that the native FabF is naturally resistant to PTM and therefore provides a second form of self-resistance to PTM; however, this native enzyme is insufficient to confer resistance to PTN, a dual inhibitor of FabF and FabH. The native FabH remains sensitive to PTN, and is insufficient to confer resistance to either PTN or PTM.

5.2 Methods

5.2.1 Bacterial strains and culture conditions

Escherichia coli DH5α was used for routine cloning (*20*). Vectors pGEM-T Easy (Promega, Madison, WI) and pCR2.1-TOPO (Invitrogen, Carlsbad, CA) were obtained from commercial sources. PTM and PTN producers, *S. platensis* MA7327 and *S. platensis* MA7339, were kindly provided by Merck Research Laboratories (Rahway, NJ). *E. coli* carrying plasmids were grown in LB medium and were selected for with appropriate antibiotics (*20*). Standard media and protocols were used for *Streptomyces* growth and sporulation (*21*). Media components and all other chemicals were from standard commercial sources. See **Appendix**, **section A1.2** for media recipes.

5.2.2 DNA manipulation and isolation

Plasmid preparation and gel extraction from *E. coli* was carried out with commercial kits (Qiagen, Valencia, CA) or according to standard protocols (*20*). Total *Streptomyces* DNA was isolated according to standard procedures (*21*), as were all restriction endonuclease digestions and ligations (*20*). Automated DNA sequencing and oligonucleotide primer synthesis were performed at the University of Wisconsin Biotechnology Center (Madison, WI), GENEWIZ (South Plainfield, NJ) and Integrated DNA Technologies (Coralville, IA).

5.2.3 Plasmids, primers, and strains

See **Appendix, Tables A1.1-A1.3**.

5.2.4 Platensimycin and platencin

The PTM and PTN utilized in this study was isolated and purified from fermentations using the strains, *S. platensis* SB12002 and *S. platensis* SB12001. Methods for purification and details regarding these overproducing strains have been reported previously (*22*, *23*).

5.2.5 Disk diffusion assay

A standard disk diffusion assay was used to determine susceptibility of wild-type (WT) and recombinant *Streptomyces* strains to PTM and PTN. In short, quantities of PTM or PTN in methanol were applied to 7 mm paper disks (Whatman 2017-006) and dried. These disks were placed onto solid R2YE agar (8 mL) plates to which ~48 hrs, dense liquid *Streptomyces* culture had been applied using sterile cotton swabs. These plates were incubated overnight at 30ºC and the zones of inhibition were subsequently observed.

5.2.6 96-well plate assay for obtaining MIC values

Aliquots of molten R2YE agar were prepared and contained either 0, 0.25, 0.5, 1, 2, 4, 8, 16, 32, 64, 128, or 256 µg/mL PTM, or 0, 0.0625, 0.125, 0.25, 0.5, 1, 2, 4, 8, 16, 32, or 64 µg/mL PTN. These aliquots were applied to sterile 96-well plates so that each well contained 100 µL agar media. Wells were inoculated with 10 µL sterile water containing ~10^3 *Streptomyces* spores (or serially diluted mycelial stocks). Plates were incubated overnight at 30ºC. Growth in wells containing PTM or PTN was compared with wells with no antibiotics.

5.2.7 Cloning of putative resistance elements and construction of expression plasmids

Putative resistance elements were amplified from *S. platensis* MA7327 genomic DNA using LA Taq with GC Buffer II (Clontech Laboratories, Inc., Madison, WI) according to the manufacturer's instructions. Resulting PCR products were cloned into TA cloning vectors: pGEM-T Easy or pCR2.1-TOPO. These constructs were used for subcloning individual

elements into pSET152ermE*, a modified *Streptomyces* integrating vector containing the apramycin resistance cassette for selection as well as the constitutively active promoter, *ermE**, upstream of the multiple cloning site to ensure a high level of expression of the downstream insert (*24*, *25*). Expression plasmids pBS12101, pBS12102, pBS12103, and pBS12104 (containing ptmP1, ptmP2, ptmP3, and ptmP4, respectively) were constructed for high-level, recombinant expression of individual elements in naïve *Streptomyces* hosts (**Table A1.2)**.

5.2.8 Site-directed mutagenesis of *ptmP3*

Point mutations were generated through site-directed mutagenesis by overlap extension using PCR (*26*). Mutagenized fragments from overlap PCR amplification methods were cloned into pGEM-T Easy vector and ultimately cloned into pSET152ermE* to yield pBS12111 (C162A) and pBS121112 (C162Q). Primers used in this procedure and the expression plasmids generated are listed in **Tables A1.1 and A1.2**.

5.2.9 Construction of recombinant *Streptomyces* strains

After transformation of each pSET152ermE* derived expression construct into *E. coli* ET12567/pUZ8002 electrocompetent cells, intergeneric conjugation between *E. coli* and *Streptomyces* was performed according to standard protocol (*21*). This resulted in stable, recombinant strains of *Streptomyces* with the various expression constructs fully integrated into the *Streptomyces* chromosome (see **Tables A1.2 and A1.3** for a full list of recombinant strains and expression constructs).

5.2.10 Construction of a Δ*ptmU4-ptmP4* mutant strain in *S. platensis* MA7327.

Cosmid pBS12005 was modified by λRED-mediated PCR targeting, using the standard protocol, to generate the construct, pBS12108 (*19*, *27*). Briefly, primers RLDC2For and RLDC2Rev were used to amplify the *aac(IV)3* cassette from pIJ773 (**Table A1.1**). Introduction

of this amplified fragment into *E. coli* BW25113/pIJ790/pBS12005 resulted in the replacement of the locus spanning *ptmU4-ptmP4* with the apramycin resistance cassette on pBS12005 to generate pBS12108. This construct was introduced into *S. platensis* MA7327 by intergeneric conjugation using *E. coli* ET12567/pUZ8002 as the donor strain. Apramycin-resistant exconjugants were picked and replica-plated to identify apramycin-resistant, but kanamycin-sensitive, clones in which homologous recombination on each side of the locus of gene replacement had taken place, resulting in isolation of the Δ*ptmU4-ptmP4* mutant strain, *S. platensis* SB12120.

5.2.11 Cloning and sequencing of *fabF* and *fabH* from S. *platensis* MA7327 and MA7339.

Sequence data for the native *fab* genes in S. *platensis* strains were unavailable. Available genome sequences of other *Streptomyces* spp. were analyzed for sequence data of the homologous *fab* cluster found in these organisms containing *fabD*, *fabH*, *acpP*, and *fabF* (**Figure 5.9**). Whole genome sequences available from the Sanger Institute database for *S. coelicolor*, *S. avermitilis*, and *S. griseus* allowed alignment of homologous *fab* clusters and design of primers specific to highly conserved regions flanking the *fabF* gene locus (**Table A1.1**). Fragments containing *S. platensis fabF* were amplified from *S. platensis* MA7327 and S. *platensis* MA7339 genomic DNA. Similar methods were used to clone a fragment containing *fabH* from *S. platensis* MA7327 and S. *platensis* MA7339 genomic DNA. These fragments were cloned into pGEM-T Easy vector for sequencing and subcloned into pSET152ermE*, to yield pBS12105, pBS12106, pBS12705, and pBS12706 (see **Appendix**, **Table A1.2** and **section A1.6**).

5.2.12 Cloning and sequencing of *fabF* and *fabH* from *S. albus* J1074

The primers designed above for amplification of *S. platensis* native *fabF* and *fabH* genes (**Section 5.2.11**) were similarly used to amplify *fab* genes from *S. albus* J1074 (**Table A1.1**).

Amplified fragments containing the *S. albus fabF* and *fabH* genes were cloned into pGEM-T Easy vector for sequencing and subcloned into pSET152ermE* to yield pBS12715 and pBS12716, respectively (see **Appendix**, **Table A1.2** and **section A1.6**).

5.2.13 Construction of Δ*fabF* and Δ*fabH* mutant strains of *S. platensis*

Isolation of cosmids containing the *S. platensis fab* cluster was carried out using the previously constructed *S. platensis* MA7327 genomic library (*22*). A 10 µL culture containing the genomic library was diluted to 10^6 cells/mL and spread onto LB plates containing 50 µg/mL kanamycin. PCR primers FabHscreenFor and FabHscreenRev were used to screen resulting single colonies for cosmids containing the *fab* cluster (**Table A1.1**). Colonies yielding the expected 432 bp band were isolated and the respective cosmids purified using standard methods. Cosmid pBS126G9 was isolated and verified to contain both *fabF* and *fabH.* This cosmid was transformed into *E. coli* BW25113/pIJ790 to generate Δ*fabF* and Δ*fabH* single knockout mutants using the previously described λRED-mediated PCR-targeting mutagenesis method (*27*). Resulting modified cosmids were introduced to *S. platensis* strains by intergeneric conjugation using *E. coli* ET12567/pUZ8002 as the donor strain. Apramycin-resistant exconjugants were selected and these putative single-crossover recombinants were replica plated to identify apramycin-resistant, but kanamycin-sensitive, clones in which homologous recombination on each side of the locus of gene replacement had taken place. Single and double crossover mutants were verified by PCR methods. Strains *S. platensis* SB12121, SB12123, and SB12717 were confirmed to be Δ*fabF*::*aac(IV)3* mutants, while *S. platensis* SB12122, SB12124, and SB12718 were confirmed to be Δ*fabH*::*aac(IV)3* mutants.

5.3 Results

5.3.1 Bioinformatics analysis reveals candidates for self-resistance genes.

Four genes within the *ptm* and *ptn* biosynthetic clusters – p*tmP1/ptmP2/ptmP3/ptmP4* or *ptnP1/ptnP2/ptnP3/ptnP4* – were previously ruled out as contributors to, or regulators of, the biosynthetic reactions leading to production of PTM and PTN (*19*). Bioinformatics analysis assigned these genes putative roles in self-resistance based on their homology to enzymes of known function (*19*). The N-terminal regions of PtmP1/PtnP1 show sequence similarity to KASIII condensing enzymes, including *E. coli* FabH (AAA23749.1, 27% identity, 42% similarity); however, while this region retains two out of three residues in a conserved Cys-Asn-His catalytic triad, it lacks the cysteine residue essential in forming an acyl-enzyme intermediate during the condensation reaction (*28*). PtmP2/PtnP2 show sequence similarity to acetyl-CoA acetyltransferases, belonging to the thiolase family of enzymes. Interestingly, structural features, including an N-terminal region containing a cysteine residue (Cys-85) and a C-terminal region containing a histidine residue (His-338), align with conserved active site regions in both thiolases and KAS condensing enzymes. However, PtmP2/PtnP2 lack additional key active site residues, critical for either thiolase or condensing enzyme activity: a C-terminal catalytic cysteine residue for type II thiolase activity, and a second C-terminal catalytic His/Asn residue for condensing enzyme activity (*29*, *30*). PtmP3/PtnP3 are FabF (KASII) homologs, retaining each of three key residues in a Cys-His-His catalytic triad conserved among KASI/II enzymes (**Figure 5.1**) (*28*). The similarity of PtmP1-P3/PtnP1-P3 to condensing enzymes, the targets of PTM and PTN, led to their classification as putative resistance elements. Finally, PtmP4/PtnP4 show high similarity to members of the major facilitator superfamily, suggesting a role in efflux activity and possible resistance (*31*).

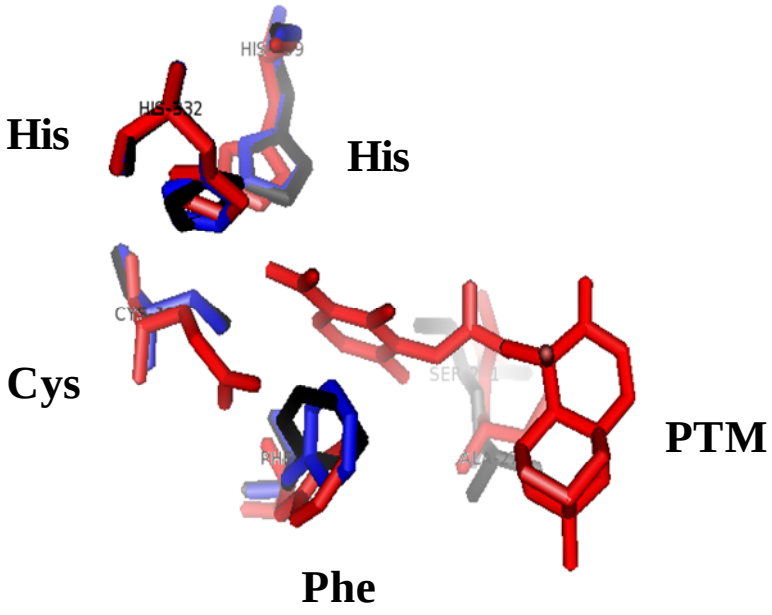

Figure 5.1 – KASII active site demonstrating conserved (Cys-His-His) catalytic triad. A sequence-based homology model of PtmP3 (black) is shown, created from a pairwise alignment with *Thermus thermophilus* HB8 KASII (blue) and aligned with *E. coli* FabF + PTM (red). PDB codes: 2GFX, 1J3N.

5.3.2 Various *Streptomyces* spp. are sensitive to both PTM and PTN.

In order to identify ideal naïve hosts for resistance studies, the susceptibility of various strains of *Streptomyces* to PTM and PTN was determined using a standard disk diffusion assay. Clear zones of growth inhibition were observed around disks impregnated with PTM as well as disks impregnated with PTN on R2YE agar plates inoculated with *Streptomyces albus* J1074, *Streptomyces lividans* K4-114, or *Streptomyces coelicolor* M512 (**Figure 5.2 and see Appendix, Figure A1.17**). These strains were selected as suitable naïve hosts for further study. Both producing strains of *S. platensis* were confirmed to be highly resistant to PTM and PTN. No zones of inhibition were observed around disks impregnated with high concentrations of either molecule (**Figure 5.2**).

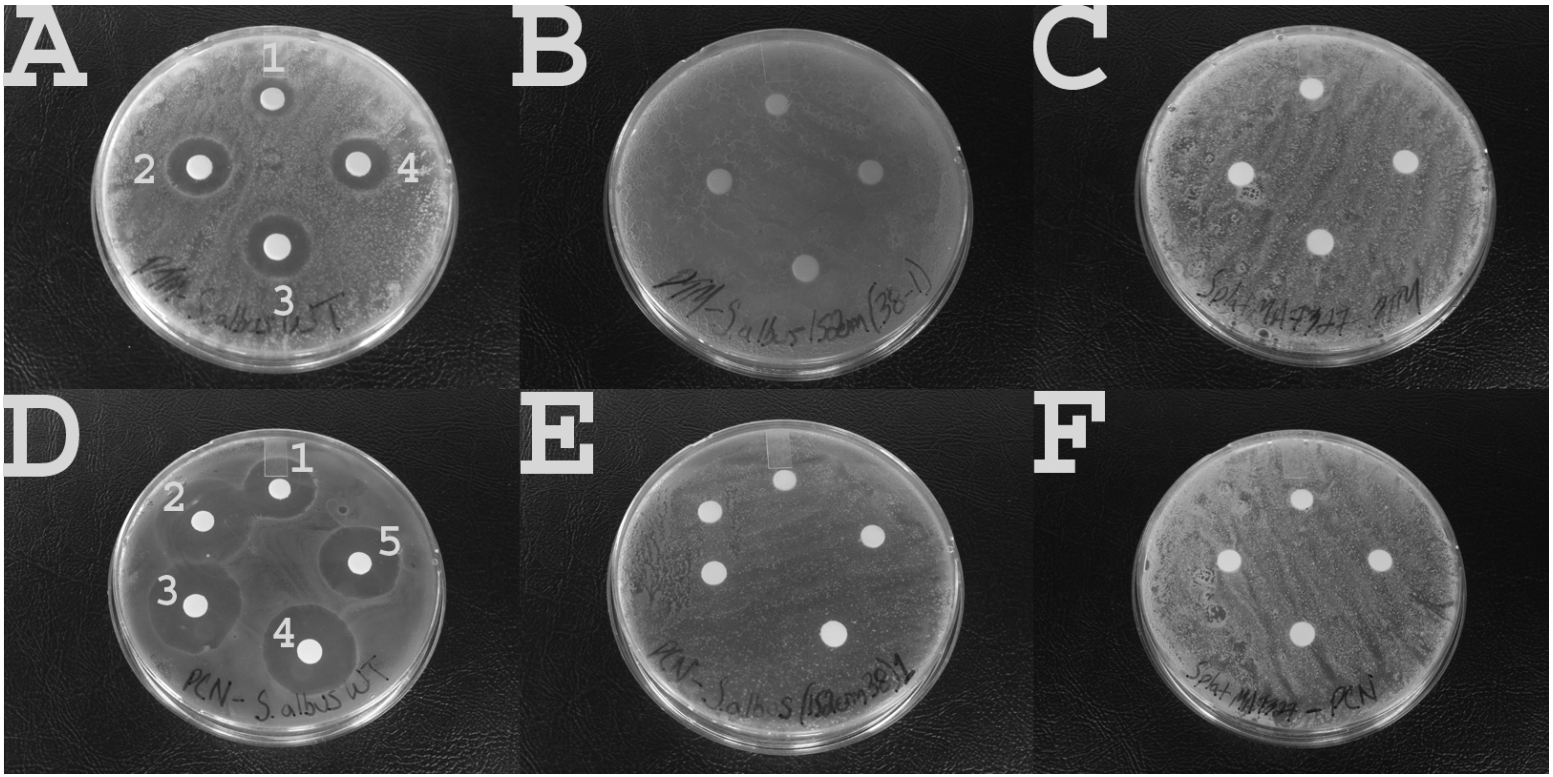

Figure 5.2 – Disk diffusion assay for PTM and PTN susceptibility. Top Row: *S. albus* WT (A), *S. albus* SB12703 (B), and *S. platensis* MA7327 (C), challenged with (1) 5 µg, (2) 10 µg, (3) 20 µg, and (4) 40 µg of PTM; Bottom Row: *S. albus WT* (D), *S. albus* SB12703 (E), and *S. platensis* MA7327 (F), challenged with (1) 1.25 µg, (2) 2.5 µg, (3) 5 µg, (4) 10 µg, and (5) 20 µg of PTN.

5.3.3 Expression of p*tmP3* in naïve *Streptomyces* hosts confers resistance to both PTM and PTN.

An *in vivo* approach was used to screen whether predicted self-resistance elements could confer resistance to PTM and/or PTN in sensitive *Streptomyces* hosts. Each candidate resistance element was cloned from isolated *S. platensis* MA7327 genomic DNA into an expression vector and transferred into a *Streptomyces* host by conjugal transfer with an *E. coli* donor strain. This resulted in stable, recombinant *Streptomyces* strains with the expression vectors containing candidate resistance elements fully integrated into the chromosomal backbone (**see Appendix, Tables A1.2 and A1.3** for full list of strains and constructs). The susceptibility of these recombinant *Streptomyces* strains to PTM and PTN was determined using the same disk diffusion assay used to assess sensitivity in the wild-type strains of each *Streptomyces* species. Recombinant *Streptomyces* strains harboring *ptmP3* (or *ptnP3*) showed high levels of resistance to both PTM and PTN, whereas strains harboring *ptmP1*, *ptmP2*, or *ptmP4* showed identical levels of sensitivity compared with their respective wild-type strains (**see Appendix, Figures A1.16-A1.18**). MIC values were also determined using a 96-well plate assay format (**Table 5.3, Figure 5.4**).

5.3.4 A point mutation at Cys-162 in PtmP3 abolishes its ability to confer resistance.

PtmP3 is homologous to type I/II β-ketoacyl-ACP synthases (FabB/KASI and FabF/KASII), a target of both PTM and PTN. Sequence alignments with characterized FabF and FabB enzymes among various genera of bacteria confirm that PtmP3 retains each of three residues (Cys-162, His-300, and His-334) in a highly conserved catalytic triad (**Figure 5.1**). The active site cysteine residue is critical for activity in FASII condensing enzymes, as it covalently binds the acyl-CoA substrate, to form an acyl-enzyme intermediate, prior to the condensation

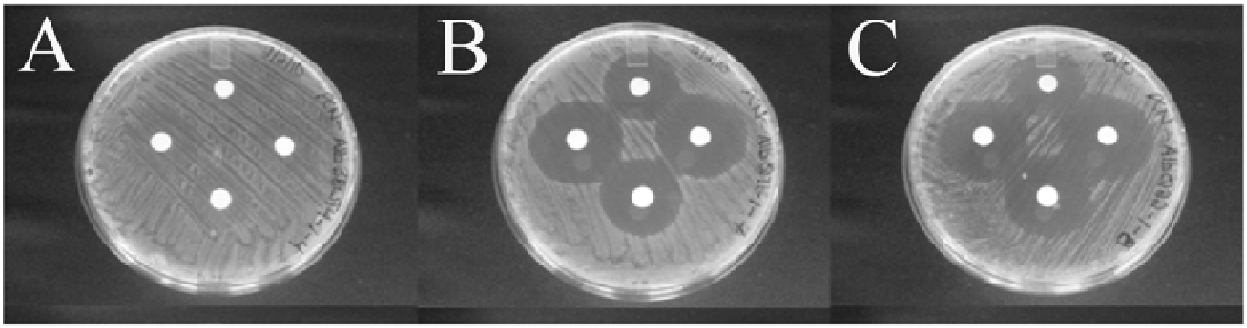

Figure 5.3 – Disk diffusion assay for PTN susceptibility. (A) *S. albus* SB12703 (+PtmP3), (B) *S. albus* SB12711 (+PtmP3-C162A), and (C) *S. albus* SB12712 (+PtmP3-C162Q) challenged with 1.25 μg, 2.5 μg, 5 μg, and 10 μg of PTN.

reaction. From these observations, PtmP3 was hypothesized to confer resistance by complementing FASII condensing activity.

We carried out site-directed mutagenesis on the Cys-162 residue of PtmP3 to determine the effect on conferred resistance. By creating a C162A mutation, we predicted that PtmP3 would be left unable to catalyze the FASII condensation reactions and thus, unable to confer resistance. Interestingly, previous structural studies examining PTM binding in *E. coli* FabF (ecFabF) demonstrate a C162Q inactivates FabF, but pre-positions nearly all components of the FabF catalytic machinery into the "acyl-enzyme conformation" – notably, the side chain of a "gatekeeping" Phe residue, is converted to an "open" conformation, allowing PTM to bind a previously inaccessible active site. PtmP3 could conceivably confer resistance by sequestering PTM or PTN, although it is unknown whether PtmP3 retains the open/closed conformation conversion upon acyl binding or C162Q mutation. The possibility for a sequestration resistance mechanism was ultimately explored by creating a C162Q mutation in PtmP3 in order to verify that a loss of conferred resistance from mutation of Cys-162 is not due to a loss in the ability of the PtmP3 to convert to an open conformation, allow sequestration of PTM or PTN. Each single

Table 5.3 – MIC values obtained for WT and recombinant strains

Strain Name	Description	MIC (µg/mL)	
		PTM	PTN
S. platensis MA7327	WT	>256 µg/mL	>64 µg/mL
S. platensis MA7339	WT	>256 µg/mL	>64 µg/mL
S. platensis SB12120	Δ*ptmU4-P4*	>256 µg/mL	16 µg/mL
S. albus J1074	WT	32 µg/mL	0.5 µg/mL
S. albus SB12703	+ *ptmP3*	>256 µg/mL	> 64 µg/mL
S. albus SB12711	+ *ptmP3-C162A*	32 µg/mL	0.5 µg/mL
S. albus SB12705	+ *S. platensis fabF*	>256 µg/mL	8 µg/mL
S. albus SB12706	+ *S. platensis fabF*	32 µg/mL	0.5 µg/mL
S. albus SB12715	+ *S. albus fabF*	32 µg/mL	0.5 µg/mL
S. albus SB12716	+ *S. albus fabH*	32 µg/mL	0.5 µg/mL

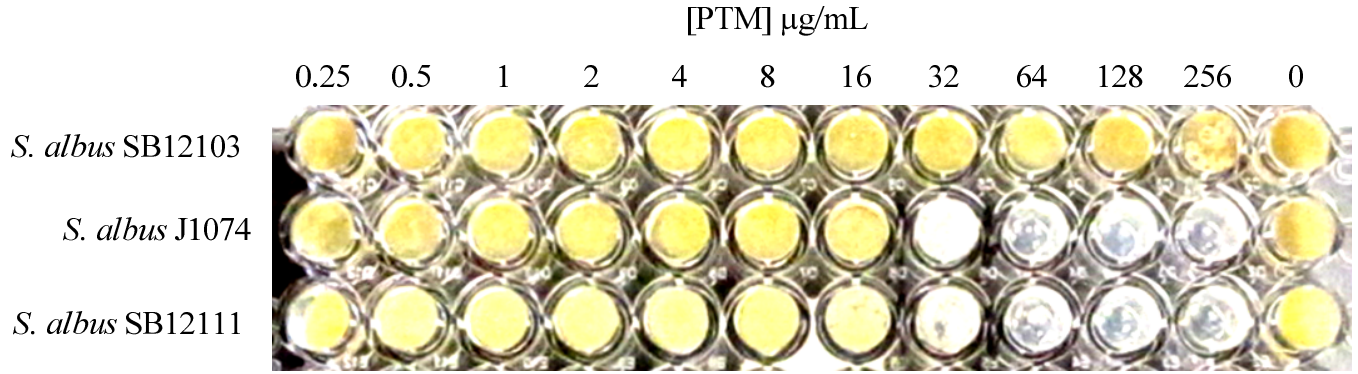

Figure 5.4 – MIC determination using a 96-well plate format. See section 5.2.6 for detailed description of protocol.

amino acid substitution at Cys-162 in PtmP3 completely abolished it ability to confer PTM and PTN resistance in a naïve host. Sensitivity in host strains containing each of the mutated versions of PtmP3 exhibited wild-type host sensitivity (**Figure 5.3, Table 5.3**).

5.3.5 Deletion of a locus spanning *ptmU4-ptmP4* , in *S. platensis* MA7327 introduces PTN susceptibility, but not PTM susceptibility

In order to assess the essentiality of PtmP3 for PTM and PTN self-resistance in the producing strains, and to explore the possibility of additional resistance elements located within the biosynthetic gene cluster or elsewhere on the *S. platensis* chromosome, a partial cluster deletion mutant strain was created in the *S. platensis* MA7327 background. A locus containing the genes *ptmU4*, *ptmA3*, *ptmP3*, and *ptmP4* was deleted. Deletion of the putative biosynthetic genes, *ptmU4* and *ptmA3*, upstream of *ptmP3* abolishes PTM and PTN production (data not shown). The susceptibility of the deletion mutant to PTM and PTN was determined by disk diffusion assay. Interestingly, the deletion mutant displayed sensitivity to PTN, but retained high-level resistance to PTM (**Table 5.3**).

5.3.6 Overexpression of native *fabF* from S. platensis MA7327 confers resistance to PTM, but not to PTN in naïve *Streptomyces* hosts.

The housekeeping *fabF* gene from *S. platensis* MA7327 was a likely candidate for contributing to the residual resistance to PTM observed in the Δ*ptmU4-ptmP4* deletion strain (**section 5.3.5**). The *S. platensis fabF* was cloned, sequenced, and utilized to construct a recombinant *S. albus* strain constitutively expressing the *S. platensis fabF*. This strain, S. albus SB12705 was assayed for PTM or PTN susceptibility and compared to both WT *S. albus* as well as a *S. albus* strain constitutively expressing a recombinant copy of its housekeeping *fabF* gene (*S. albus* SB12715). Only *S. albus* SB12705 showed high-level resistance to PTM. All strains

remained sensitive to PTN, although the MIC was slightly increased in *S. albus* SB12705 (**Table 5.3**).

5.3.7 Overexpression of native *fabH* from S. platensis MA7327 does not confer resistance to either PTM or PTN in naïve *Streptomyces* hosts.

We similarly investigated *S. platensis* FabH. The *S. platensis fabH* was cloned, sequenced, and utilized to construct *S. albus* SB12706. This strain was assayed for PTM or PTN susceptibility and compared with WT *S. albus* as well as a strain constitutively expressing a recombinant copy of its housekeeping *fabH* gene, *S. albus* SB12716. Overexpression of *fabH* genes from *S. platensis* or *S. albus* was insufficient to confer resistance to either PTN or PTM in a naïve host (**Table 5.3**).

5.3.8 The *fabF* and *fabH* from the *Streptomyces* chromosomal *fab* gene cluster can be deleted in strains expressing *ptmP3.*

We sought further confirmation that the resistance element, PtmP3, can functionally replace both FASII condensing enzymes, FabF and FabH, as a mechanism of conferred resistance to PTM and PTN. A strategy for deletion of *fabF* and *fabH* in strains of *S. platensis* MA7327 expressing *ptmP3* was designed and carried out (**Figures 5.5 and 5.6**). A cosmid harboring the conserved *Streptomyces fab* gene cluster (*fabD-fabH-acpP-fabF)* was isolated from a previously constructed *S. platensis* MA7327 genomic library (*22*). This cosmid was modified by λRED-mediated PCR targeted gene replacement of *fabF* or *fabH* with an apramycin resistance cassette to yield cosmids, pBS12109 and pBS12110. A pSET152 derivative, pBS12107, containing *ptmP3* under the expression of the *ErmE** promoter, was introduced into

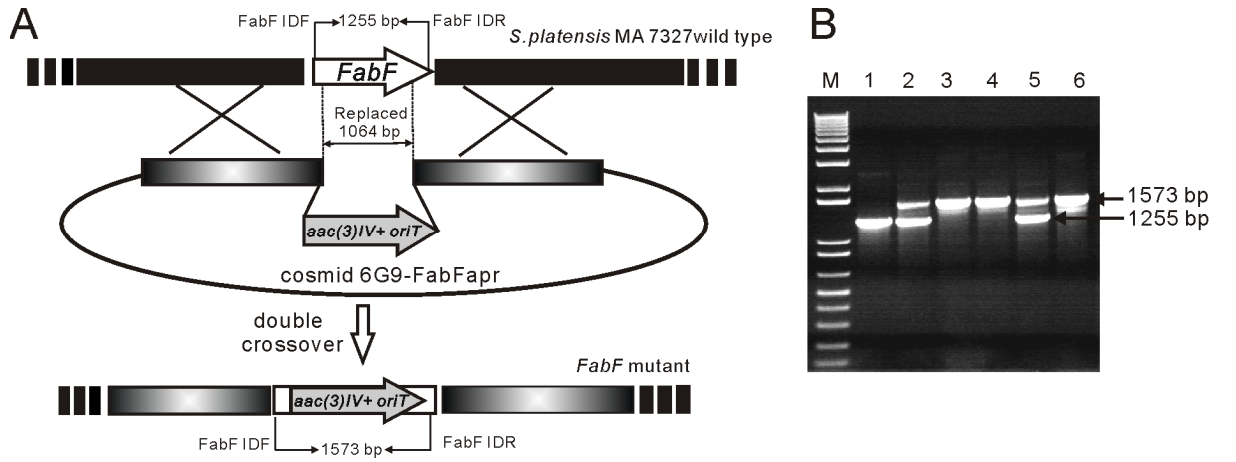

Figure 5.5 – Inactivation of *fabF* in *S. platensis*. (A) Schematic of the inactivation of *S. platensis fabF* by insertion of an apramycin resistance-oriT cassette *(aac(3)IV +oriT*) (B) PCR verification of WT, single crossover mutant, and double crossover mutant genotypes, using the primers FabF_IDFor and FabF_IDRev: *S. platensis* MA7327 (lane 1); single crossover mutants (lanes 2 and 5); double crossover mutants, *S. platensis* SB12121 and SB12123 (lanes 3 and 4); cosmid 6G9 control (lane 6).

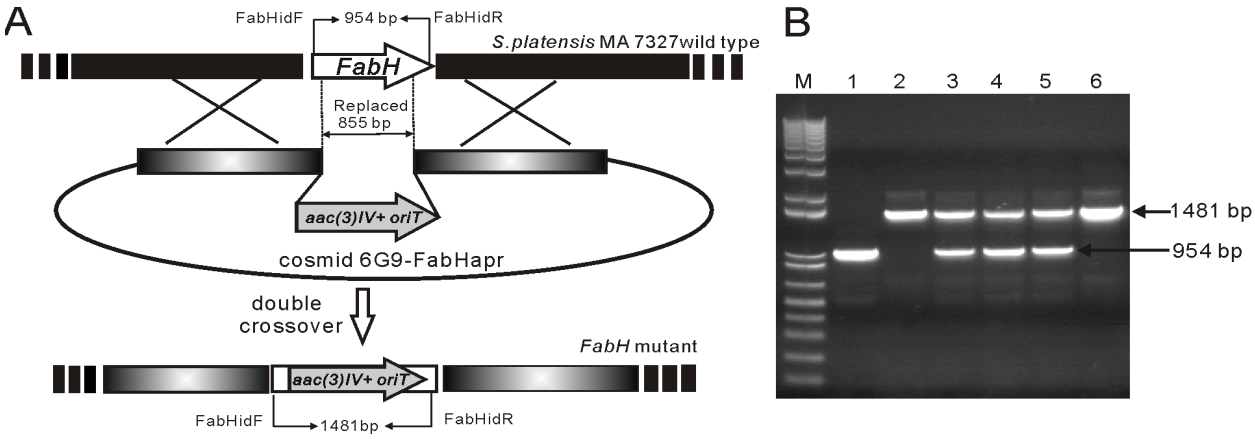

Figure 5.6 – Inactivation of *fabH* in *S. platensis*. (A) Schematic of the inactivation of *S. platensis fabH* by insertion of an apramycin resistance-oriT cassette *(aac(3)IV +oriT*) (B) PCR verification of WT, single crossover mutant, and double crossover mutant genotypes, using the primers FabH_IDFor and FabH_IDRev: WT MA7327 (lane 1); single crossover mutants (lanes 3, 4, and 5); double crossover mutants, *S. platensis* SB12122 and SB121224 (lane 2); cosmid pBS006G9 control (lane 6).

S. platensis MA7327, to yield *S. platensis* SB12127, which constitutively expresses *ptmP3*. Introduction of cosmids, pBS12109 or pBS12110, into *S. platensis* SB12127 and *S. platensis* MA7327, by conjugation from *E. coli* yielded apramycin-resistant, single-crossover recombinants, which were screened for a second crossover event, indicating deletion of *fabF*, or *fabH*, from the chromosomal *fab* gene cluster in *S. platensis* (**Figures 5.5 and 5.6**). Successful isolation of ΔfabF and ΔfabH single knockout *S. platensis* strains, SB12121 and SB12122, respectively, demonstrated that either *fabF* or *fabH* can be readily deleted from the chromosome of *S. platensis* strains expressing *ptmP3*.

5.4 Discussion

5.4.1 PtmP3 is the major self-resistance element in PTM/PTN-producing strains of *S. platensis*

Bioinformatics analysis of the gene clusters responsible for PTM and PTN biosynthesis revealed four candidate genes for encoding self-resistance to the producers. The results from this study have now identified PtmP3 (and its homolog, PtnP3, from the *ptn* cluster) as the major resistance element(s) in PTM/PTN-producing strains of *S. platensis*. Although the results from this study do not specifically exclude PtmP1/PtnP1, PtmP2/PtnP2, or PtmP4/PtnP4 from contributing to PTM and PTN resistance, their functions or other contributions to the biosynthesis of PTM or PTN remain unclear. PtmP3 confers high-level resistance to PTM, a specific inhibitor of FabF, and PTN, a dual inhibitor of FabF and FabH, in naïve *Streptomyces* hosts. Furthermore, PtmP3 retains a catalytic triad conserved among KASI/II enzymes. A single amino acid substitution, C162A, the conserved catalytic cysteine residue, abolished the ability of PtmP3 to confer resistance in a naïve host, demonstrating that the predicted catalytic cysteine residue was essential in PtmP3 to confer resistance. Furthermore, a C162Q substitution also

abolished its ability to confer resistance and verified an aforementioned mechanism for sequestration of PTM and PTN (**section 5.3.4**) is not likely responsible for the observed PtmP3-mediated resistance. While these data support an initial hypothesis that PtmP3 is likely a resistant isoform of a FASII condensing enzyme, the dual capacity of PtmP3 to provide resistance to both antibiotics and apparently carry out the disparate functions of both the FabF (KASII) and the FabH (KASIII) enzymes in *Streptomyces* was unexpected.

5.4.2 An evolutionary relationship between PtmP3 and *S. platensis* FabF.

The S. *platensis* MA7327 Δ*ptmU4-ptmP4* partial cluster deletion strain, SB12120, is sensitive to PTN, but retains high-level resistance to PTM. This confirmed the presence of another form of resistance to PTM in S. *platensis*. Lacking any remaining candidates within the *ptm* biosynthetic gene cluster, we investigated the native *S. platensis fab* genes: namely *fabF,* the target of PTM (**Figure 5.9**). Overexpression of native *S. platensis fabF* in a naïve host conferred high-level resistance to PTM (but not to PTN) and confirmed that it was likely responsible for the residual PTM resistance observed in the SB12120 deletion strain. Our findings have revealed that the producing organisms have adapted two complementary mechanisms for resistance to PTM and PTN: target replacement – PtmP3, within the ptm biosynthetic cluster; and target modification – *S. platensis* FabF, in the conserved *fab* primary metabolic gene cluster. PtmP3 (GenBank: ACS13710.1) shows 51% identity / 67% similarity to the *S. platensis* MA7327 FabF (see **Appendix, section A1.6**) and 38% identity / 55% similarity to the *E. coli* FabF (GenBank: CAA84431.1). As a comparison, *S. platensis* MA7327 FabF shows an average of 80% sequence identity / 90% similarity to other *Streptomyces* spp. FabF enzymes, including *S. coelicolor* (GenBank: AL939112.1), *S. griseus* (GenBank: NC_010572.1), and *S. avermitilis* (GenBankNC_003155.4), and 39% identity / 57% similarity to the *E. coli* FabF (GenBank:

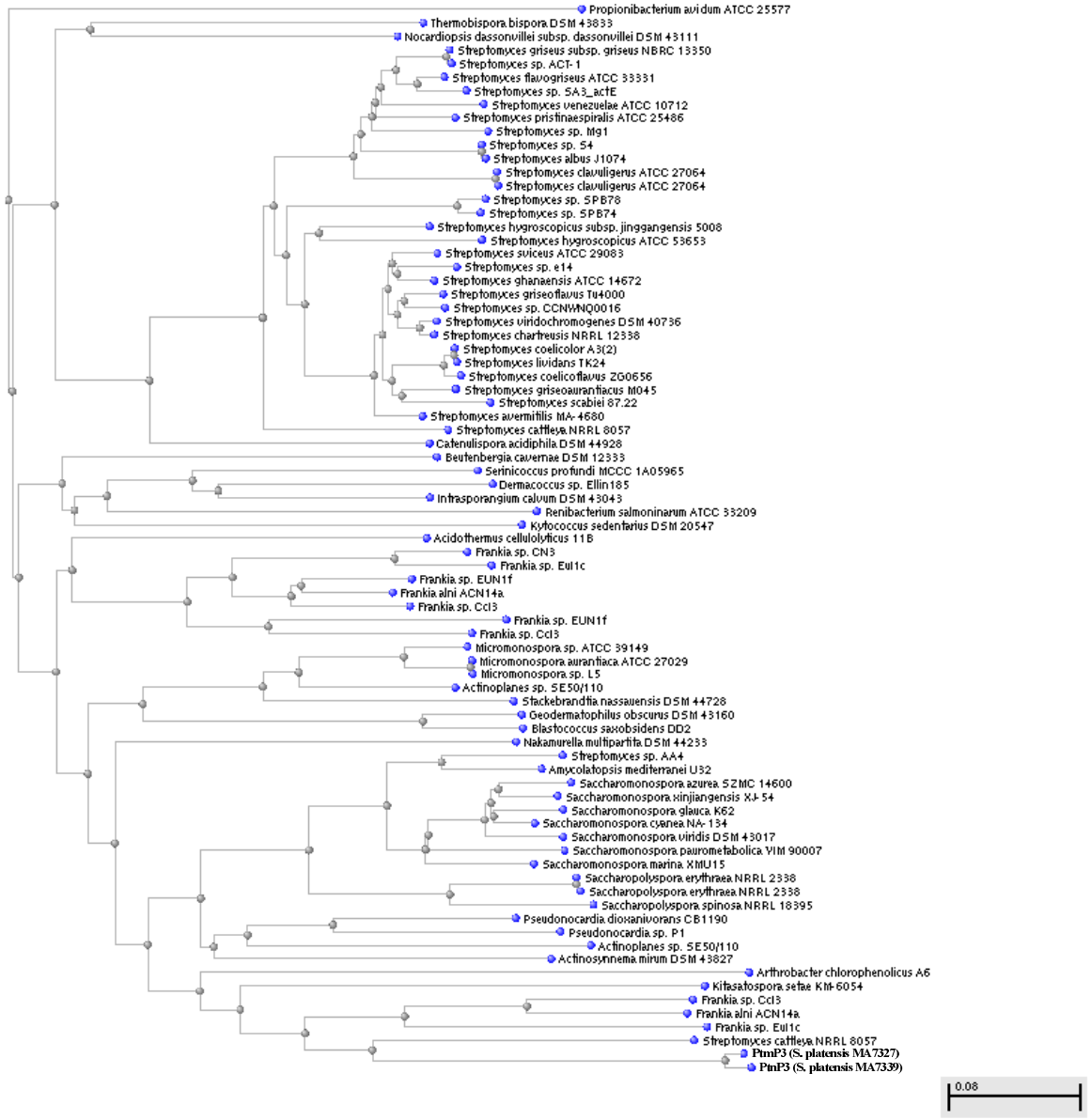

Figure 5.7 - Fast minimal evolution tree of primary amino acid sequences of PtmP3/PtnP3 and closest homologs (by species). Identified by a BLAST pairwise alignment of database sequences; closest homologs are all KASII homologs and originate from high-GC, Gram positive organisms.

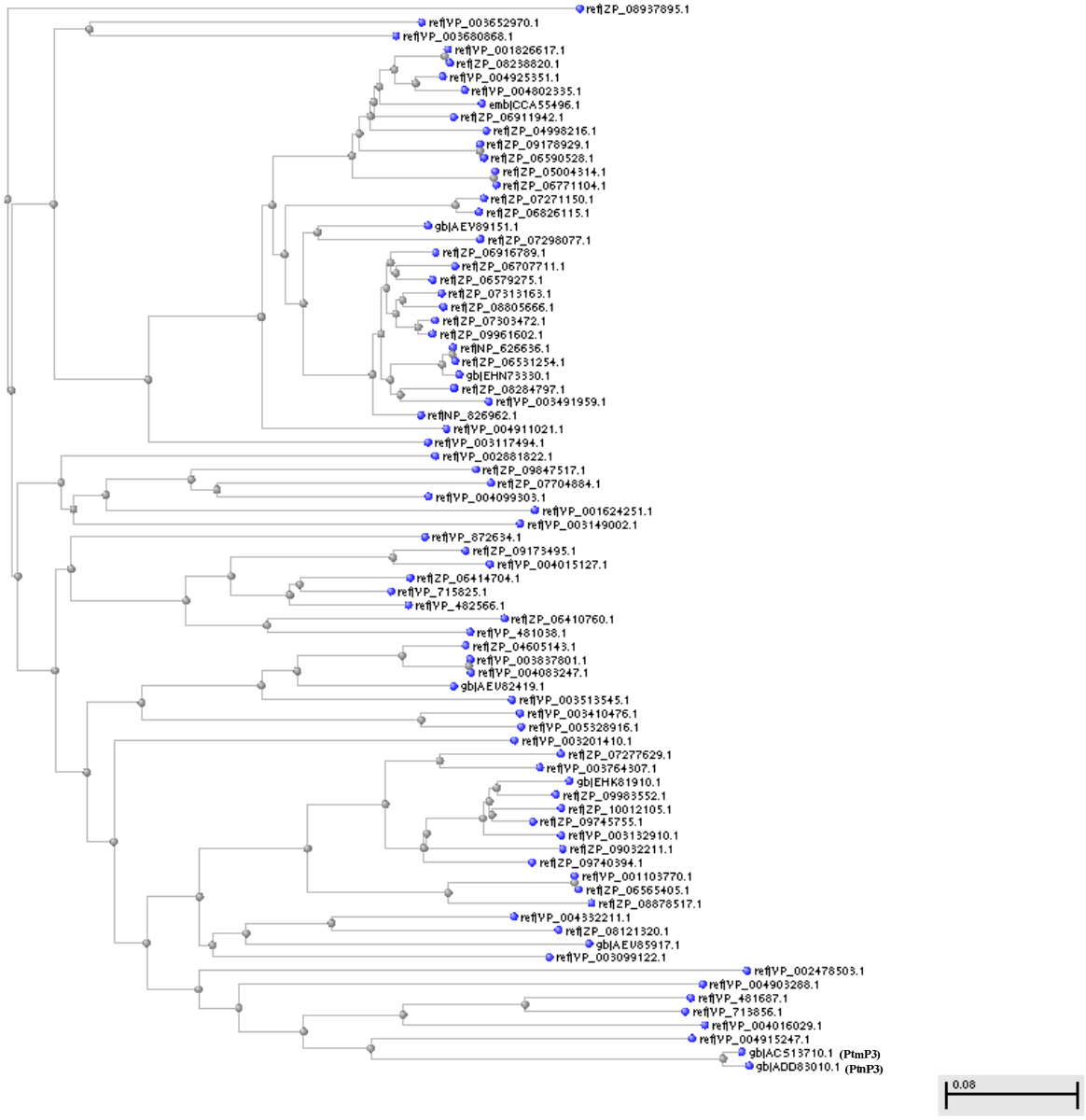

Figure 5.8 - Fast minimal evolution tree of primary amino acid sequences of PtmP3/PtnP3 and closest homologs (by accession number). Identified by a BLAST pairwise alignment of database sequences; closest homologs are all KASII homologs and originate from high-GC, Gram positive organisms.

CAA84431.1). A BLASTP search for sequences homologous to PtmP3 revealed its closest homologs range from ~49%-67% sequence identity. Notably, all are annotated as KASII homologs and originate from high-GC, Gram-positive bacteria. A minimal evolution tree generated from the primary amino acid sequences from PtmP3 and these closest homologs illustrates these results (**Figures 5.7 and 5.8**). Although *S. platensis* MA7327 FabF is not included in this comparison, KASII enzymes from a variety of other *Streptomyces* spp. are present. Point mutations arising in the *S. platensis* FabF, reducing its affinity for PTM, might explain its resistance to PTM. However, this essential and highly conserved gene involved in primary metabolism would likely have a very low tolerance for subsequent mutations (*32*), as demonstrated by the high sequence identity and similarity to and among other *Streptomyces* spp. housekeeping FabF enzymes. Acquisition of a second *fabF* gene from the environment, or more likely, a duplication of its own *fabF* gene near the *ptm* biosynthetic locus, would provide a gene locus capable of diverse mutation and genetic variation, and importantly, without affecting primary metabolism and growth. Co-evolution with the *ptm* cluster, and production of PTM and PTN, might exemplify one path for evolution of such a highly efficient resistance element such as PtmP3. As with other biosynthetic gene clusters among bacteria, having a resistance element such as PtmP3 located within the *ptm* cluster locus – as opposed to a conserved region, such as the *fab* cluster locus of the chromosome (**Figure 5.9**) – provides an additional advantage of supporting horizontal cluster transfer among organisms to afford other PTM, PTN, or PTM-PTN dual producers.

5.4.3 Metabolic simplification as a mechanism of resistance to FASII inhibitors

PtmP3 is capable of providing high-level resistance to both PTM, an inhibitor of FabF (KASII), and PTN, a dual inhibitor of FabF (KASII) and FabH (KASIII), in naïve *Streptomyces*

hosts. The isolation of viable *S. platensis* strains containing Δ*fabF* or Δ*fabH* deletions in backgrounds expressing *ptmP3* further demonstrates that PtmP3 is able to functionally complement the activities of each of these enzymes. β-ketoacyl-ACP synthases (KAS) are an example of a group of enzymes that ultimately perform the same chemical reaction (i.e. a decarboxylative Claisen condensation), but its various members are defined by their individual substrate preferences. This is highlighted by the unique substrate preferences of KAS III and KASII, defining their roles in fatty acid biosynthesis: FabH (KAS III) utilizes short-chain acyl CoA substrates and "initiates" the fatty acid biosynthetic pathway by catalyzing the first decarboxylative condensation with malonyl-ACP. Alternatively, FabF (KASII) catalyzes the same decarboxylative condensation reaction, but condenses acyl-ACP substrates of varying lengths with malonyl-ACP to carry out the consecutive rounds of elongation growing fatty acid chains. FabH has been shown to be essential for viability in *E. coli*, *Streptomyces coelicolor*, and *Lactococcus lactis*, demonstrating FabH is the key contributor for initiating fatty acid biosynthesis (*33–35*). That PtmP3, a KAS II homolog, can apparently replace both the functions of FabF (KASII) and FabH (KASIII) in *Streptomyces* is unexpected, but plausible. In *L. lactis*, a *fabH* "byass strain" (viable in media supplemented with either octanoate or oleate) can be fully complemented by engineered overproduction of the *L. lactis* FabF (*36*). The authors have proposed a mechanism for this complementation, based on previously observed activities of *E. coli* FabF/B enzymes *in vitro* (although comparable detailed mechanistic studies of the *L. lactis* enzymes *in vitro* have not been reported): in the absence of acyl-ACP substrate, the FabF decarboxylates the excess malonyl-ACP substrate to yield acetyl-ACP, which then becomes an available substrate for condensation with malonyl-ACP to yield a traditional FabH product, acetoacetyl-ACP (*36–39*). While the evolutional tendency of *L. lactis* is heavily biased toward

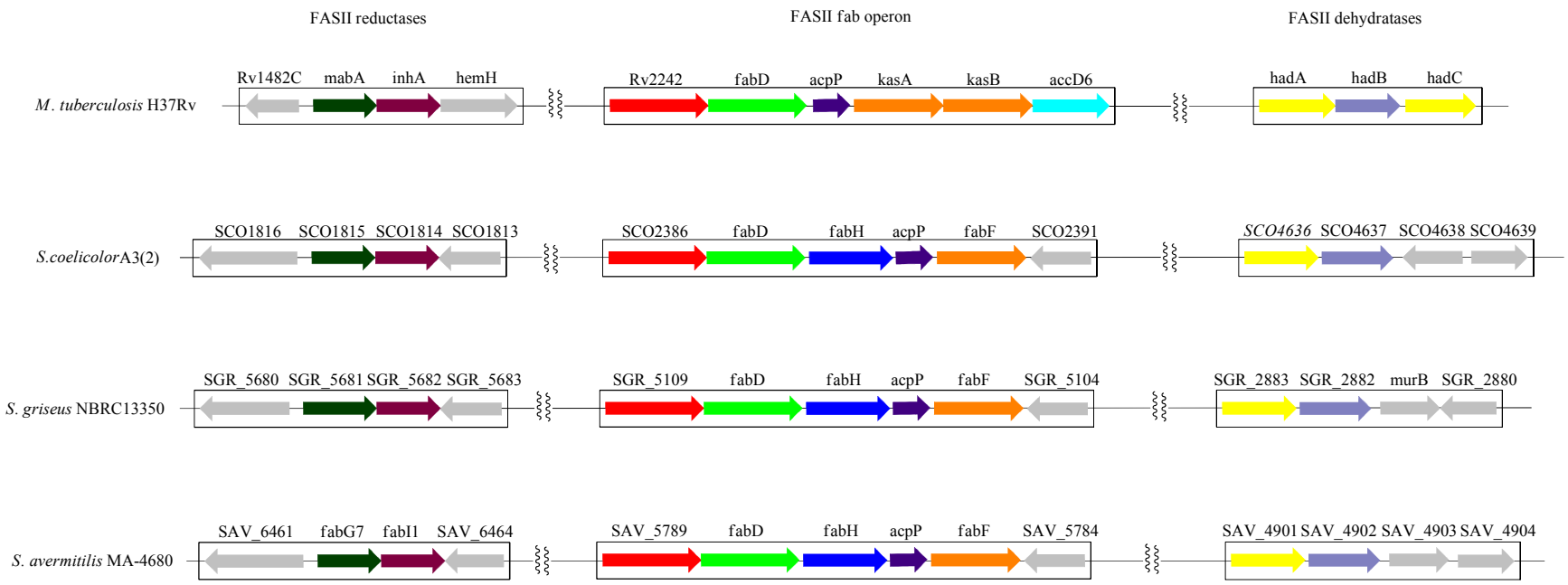

Figure 5.9 - Genetic organization of the FASII genes in actinomycetes. Alignments constructed from whole genome sequences available in NCBI database for *M. tuberculosis* H37Rc (GenBank: BX842576.1, BX842579.1, and BX842574.1), *S. coelicolor* A3(2) (GenBank: AL939110.1, AL939112.1, and AL939120.1), *S. griseus* NBRC13350 (GenBank: NC_010572.1), and *S. avermitilis* MA-4680 (GenBank: NC_003155.4).

genome minimization and metabolic simplification, it is a significant precedent for a bacterium to evolve toward a capability to survive with only a single functional KAS enzyme (*36, 40*). Although these observations were in engineered strains of *L. lactis*, and naive strains retain functional FabH and FabF enzymes, it nonetheless adds complexity to the current understanding of fatty acid synthesis in bacteria. *S. platensis* has apparently exploited a similar evolutionary pathway towards metabolic simplification as a mechanism of resistance: the functions of two discrete targets of unique antibiotics can be replaced by a single enzyme that provides traditional insensitivity to antibiotics. Future detailed mechanistic studies will provide insight on how PtmP3 balances apparently expanded substrate preferences while maintaining catalytic efficiency compared with native FabF and FabH enzymes (**Figure A1.20**).

5.4.4 Predicting clinical resistance to platensimycin and platencin

Bacterial fatty acid synthesis (FASII) – like cell wall synthesis, protein synthesis, and DNA replication – is an example of an essential cellular pathway and represents an attractive target for clinically useful antibiotics. The effectiveness of targeting FASII enzymes has been validated through the successful use of isoniazid and triclosan, as antitubercular and antiseptic agents, respectively. Furthermore, the limited clinical use of antibiotics targeting this pathway only increases the value of developing novel drugs targeting FASII, since the probability of key antibiotic resistant pathogens exhibiting cross-resistance to antibiotics with a novel mode of action is low. The discovery of PTM and PTN, as well as other natural products that specifically target FASII enzymes further highlights the wisdom of developing antimicrobial agents inhibiting bacterial fatty acid synthesis. Yet, clinical resistance to antibiotics of natural product origin is likely unavoidable. PtmP3, identified here as the major natural resistance determinant in PTM and PTN producing organisms, *S. platensis*, is one such potential and unwanted source

of acquired clinical resistance to antibiotics inhibiting FASII. Its identity as an apparent "hybrid" KASII/III isoform capable of complementing both native FabF (KASII) and FabH (KASIII) enzymes in *Streptomyces*, highlights how even a molecule such as PTN, an inhibitor of two separate essential targets, can be quickly counteracted through a clever resistance mechanism evolved in a natural producer of the antibiotic. The potential for PtmP3/PtmP3 to confer resistance to other clinically relevant FabF/FabH inhibitors as well as its ability to complement FabF/FabH and/or confer resistance in other organisms and pathogens should be investigated. These answers will hopefully guide future development of the PTM/PTN class of antibiotics, as well as lead compounds targeting FASII enzymes, and contributing towards the development of new and effective therapeutics.

5.5 References

1. Demain AL (2009) Antibiotics: natural products essential to human health. *Medicinal Research Reviews* 29:821–842.

2. Levy S (2005) Antibiotic resistance--the problem intensifies. *Advanced Drug Delivery Reviews* 57:1446 - 1450.

3. Levy SB, Marshall B (2004) Antibacterial resistance worldwide: causes, challenges and responses. *Nature Medicine* 10:S122-S129.

4. French GL (2005) Clinical impact and relevance of antibiotic resistance. *Advanced Drug Delivery Reviews* 57:1514-1527.

5. Taubes G (2008) The bacteria fight back. *Science* 321:356-361.

6. Mayers DL (2009) *Antimicrobial Drug Resistance* (Humana Press, Totowa, NJ).

7. Abraham E, Chain E (1940) An enzyme from bacteria able to destroy penicillin. *Nature* 146:837-837.

8. El'Garch F, Jeannot K, Hocquet D, Llanes-Barakat C, Plésiat P (2007) Cumulative effects of several nonenzymatic mechanisms on the resistance of Pseudomonas aeruginosa to aminoglycosides. *Antimicrobial Agents and Chemotherapy* 51:1016-1021.

9. Wehrli W (1983) Rifampin: mechanisms of action and resistance. *Reviews of Infectious Diseases* 5:S407-S411.

10. Gould SJ, Lloyd EA (1999) Individuality and adaptation across levels of selection: how shall we name and generalize the unit of Darwinism? *Proceedings of the National Academy of Sciences of the United States of America* 96:11904-11909.

11. D'Costa VM, McGrann KM, Hughes DW, Wright GD (2006) Sampling the antibiotic resistome. *Science* 311:374-377.

12. Hopwood DA (2007) How do antibiotic-producing bacteria ensure their self-resistance before antibiotic biosynthesis incapacitates them? *Molecular Microbiology* 63:937-940.

13. Benveniste R, Davies J (1973) Aminoglycoside antibiotic-inactivating enzymes in actinomycetes similar to those present in clinical isolates of antibiotic-resistant bacteria. *Proceedings of the National Academy of Sciences of the United States of America* 70:2276-2280.

14. Marshall CG, Broadhead G, Leskiw BK, Wright GD (1997) D-Ala-D-Ala ligases from glycopeptide antibiotic-producing organisms are highly homologous to the enterococcal

vancomycin-resistance ligases VanA and VanB. *Proceedings of the National Academy of Sciences of the United States of America* 94:6480-6483.

15. Pootoolal J, Neu J (2002) Glycopeptide antibiotic resistance. *Annual Review of Pharmacology and Toxicology* 42:381-408.

16. Hopwood DA (2007) How do antibiotic-producing bacteria ensure their self-resistance before antibiotic biosynthesis incapacitates them? *Molecular Microbiology* 63:937-940.

17. Wright GD (2007) The antibiotic resistome: the nexus of chemical and genetic diversity. *Nature Reviews Microbiology* 5:175-186.

18. Davies J, Davies D (2010) Origins and evolution of antibiotic resistance. *Microbiology and Molecular Biology Reviews* 74:417-433.

19. Smanski MJ, Yu Z, Casper J, Lin S, Peterson RM, Chen Y, Wendt-Pienkowski E, Rajski SR, Shen B (2011) Dedicated ent-kaurene and ent-atiserene synthases for platensimycin and platencin biosynthesis. *Proceedings of the National Academy of Sciences of the United States of America* 108:13498-13503.

20. Sambrook J, Russel D (2001) *Molecular cloning: a laboratory guide* (Cold Spring Harbor Laboratory Press, Cold Spring Harbor).

21. Kieser T, Bibb MJ, Buttner M, Chater KF, Hopwood DA (2000) *Practical streptomyces genetics* (The John Innes Foundation Norwich, UK).

22. Smanski MJ, Peterson RM, Rajski SR, Shen B (2009) Engineered Streptomyces platensis strains that overproduce antibiotics platensimycin and platencin. *Antimicrobial Agents and* Chemotherapy 53:1299-1304.

23. Yu Z, Smanski MJ, Peterson RM, Marchillo K, Andes D, Rajski SR, Shen B (2010) Engineering of Streptomyces platensis MA7339 for overproduction of platencin and congeners. *Organic Letters* 12:1744-1747.

24. Bierman M, Logan R, O'Brien K, Seno E, Nagaraja R (1992) Plasmid cloning vectors for the conjugal transfer of DNA from Escherichia coli to Streptomyces spp. *Gene* 116:43-49.

25. Bibb MJ, White J, Ward JM, Janssen GR (1994) The mRNA for the 23S rRNA methylase encoded by the ermE gene of Saccharopolyspora erythraea is translated in the absence of a conventional ribosome-binding site. *Molecular Microbiology* 14:533-545.

26. Ho SN, Hunt HD, Horton RM, Pullen JK, Pease LR (1989) Site-directed mutagenesis by overlap extension using the polymerase chain reaction. *Gene* 77:51-59.

27. Gust B, Challis GL, Fowler K, Kieser T, Chater KF (2003) PCR-targeted Streptomyces gene replacement identifies a protein domain needed for biosynthesis of the sesquiterpene soil odor geosmin. *Proceedings of the National Academy of Sciences of the United States of America* 100:1541-1546.

28. White SWS, Zheng J, Zhang YY-M, Rock C, Rock (2005) The structural biology of type II fatty acid biosynthesis. *Annual Review of Biochemistry* 74:791-831.

29. Huang W et al. (1998) Crystal structure of beta-ketoacyl-acyl carrier protein synthase II from E.coli reveals the molecular architecture of condensing enzymes. *EMBO Journal* 17:1183-1191.

30. Kursula P, Ojala J, Lambeir A, Wierenga R (2002) The catalytic cycle of biosynthetic thiolase: a conformational journey of an acetyl group through four binding modes and two oxyanion holes. *Biochemistry* 41:15543-15556.

31. Kumar A, Schweizer HP (2005) Bacterial resistance to antibiotics: active efflux and reduced uptake. *Advanced Drug Delivery Reviews* 57:1486-1513.

32. Andersson DI, Levin BR (1999) The biological cost of antibiotic resistance. *Current Opinion in Microbiology* 2:489-493.

33. Lai C-Y, Cronan JE (2003) Beta-ketoacyl-acyl carrier protein synthase III (FabH) is essential for bacterial fatty acid synthesis. *Journal of Biological Chemistry* 278:51494-51503.

34. Li Y, Florova G, Reynolds KA (2005) Alteration of the fatty acid profile of Streptomyces coelicolor by replacement of the initiation enzyme 3-ketoacyl acyl carrier protein synthase III (FabH). *Journal of Bacteriology* 187:3795-3799.

35. Revill W, Bibb MJ, Scheu A, Kieser H, Hopwood DA (2001) Beta-ketoacyl acyl carrier protein synthase III (FabH) is essential for fatty acid biosynthesis in Streptomyces coelicolor A3 (2). *Journal of Bacteriology* 183:3526-3530.

36. Morgan-Kiss RM, Cronan JE (2008) The Lactococcus lactis FabF fatty acid synthetic enzyme can functionally replace both the FabB and FabF proteins of Escherichia coli and the FabH protein of Lactococcus lactis. *Archives of Microbiology* 190:427-437.

37. Alberts A, Bell R, Vagelos PR (1972) Acyl carrier protein. XV. Studies of beta-ketoacyl-acyl carrier protein synthetase. *Journal of Biological Chemistry* 247:3190-3198.

38. Mcguire KA, McGuire JN, von Wettstein-Knowles P (2000) Acyl carrier protein (ACP) inhibition and other differences between beta-ketoacyl synthase (KAS) I and II. *Biochemical Society Transactions* 28:607-610.

39. McGuire KA, Siggaard-Andersen M, Bangera MG, Olsen JG, von Wettstein-Knowles P (2001) Beta-ketoacyl-[acyl carrier protein] synthase I of Escherichia coli: aspects of the condensation mechanism revealed by analyses of mutations in the active site pocket. *Biochemistry* 40:9836-9845.

40. Makarova K et al. (2006) Comparative genomics of the lactic acid bacteria. *Proceedings of the National Academy of Sciences of the United States of America* 103:15611-15616.

Appendix

A1.1 Primers, plasmids, and strains

Table A1.1 – Primers

Primer	Sequence	Description	Chapter
M13 Forward	5’-CGCCAGGGTTTTCCCAGTCACGAC-3’	pUC/M13 primers	3
M13 Reverse	5’-GAGCGGATAACAATTTCACACAGG-3’	pUC/M13 primers	3
ptmForward	5’-CCAAGATCCCGCTGGAGATC	GriH amplify	3
ptmReverse	5’-GGCAGAACTCGTTGATCGGG	GriH amplify	3
ΔptmT1Forward	5’-AGACCTGAGAATGACGGTGACCGAGTGTCCAGCATGACGATTCCGGGGATCCGTCGACC-3’	Amplification of *ptmT1* disruption cassette	4
ΔptmT1Reverse	5’-CTCCCGCGAGATGCTCCGCAGCAGTTTGATCTTGTCCACTGTAGGCTGGAGCTGCTTC-3’	Amplification of *ptmT1* disruption cassette	4
ΔptmT3Forward	5’-GGGGCTGACATCGGCGACCGTGAGGAAGCAGGAATGAACATTCCGGGGATCCGTCGACC-3’	Amplification of *ptmT3* disruption cassette	4
ΔptmT3Reverse	5’-CGCGGCGGCGGAGGCCGGGGCGCTGCGGTGCAGCTCGTCTGTAGGCTGGAGCTGCTTC-3’	Amplification of *ptmT3* disruption cassette	4
Sros_3708For	5’-CCACACTCAAGGAGATTCGATGACC-3’	Amplification of *sros_3708*	4
Sros_3708Rev	5’-GTCACCGCGGCTGTCTCATC-3’	Amplification of *sros_3708*	4
PtmT2pCDF2For	5’-GACGACGACAAGATGGTGCTCGAAGTTCCCGCTCAGC-3’	Amplification of *ptmT2*	4
PtmT2pCDF2Rev	5’-GAGGAGAAGCCCGGTTCAAGCACCTCCGGAAGC-3’	Amplification of *ptmT2*	4
PtmT3pCDF2For	5’-GACGACGACAAGATGAACAACAAGCTCGTCTCCCAC-3’	Amplification of *ptmT3*	4
PtmT3pCDF2Rev	5’-GAGGAGAAGCCCGGTCTAGCCGACGGCCTGTTC-3’	Amplification of *ptmT3*	4
PtmT1pCOLDFor	5’-GGAATTCCATATGACGTCGGAACTGCCCG-3’	Amplification of *ptmT1*	4

PtmT1pCOLDRev	5’-CGGAATTCTCAGAGCGCGAGCAGC-3’	Amplification of *ptmT1*	4
PtmP1For	5'-GACCTCGACGTCGCTGAC-3'	Amplification of *ptmP1*	5
PtmP1Rev	5'-TGGTTCCGTGCGCAGTAC-3'	Amplification of ptmP1	5
PtmP2For	5'-CGTGGTGTTGATGACCCGTC-3'	Amplification of ptmP2	5
PtmP2Rev	5'-GCCAGTTCGACGGCCATG-3'	Amplification of ptmP2	5
PtmP3For	5'-TGTGGAAGGGACACAACTTACC-3'	Amplification of ptmP3	5
PtmP3Rev	5'-GTGGTCACTTGGTGAACACCAGG-3'	Amplification of ptmP3	5
PtmP4For	5'-TGTTCACCAAGTGACCACGGC-3'	Amplification of ptmP4	5
PtmP4Rev	5'-CGTCATCACTCACTCCAGGATG-3'	Amplification of ptmP4	5
PtmP3C162AFor	5'-TCAGCGCCGCGGCGTCCG-3'	Site-directed mutagenesis of ptmP3	5
PtmP3C162ARev	5'-CGGACGCCGCGGCGCTGA-3'	Site-directed mutagenesis of ptmP3	5
PtmP3C162QFor	5'-TCAGCGCCCAGGCGTCCG-3'	Site-directed mutagenesis of ptmP3	5
PtmP3C162QRev	5'-CGGACGCCAGGGCGCTGA-3'	Site-directed mutagenesis of ptmP3	5
pSETmutFor	5'-TGACCGACGCGGTCCACACGTGG-3'	Site-directed mutagenesis of ptmP3	5
pSETmutRev	5'-CGGTGCGGGCCTCTTCGCTATTACGC-3'	Site-directed mutagenesis of ptmP3	5
SeqC162mutUp	5'-GACGACATCTTCGAGGAGTCCG-3'	Sequencing of PtmP3 C162 mutation	5
SeqC162mutDown	5'-CGGACTCCTCGAAGATGTCGTC-3'	Sequencing of PtmP3 C162 mutation	5

RLDC2For	5'-ACACCAGCCGTACTACGCGGATCGGAGGGCCGAGTCGTGATTCCGGGGATCCGTCGACC-3'	Amplification of *ptmU4-ptmP4* disruption cassette	5
RLDC2Rev	5'-CTACTTGCCGGGCTGCCGGGTACGGACGAGCAGTCCGGCTGTAGGCTGGAGCTGCTTC-3'	Amplification of *ptmU4-ptmP4* disruption cassette	5
UpstreamFabH(1)	5'-TGGTCGGCCAGGTCGCC-3'	Amplification of *Streptomyces fabH*	5
UpstreamFabH(2)	5'-TGGGACCTGTGCATGGAGAC-3'	Amplification of *Streptomyces fabH*	5
DownstreamFabH(1)	5'-GGTCGTCGGTGAAGGACTTGTC-3'	Amplification of *Streptomyces fabH*	5
DownstreamFabH(2)	5'-TCGACCATGGACAGCGAGTCG-3'	Amplification of *Streptomyces fabH*	5
UpstreamFabF(1)	5'-GGACAAGTCCTTCACCGACGAC-3'	Amplification of *Streptomyces fabF*	5
UpstreamFabF(2)	5'-GCTGTCCATGGTCGAGGTCG-3'	Amplification of *Streptomyces fabF*	5
DownstreamFabF(1)	5'-TCCGCTGGCTGCACCAGG-3'	Amplification of *Streptomyces fabF*	5
DownstreamFabF(2)	5'-ACGACGAACTGGAGCCCTTCC-3'	Amplification of *Streptomyces fabF*	5

ΔFabF-Forward	5'-ACACCGCTGGGTGGCGACAGCG CTTCGTCCTGGGAGGCCATTCCGGG GATCCGTCGACC-3'	Amplification of *fabf* disruption cassette	5
ΔFabF-Reverse	5'-CTCGGCGGGCAGCTTGCGGGGC TCGCCGCGGACGATGTCTGTAGGCT GGAGCTGCTTC-3'	Amplification of *fabf* disruption cassette	5
ΔFabH-Forward	5'-GGCGGCTACCGCCCGACCCGGG TCGTGCCCAACGAGGAGATTCCGGG GATCCGTCGACC-3'	Amplification of *fabH* disruption cassette	5
ΔFabH-Reverse	5'-CAACAGTCGCTCCATGGCGAGC GGAATGGAGGCGGCCGATGTAGGCT GGAGCTGCTTC-3'	Amplification of *fabH* disruption cassette	5
FabFscreenFor	5’-ATCGCACCGTGGTCGTCAC-3'	Isolation of cosmids containing *S. platensis fabF*	5
FabFscreenRev	5’-GGCCGTTGGGCATCAGCAT-3'	Isolation of cosmids containing *S. platensis fabF*	5
FabHscreenFor	5’-TCCACCGTTTCGCACTTCA-3'	Isolation of cosmids containing *S. platensis fabH*	5
FabHscreenRev	5’-GGCCGTTGGGCATCAGCAT-3'	Isolation of cosmids containing *S. platensis fabH*	5
FabF_IDFor	5'-AACGCGACCAATCGCACCG-3'	Confirmation of Δ*fabF* in *S. platensis*	5
FabF_IDRev	5'-TCCGGAAGGCCAGCACCAC-3'	Confirmation of Δ*fabF* in *S. platensis*	5
FabH_IDFor	5'-GACCTCGAAGGTCAAGCCC-3'	Confirmation of Δ*fabH* in *S. platensis*	5
FabH_IDRev	5'-GTCGCCAACAGTCGCTCCA-3'	Confirmation of Δ*fabH* in *S. platensis*	5

Table A1.2 – Plasmids

Plasmid	Description	Chapter
SuperCos1	Used for construction of MA7327 cosmid library	3
pIJ773 (*1*)	Contains apramycin resistance cassette (*aac(IV)3*)	4
pSET152 (*2*)	*E. coli – Streptomyces* shuttle vector	4,5
pSET152ermE*	pSET152 derivative with *ermE** promoter cloned upstream of a multiple cloning site	4,5
pSET152ampthio A (pBS9010) (*3*)	pSET152 derivative with ampicillin (*bla*) and thiostrepton (*tsr*) resistance genes replacing apramycin (*aac(3)IV*) resistance gene	4
pGEM-T Easy	TA cloning vector	4,5
pCR2.1-TOPO	TA cloning vector	5
pANT841	Cloning vector	4
pCDF-2 Ek/LIC	Cloning and expression vector	4
pCold Tf	Cloning and expression vector	4
pBS12003 (*4*)	Cosmid harboring partial *ptm* gene cluster	4
pBS12005 (*4*)	Cosmid harboring partial *ptm* gene cluster	4
pBS126G9	Cosmid harboring *fab* cluster from *S. platensis* MA7327	5
pBS12101	pSET152ermE* derivative harboring *ptmP1* under control of *ermE** promoter	5
pBS12102	pSET152ermE* derivative harboring *ptmP2* under control of *ermE** promoter	5
pBS12103	pSET152ermE* derivative harboring *ptmP3* under control of *ermE** promoter	5
pBS12104	pSET152ermE* derivative harboring *ptmP4* under control of *ermE** promoter	5
pBS12105	pSET152ermE* derivative harboring *S. platensis* MA7327 *fabF* under control of *ermE** promoter	5
pBS12106	pSET152ermE* derivative harboring *S. platensis* MA7327 *fabH* under control of *ermE** promoter	5
pBS12705	pSET152ermE* derivative harboring *S. platensis* MA7339 *fabF* under control of *ermE** promoter	5
pBS12706	pSET152ermE* derivative harboring *S. platensis* MA7339 *fabH* under control of *ermE** promoter	5
pBS12107	pBS9010 derivative harboring *ptmP3* under control of *ermE** promoter	5
pBS12108	pBS12005 Δ*ptmU4-ptmP4::aac(IV)3*, generated by PCR targeting with primers RLDC2-For and RLDC2-Rev	5
pBS12109	pBS126G9 Δ*fabF::aac(IV)3*, generated by PCR targeting with primers FabF-TgtFor and FabF-TgtRev	5
pBS12110	pBS126G9 Δ*fabH::aac(IV)3*, generated by PCR targeting with primers FabH-TgtFor and FabH-TgtRev	5
pBS12111	pSET152ermE* derivative harboring *ptmP3*(C162A) under control of ermE* promoter	5

pBS12112	pSET152ermE* derivative harboring *ptmP3*(C162Q) under control of *ermE** promoter	5
pBS12713	pSET152ermE* derivative harboring *ptnP3* under control of *ermE** promoter	5
pBS12114	pSET152ermE* derivative harboring *ptmP2* and *ptmP1* under control of *ermE** promoter	5
pBS12715	pSET152ermE* derivative harboring *S. albus fabF* under control of *ermE** promoter	5
pBS12716	pSET152ermE* derivative harboring *S. albus fabH* under control of *ermE** promoter	5
pBS12011	pBS12003 Δ*ptmT1*	4
pBS12012	pBS12003 Δ*ptmT3*	4
pBS12603	pSET152ermE* derivative harboring "PTM cassette" from *S. platensis* MA7327 under control of *ermE** promoter	4
pBS12017	pSET152AT derivative harboring *sros_3708* from *S. roseum* DSM43021 under control of *ermE** promoter	4
pBS12250	pCDF-2 harboring *ptmT2* (N-terminal His_6-tag)	4
pBS12251	pCDF-2 harboring *ptmT3* (N-terminal His_6-tag)	4
pBS12252	pCold harboring *ptmT1* (N-terminal His_6-tag)	4

Table A1.3 – Strains

Strains	Description	Chapter
Escherichia coli DH5α	*E. coli* host for routine cloning	4,5
E. coli BL21 (DE3)	*E. coli* host for protein expression	4
E. coli BW25113/pIJ790 (*1*)	*E. coli* host for PCR targeting (contains recombination plasmid, pIJ790)	4,5
E. coli ET12567/pUZ8002 (*5*)	Methylation-deficient *E. coli* host for intergenic conjugation; contains pUZ8002, a non-transmissible *oriT* mobilizing plasmid	4,5
Streptomyces platensis MA7327 (*6*)	Wildtype PTM/PTN producer	3,4,5
S. platensis MA7339 (*7*)	Wildtype PTN producer	3,4,5
Streptosporangium roseum DSM43021	ATCC strain 12428 (Complete genome sequence available through GenBank: NC_013595)	4
S. platensis SB12001 (*8*)	PTM/PTN overproducing strain	3,4,5
S. platensis SB12002 (*8*)	PTM/PTN overproducing strain	3,4,5
Streptomyces albus J1074	Naïve host for expression constructs	5
Streptomyces lividans K4-114	Naïve host for expression constructs	5
Streptomyces coelicolor M512	Naïve host for expression constructs	5
S. albus SB12701	J1074 harboring pBS12101	5
S. albus SB12702	J1074 harboring pBS12102	5
S. albus SB12703	J1074 harboring pBS12103	5
S. albus SB12704	J1074 harboring pBS12104	5
S. albus SB12705	J1074 harboring pBS12105	5
S. albus SB12706	J1074 harboring pBS12106	5
S. albus SB12711	J1074 harboring pBS12111	5
S. albus SB12712	J1074 harboring pBS12112	5
S. albus SB12713	J1074 harboring pBS12713	5
S. albus SB12714	J1074 harboring pBS12114	5
S. albus SB12715	J1074 harboring pBS12715	5
S. albus SB12716	J1074 harboring pBS12716	5
S. lividans SB12723	K4-114 harboring pBS12103	5
S. *coelicolor* SB12733	M512 harboring pBS12103	5
S. platensis SB12127	MA7327 harboring pBS12107	5
S. platensis SB12727	MA7339 harboring pBS12107	5
S. platensis SB12120	MA7327 Δ*ptmU4-ptmP4::aac(IV)3*	5
S. platensis SB12121	MA7327 Δ*fabF::aac(IV)3*	5
S. platensis SB12122	MA7327 Δ*fabH::aac(IV)3*	5
S. platensis SB12123	SB12127 Δ*fabF::aac(IV)3*	5
S. platensis SB12124	SB12127 Δ*fabH::aac(IV)3*	5
S. platensis SB12717	SB12727 Δ*fabF::aac(IV)3*	5
S. platensis SB12718	SB12727 Δ*fabH::aac(IV)3*	
S. platensis SB12007	MA7237 Δ*ptmT1::aac(IV)3*	4
S. platensis SB12008	MA7327 Δ*ptmT3::aac(IV)3*	4

S. platensis SB12604	MA7339 harboring pBS12603	4
S. platensis SB12140	SB12007 harboring pBS12017	4

A1.2 Common media, buffers, and reagents

R2YE Medium (1L):

Sucrose	103g
K2SO4	0.25g
MgCl2*6H2O	10.12g
Glucose	10g
Casaminoacids	0.1g
Yeast Extract	5g
TES	5.73g
H2O	850mL
(agar)	(22g)
Autoclave above first, then add:	
1M NaOH	5mL
0.5% KH2PO4	10mL
1M CaCl2	20mL
20% Proline	15mL
Trace Elements Solution	2mL

Trace Elements Solution (1L)

ZnCl2	0.04g
FeCl3*6H2O	0.2g
CuCl2*2H2O	0.01g
MnCl2*4H2O	0.01g
(NH4)6Mo7O24*H2O	0.01g
Na2B4O7*10H20	0.01g
H2O	1000mL

IWL4 Medium (1L):

ISP4	37g
Yeast Extract	0.5g
Tryptone	1g
H2O	1000mL
Autoclave above first, then add:	
1M MgCl2	10mL

ISM-3 Seed Medium (1L):

Yeast Extract	15g
Malt Extract	10g
Anhydrous MgSO4*7H2O	0.244g
FeCl3*6H2O	0.3g
Glucose	20g
H2O	1000mL

[Adjust to pH 7.0 with NaOH]

SLY Medium or "PTM" Medium (1L):

Stadex 60	40g
Lactose	40g
Yeast Extract	5g
H2O	1000mL

[Adjust to pH 7.0 with NaOH]

SLYM Medium or "PTMM" Medium (1L):

Stadex 60K	40g
Lactose	40g
Yeast Extract	5g
MOPS (sodium salt)	20g
H2O	1000mL

[Adjust to pH 7.3 with NaOH]

PTN Medium (1L):

Yeast Extract	6g
Malt Extract	15g
Dextrose	6g
MOPS (sodium salt)	20g
H2O	1000mL

[Adjust to pH 7.4 with NaOH]

Merck PTM production, "CLA" (1L):

Amberex pH	5g
Yellow corn meal	40g
Lactose	40g
H2O	1000mL

[Adjust to pH 7.0 with NaOH]

SOC Medium (1L):

Bacto Tryptone	10g
Glucose	1.8g
Yeast Extract	2.5g
NaCl	0.29g
KCl	0.093g
MgCl2*6H20	1.02g
MgSO4*7H20 (or anhydrous)	1.23g (0.6g)
H2O	1000mL

[Adjust to pH 7.0 with NaOH]

2xYT Medium (1L):

Tryptone	16g
Yeast Extract	10g
NaCl	5g
H2O	1000mL

[Adjust to pH 7.0 with NaOH]

SOB Medium (1L):

Bacto Tryptone	20g
Yeast Extract	5g
NaCl	0.58g
KCl	0.186g
H2O	1000mL

[Adjust to pH 7.0 with NaOH]

LB Medium (1L):

Tryptone	10g
Yeast Extract	5g
NaCl	10g
(agar)	(15g)
H2O	100mL

[Adjust to pH 7.0 with NaOH]

TE Buffer (1L):

1M Tris-HCl (pH 8.0)	10mL
0.5M EDTA (pH 8.0)	2mL
H20	988mL

TSE Buffer (1L):

1M Tris-HCl (pH 8.0)	25mL
0.5M EDTA (pH 8.0)	5mL
Sucrose	103g
H20	To 1000mL

TB Buffer (1L):

Pipes	3g
CaCl2*2H2O	2.2g
KCl	18.65g
<u>Adjust to pH 6.7 with KOH, then add:</u>	
MnCl2	10.9g

RNase A stock (1mL):

Ribonuclease A (RNase A)	10mg
0.3M Sodium Acetate (pH 4.8)	1mL

[Incubate at 90ºC for 10 min; store at -20 ºC]

A1.3 List of vectors and vector maps

Figure A1.1 – SuperCos 1 (Agilent Technologies, Santa Clara, CA)

Figure A1.2 – pGEM-T Easy (Promega Corporation, Madison, WI)

Figure A1.3 – pGEM-3Zf(+) (Promega Corporation, Madison, WI)

Figure A1.4 – pCR2.1-TOPO (Life Technologies Corporation, Grand Island, NY)

Figure A1.5 – pANT841 (GenBank: AF438749)

Figure A1.6 – pSET152ermE* (Derivative of pSET152, GenBank: AJ414670)

Figure A1.7 – pSET152ampthio A (Derivative of pSET152, GenBank: AJ414670)

Figure A1.8 – pCDF-2 Ek/LIC (EMD Millipore, Billerica, MA)

Figure A1.9 – pCold Tf (GenBank: AB213654; Clontech Laboratories, Inc., Mountain View, CA)

Figure A1.1

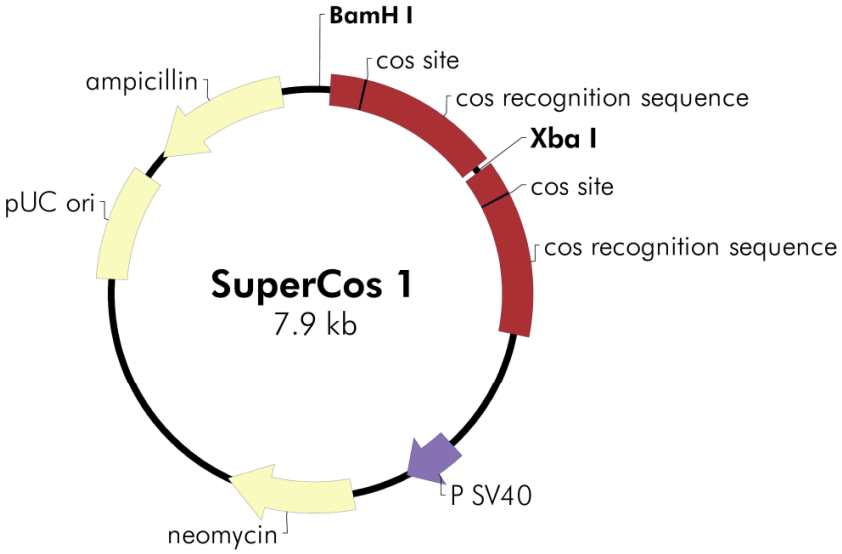

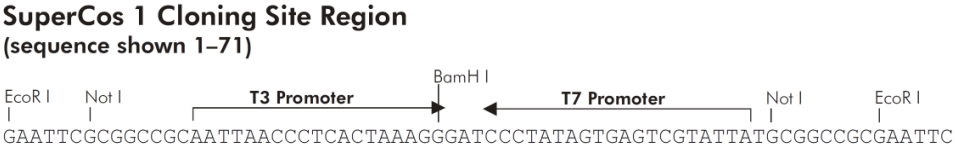

Figure A1.2

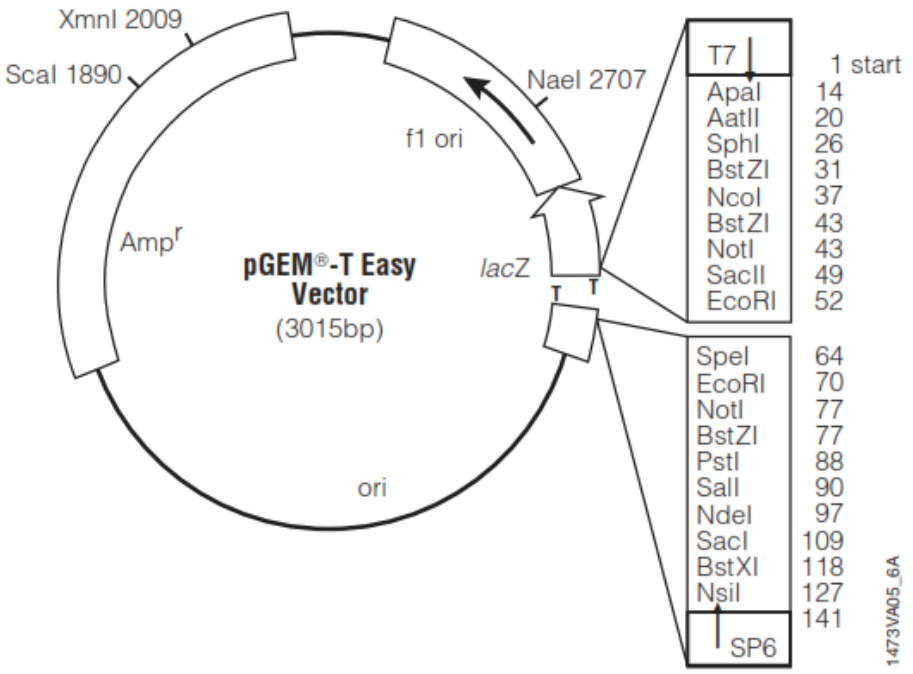

Figure A1.3

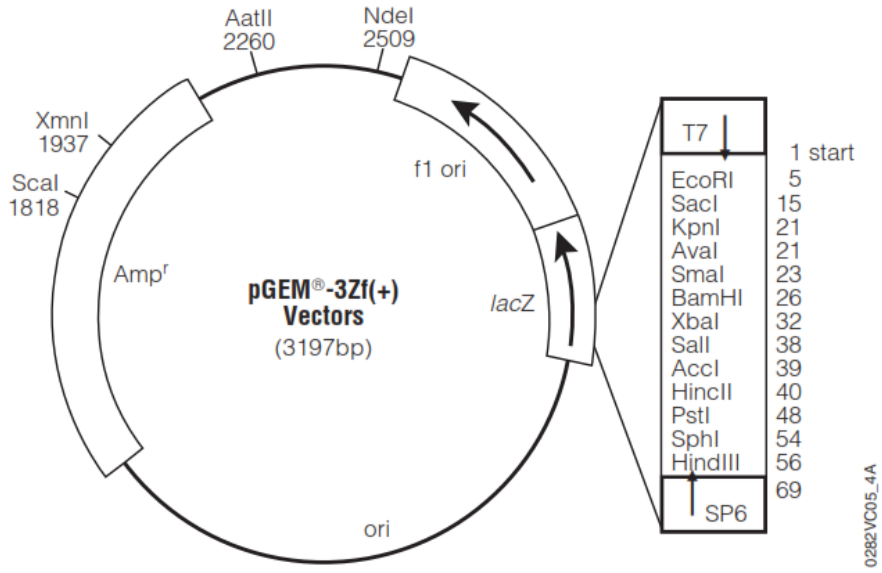

Figure A1.4

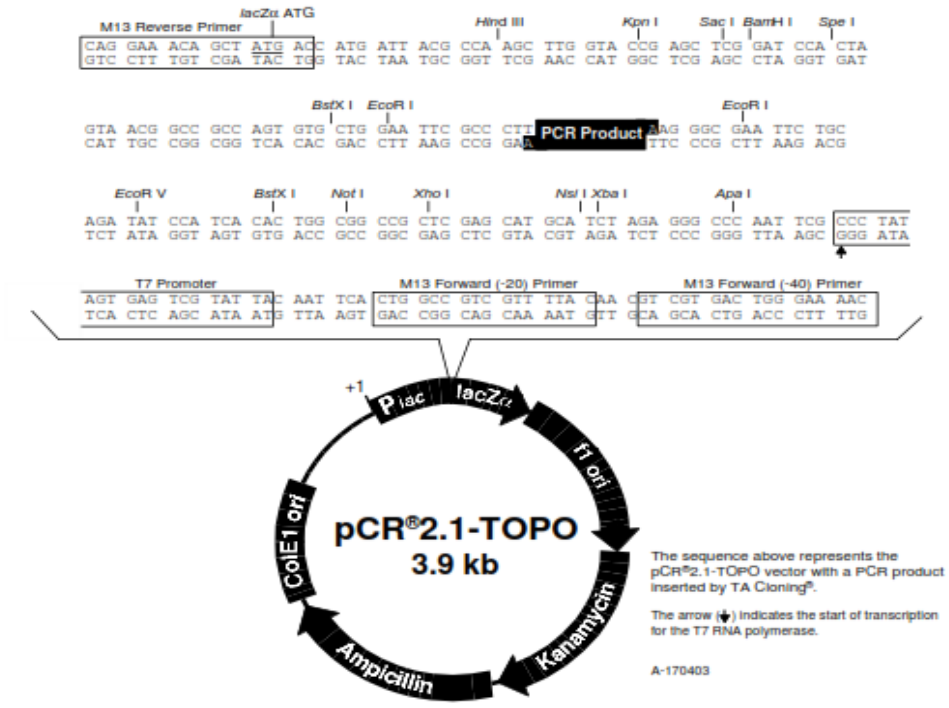

Figure A1.5

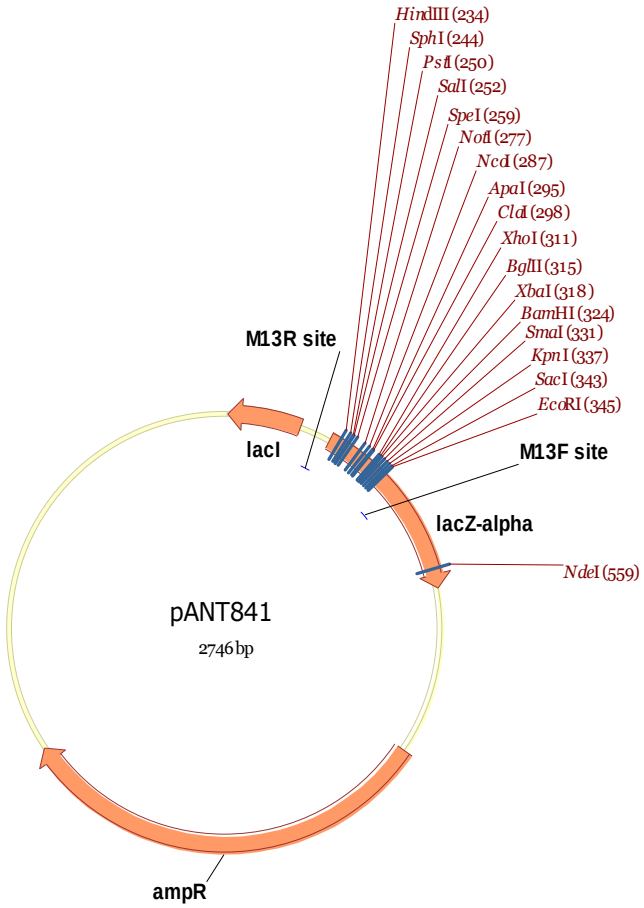

Figure A1.6

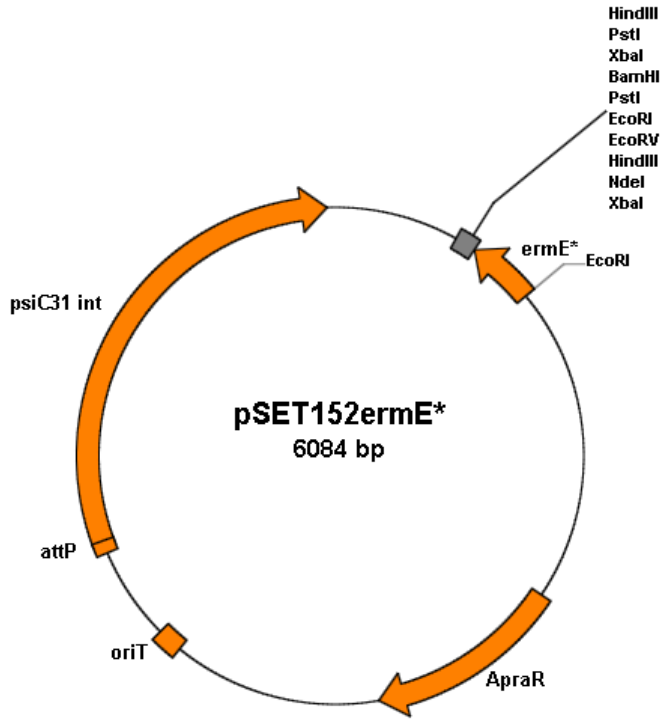

Figure A1.7

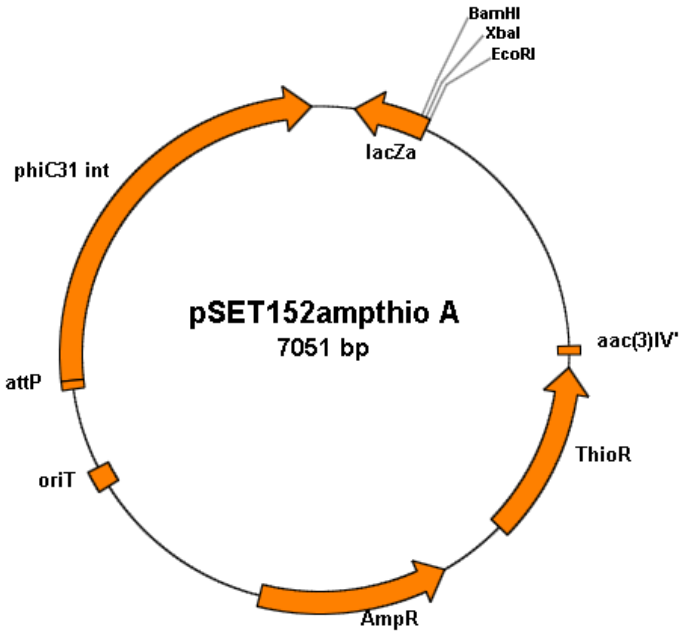

Figure A1.8

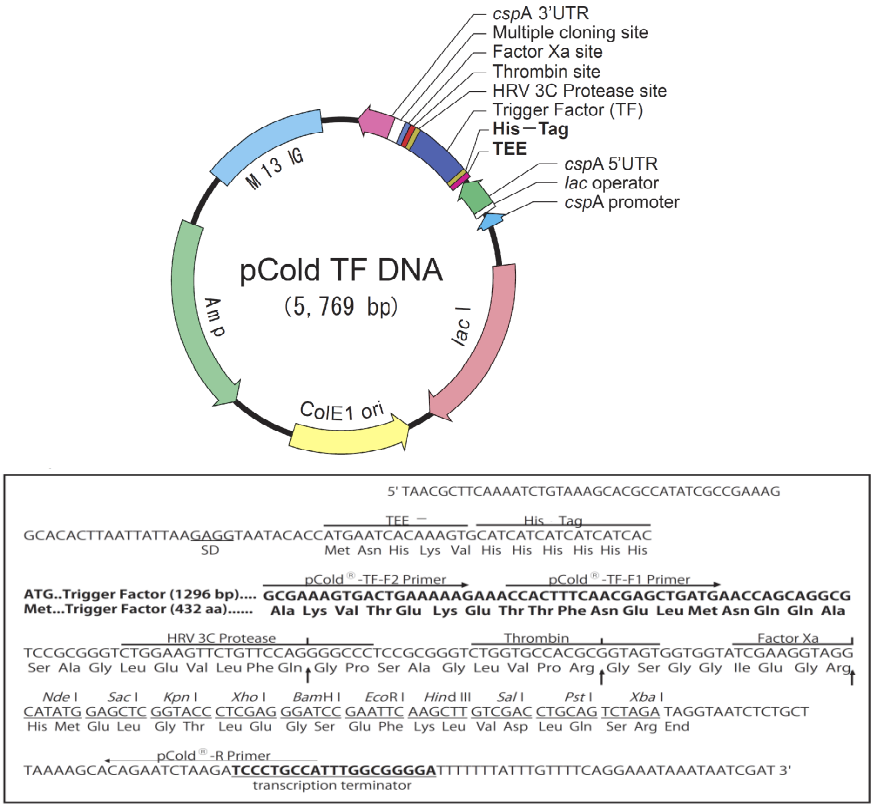

Figure A1.9

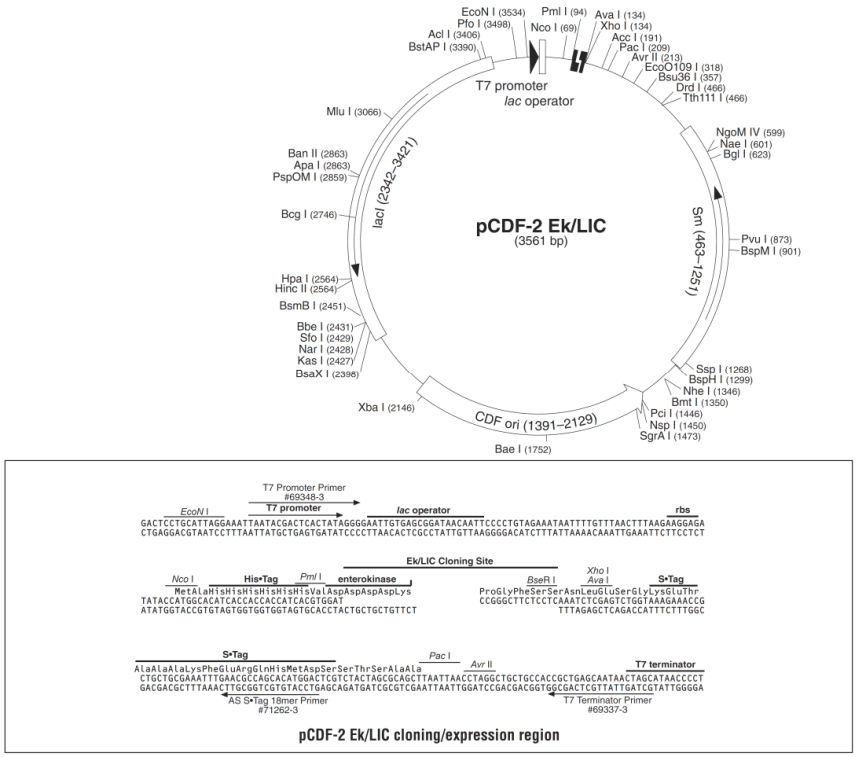

A1.4 Supplementary materials and methods.

A1.4.1 Total DNA isolation from *Streptomyces* (*5*):

A 1-2 mL aliquot of an early stationary phase *Streptomyces* culture is spun down in a microcentrifuge tube to obtain ~100 µL packed cells. The cells are washed once with 1 mL 10.3% sucrose. The washed cell pellet is resuspended in 450 µL TSE containing lysozyme (5 mg/mL) and incubated for 30-45min at 37˚C. After incubation, 225µL 2% SDS (diluted from 10% SDS stock) is added to the tube, mixed in gently to lyse cells, and the mixture incubated at room temperature for 5 min. A 100 µL aliquot of neutral phenol and 50µL aliquot of chloroform is added to the tube and the contents are mixed/vortexed very well. The sample is centrifuged for 10-15 min and the supernatant carefully transferred to a new tube containing 60µL 3M NaOAc before adding 700µL isopropanol. The sample is mixed gently by inversion as the DNA visibly transforms from cloudy mixture to a white, stringy clump. The sample is centrifuged briefly to pellet the DNA. The DNA is subsequently dissolved in 500 µL TE buffer containing 10uL RNase solution (10 mg/mL) and incubated at room temperature for 15 min. After incubation, 300 µL of neutral phenol and 150 µL chloroform is added to the tube, the sample mixed/vortexed very well and centrifuged for 15 sec before transfer of the supernatant to a new tube and addition of a second aliquot of 300 µL chloroform. The tube is mixed well and centrifuged for 5 min. The supernatant is again transferred to a new tube containing 50 µL 3M NaOAc, before addition of 350uL isopropanol. The contents are mixed gently until white strings (DNA) appear and incubated on ice for 30 min. The mixture is finally centrifuged for 15 sec, the supernatant is removed, and the pellet is allowed to air dry for a few minutes before addition of 150 µL TE.

A1.4.2 Introduction of DNA into *Streptomyces* by conjugation with *E. coli* (*5*):

Chemically competent *E. coli* ET12567/pUZ8002 cells are transformed with pSET152-derived constructs (or other *oriT*-containing vectors) and plated on LB containing antibiotic selection for the incoming plasmid (i.e. apramycin for pSET152). A single transformant is used to inoculate 5 mL LB containing kanamycin (25 mg/mL), chloramphenicol (25 mg/mL), and the antibiotic used for selection of the *oriT*-containing plasmid, and incubated overnight at 37°C with 250 rpm shaking. A 250 μL aliquot of the overnight culture is used to inoculate 25 mL of fresh LB containing appropriate antibiotics, which is incubated at 37°C with shaking until an OD_{600} of ~0.6 is reached. The cells are harvested by centrifugation, washed twice with equal volumes of LB to remove antibiotics, and resuspended in 2.5 mL LB before incubating on ice prior to conjugation. *Streptomyces* spores (or mycelial fragments – see Chapter 4) are prepared for conjugation by adding ~10^8 spores to 500 μL 2xYT liquid media and heat-shocking at 50°C for 10 min. After a brief cool down, 500 μL of the prepared E. coli cells are added to the heat-shocked spores, mixed briefly, and centrifuged for 15 sec. The supernatant is poured off and the spore/*E. coli* cell pellet is resuspended in residual liquid, which is plated onto a freshly prepared ISP-4 plate supplemented with 10 mM $MgCl_2$ and incubated for 20 h at 30°C. After initial incubation, the plate is overlaid with 1 mL of water containing 20 uL nalidixic acid (25 mg/mL in 0.15M NaOH) and the antibiotic for selection of plasmid being introduced into *Streptomyces*. The overlaid plate is incubated at 30°C until potential exconjugants are visible (petand able to be picked and streaked onto selective media containing nalidixic acid.

A1.4.3 Methods for small-scale synthesis of geranylgeranyl diphosphate from geranylgeraniol starting material (*9*)

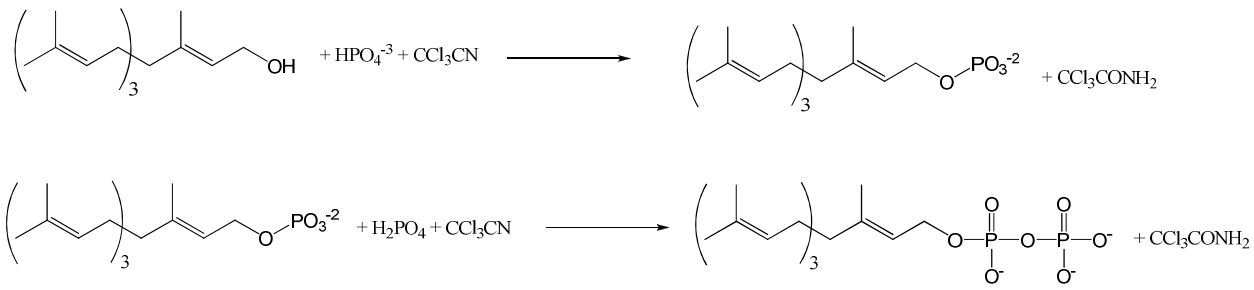

Figure A1.10 – Scheme for phosphorylation of geranylgeraniol.

Solution A: dilute 25 mL of concentrated phosphoric acid (HPLC grade) into 94 mL acetonitrile

Solution B: dilute 110 mL triethylamine into 100 mL acetonitrile

Mobile phase 1: isopropanol:NH_4OH:H_2O (6:2.5:0.5, v/v)

Mobile phase 2: isopropanol:NH_4OH:H_2O (6:3:1, v/v)

Geranylgeraniol (100 mg, 344 µmol neat alcohol) was transferred equally into two 50 mL polypropylene tubes with trichloroacetonitrile (0.5 mL, ~5 mmol). A TEAP solution was prepared by slowly adding 1.82 mL of solution A to 3.0 mL solution B with constant stirring. After mixing, 0.5 mL of the TEAP solution was added to each of the tubes containing GGOH. The reactions were placed in a 37°C bath for 5 min. Two more 0.5 mL additions of TEAP were added to each of the tubes followed by 5 min incubations at 37°C after each addition.

The reaction mixtures were streaked onto two 20 x 20 cm silica preparative TLC plates (Whatman 4861-840) using a Pasteur pipette, and the plates were allowed to dry for 1 h. The plates were placed into a covered prep-TLC tank containing ~130 mL mobile phase 2 and

allowed to develop overnight. After development, the plates were allowed to dry for ~2 h (until plates were dry and the smell of ammonia had dissipated).

Short-wave UV analysis revealed 5 fluorescent bands at approximately 5 cm (band 1), 7 cm (band 2), 11.5 cm (band 3), 13.5 cm (band 4), and 15.5 cm (band 5) from the bottom of the 20 cm plates. In addition, a visible yellow band from ~17 cm to 19 cm from the bottom of the plate. In a previous study, the GGDP band had a reported R_f value of approximately 0.5 and was not visible under UV. The plates were subsequently sprayed with ddH20 (~10-20mL) until three thick "white bands" were revealed between fluorescent bands: between bands 1 and 2, between bands 2 and 3, and between bands 3 and 5. The largest white band (between fluorescent bands 2 and 3), and at approximately 8-11 cm from the bottom of the plates (average R_f value ~0.5), was expected to be the GGDP product. This area on each of the two plates was subsequently scraped off and collected in 50 mL polypropylene tubes.

The recovered silica was washed thoroughly with 20 mL of 10 mM NH_4HCO_3 (pH 8), vortexing for ~1 min to ensure maximum recovery. The tubes were spun down at 3000 g for 10 min, the supernatant decanted, and the pellet washed again with 10 mL of 10 mM NH_4HCO_3 (pH 8). The tubes were spun once more and the combined supernatants were filtered (to eliminate very fine silica particles) using disposable SFCA bottletop filters (150 mL).

The samples (~30 mL total volume) were frozen at -80°C and lyophilized until dry. Dried samples were resuspended in 4 mL of 10 mM NH_4HCO_3-MeOH (1:1, v/v). Samples were spun down at 4150 rpm for 30 min and finally syringe filtered (0.22 µm – Millex GV PVDF) to eliminate any remaining silica particles. Samples were stored at -20°C.

A1.4.4 Analytical TLC of fractions collected from MPLC purification of large-scale synthesis of GGDP from geranylgeraniol:

Analytical TLC was carried out using silica gel 60 glass plates (0.25mm). Plates were developed in a TLC chamber using mobile phase 2 (see Section A1.4.3) and detection was achieved by spraying developed and dried plates with anisaldehyde solution (90:5:5, ethanol:p-anisaldehyde:H_2SO_4, v/v) and heating. TLC analysis facilitated pooling of GGDP-containing fractions, which were concentrated by rotary evaporation and diluted with equal volumes MeOH and 10 mM NH_3HCO_3. Pool 1, final volume of 80 mL, containing mostly pure GGDP, was stored in two separate 50 mL polypropylene tubes, labeled "GGDPSynth1A" and "GGDPSynth1B", at -20ºC. Pool 2 (final volume of 15 mL), pool 3 (final volume of 45 mL), and pool 4 (final volume of 30 mL) were also stored at -20°C.

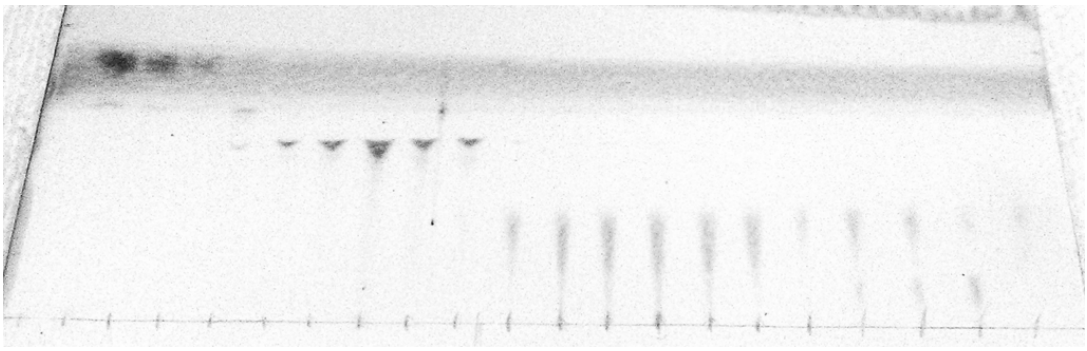

Frxn #: 1 5 10 11 15 20 21 25 30 31 35 40 41 45 50 51 55 60 61 65 Std

[----**Pool 4**, Frxns 15-33-------]

Figure A1.11 – TLC analysis of MPLC fractions 1 – 65. Fractions 15-33 were pooled to yield mostly pure GGTP in "pool 4". Authentic GGDP was spotted for comparison indicated as "Std" to the right of fraction 65.

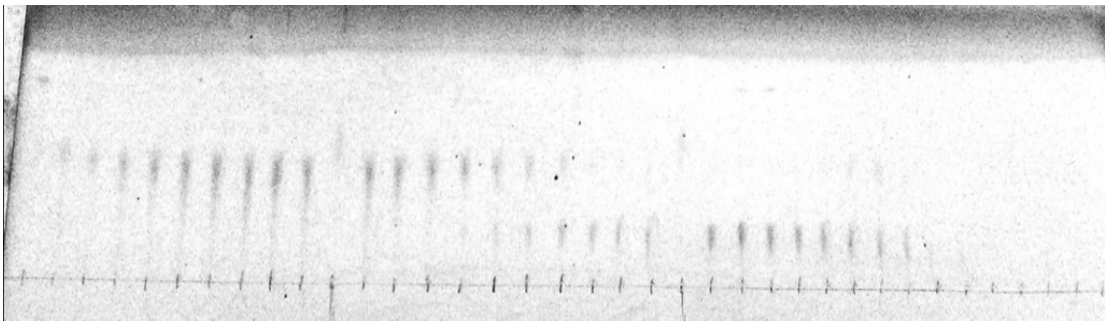

Frxn #: [----------**Pool 1** (Frxns 34-56)----------] [--**Pool 2**--][---------**Pool 3** (Frxns 70-88)-------] 94
(Frxns 58-64)

Figure A1.12 - TLC analysis of MPLC fractions 34 – 94. Fractions 34-56 were pooled to yield "pool 1", containing mostly pure GGDP; fractions 58-64 were pooled to yield "pool 2", containing a mix of GGDP and GGMP; and fractions 70-88 were pooled to yield "pool 3", containing mostly GGMP.

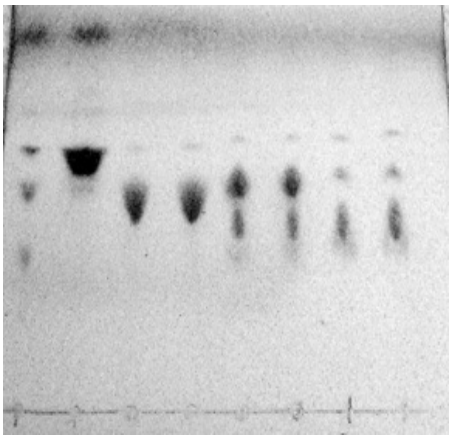

Lane: 1 2 3 4 5 6 7 8

Figure A1.13 – TLC check of pooled fractions. Pool 1 (lanes 3-4, mostly pure GGDP), pool 2 (lanes 5-6, GGDP- and GGMP-containing mixture), pool 3 (lanes 7-8, mostly pure GGMP, some GGDP), pool 4 (lane 2, mostly pure GGTP), and crude reaction mixture (lane 1).

A1.4.5 Analysis by HPLC of fractions collected from MPLC purification of large-scale synthesis of GGDP from geranylgeraniol:

A Waters 510 HPLC system with a photodiode array detector (Waters, Milford, MA) and an Apollo C_{18} column (particle size, 5μm; 4.6mm x250 mm; Grace Davison Discovery Sciences, Deerfield, IL) was used to analyze GGDP-containing fractions. Analysis was performed at a flow rate of 1 mL/min, using a linear gradient from 5% solvent B (acetonitrile) and 95% solvent A (25 mM NH_4HCO_3 in water, pH 8) to 95% solvent B over 20 min followed by 5 min isocratic 95% solvent B. Absorbance at 214nm was monitored.

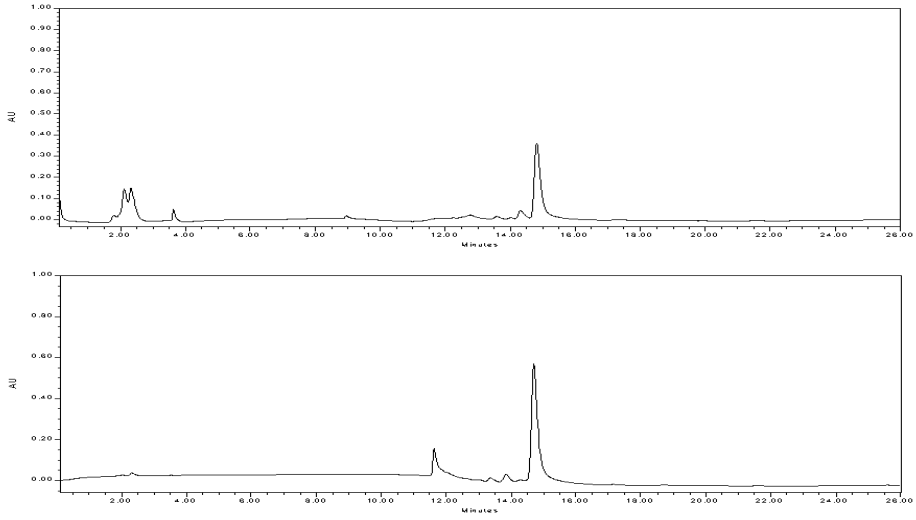

Figure A1.14 – HPLC analysis of GGDP. HPLC chromatograms of a 30 μL injection of prep-TLC purified GGDP sample (top panel) and 10 μL injection of a commercially obtained GGDP standard (bottom panel). Absorbance monitored at 214 nm.

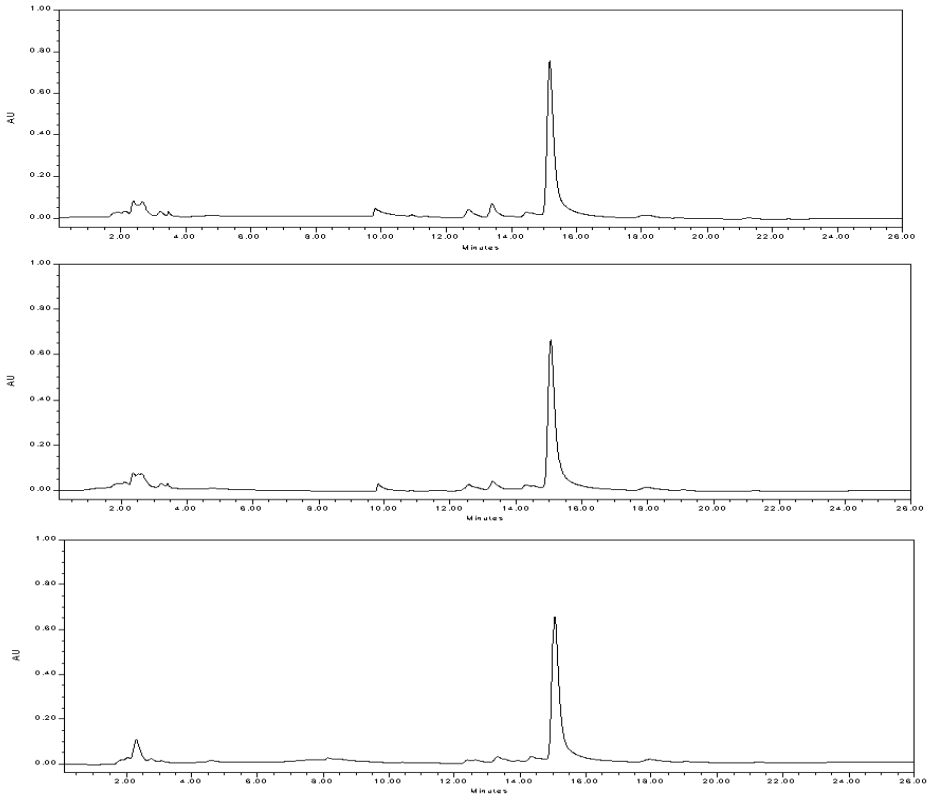

Figure A1.15 – HPLC analysis of GGDP samples during purification steps. HPLC chromatograms of 15 μL injections of prep-TLC purified samples of GGDP before (top panel) and after (middle and bottom panels) centrifugation/filtration steps to remove silica particles. Absorbance monitored at 214 nm.

A1.4.6 Large-scale bioconversion of GGDP to ent-CPP and kauran-16-ol using purified recombinant PtmT2 and PtmT3 enzyme:

(A) Bioconversion of GGDP to *ent*-CPP:

A 400 mL reaction mixture was prepared in a 1 L flask containing 50 mM Tris-HCl (pH 6.8), 1 mM $MgCl_2$, 5 mM 2-mercaptoethanol, 0.1% Tween 80, 10% glycerol and 8.4 mg GGDP (~47 µM, "RMPSynth1A"). The reaction was initiated by addition of 0.75 mL PtmT2 (~24 mg/mL). The reaction was mixed thoroughly and incubated in a 30°C water bath. An additional 0.25 mL PtmT2 (~24 mg/mL) was added after 3hrs of incubation. The reaction was incubated an additional 9 hrs before column purification methods.

(B) Bioconversion of GGDP to kauran-16-ol:

A 400 mL reaction mixture was prepared in a 1 L flask containing 50 mM Tris-HCl (pH 6.8), 1 mM $MgCl_2$, 5 mM 2-mercaptoethanol, 0.1% Tween 80, 10% glycerol and ~8.4 mg GGDP (~47 µM, "RMPSynth1A"). The reaction was initiated by addition of 0.5 mL PtmT2 (~24 mg/mL) and 0.5 mL PtmT3 (~10.5 mg/mL). The reaction was mixed thoroughly and incubated in a 30°C water bath. An additional 0.5 mL PtmT3 (~10.5 mg/mL) was added after 3 hrs of incubation. The reaction was incubated an additional 9 hrs before extraction with hexanes.

(C) Isolation and purification of *ent*-CPP reaction product:

A 20 g quantity of Diaion HP-20 resin (Itochu Chemicals America) was added directly to the terminated reaction mixture (400 mL) and incubated at room temperature with constant stirring for 3 hrs. The mixture containing resin was then poured into a glass column (Chemglass Life Sciences, 1 in I.D. x 18 in E.L.). The reaction mixture was allowed to flow

through the column and the resin allowed to settle. The resin was then washed with 10 column volumes of 100 mM EDTA to remove Mg^{2+}. Material bound to the resin was eluted with 5 column volumes of methanol and the eluate was concentrated on a rotary evaporator.

(D) Isolation and purification of kauran-16-ol reaction product:

After incubation, the 400 mL reaction mixture was extracted three times with equal volumes (~1.2 L total) of hexanes. Washing the organic phase and a resulting "emulsion" layer with a saturated NaCl solution after removing the aqueous layer eliminated the emulsion layer and assisted in cleanly separating the organic phase from an aqueous phase. The organic layers from the extractions, and subsequent washings, were decanted, collected and concentrated on a rotary evaporator.

A1.4.7 Assays for determining PTM/PTN susceptibility in *Streptomyces* strains using disk diffusion methods

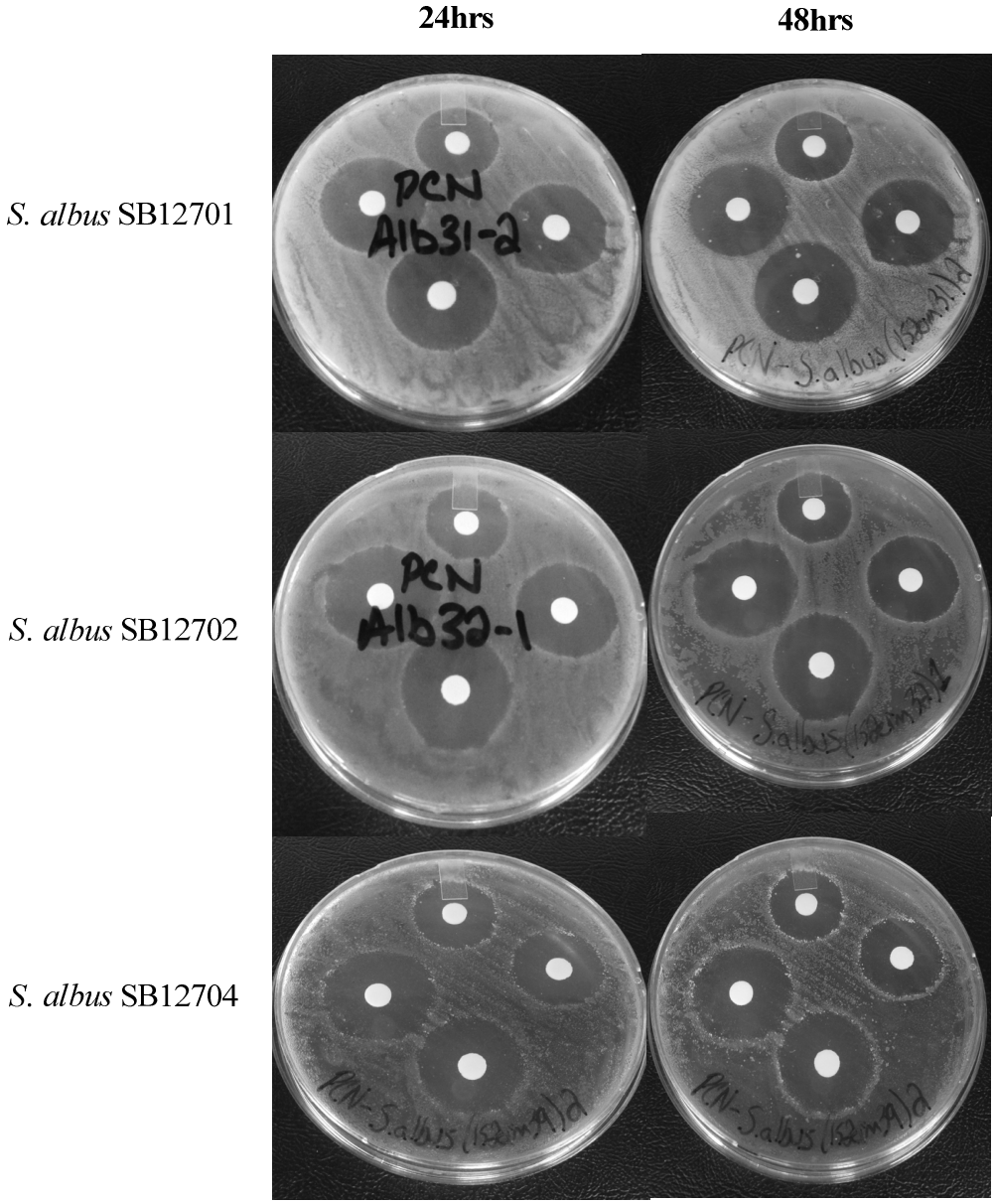

Figure A1.16 – Comparison of susceptibility to PTN among *S. albus* strains expressing *ptmP1*, *ptmP2*, or *ptmP4*. No significant change is seen in zones of inhibition after 24 hrs and 48hrs of growth at 30°C after application of disk containing PTN. Amount of PTN/disk ranges from 1.25 µg - 10 µg.

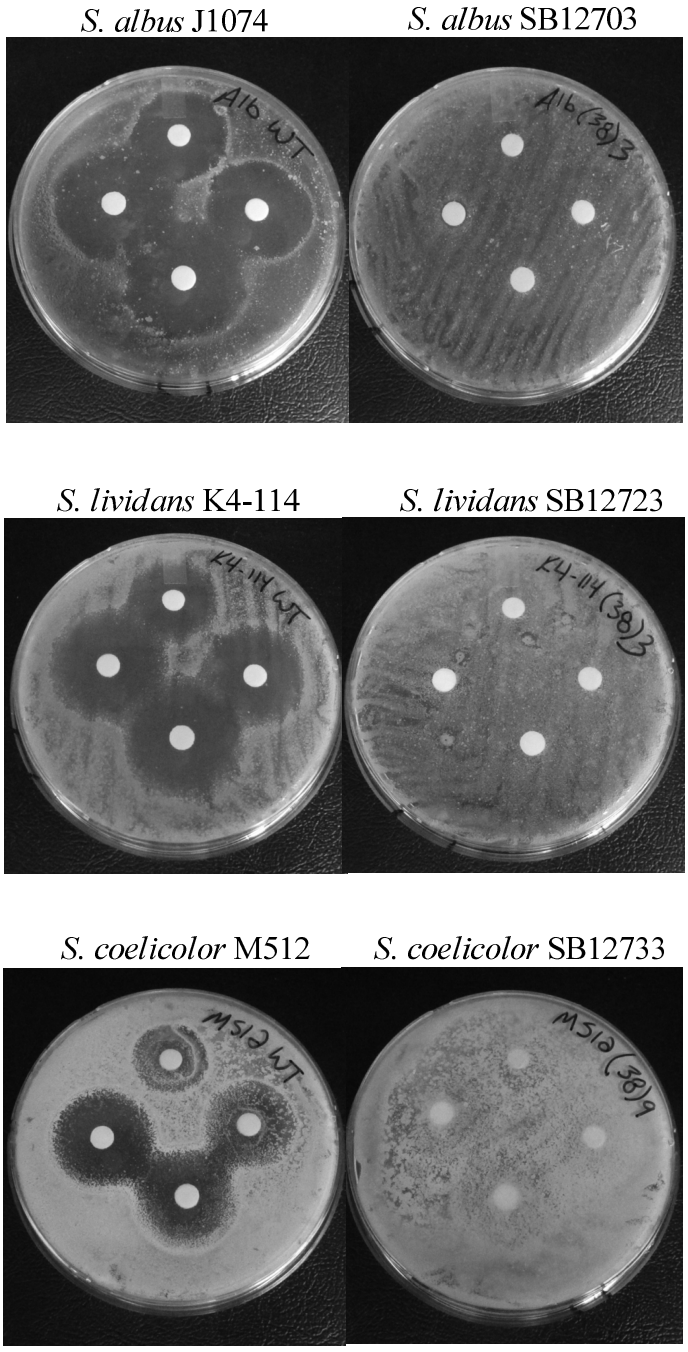

Figure A1.17 – Comparison of PTN susceptibilities among WT and recombinant *Streptomyces* strains overexpressing *ptmP3*. Amount of PTN/disk ranges from 1.25 μg - 10 μg.

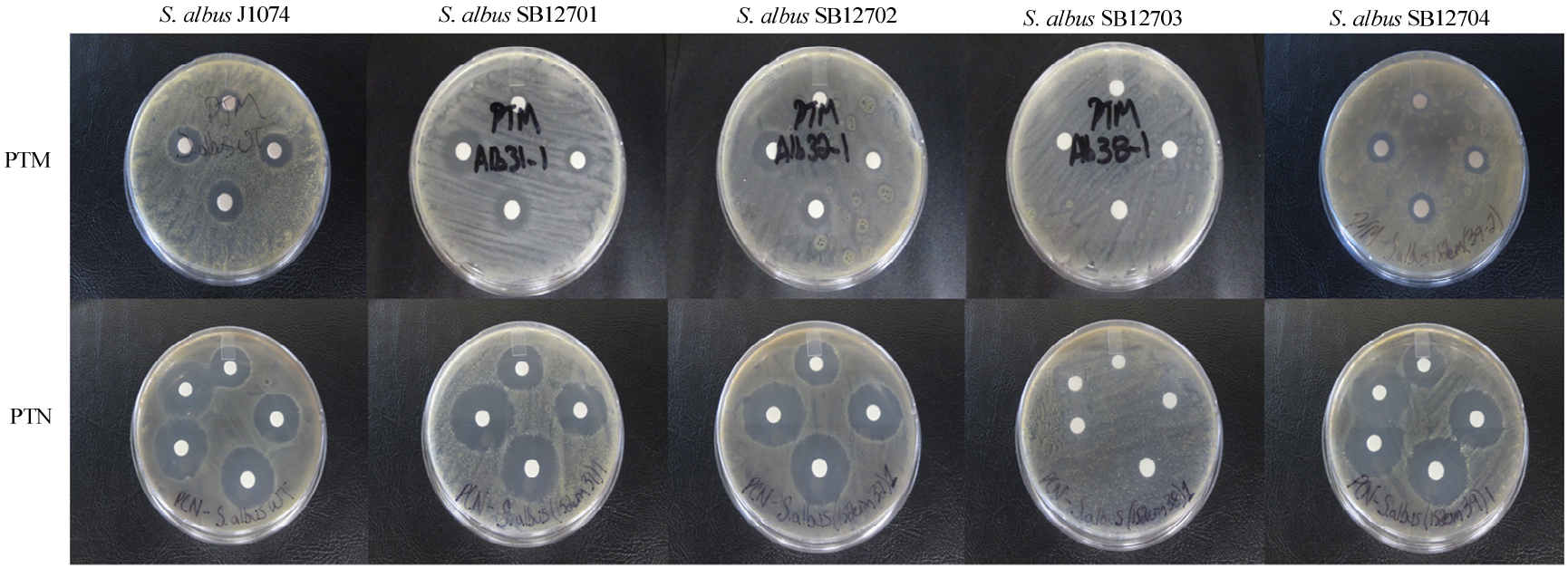

Figure A1.18 – Comparison of PTM and PTN susceptibility of WT and recombinant *S. albus* strains overexpressing *ptmP1*, *ptmP2*, *ptmP3*, or *ptmP3*. Amount of PTN/disk ranges from 1.25 µg - 10 µg; amount of PTM/disk ranges from 5 µg – 40 µg.

S. albus J1074

S. albus SB12705

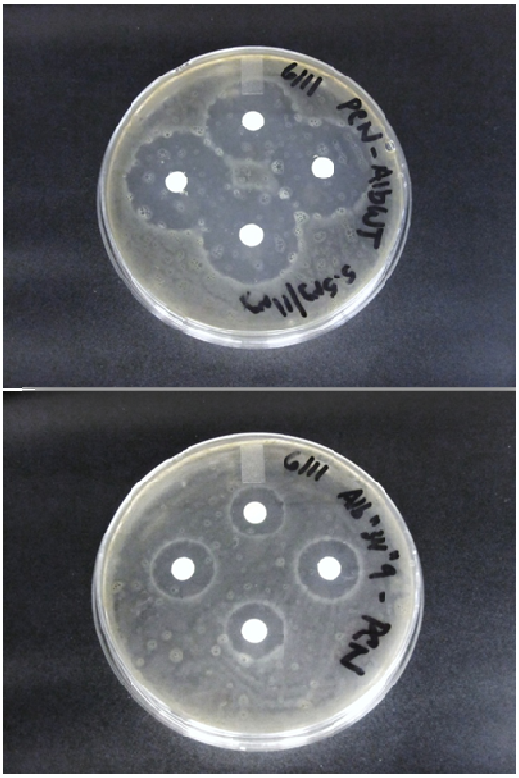

Figure A1.19 – Comparison of PTN susceptibility between a WT *S. albus* strain and a recombinant strain overexpressing *S. platensis fabF*. Amount of PTN/disk ranges from 1.25 μg – 10 μg.

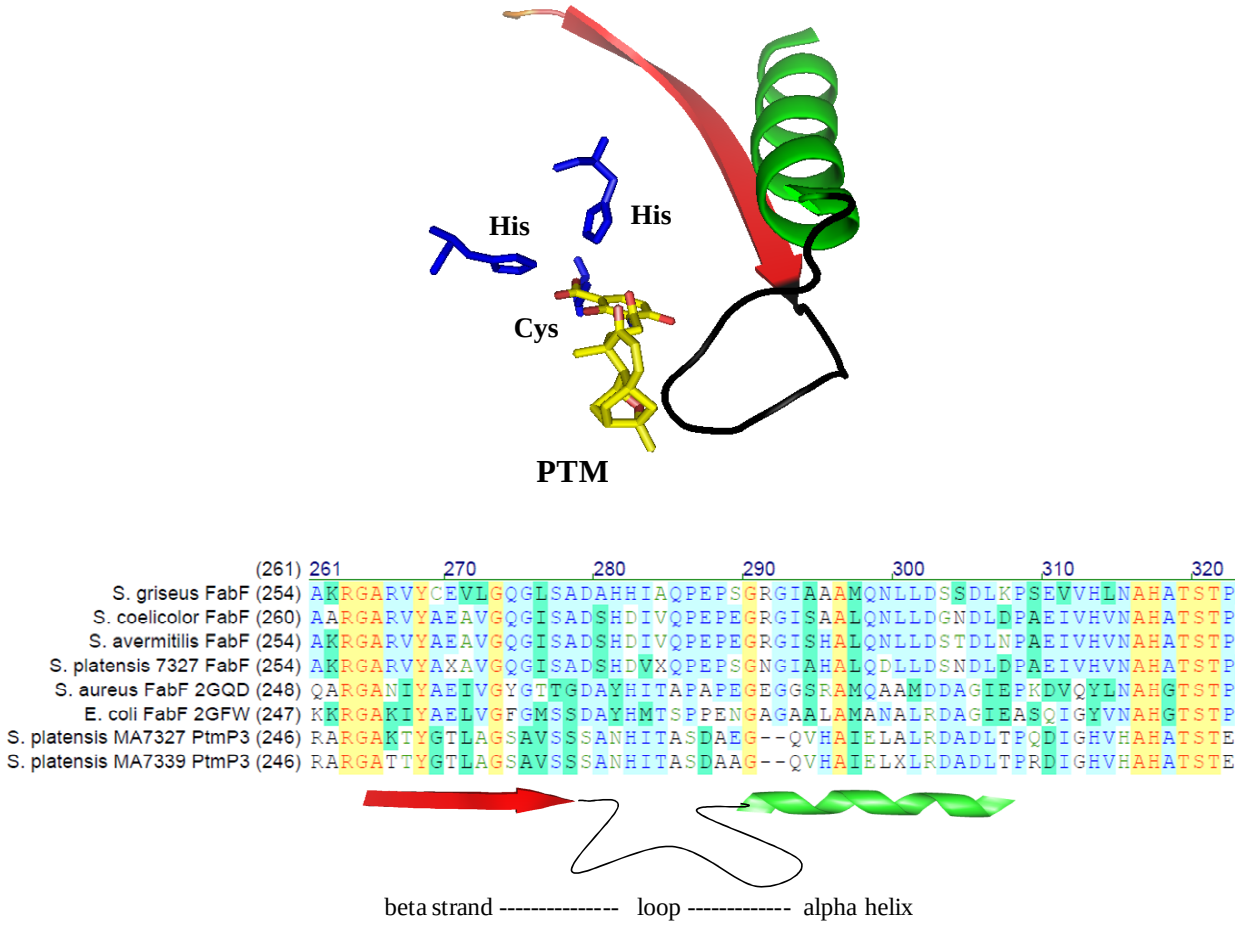

Figure A1.20 – Identifying a basis for PtmP3 resistance to PTM and PTN antibiotics. Primary sequence differences between PtmP3 and native FabF may reveal structural basis for PTM/PTN insensitivity with no affect on FASII reactions; one area of interest includes a “loop” involved in PTM/PTN “induced fit” binding that exhibits sequence variation between PtmP3 and native FabF from other *Streptomyces* spp.

A1.5 Reference GC-MS mass spectral data

Figure A1.21 – Mass spectra of geranylgeraniol ($C_{20}H_{34}O$), CAS Reg. No. 7614-21-3, Spectral Database for Organic Compounds (SDBS) (*10*)

Figure A1.22 – Mass spectra of *ent*-copalol ($C_{20}H_{34}O$) authentic standard (*11*).

Figure A1.23 – Mass spectra of *ent*-kaur-16-ene ($C_{20}H_{32}$), CAS Reg. No. 562-28-7, The Pherobase: Database of pheromones and semiochemicals (*12*).

Figure A1.24 – Mass spectra of *ent*-kauran-16-ol ($C_{20}H_{34}O$), CAS Reg. No. 524-17-4, The Pherobase: Database of pheromones and semiochemicals (*12*).

Figure A1.25 – Mass spectra of *ent*-kauran-16α-ol (*13*).

Figure A1.26 – Mass spectra of *ent*-kauran-16β-ol (*13*).

Figure A1.27 – Known contaminating peaks due to GC septum bleed (*14*).

Figure A1.21

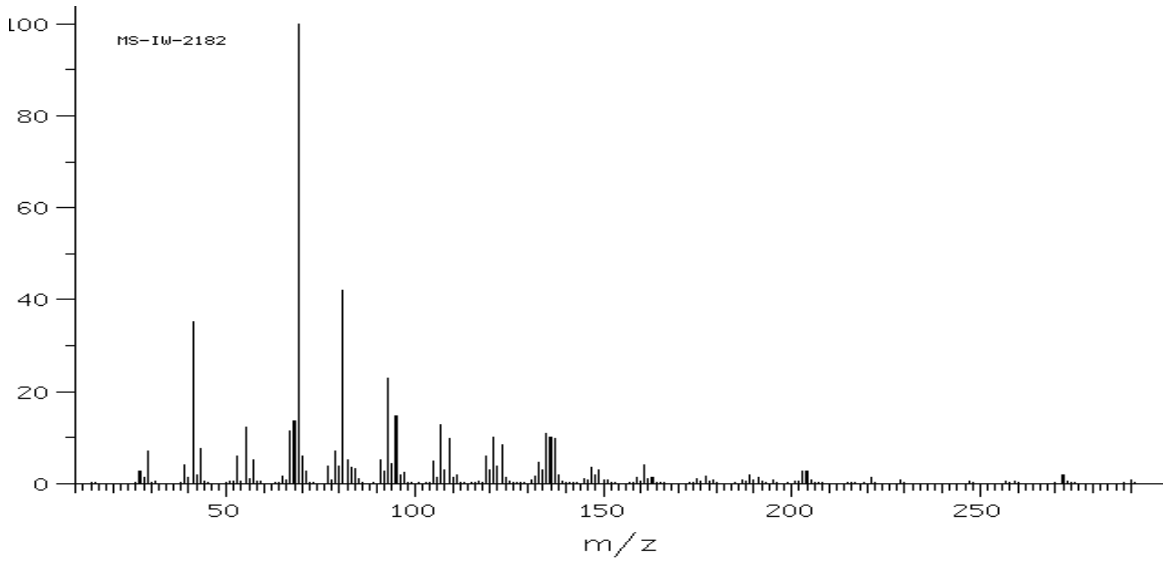

Figure A1.22

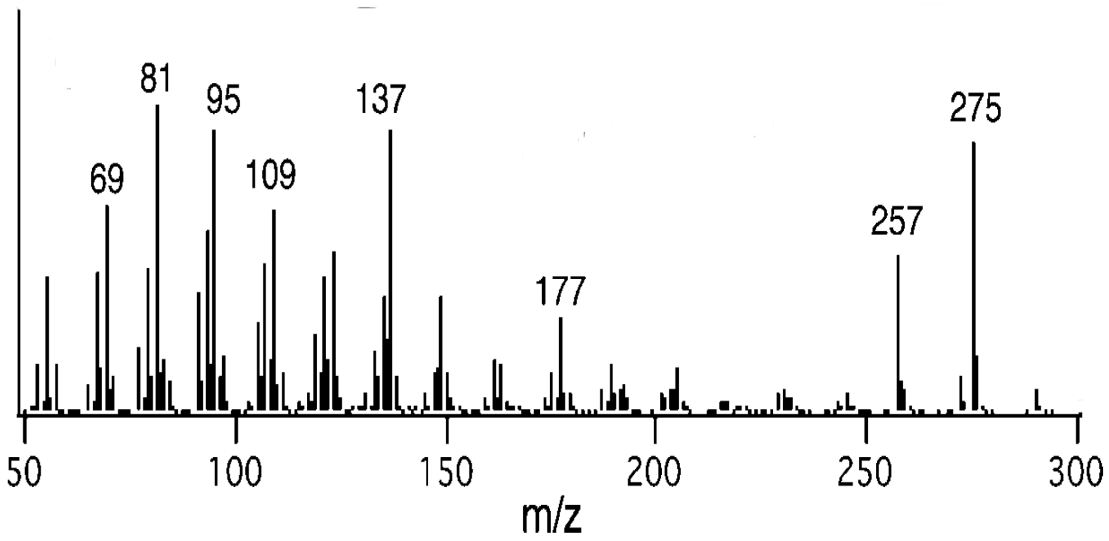

Figure A1.23

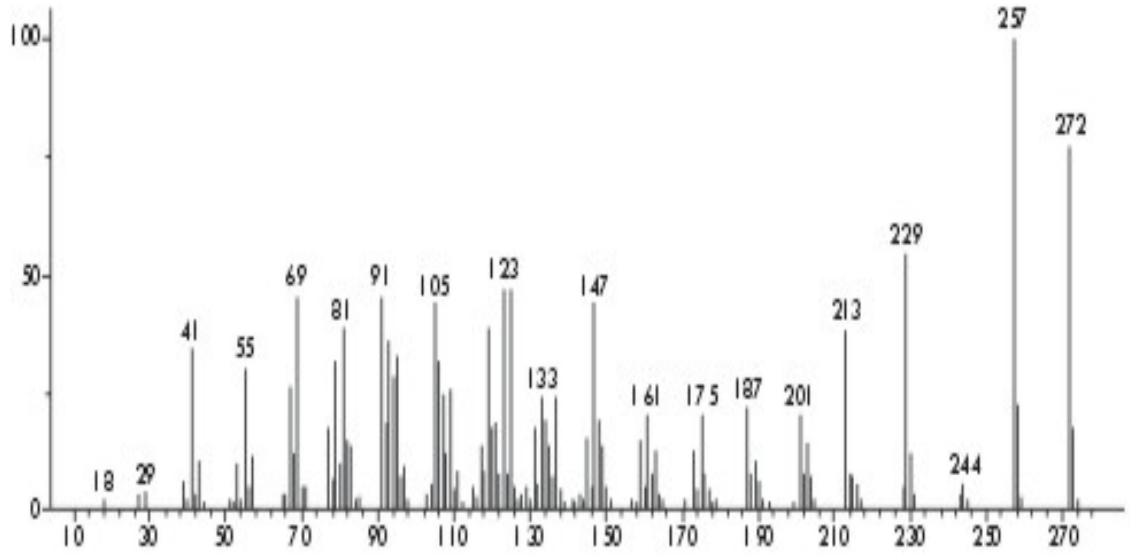

Figure A1.24

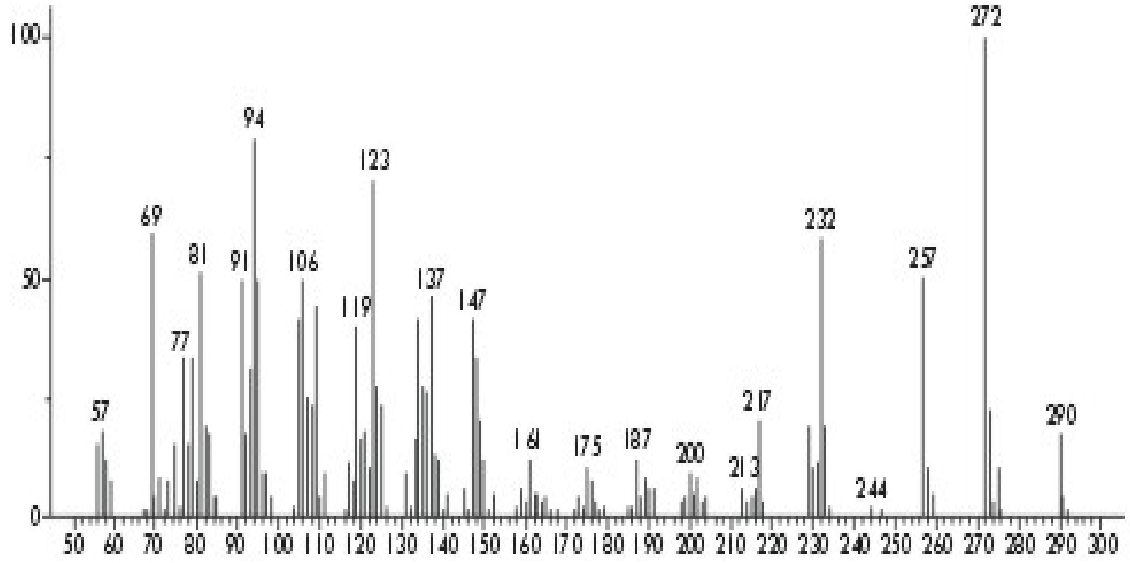

Figure A1.25

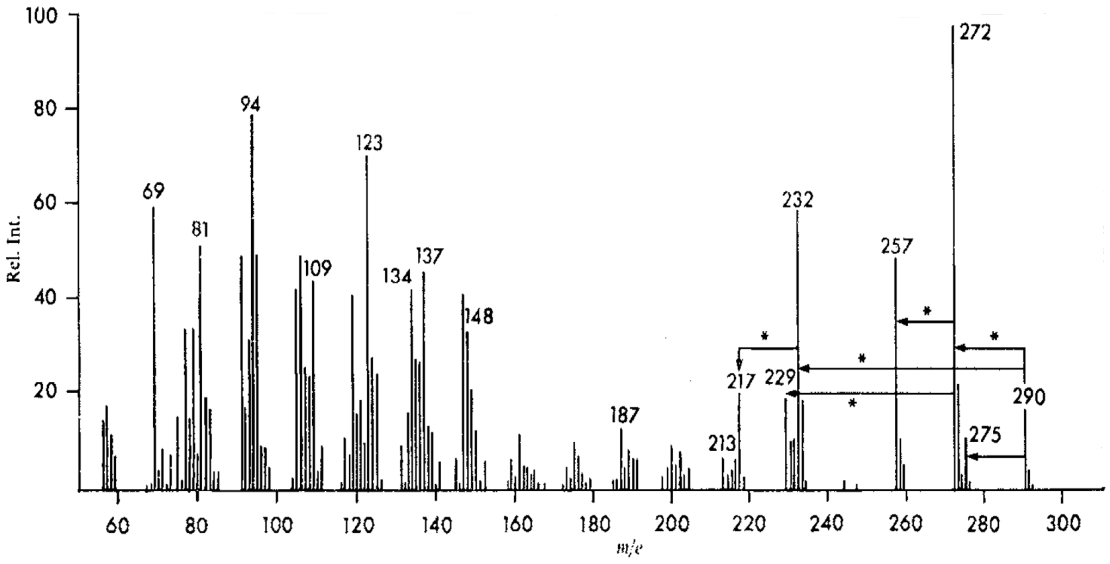

Figure A1.26

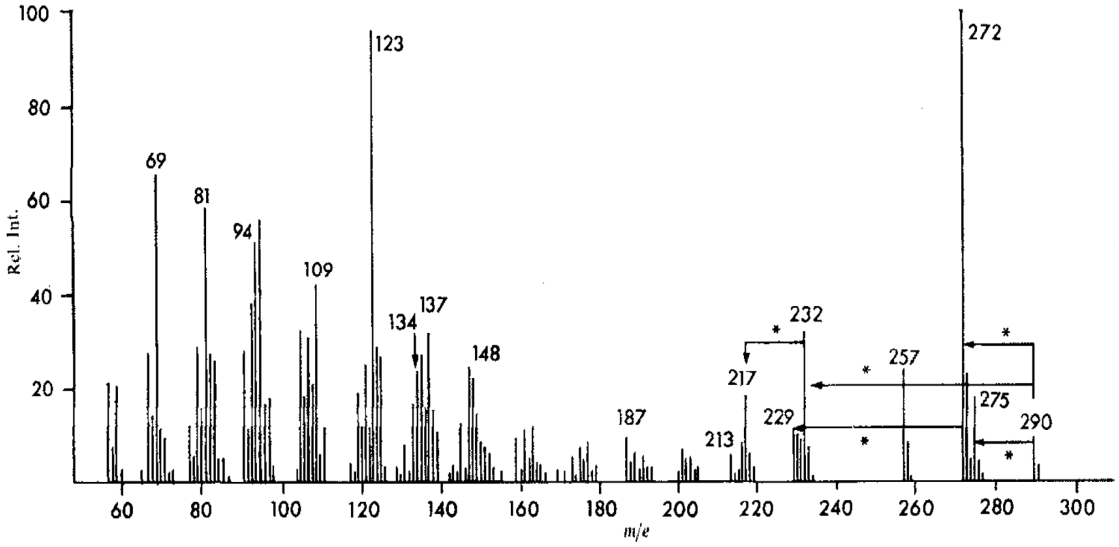

Figure A1.27

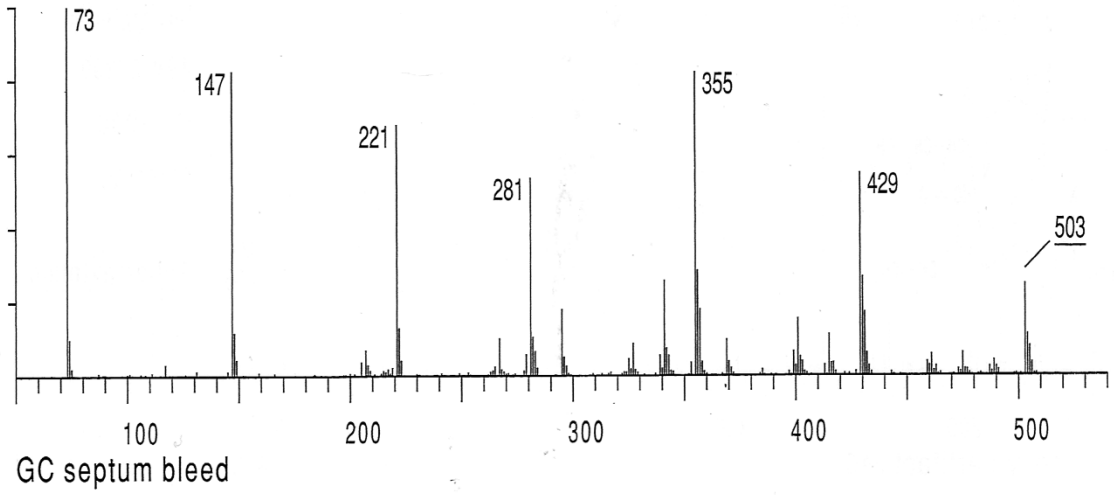

A1.6 DNA sequences of *fabF* and *fabH* genes cloned from *Streptomyces albus* J1074 and *Streptomyces platensis* MA7327 genomic DNA

S. platensis MA7327 *fabF*: (1266bp)

gtgaacgcgaccaatcgcaccgtggtcgtcaccggtatcggcgcaaccacaccgctgggtggcgacagcgcttcgtcctgggaggccat
gctcgccggacgttccggtgtcggcacgctcgaccaggactgggcggccgagcttcccgtccggatcgccgcacaggcggccgtggac
ccggcggacgtcctcccccgggcgcaggcccgcaagctggaccgctcggcgcagctcgcgctgatcgcggcccgcgaggcctgggc
ggacgccggtttcaccgccagggccggtgaggacacctcggtggaccccgaccggctcggcgccgtcattgcctccggcatcggcggc
gtgaccaccctgctcggccagtacgacgtgctcaaggagaagggcgtccgccgcgtctccccgcacaccgtgccgatgctgatgcccaa
cggcccgtccgccaacgtcggcctggatgtgaacgcccgcgccggtgtgcacaccccggtcagcgcctgtgcgtccggctccgaggcg
atcggctacgccntcgagatgatccgtacgggccgcgccgacttcgtcatcgcgggcggtacggaggcggccatccacccgctgccgat
cgccgccttcggcaacatgatggcgatgtcgaagtccaacgacnacccgcagggcgcctcccgtcccttcgacaccgcgcgcaacggtt
tcgtcatgggtgagggcgccggngtgatcgtcctggagtcggccgagcacgccgccaagcgcggcgcccgggtctacgccnaggccg
tcggccagggcatctccgccgacagccacgacgtcntgcagcccgagccgtccggcaacggcattgcacacgccctccaggacctcct
ggactccaacgacctcgacccggcggagatcgtgcacgtcaatgcgcacgccacctccacgccgcanggcgacctggccgaactgaa
ggcgctgcgcaaggtcttcggcgacgacaccgaccacatggcggtctccgccacgaagtcgatgacgggccacctcctgggcggcgcc
ngcggtgtcgagaccgtcgccgcgatcctggcgctgtaccaccgggtggcaccgccnacgatcaacgtcgacgagctcgacccggag
gtcgacgcggacatcgtccgcggcgagccccgcaagctgcccgccgagggccgcatcgcggcgctgaacgactcgttcggcttcagcg
gccacaacgtggtgctggccttccggacggtctga

S. albus* J1074 *fabF: (1289bp)

gtgagctcgaccaattgcaccgtggtcgtcaccggtatcggcgcaaccacaccgntgggtggcgacgcagcctcgacctgggagggtct
ggtcgccggcaggtccggcgtccggcccctggagcaggagtgggctgccgaccaggcggtccgtatcgtcgcgccggccgccttctcc
ccctccaaggtcatcccgcggccgcaggcccgccgtctggaccgctcggcgcagttcgcgctgatcgcggcgcaggatgcctggaagg
gcgccgggtattccggcaaggcgggcgagagtcccgccgaggacngcgcggcccacgtcgaccccgaccggctcggtgcggtcatc
gcctccngnatcggcggcgtgaccacgctgctcnaccannatgacgtgctgantgagaantgcgtccgcngcgtctccccgcanacgtc
ncnntgctgatgncnancngtccctccgccaanntnngtctggccgtgggngcccntgcggncgtgcactccccggtctcgncctgcg
cgtcgggcgccgaggccatnggntacgccatcgagatgatccgcnccgnnnngccgacgtcgncgtcgcgggtggncacggaggcg
gcgatccacccgntgcccatcgccgcgntnggcaacacgatggcgatgtccaagaacaacgacgacccgcagggcgcctcccgcccn
ttcgacacggcgcgcgacggcttcgtcctcggcgagggcgccggcgtcctggtcctggagtccgccgagcacgccgccgcgcgcggc
ncccgcgtctacgcggaggcggtcggccagggcatctccgccgacagccactacatcgtgcagccggagccggagggccgcggcatn
tccgccgccctgcagaacctgctggacggcaacgacctggacccggccgagatcgtgcacgtcaacgcgcacgccacctcgacgccg
gccggtgacatcgccgagctgaaggcgctgcgcaaggtcctcggcgacgacgtcgaccacatggcggtctccggcaccaagtcgatga
ccggtcacctgctcggtggcgcgggcggcgtggagtccgtggcgaccgtgctcgcgctgtaccaccgggtggcgccgccgaccatcag
cgtcgagaacctcgacccggaggccgaggccaacgcggacatcgtccgcggggaggcccgcaagctcccggtggagggccgtatcg
ccgcgctgaacgactcgttcggcttcggcgggcacaacgtggtgctcgcgttccggtcggtctga

***S. platensis* MA7327 *fabH*: (1047bp)**

atgacctcgaaggtcaagccctcgaagggcgccccgtacgcgcggatcatgggcgtcggcggctaccgcccgacccgggtcgtgccca
acgaggagatcctcaagcacatcgactcgtccgacgagtggatccgctcgcggtccggtatcgcgacccgccactgggcgggccccga
cgagaccgtcgcgaccatgtcggtcgaggcgtccggcaaggccatcgccgacgccgggatcacgcccgagcagatcggcgccgtgat
cgtctccaccgtttcgcacttcaagcagaccccggcgatcgcgaccgagatcgcgcaccgcatcggtgccggcaagccggccgcgttcg
acatctcggcgggctgcgcgggcttcggctacggcctgaccctggccaagggcctggtgaccgagggctcggcggagtacgtcctggtc
ctcggcgtcgagcggctctcggacctgaccgacctggaggaccgcgcgacggccttcctgttcggtgacggtgccggcgcggtgatcgt
cggcccggccacggagcccgagatcggcccgaccgtgtggggctcggagggcgacaagtccgagaccatcaagcagaccctgggct
gggacgtctaccgctcccacccgctccccggaggggacgcccctgagggccgccccgctccggaggagatccgttaccccgccatcac
gcaggagggccaggcggtcttccggtgggcggtgttcgagatggcgaaggtcgcccagcaggcactggacgcggccggagtcagccc
ggacgacctggacgtcttcatcccgcaccaggccaacatgcggatcatcgactcgatggtgaagactctgaagctgccggagagcgtgac
ggtcgcccgcgacgtggagaccaccggcaacacctcggccgcctccattccgctcgccatggagcgactgttggcgaccggacaggcc
aagagcggcgacaccgcgctggtcatcggcttcggggcgggtctcgtctacgccgcgacggtcgttaccctcccctag

S. *albus* J1074 *fabH*: (1023bp)

atggcgaagatcaagcccagcaagggtgcaccgtacgcgcgcattctcggggtcggcggctaccgcccgacgcgggtggtgcccaac
gaggtgaccctggagcggatcgactcgtccgacgagtggatccgctcgcgttcgggcatcgcgacccggcactgggccgacgaccagg
agaccgtcaccgcgatgtcggtggaggcggcgggcaaggccatcgcggacgccggtatagccccggccgacatcggcgccgtcgtcg
tctcgacggtctcgcacttcaagcagacccccgcggtcgccaccgagatcgcccacctggtgggcgccggcaagcccgccgccttcgac
atctccgccggctgcgcggggttcggctacggcctgaccctggccaagggcatgatcgtcggcgggtcggccgagcacgtgctggtcat
cggcgtggagcggctcagcgacctcaccgaccacgaggaccgcgcgacggccttcctcttcggtgacggcgcgggcgcggtcgtcgtc
ggcccctccgacgtcccggccatcgggcggacggtgtggggctccgagggcgacaagtcggagaccatcaagcagacggtgtcgtgg
gcggagtaccgcgacggccacccggagaagttcccggcgatcacgcaggagggccaggcggtcttccgctgggccgtcttcgagatgg
ccaaggtcgcccagcaggcgctggaggccgccgggatcaccgcggacgacctggacgtcttcattccgcaccaggccaacatgcggat
catcgactcgatggtgaagaccctcaaactgccggagcacgtcacggtcgcccgtgacatcgagaccaccggcgacacctcggccgcgt
cgatcccgctcgcgatggagcggcttctggcgacgggcgaggccaagagcggcgacacggcactcgtcatcggcttcggggcggggc
ttgtcccaaccgaatcgctcggcagcacatcctcggttccccacccgtcgtaatag

A1.7 References

1. Gust B, Challis GL, Fowler K, Kieser T, Chater KF (2003) PCR-targeted Streptomyces gene replacement identifies a protein domain needed for biosynthesis of the sesquiterpene soil odor geosmin. *Proceedings of the National Academy of Sciences of the United States of America* 100:1541-1546.

2. Bierman M, Logan R, O'Brien K, Seno E, Nagaraja R (1992) Plasmid cloning vectors for the conjugal transfer of DNA from Escherichia coli to Streptomyces spp. *Gene* 116:43-49.

3. Galm U et al. (2009) The biosynthetic gene cluster of zorbamycin, a member of the bleomycin family of antitumor antibiotics, from Streptomyces flavoviridis ATCC 21892. *Molecular Biosystems* 5:77-90.

4. Smanski MJ, Yu Z, Casper J, Lin S, Peterson RM, Chen Y, Wendt-Pienkowski E, Rajski SR, Shen B (2011) Dedicated ent-kaurene and ent-atiserene synthases for platensimycin and platencin biosynthesis. *Proceedings of the National Academy of Sciences of the United States of America* 108:13498-13503.

5. Kieser T, Bibb MJ, Buttner M, Chater KF, Hopwood DA (2000) *Practical streptomyces genetics* (The John Innes Foundation Norwich, UK).

6. Wang J et al. (2006) Platensimycin is a selective FabF inhibitor with potent antibiotic properties. *Nature* 441:358-361.

7. Wang J et al. (2007) Discovery of platencin, a dual FabF and FabH inhibitor with in vivo antibiotic properties. *Proceedings of the National Academy of Sciences of the United States of America* 104:7612-7616.

8. Smanski MJ, Peterson RM, Rajski SR, Shen B (2009) Engineered Streptomyces platensis strains that overproduce antibiotics platensimycin and platencin. *Antimicrobial Agents and Chemotherapy* 53:1299-1304.

9. Keller RK, Thompson R (1993) Rapid synthesis of isoprenoid diphosphates and their isolation in one step using either thin layer or flash chromatography. *Journal of Chromatography A* 645:161-167.

10. National Institute of Advanced Industrial Science and Technology (AIST) (2012) Spectral Database for Organic Compounds SDBS. Available at: <http://riodb01.ibase.aist.go.jp/sdbs/cgi-bin/direct_frame_top.cgi> [Accessed January 5, 2012].

11. Prisic S, Xu M, Wilderman P, Peters R (2004) Rice contains two disparate ent-copalyl diphosphate synthases with distinct metabolic functions. *Plant Physiology* 136:4228-4236.

12. El-Sayed A (2012) The Pherobase: Database of Pheromones and Semiochemicals. Available at: <http://www.pherobase.com> [Accessed January 5, 2012].

13. Kalinovsky AI et al. (1970) Mass spectrometry of kaurene derivatives I. The mass spectra of some (−)-kauran-16-ols. *Organic Mass Spectrometry* 3:1393-1400.

14. Pfleger K, Maurer H, Weber A (1992) *Mass Spectral and GC Data of Drugs, Poisons, Pesticides, Pollutants, and Their Metabolites* (VCH, New York).